UC Merced

UC Merced Electronic Theses and Dissertations

Title

Investigating groundwater and surface water interactions using novel isotopes and geochemical tracers in the upper Merced River Basin, Sierra Nevada, California

Permalink

https://escholarship.org/uc/item/2w97s9qk

Author

Shaw, Glenn David

Publication Date

2009-08-05

Peer reviewed|Thesis/dissertation

eScholarship.org Powered by the California Digital Library
University of California

INVESTIGATING GROUNDWATER AND SURFACE WATER INTERACTIONS USING NOVEL ISOTOPES AND GEOCHEMICAL TRACERS IN THE UPPER MERCED RIVER BASIN, SIERRA NEVADA, CALIFORNIA

by

Glenn David Shaw

A dissertation submitted to the faculty of
The University of California, Merced
in partial fulfillment of the requirements for the degree of

Doctor of Philosophy

in

Environmental Systems

School of Engineering

The University of California, Merced

August 2009

Copyright © Glenn David Shaw 2009

All Rights Reserved

ABSTRACT

Groundwater and surface water interactions in mountain catchments occur at much larger scales than previously recognized. Because mountains are "water towers" and provide much of the water needed to adjacent low lands, it is important to understand these interactions to accurately assess water fluxes within a mountain system. This dissertation presents an approach using several environmental tracers to identity source waters, establish groundwater residence times, and identify groundwater discharge locations in the Merced River basin between Yosemite Valley and El Portal.

^{36}Cl and Cl^- were used to identify source waters and to characterize their discharge contributions to stream flow in the Upper Merced River. Near-surface water was found to be the largest endmember. Low-Cl^- evapotranspired water was second, and high-Cl^- was third. Near-surface water was primarily released during snowmelt, but snow was not an obvious endmember. Snow and near-surface water had Cl^- concentrations <0.25 mgL^{-1}, but the $^{36}Cl/Cl$ in near-surface water was much greater than in snow (i.e. ~$10000x10^{-15}$ compared to <$306x10^{-15}$). The elevated ratio is likely from bomb-pulse ^{36}Cl still circulating in the biosphere. One possible mechanism may be retention of bomb-pulse ^{36}Cl into organic matter, which later remineralizes, providing Cl^- to near-surface water. This process would indicate that retention of organochlorines has timescales up to 40-50 years. Low-

Cl^- evapotranspired water was only observed in tributaries, during baseflow, and in Yosemite Valley groundwater samples. High-Cl^- groundwater was observed in El Portal groundwater, a spring at the top of Yosemite Valley, and the Merced River during baseflow. Although its contributions to stream flow is lowest compared to other endmembers, its flow rates are more stable.

Low-Cl^- groundwater is characterized by $^3H/^3He$ ages between 7 and 28 yrs, 0-50% premodern water, and $^4He_{RAD}$ ranging between $1.0x10^{-8}$ to $5.7x10^{-8}$ cm^3 (STP) g^{-1}. High-Cl^- groundwater is characterized by $^3H/^3He$ ages between 23 and 49 yrs, >75% premodern water, and $^4He_{RAD}$ ranging between $6.7x10^{-7}$ and $1.6x10^{-6}$ cm^3(STP) g^{-1}. $^3H/^3He$ ages in a spring and a groundwater well increase ~10 to 20 yrs, from snowmelt to baseflow.

^{222}Rn in the Merced River along the reach in Yosemite Valley remains spatially uniform in comparison to downstream of Yosemite Valley, which suggests a constant groundwater flux. Downstream of Yosemite Valley groundwater discharge to the river is typically much lower than in Yosemite Valley, but there are point-source locations of elevated groundwater discharge occurring at fracture zones. The differences between these two river reaches appear to be controlled by the amount of alluvium (i.e. Yosemite Valley consists of ~300 m of alluvium in comparison to <30 m of alluvium downstream).

This study improves our understanding of how stream flow is generated in snowmelt-dominated catchments and how climate change may affect stream flow regime. The small contributions and young ages of groundwater mixing with surface water in the Merced River basin, suggests that the Sierra Nevada may be even more vulnerable to the climate change than other mountain systems.

TABLE OF CONTENTS

LIST OF TABLES

LIST OF FIGURES

PREFACE

This dissertation consists of four main chapters between the Introduction and Conclusions chapters. Chapters 2, 3, and 4 are chapters intended for publication, while Chapter 5 is written as an idea for future work.

Chapter 2, "Groundwater and surface water flow to the Merced River, Yosemite Valley, California: ^{36}Cl AND Cl^- evidence," is intended to be submitted to the journal *Water Resources Research*. The paper discusses how ^{36}Cl and Cl^- can be used to identify and separate surface and subsurface endmembers mixing in an alpine catchment. It is the ^{36}Cl bomb pulse that is especially useful in assessing hydrology of the area. This study is one of the first known to the author where ^{36}Cl is successfully used as a tracer in primarily surface water samples to determine quantities and mixing of subsurface flow paths. In particular, ^{36}Cl indicates that all water types exchange with soil, and that chlorine biogeochemical processes, or other processes, may result in retention of bomb-pulse ^{36}Cl.

Chapter 3 is titled, "Groundwater Residence Times in the Merced River Basin, California, from analyses of tritium and noble gases." This chapter is intended for submission to the journal *Water Resources Research*. This paper builds on the identification of subsurface endmembers from Chapter 2, and uses noble gas measurements to characterize recharge temperatures, elevations, and groundwater residence times for at least two distinct groundwater bodies mixing in the watershed.

Chapter 4 is titled, "Local groundwater discharge to surface water in the Merced River basin: Comparing glacial and river-cut reaches using ^{222}Rn and ^{3}He/^{4}He." This is a short chapter intended for publication in the journal *Ground Water*. The purpose of this chapter is to use ^{222}Rn and helium isotopes to characterize local groundwater discharge occurring in Yosemite Valley and downstream of Yosemite Valley. Yosemite Valley has thick and wide glacial till alluvium, and the river alluvium is shallow and laterally narrow downstream of Yosemite Valley.

Finally, Chapter 5 is titled, "Why is Near-Surface ^{36}Cl/Cl Elevated in the Merced River Basin: A Closer Look at Chlorine Biogeochemistry". This is a short chapter proposing a mechanism that could explain why ^{36}Cl/Cl ratios are elevated in the Merced River basin. This mechanism cannot be validated from the current data, but observations from the Merced River basin are compared with previous studies that focus on chlorine biogeochemical processes occurring in forested areas. The answer to this hypothesis depends on conducting further work. .

Many people need to be acknowledged for helping this dissertation become a reality. I'd like to first thank my advisor Martha Conklin. When I agreed to come to UC Merced, the campus had not even opened to students. After agreeing to work with Martha at UC Merced, she said in an email, "Thank you for your faith." I'd like to now thank Martha for her faith in me. Martha has been extremely patient with me, even during times when I flailed more than progressed. In particular she has helped me see hydrology in a larger context, encouraged me to think in terms of research and new ideas rather than just conducting another consulting project, and especially, taught me how to present

research to professionals and information to students in the classroom. Her energy has inspired me.

My thanks also extend to Roger Bales and Tom Harmon for the hours spent serving on my oral defense and final defense committees

I'm also grateful to Gregory Nimz for providing the backbone for the ^{36}Cl work conducted in this study, and for serving on my oral and final defense committee. It was Greg who first encouraged Martha and me to apply for funding to look at ^{36}Cl in the Merced River basin. Greg has patiently mentored me to learn how to successfully analyze and interpret ^{36}Cl data. Several times he has sat down with me for several hours to "brainstorm" about this project, and he has spent numerous hours going through all of my chapters helping me prepare for my final defense and for publishing these results.

I'd like to Bryant Hudson and Jean Moran for providing summer employment, providing all the noble gas analyses, and getting me started with my work using ^{222}Rn.

I also owe thanks to many fellow grad students, postdocs and research staff for their role in keeping me sane and allowing me to express frustration at times—especially my running buddies Don Schweizer and Jason Fisher. Others include Rob Root, Nelson Rivera, Peter Kirchner, Chris Butler, Ryan Lucas, Eric Haux, Alex Radko, Heidi Deitrich, Gyami Shrestha, Ricardo Cisneros, Sarah Martin, Phil Saksa, Matt Meadow, Basha Stankovich, Dorie Beals, Cristiane Cruz, and many more who I'm probably neglecting. Also to my good friend,

colleague Fengjing Liu, who was always there to listen, give ideas, help with this project, and bring sanity to my whole perception of this project.

Most importantly, I'd like to thank my wife Ana for her dedication and companionship to me. She has been the greatest support through the good and bad times spent here in Merced. She helps me see that my cup has always been half full. With her patience, love, devotion, and sacrifice, she has helped make this experience seem less like an ordeal, and more like a great opportunity.

I owe thanks to my four children, Samuel, Abraham, Kimori, and Zora. Thank you, Samuel and Abraham, for letting me uproot you from the security of Mom being at home with you, from Sunday dinners with Grandma and Grandpa, and from living in a place with lots of nearby snow. Zora and Kimori, you have inspired me to work a little harder so I can actually finish this dissertation.

I express gratitude to my Grandmother Camille Decelles Shaw for pushing my Grandfather Joseph Shaw to pursue a B.S. and M. S. in Metallurgical Engineering at Butte School of Mines during the Great Depression. Because of her tenacity, Grandpa Shaw started up the successful Butte Machinery Company. It was this education and exposure to machinery that fed my father's unquenchable thirst for science—eventually leading him to become a successful professor of atmospheric physics at the University of Alaska, Fairbanks. Grandpa's education paved the way for Dad's education, which has in turn created the path for my two brothers and myself. Their examples motivated me through action, not words, to forego a perfectly fine job in industry to pursue science more deeply.

CHAPTER 1

INTRODUCTION

Although major urban and agricultural centers in mountainous regions are usually located in valleys adjacent to mountains, most water use by these communities originates in the mountains (Bales et al., 2006; Earman, 2006; Viviroli et al., 2007). Over 60 million people in the western United States depend on mountain water as a resource (Bales et al., 2006). More specifically, runoff from the Sierra Nevada provides approximately 30% of all runoff in California (Kattelman, 1996).

Two major problems remain associated with mountain hydrology. The first problem is that, in spite of the importance of water to the communities surrounding mountains, current understanding of water resources in mountains is limited because of a lack of observations. The second problem is that water in mountain systems is the most vulnerable to climate change. To address these two problems, characterization of the distribution and timing of mountain water is necessary. One technique that has been useful in mountain systems is through the use of geochemical and isotope tracers (Manning and Solomon, 2005; Liu et al., 2008). This chapter will, i) discuss the two previously mentioned problems in greater detail, ii) provide background information on current understanding of

groundwater in Yosemite National Park, which is part of the setting for this dissertation, and iii) present an isotopic approach for characterizing the distribution of water fluxes and residence times in the Merced River basin, which is a representative basin in the southern Sierra Nevada.

Mountain water systems, in spite of their vulnerability to human perturbations and other changes, are largely under-observed (Bales et al., 2006). Hydrologic processes in mountains have been studied in detail at the hillslope scale, with a focus on stream flow response to precipitation (Wilson and Guan, 2004), but accurate characterization of snow pack volumes, source waters, flow paths and other hydrologic fluxes is lacking because of limited observations (Bales et al., 2006). Precipitation amounts, snow depth, and stream flow measurements are particularly lacking in high elevations where a large fraction of the snowpack exists. This is partly due to the difficulties of accessing locations.

Understanding of mountain groundwater is particularly limited because of the absence of groundwater wells in these systems. Mountain groundwater systems are also complicated by numerous fractures, faults, and folds, resulting in significant difficulty in determining flow paths, fluxes, and residence times (Maloszewski and Zuber, 1983; Moline et al., 1998; Manning and Caine, 2007). However, recent studies show that mountain groundwater provides a major component of water in the aquifers in adjacent basins (Manning and Solomon, 2003; Wilson and Guan, 2004; Manning and Solomon, 2005). Groundwater also interacts with surface water in large quantities (commonly >50% during low-flow months), even in high-elevation catchments where there is little soil (Sueker et al., 2000; Liu et al., 2004).

In recent decades, warming trends have already been observed in western North America (Cayan et al., 2006). Earlier snowmelt is a result of warming, and climate predictions estimate that the timing and form of precipitation in the Sierra Nevada will shift from snow-dominated to rain-dominated systems at moderate elevation zones (Cayan et al., 2001; Dettinger et al., 2004; Knowles et al., 2006).

It is unclear exactly how changes in type and timing of precipitation will affect groundwater, but it has been suggested that groundwater recharge may decrease as the system experiences these changes (Earman et al., 2006). Furthermore, groundwater discharging to streams during low flowing months may also be threatened as summers lengthen from earlier snowmelt, but the system is largely controlled by the bedrock type and porosity of the bedrock (Tague et al., 2008). Perhaps some basins may even experience changes from perennial streams to ephemeral streams as summer months are lengthened and groundwater recharge decreased. Water deficits are already suggested as a probable contributor to increased tree mortality that has been observed in mountain regions of the western United States (van Mantgem and Stephenson, 2007; van Mantgem, et al., 2009).

The use of environmental tracers in mountain systems is gaining popularity for characterizing groundwater and surface water fluxes and flow paths. Examples of tracer studies include quantification of groundwater and surface water discharge to streams by continuous injection of salt tracers (Kimball et al., 2004), characterization of groundwater discharge to streams using heat as a tracer (Constanz, 1998), characterization of local subsurface fluxes to streams using ^{222}Rn (Wanninkof et al., 1990; Cook et al., 2003), separating surface water and groundwater hydrographs

using major ion chemistry and stable isotopes (Sueker et al., 2000; Liu et al., 2004), estimating groundwater storage in catchments using tritium and stable isotopes (Martinec et al., 1982; Maloszewski et al., 1983; Mattle, 2001), and estimating groundwater residence times and recharge temperatures using noble gases and tritium (Manning and Solomon, 2003; Manning and Caine 2007). These studies are powerful for characterizing unique hydrologic processes occurring within montane catchments, but it is anticipated that a combination of several tracers would provide a more complete understanding for building a conceptual model of water fluxes in these systems (Burns, 2002).

The primary focus of this dissertation is to present data from several geochemical tracers, and discuss how they can be used to identify groundwater and surface water interactions in an alpine catchment and determine groundwater residence times in the Merced River basin, focusing on Yosemite Valley and ending in the foothills below Yosemite Valley (Figure 1.1).

Groundwater in Yosemite National Park

In addition to the large-scale regional implications concerning mountain hydrology (e.g. whole mountain ranges and basins), there are also local implications. Yosemite National Park is one of the most popular national parks in the United States and typically receives more than 3.5 million visitors annually. All drinking water for Yosemite comes from groundwater production wells (personal communication with National Parks Service well operators). As popularity of the park increases, demand for water may follow. However, current understanding of groundwater within Yosemite is limited.

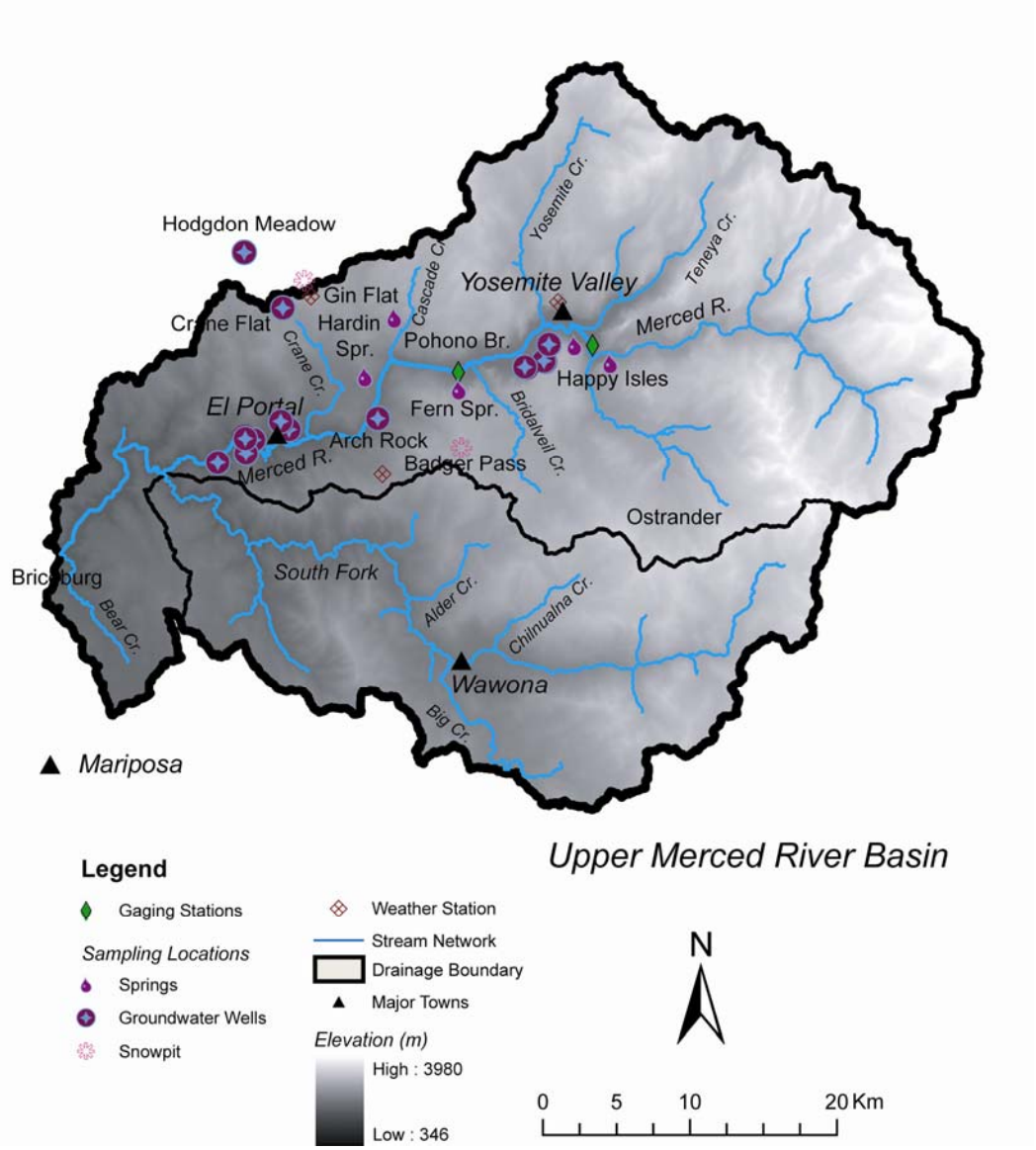

Figure 1.1: Study Site of the upper Merced River basin.

Most studies on water in Yosemite pertain to water quality (Sorenson and Hoffman, 1981; and Sorenson, 1982), mineral weathering and nutrient cycling (Clown et al., 1996; and Peterson et al., 2005), or mass wasting (Wieczorek and Jäger, 1996; Wieczorek et al., 2007; and Harp et al., 2008). The focus of these studies is primarily on surface water or geology, and they briefly discuss the role of groundwater or soil water. For example, increases in major ion chemical concentrations in surface water during baseflow (September-November) indicate longer and deeper flow paths with more solutes released from mineral weathering (Clow et al., 1996; Peterson et al., 2005). Mass wasting studies discuss how springtime increases in water flow through fractures enhanced rock falls in Yosemite Valley and just downstream of the Park.

Two more detailed efforts have investigated groundwater resources, residence times, and/or recharge in Yosemite (Borchers, 1996; Nimz, 1998; Flint et al., 2008). Groundwater recharge was estimated at Gin Flat (Figure 1.1) using time domain reflectometry (TDR) and heat dispension probes (HDP) (Flint et al., 2008). This study indicates a diurnal wetting and draining cycle from meltwater infiltrating into a shallow sandy loam (~72 cm deep). In this cycle, meltwater infiltrates into soil and ponds at the bedrock soil interface. After soil is completely saturated near bedrock, water begins to infiltrate into bedrock fractures. This continues until the soil is drained after night time temperatures go below freezing and melting of snowpack decreases. Bedrock permeability was estimated to be 1.6 cm d^{-1}. Using TOUGH2 (Pruess et al., 1999), Flint et al. (2008) showed that the

most likely fate of soil water was through infiltration into bedrock rather than lateral soil flow.

Although the findings from Flint et al. (2008) provide a reasonable conceptual model for mountain-block recharge, Gin Flat consists of a small low gradient (nearly flat) area. Findings from this study may not apply to locations with steep gradients, and there may be more lateral soil throughflow and less fracture recharge in these areas. Bedrock permeability determined from this study can only be applied to the shallow fractures, and cannot be extended to deeper fractures.

The most comprehensive groundwater study in Yosemite was conducted near Wawona (Figure 1.1), where water resources and water supply were being assessed for potentially moving Yosemite administrative facilities to Wawona (Borchers, 1996). Several groundwater wells in fractured granitic rocks were sampled, and two deep test holes were drilled in fractured granite. Several approaches were used to assess groundwater including analyses for major ion chemistry, ^{222}Rn, ^{3}H, ^{36}Cl, ^{2}H, and ^{18}O, geophysical seismic refraction, borehole geophysical surveys, geomorphology and fracture mapping, and well hydraulic testing to better assess groundwater. Two distinct fractured bedrock aquifers were characterized (Borchers, 1996); these aquifers were geochemically, hydraulically, and physically isolated.

The shallow aquifer is less than 100 m deep and characterized by lower conductivity water, enriched stable isotopes, greater tritium, and higher well driller pumping rates than the deep aquifer below 100 m deep. Conductivity

ranged between 126 and 207 μS cm^{-1} in the shallow aquifer, and it ranged between 369 and 2350 μS cm^{-1} in the deep aquifer. $\delta^{18}O$ and δD in the shallow aquifer ranged from -11.7 to -12.2‰ and -81.5 to -86.5‰ respectively. $\delta^{18}O$ and δD in the deep aquifer ranged from –13.3 to -13.6‰ and -94.5 to -99.4‰ respectively. The difference in stable isotopes indicates higher elevation or colder recharge for the deep groundwater. Tritium in the shallow aquifer range between 7.5 and 16.2 tritium units, which indicates that this water is modern (recharged < 50 yrs ago). Tritium concentrations in the deep aquifer were <0.3 tritium units, which indicates this water is premodern (recharged >50 yrs ago). Well driller pumping rates lasted from minutes to < 1 hr, and they ranged between 0 to 75 L min^{-1} in the shallow aquifer, and 0 to 26 L min^{-1} in the deep aquifer.

The overall median sustainable pumping rate for wells in Wawona was 15-19 L min^{-1} (Borchers, 1996), but well driller reports for two wells placed in fractured granite underlying meadows at Crane Flat and Hodgdon Meadow had sustained pumping rates at 114 and 159 L min^{-1} respectively.

Other National Park Service wells are set in Merced River alluvium, and typically have much higher yields for groundwater. Downstream of Yosemite Valley, alluvium is thin (<30 m) and the river corridor is a narrow, V-shaped valley; therefore, there is not much lateral extent of alluvium. 24-hr pumping tests indicate that these wells could sustain pumping rates between and 110 to 360 L min^{-1} (Table 1.1). Three wells placed in Yosemite Valley, where alluvium ranges between 300-600 m deep (Gutenberg et al, 1956), and the valley is much wider from glacial scouring (Bateman and Warhaftig, 1966), had sustained yields

Table 1.1: Sustained Flows for Yosemite National Park Service Wells

Well Location	**Pumping rate (L min^{-1})**
Meadow Wells	
Crane Flat	114
Hogdon's Meadow	159
River Wells	
Arch Rock	193
El Portal Well 2	265
El Portal Well 3	379
El Portal Well 4	114
El Portal Well 5	360
El Portal Well 6	170
El Portal Well 7	110
Yosemite Valley Wells	
Valley Well 1	4542
Valley Well 2	2422
Valley Well 4	4542
Average	1310
Median	229
Standard Deviation	1838

ranging between 2422-4542 L min^{-1} (Table 1.1). Transmissivity estimates range between 1490-2111 m^2 d^{-1} at Valley Well 2, and 621-1316 m^2 d^{-1} at Valley Well 4, but were not estimated at other well locations.

The variability of sustained pumping flow rates in individual Yosemite National Park Service wells suggests that groundwater does not behave uniformly throughout the Merced River basin, and that it may be compartmentalized. There may be locations where groundwater is easily replenished (e.g. the high sustained flow rates in Yosemite Valley wells) and other locations where groundwater is isolated and limited as a resource (e.g. low sustained wells in Wawona).

Hypotheses

Based on observations in Yosemite National Park, it was hypothesized that sampling of several environmental tracers in surface and groundwater would provide a greater understanding of how water partitions and distributes throughout mountain watersheds, and that at least two groundwater bodies would interact with surface water in the basin. These two groundwater bodies would reflect geochemistry and residence time characteristics of the deep and shallow groundwater observed in Wawona.

Approach

This dissertation presents an approach for investigating subsurface flow paths and how they interact with surface water in the upper Merced River basin from the headwaters to Briceburg, which is just upstream of Lake McClure, a reservoir in the foothills (Figure 1.1). Specifically, major ion chemistry (Na^+, K^+,

Mg^{2+}, Ca^{2+}, Cl^-, SO_4^{2-}) stable isotopes (^{18}O, ^2H), radioactive isotopes (^{222}Rn, ^{36}Cl, ^3H), and noble gases (^3He, ^4He, Ne, Ar, Kr, Xe) were used to investigate groundwater and surface water processes. Samples were collected both spatially and temporally in surface water, springs, and groundwater between July 2004 and October 2007. Each tracer used in this study provides specific information about water fluxes and flow paths in the watershed.

Major ion chemistry and ^{36}Cl were used to investigate surface and subsurface water contributions to the Merced River, as well as some of the geochemical and hydrologic processes controlling source water chemistry. These processes include, incorporation of the ^{36}Cl bomb-pulse in recent snowmelt, incorporation of rock Cl^-, evapotranspiration, and possibly biogeochemistry (see Chapter 2). Groundwater noble gas and ^3H analyses were combined to investigate groundwater mixing, recharge locations, and residence times (see Chapter 3). Recharge temperatures, apparent $^3H/^3He$ ages, the fraction of premodern water (recharged > 50 yrs ago) and modern water (recharge less than 50 yrs ago), and radiogenic ^4He ($^4He_{RAD}$) ages were investigated. ^{222}Rn activity in the Merced River basin was also used to investigate how local groundwater fluxes to surface water vary along the Merced River both spatially and temporally (see Chapter 4). Finally, current understanding of ^{36}Cl sources, deposition of bomb-pulse ^{36}Cl ($^{36}Cl_{BP}$), and chlorine biogeochemistry were combined with Merced River flows and past and present ^{36}Cl measurements in the Merced River to investigate the occurrence of anomalously high $^{36}Cl/Cl$ ratios in recent meltwater (see Chapter 5). This investigation discusses the possibility of rapid retention of Cl^- into

organochlorines and slow release of Cl^- from decaying organochlorines as the major contributor to current observations.

The major questions addressed in this dissertation are i) What are the major flow paths and residence times associated with source waters in high elevation granitic watersheds? ii) What major geologic controls influence groundwater recharge and discharge to surface water? iii) What information can specific isotopes provide about hydrologic and geochemical processes mountain watersheds? iv) How can information on source waters and residence times be used to assess the vulnerability of water resources to climate change in the Sierra Nevada?

Conceptual Model

Throughout this dissertation, novel isotopes and geochemical tracers will be used to understand water fluxes, flow paths, and residence times. A conceptual model of these flow paths and residence times is discussed below, and illustrated in Figure 1.2. Water in the Merced River basin takes several near-surface and subsurface flow paths from snowmelt to the Merced River. In this study, the catchment is broken into two major reaches. They are, 1) flow paths leading to the Merced River within Yosemite Valley, and 2) flow paths leading to the Merced River downstream of Yosemite Valley (e.g. at El Portal). Many of the flow paths interacting within these two reaches are related, but the difference in alluvium depth and width, largely contribute to differences observed within the watershed. Yosemite Valley consists of valley fill that is ~300 m thick and 1 km wide. River alluvium in El Portal, on the other hand, is ~20-30 m thick and 100 m wide. There are seven major flow paths identified in this study. They are, 1) near-surface flow,

2) shallow fracture flow, 3) recharged tributary flow into alluvium, 4) deep fracture flow discharging laterally to river alluvium, 5) inflows and/or outflows between deep fractures underlying river alluvium, 6) alluvium flow parallel to the Merced River, and 7) Merced River water recharging river alluvium (Figure 1.2). The proceeding paragraphs describe each of these flow paths and the relative quantities and residence times associated with them.

Flow Path 1

The largest flux of water through the catchment occurs as near-surface flow paths occurring throughout the entire watershed. The majority of this water is released during snowmelt. Part of the flow path may be overland flow, but at some point prior to entering surface water bodies, it interacts with soil, alluvium, and perhaps even shallow exfoliation fractures. The residence time for this water is on the order of days to months.

Flow Path 2

Snowmelt or flow path 1 water may recharge shallow fractures less than 100 m thick and eventually discharge to surface water tributaries above the Merced River. This flow path may also occur throughout the entire watershed, and the residence times are on the order of years to decades.

Flow Path 3

The third flow path consists of water in river and valley alluvium flowing from canyon walls to the Merced River. A large fraction of this water is recharged

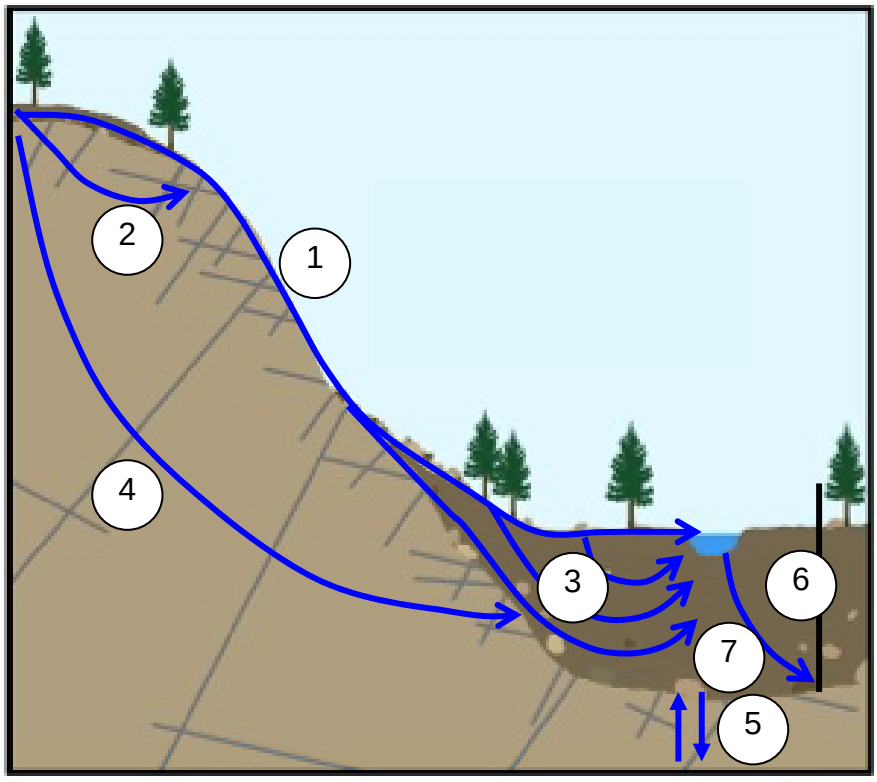

Figure 1.2: Flow paths in the Merced River basin.

from tributaries spilling over the canyon walls (e.g. Yosemite Valley) or flowing directly to river alluvium from small canyons (e.g. El Portal). However, some of this water enters alluvium from fractured groundwater flow. The residence times of groundwater within Yosemite Valley alluvium is on the order of years to a few decades. The river alluvium in El Portal is primarily recharged locally from near surface water, and the mean residence time for this water is less than 1 yr.

Flow Path 4

Snowmelt, near-surface water, and/or shallow groundwater in fractures may recharge deep fractures, which may later discharge to river and valley alluvium. This water consists of the smallest flux of water that mixes with the Merced River, and the residence time ranges between several decades to even millennia. This water is typically deeper than 100 m, and these fractures appear to be more regional, occurring at sub-basin drainage locations.

Flow Path 5

The least well understood flow path is the flux of groundwater between the river and valley alluvium and deep fractures parallel to the Merced River. It is unclear which direction the flow is, what the flux may be, and the residence times of these fluxes.

Flow Path 6

Both upstream and downstream of Yosemite Valley, groundwater may also be transported within the valley and river alluvium parallel to the Merced River; this is often referred to as sub-alluvial flow.

Flow Path 7

Many of the production wells in the Merced River basin are located in valley or river alluvium. Each well creates a cone of depression, resulting in enhanced flow to the wells. In Yosemite Valley, the wells are placed near the Merced River and Yosemite Creek. Even though Yosemite Valley wells are relatively deep, there may be flow from recharging surface water to the wells. In El Portal, the alluvium is thinner, and it may be more likely that production wells are drawing recently recharged surface water to them.

Conclusion

The sum of these flow paths provides a more complete understanding of how water transports through the basin, and the spatial differences between Yosemite Valley and El Portal. There may be other complexities not mentioned, such as the role of upland meadows serving as collection basins for snowmelt and slowly recharging underlying fractures. These other complexities are discussed in greater detail throughout this dissertation. The major focus is to provide useful techniques for understanding the transport processes of water through a complex montane catchment.

References

Bales, R. C., N. P. Molotch, T. H. Painter, M. D. Dettinger, R. Rice, and J. Dozier, Mountain hydrology of the Western United States, *Water Resources Research*, 42, W08432, 2006.

Bateman, P. C., and C, Wahrhiftig, Geology of the Sierra Nevada, In Bailey, E, H., ed. Geology of Northern California, *California Division of Mines and Geology Bulletin*, 190: 107-172, 1966.

Borchers, James, W., Ground-water resources and water-supply alternatives in the Wawona area of Yosemite National Park, California, *U.S. Geological Survey Water-Resources Investigations Report 95-4229*, pp 77, 1996.

Burns, D. A., Stormflow-hydrograph separation based on isotopes: the thrill is gone—what's next? *Hydrological Processes*, 16, 1515-1517, 2002.

Cayan, D. R., S. Kammerdiener, M. D. Dettinger, J. M. Caprio, and D. H. Peterson, Changes in the onset of spring in the western United States, *Bulletin, American Meteorology Society*, 82, 399-415, 2001.

Clow, David W., M. Alisa Mast, and Donald H. Campbell, Controls on surface water chemistry in the upper Merced River Basin, Yosemite National Park, California, *Hydrological Processes*, 10, 727-746, 1996.

Constantz, J., Interaction between stream temperature, stream flow, and groundwater exchanges in alpine streams, *Water Resources Research*, 34, 1609-1616, 1998.

Dettinger, M. D., D. R. Cayan, M. K. Meyer, and A. E. Jeton, Simulated hydrologic response to climate variations and change in the Merced, Carson, and American River Basins, Sierra Nevada, California, *Climate Change*, 62, 283-317, 2004.

Earman, S. A. R. Campbell, B. D. Newman, and F. M. Phillips, Isotopic exchange between snow and atmospheric water vapor: Estimation of the snowmelt component of groundwater recharge in the southwestern United States, *Journal of Geophysical Research*, 111, D09302, doi: 10.1029/2005JD006470, 2006.

Flint, A. L., L. E. Flint, and M. D. Dettinger, Modeling soil moisture processes and recharge under a melting snowpack, *Vadose Zone Journal*, 7, 350-357, 2008.

Gutenberg, B., J. P. Buwalda, and P. Sharp, Seismic explorations on the floor of Yosemite Valley, California, *Bulletin of the Geological Society of America*, 67, 1051-1078, 1956.

Harp, E. L., M. E. Reid, J. W. Godt, J. V. DeGraff, and A. J. Gallegos, Ferguson rock slide buries California State Highway near Yosemite National Park, *Landslides*, 5, 331-337, 2008.

Kattelman, R., Hydrology and Water Resources, in Status of the Sierra Nevada, Vol. 2, *Wildland Resources Center Report No. 37, University of California, Davis*, 1528 pp., 1996.

Kimball, B. A., R. L. Runkel, and L. J. Gerner, Quantification of mine-drainage inflows to Little Cottonwood Creek, Utah, using a tracer-injection and synoptic-sampling study, *Environmental Geology*, 40, 1390-1404.

Knowles, N., M. D. Dettinger, and D. R. Cayan, Trends in snowfall vs. rainfall in the Western United States, *Journal of Climate*, 119, 4545-4559, 2006.

Liu, F., R. Parmenter, P.D. Brooks, M. H. Conklin, and R. C. Bales, Seasonal and interannual variation of streamflow pathways and biogeochemical implications in semi-arid, forested catchments in Valles Caldera, New Mexico, *Ecohydrology*, 1, 239-252, 2008.

Liu, F., M. W. Williams, and N. Caine, Source waters and flow paths in an alpine catchment, Colorado Front Range, United States, *Water Resources Research*, 40, W09401, 2004.

Maloszewski, P, W. Rauert, W. Stichler, and A. Herrmann, Application of Flow Models in an Alpine Catchment Area Using Tritium and Deuterium Data, *Journal of Hydrology*, 66, 319-330, 1983.

Manning, A. H., and D. K. Solomon, Using noble gases to investigate mountain-front recharge, *Journal of Hydrology*, 275, 194-207, 2003.

Manning A. H., and D. K. Solomon, An integrated environmental tracer approach to characterizing groundwater circulation in a mountain block, *Water Resources Research*, 41, W12412, 2005.

Manning, A. H., J. S. Caine, Groundwater noble gas, age, and temperature signatures in an alpine watershed: Valuable tools in conceptual model development, *Water Resources Research*, 43, WO4404, 2007.

Martinec, J, H. Oeschger, U. Schotterer, and U. Siegenthaler, Snowmelt and groundwater storage in an alpine basin, in hydrological aspects of alpine and high-mountain areas, *IAHS Publication No. 138, Proceedings of a Symposium at the First Scientific General Assembly of the IAHS*, July 19-30, 1982, England, 169-175, 1982.

Mattle, N., W. Kinzelbach, U. Beyerle, P. Huggenberger, H. H. Loosli, Exploring an aquifer system by integrating hydraulic, hydrogeologic and environmental tracer data in a three-dimensional hydrodynamic transport model, *Journal of Hydrology*, 242, 183-196, 2001.

Moline, G. R., M. R. Schreiber, J. M. Bahr, Representative ground water monitoring in fractured porous systems, *Journal of Environmental Engineering*, 124 (6), 530-538, 1998.

Nimz, G., Lithogenic and cosmogenic tracers in catchment hydrology, in *Isotope Tracers in Catchment Hydrology*, edited by K. Kendall and J. J.McDonnell, 1, Elsevier, New York, 291-318, 1998.

Peterson, D. H., R. Smith, S. Hager, J. Hicke, M. Dettinger, and K. Huber, River Chemistry as a monitor of Yosemite Park mountain hydroclimates, *EOS, Transactions, American Geophysical Union*, 86 (31), 285-288, 2005.

Pruess, K., C. Oldneburg, and G. Moridis, TOUGH2 user's guide, version 2.0. LBNL-43134. Lawrence Berkeley National Laboratory, Berkeley, CA, 1999.

Sorenson, S. K., and R. J. Hoffman, Water-quality assessment of the Merced River, California, in the 1977 water year, *U. S. Geological Survey, Water-Resources Investigations 80-75*, 30 pp., 1981.

Sorenson, S. K. Water-quality assessment of the Merced River, California, *U. S. Geological Survey, Open-File Report 82-450*, 46 pp., 1982.

Sueker, J. K., J. N. Ryan, C. Kendall, and R. D. Jarrett, Determination of Hydrologic Pathways during snowmelt for alpine/subalpine basins, Rocky Mountain National Park, Colorado, *Water Resources Research*, 36 (1), 63-75, 2000.

Tague, C., G. Grant, M. Farrell, J. Choate, and A. Jefferson, Deep groundwater mediates streamflow response to climate warming in the Oregon Cascade, Climate Change, 86, 189-210, 2008.

van Mantgem, P. J., and N. L. Stephenson, Apparent climatically induced increase of tree mortality rates in a temperate forest, *Ecology Letters*, 10, 909-916, 2007.

van Mantgem, P. J., N. L. Stephenson, J. C. Byrne, L. D. Daniels, J. F. Franklin, P. Z. Fule, M. E. Harmon, A. J. Larson, J. M. Smith, A. H. Taylor, T. T. Veblem, Widespread increase of tree mortality rates in the western United States, Science, 323, 521-524, 2009.

Viviroli, D., H. H. Durr, B. Messerli, M. Meybeck, Mountains of the world, water towers for humanity: typology, mapping, and global significance, *Water Resources Research*, 43, W07447, 2007.

Wanninkof, R., P. J. Mulholland, and J. W. Elwood, Gas exchange rates for a first-order stream determined with deliberate and natural tracers. *Water Resources Research*, 26, 1621-1630, 1990.

Wieczorek, G. F., and S. Jäger, Triggering mechanisms and depositional rates of postglacial slope-movement processes in Yosemite Valley, California, *Geomorphology*, 15, 17-31, 1996.

Wieczorek, G. F., J.B. Snyder, J. W. Borchers, and P. Reichenbach, Staircase Falls rockfall on December 26, 2003, and geologic hazards at Curry Village, Yosemite National Park, California, *USGS Open-file report 2007-1378*, 2007.

Wilson, J. L., and H. Guan, Mountain-block hydrology and mountain-front recharge, in *Groundwater Recharge in a Desert Environment: The Southwestern United States*, edited by F. M. Phillips, J. H. Hogan, and B. Scanlon, AGU, Washington, DC, 2004.

CHAPTER 2

GROUNDWATER AND SURFACE WATER FLOW TO THE MERCED RIVER, YOSEMITE VALLEY, CALIFORNIA: ^{36}Cl and Cl^- EVIDENCE.

Abstract

^{36}Cl and Cl^- were utilized as tools to characterize flow paths and fluxes in the Merced River basin, extending from Yosemite Valley to El Portal. Surface water, snow, groundwater, and springs were sampled seasonally from July 2004 to October 2007. Three endmembers were identified, and they include, 1) near-surface water with chloride concentrations < 0.25 mgL^{-1} and $^{36}Cl/Cl$ up to $10000x10^{-15}$, 2) low-Cl^- evapotranspired water with Cl^- concentrations between 0.35 and 1.0 mgL^{-1} and $^{36}Cl/Cl > 10000x10^{-15}$, and 3) high-$Cl^-$ groundwater with Cl^- greater than 12 mgL^{-1} and $^{36}Cl/Cl < 500x10^{-15}$. Chloride and $^{36}Cl/Cl$ measured in snow ranged between 0.07-0.14 mgL^{-1} and $220\text{-}306x10^{-15}$ respectively. Snow is not an obvious endmember, with significantly lower $^{36}Cl/Cl$ ratios than any of the identified endmembers. In particular, the $^{36}Cl/Cl$ ratio increases substantially in the Merced River during snowmelt. The source of the elevated ratios is attributed to bomb-pulse ^{36}Cl from above-ground thermonuclear weapons testing. The majority of the near-surface water is recently released during snowmelt, so bomb-

pulse ^{36}Cl must be efficiently retained in the system, and slowly released as meltwater interacts with the soil. The low-Cl^- evapotranspired water is observed in a 159 m deep Yosemite Valley drinking water well set in coarse-grained alluvium and in tributaries feeding the Merced River during baseflow. It is unclear whether this water exists only as evaporated surface water above Yosemite Valley, or if shallow groundwater of this composition discharges to the upper tributaries. The high-Cl^- groundwater mixes with the Merced River but not the tributaries, and it is attributed to saline springs discharging to the river. Although other major ions show similar temporal trends, the degree of seasonal fluctuations is not as great as Cl^-, indicating that there may be several sub-compartments representing either physical flow paths or processes controlling water chemistry. Therefore, the three major compartments are best elucidated by $^{36}Cl/Cl$ and Cl^-. A possible mechanism for the retention of bomb-pulse ^{36}Cl is incorporation into organic matter and formation of organochlorines, which later remineralize providing Cl^- to near-surface water. This mechanism suggests that turnover of organic matter may be on the order of 40-50 years, and care must be taken in any tracer study that depends on Cl^- being conservative.

Introduction

Water resources in the arid and semi-arid Western United States depend heavily on precipitation in mountains. This is especially true in the Sierra Nevada of California, where future demand for water is expected to increase and hydrologic fluxes are expected to change as climate warms (Bales, et al., 2006). Our current understanding of water fluxes and flow paths within the mountain

block is limited, and improved understanding is necessary to more accurately assess hydrology above the mountain front (Wilson and Guan, 2004). Future climate models predict increased warming and shifts in timing and type of precipitation (Dettinger et al., 2004; Knowles et al., 2006). It is anticipated that precipitation will shift from snow to rain, and that the snow line will shift upwards in the Sierra Nevada. It therefore has become crucial to establish a current baseline quantifying water fluxes and flow paths as precipitation transitions to surface water and groundwater. It is difficult to assess groundwater transport in mountain systems because of the complexity of the terrain—fractures, faults, and folds (Maloszewski and Zuber, 1982; Moline et al., 1998; Manning and Caine, 2007). With limited numbers of wells and access to groundwater, utilization of environmental tracers and isotopic techniques at groundwater discharge locations, such as springs, rivers, and river alluvium, becomes a key component in understanding groundwater flow processes occurring within the mountain block (Martinec et al., 1982; Maloszewski et al., 1983; Maurer, 1986; Constanz, 1998; Sueker et al., 2000; Mattle, 2001; Rademacher et al., 2001; Maurer, 2002).

The focus of this study was to determine surface and subsurface flow paths and fluxes, and to determine how groundwater interacts with surface water in the Sierra Nevada. Previous work determined that bomb-pulse ^{36}Cl ($^{36}Cl_{BP}$) occurs in Sierran streams, but not in precipitation (Nimz, unpublished data). This suggests that ^{36}Cl combined with water chemistry could elucidate sources of water in Sierran streams, and possibly groundwater flow paths. This study

examined water within the Merced River drainage basin from the eastern end of Yosemite Valley westward to the confluence of the South Fork of the Merced River, 40 km downstream (Figure 2.1). Water was sampled from the river and its tributaries, area wells and springs, and precipitation. The questions addressed in this paper are, 1) What are the major source waters in the Merced River? 2) What processes control source water chemistry? 3) How is mixing between source waters elucidated in surface water? and 4) Why are the surface water $^{36}Cl/Cl$ ratios elevated during snowmelt? It was hypothesized that 1) source waters and their fluxes will be distinguishable by analyzing spatial and temporal variations of ^{36}Cl and major chemistry in the Merced River and its tributaries, 2) ^{36}Cl and major ion chemistry can help determine processes controlling source water geochemistry, and 3) the behavior of ^{36}Cl documented in this study will demonstrate how ^{36}Cl can be applied to hydrologic research in other systems.

Origins of ^{36}Cl

Chlorine has three naturally occurring isotopes, with ^{36}Cl being the only radioactive isotope with a half-life of 301,000 years. ^{36}Cl in the watershed depends on several key factors, namely natural background meteoric ^{36}Cl, bomb-pulse ^{36}Cl ($^{36}Cl_{BP}$), and lithogenic ^{36}Cl. ^{36}Cl is produced in the atmosphere as a result of several nuclear reactions resulting from cosmic ray interactions, the most common being the interaction with ^{40}Ar (Bentley et al., 1986; Phillips, 2000; Moran and Rose, 2003). Several attempts have been made to determine natural meteoric ^{36}Cl deposition over the continental United States (Bentley et al., 1986; Hainsworth et al., 1994; Phillips, 2000; Davis et al., 2000; Moysey et al., 2003; Davis et al., 2003). These studies show

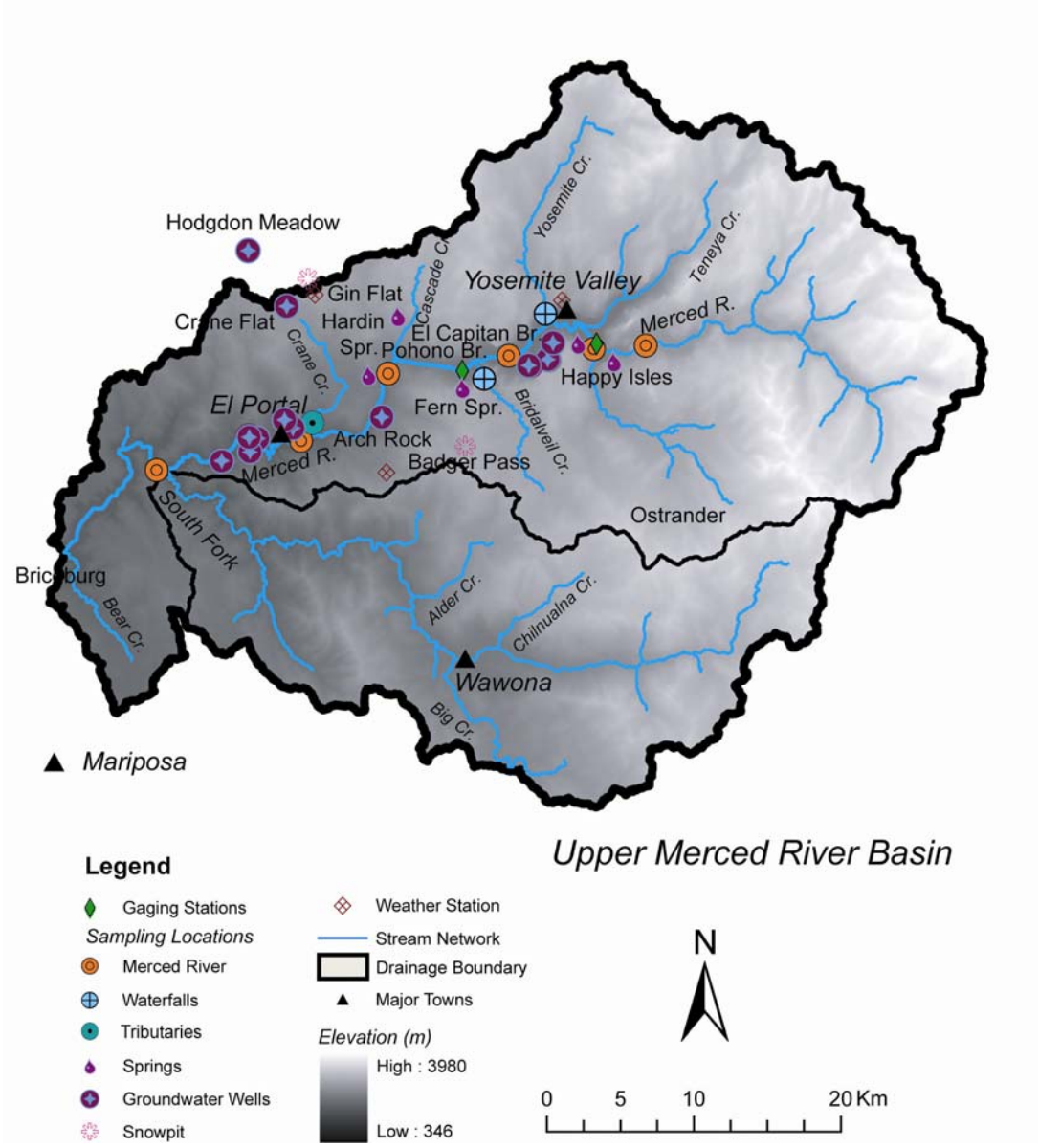

Figure 2.1: The Upper Merced River basin, with water sampling locations.

that natural background $^{36}Cl/Cl$ in the Sierra Nevada would be expected to range between $150x10^{-15}$ and $500x10^{-15}$.

Large quantities of ^{36}Cl were also produced from neutron activation of ^{35}Cl in seawater from above-ground thermonuclear weapons testing during the 1950s and 1960s. Global ^{36}Cl fallout was significantly elevated during this time, a record of which is preserved in the Greenland Dye-3 ice core (Bentley et al., 1982; Elmore et al., 1982; Synal et al., 1990). Deposition of $^{36}Cl_{BP}$ was highest at mid latitudes (Phillips, 2000). There is also subsurface production of ^{36}Cl as a result of activation of ^{35}Cl by neutrons derived from decay of U and Th. Chloride in secular equilibrium with common rock types will have relatively low $^{36}Cl/Cl$ ratios (Bentley et al., 1986)—ranging from $\sim 4x10^{-15}$ (in low U-Th rocks like common limestone) to $\sim 50x10^{-15}$ (in higher U-Th rocks like common granitic rocks). Meteoric waters interacting with rock will gradually assume the $^{36}Cl/Cl$ values of the rock (Davis et al., 1998; Lehmann et al., 2003; Metcalfe et al. 2007).

Several hydrologic studies have successfully used ^{36}Cl as a tracer (Bentley et al., 1982: Elmore et al., 1982: Phillips, 2000). Typically ^{36}Cl has been used to understand groundwater transport and evolution in deep groundwater basins with residence times on the order of thousands to millions of years (Phillips et al., 1986; Lehmann et al., 2003; Metcalfe et al. 2007). It has been suggested that groundwater residence times could be established from the ^{36}Cl released from above-ground thermonuclear weapons testing, similar to ^{3}H in groundwater (Bentley et al., 1982; Elmore et al., 1982; Synal et al., 1990; Cook et al., 1994; Balderer et al, 2004; Tosaki et al., 2007). However, this may not always be possible due to recycling, retardation,

or retention of $^{36}Cl_{BP}$ (Cornett et al., 1997; Milton et al., 1997; Blinov et al., 2000; Phillips, 2000; Moysey et al., 2003; Corcho Alvarado et al., 2005).

Field Area

The Merced River basin is on the western slopes of the Sierra Nevada with headwater elevations as high as 4000 m above sea level (m. a. s. l.) at Mt Lyell. The Merced River is a protected river under the National Wild and Scenic Act, and flows freely from the headwaters to downstream of the study area. The study site consists of a 40 km reach of the Merced River beginning at Happy Isles, which is the upper end of Yosemite Valley at 1,224 m. a. s. l. and ending at El Portal which has an elevation of 640 m. a. s. l. (Figure 2.1). The topography is stepped so that parts of the river in Yosemite Valley have a low gradient, whereas, other reaches have swift flows, and sometimes pools and riffles (Warhaftig, 1965). There are also several high Cl^- springs that discharge to the Merced River above Happy Isles (Clow et al., 1996).

Yosemite Creek and Bridalveil Creek are two major tributaries that enter the Merced River in Yosemite Valley. Yosemite Creek flows mostly southwest, and Bridalveil Creek flows mostly northwest. Both creeks form waterfalls as they enter Yosemite Valley, prior to entering the Merced River (Yosemite Falls drops 777 m). Crane Creek enters the Merced River near El Portal, but there are no extensive waterfalls associated with it. Twelve drinking water wells are located in the Merced basin. Three wells (Yosemite Valley Wells 1, 2, and 4) are located near Yosemite Creek, and range in depths from 159 to 244 m. Meadows at Crane Flat and Hodgdons Meadow both have wells that are set in bedrock at depths of 112 and 63 m respectively. Arch Rock Well is located near the west entrance of Yosemite National

Park, and is set in river alluvium at a depth of 28 m. There are six wells located near El Portal (El Portal Wells 2-7), which are set near the bedrock alluvium interface near the Merced River with depths ranging from 17 to 21 m deep.

The terrain is mountainous with steep slopes and cliffs, and a complex network of joints, fractures, and faults (Bateman, 1992; Clow et al., 1996). The Merced River basin is underlain by mostly Mesozoic granitic basement (Bateman, 1992), but there are outcrops of metavolcanic and metasedimentary rocks at the upper end of the basin. In contrast, most of the basement rock near El Portal consists of metasedimentary and metavolcanic rock.

Fractures in the Sierra range in size and frequency (Segall et al., 1990; Ericson et al., 2005; Wakabayashi & Sawyer, 2005). There are regional fractures consisting of spacing on the order of hundreds to thousands of meters. There are also numerous well-connected shallow fractures in granitic rocks resulting from exfoliation, with spacing on the order of 1-4 m and three primary orientations perpendicular to each other (Jahns, 1943; Warhaftig, 1965). Two orientations are perpendicular to the bedrock surface, while the third fracture forms as concentric shells parallel to the bedrock surface. In many locations the granitic rocks in the Sierra Nevada have gruss formed from weathering of the minerals surrounding the exfoliation fractures which may create impermeable zones (Warhaftig, 1965). Fractures from exfoliation are commonly less that a few tens of meters in depth, but fractures may be impermeable at shallower depths due to formation of gruss (Figure 2.2).

Basement rock is exposed in many locations in the basin, but surficial deposits of alluvium are scattered throughout the basin at largely unknown but probably

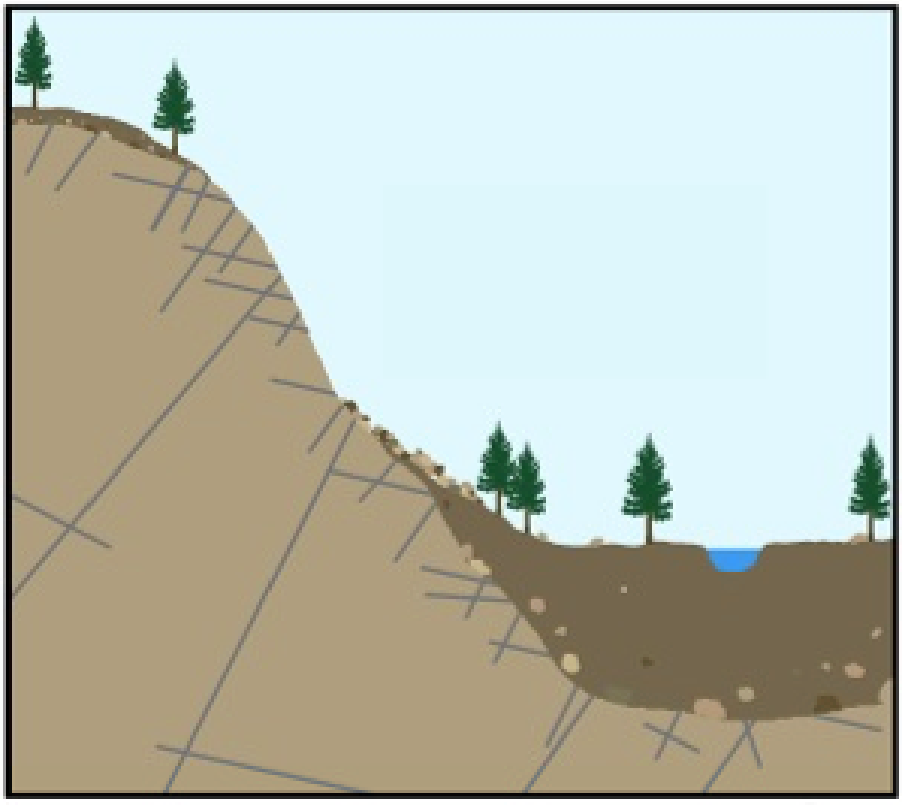

Figure 2.2: A conceptual model of the system, which consists of shallow soil cover over the mountain system, with some exposed bedrock on steep slopes. River valleys and/or meadows often have deeper alluvial fill. This model assumes at least two sets of fractures, with shallow numerous fractures near the surface, and deeper less-numerous regional fractures.

shallow depths. Above Happy Isles, only 20% of the basin is covered by surficial deposits (Clow et al., 1996). Alluvium is typically assumed to be thin (< 1m) above the river corridor. At Gin Flat, a small forested location at 2149 m above sea level, has loamy sand on average of 72 cm thick (Flint et al., 2008). Tuolumne meadows, which is a meadow in the Tuolumne drainage basin has approximately 1 m of alluvium (Alan Flint and Jessica Lundquist, October 2007 Yosemite Hydroclimate Meeting). Well logs for Hodgdons Meadow and Crane Flat Wells (both located in meadows) indicate that alluvial fill reaches depths of 27 to 18 m respectively. Well logs for Yosemite Valley wells verify that alluvium is greater than 309 m deep, and seismic surveys of Yosemite Valley indicate that alluvial fill reaches a maximum depth of 600 m near the center of the valley (Gutenberg et al., 1956). Most alluvium in Yosemite Valley consists of glacial till, with three layers of approximately equal thickness. The middle layer consists of mostly glacial flour, while the upper and lower alluvial fill consists of mostly coarse-grained sands and gravels, with cobbles and boulders dominating near bedrock (Gutenberg et al., 1956). Well logs for wells set in river alluvium downstream of Yosemite Valley show that alluvium is greater than 28 m thick near Arch Rock, and alluvium ranges between 15 and 25 m thick near El Portal. Virtually all alluvium within the river corridor is primarily coarse-grained sands, gravels, cobbles, and boulders. Estimates of soil thickness based on hydrochemical signatures suggest that there is an apparent low-mean soil thickness in the upper Merced River basin compared to the Stanislaus River in the Sierra Nevada (Peterson et al., 2005).

The climate in the Merced River basin is dry in the late spring through early fall, and wet from mid fall to mid spring. The dominant form of precipitation comes as snow above ~2000 m, and rain below ~1500 m. As air temperatures warm, snow melts resulting in a snowmelt pulse between early March and mid July, peaking in mid May.

Methods

Samples were collected seasonally in the Merced River basin from July 2004 to October 2007, consisting of 123 groundwater, surface water, spring, and snow samples. The Merced River was sampled at several locations including springs and tributaries from Happy Isles to El Portal (Figure 2.1). Groundwater samples at 12 wells were also collected in June 2005, May 2006, November 2006, and October 2007. Snow samples were collected at Gin Flat, Badger Pass, Tuolumne Meadows, and Tioga Pass which have elevations at 2148, 2194, 2627, and 3031 m respectively. Samples and parameters measured were temperature and conductivity, major ions (Cl^-, Na^+, Ca^{2+}), ^{18}O, D, ^{36}Cl, ^{222}Rn.

Temperature and conductivity were measured using a YSI 30 EC meter. Samples for major ion chemistry were collected in 125 HDPE plastic bottles, stored at 4 C°, and filtered before analyzing. The analyses were completed using a Dionex ICS 2000 in the Sierra Nevada Research Institute (SNRI) Laboratory at the University of California, Merced (UC Merced). ^{222}Rn was analyzed by mixing 20 ml of mineral oil scintillation cocktail with 1 L of water in a glass volumetric flask. Samples were shaken for 10 minutes, and mineral oil was extracted and placed in 20 ml scintillation vials. Samples were analyzed using a Beckman

Coulter LS 6500 Multipurpose Scintillation Counter within 3 days after field collection.

Analysis of $\delta^{18}O$ and δD for all samples collected during years 2004 and 2006 were completed at the University of California, Berkeley (UCB), using a VG PRISM isotope ratio mass spectrometer. Oxygen isotopes were prepared using automated water-CO_2 equilibration, and hydrogen isotopes were prepared using a Cr reduction furnace. Their compositions are expressed as δ (per mil) values and calculated by $(R_X/R_{VSMOW} - 1)\times 1000$, where R is isotopic ratio $^{18}O/^{16}O$ or D/H, *X* indicates sample and VSMOW stands for Vienna Standard Mean Ocean Water. The precision was ±0.05‰ for $\delta^{18}O$ and ±0.3‰ for δD based on replicate samples. Samples during the year 2007 were analyzed at UC Merced using a Los Gatos DLT-100 Liquid-Water Isotope Analyzer. The precision was ±0.3‰ for $\delta^{18}O$ and ±1‰ for δD.

One liter HDPE plastic bottles were used for collection of ^{36}Cl. Samples were stored at room temperature. One hundred ml of sample was prepared by precipitating silver chloride from solution by adding enough 10 mg/g solution of silver nitrate to precipitate all the chloride in the solution. The pH of the solution was lowered to below 4.0. Samples from the Merced River have low chloride concentrations (approximately 0.2-2 μg /g Cl-), requiring 10 μg/g carrier solution to be added to samples to bulk up the precipitated chloride mass to greater than 1 mg. Two ml of a saturated barium nitrate solution was added to the 100 ml of sample, covered gently with tin foil, and left for two to three days in a fume hood to scavenge sulfur from the sample with precipitation of barium sulfate and

barium carbonate. Samples were centrifuged, filtered, and washed five times by decanting supernatant, adding de-ionized water, vortexing, and centrifuging for 5 minutes at 3000 RCF. Samples were then dried at 70 C°, silver chloride precipitate was packed in sample targets containing silver bromide, and analyzed for ^{36}Cl using an Accelerator Mass Spectrometer at Lawrence Livermore National Laboratory. Every sample batch prepared had at least one process blank resulting in a total of 20 analyzed process blanks. 18 Ω-Ohm de-ionized water was used for the process blank, and each process blank was prepared and processed identically with other samples. All process blanks had non-detect Cl^-, and maximum $^{36}Cl/Cl$ ratios were $1.9x10^{-14}$.

Results

Forty three samples in the Merced River had mean Cl^-, ^{36}Cl, and $^{36}Cl/Cl$ of 1.9 ± 1.5 mgL^{-1}, $3.23x10^4$ atoms/g $\pm$ $1.56x10^4$, and $1813x10^{-15} \pm 1522x10^{-15}$ respectively (Table 2.1). Twenty four tributary samples located at Yosemite Creek, Bridalveil Creek, and Crane Creek had mean Cl^-, ^{36}Cl, and $^{36}Cl/Cl$ of 0.32 ± 0.2 mgL^{-1}, $4.3x10^4 \pm 2.50x10^4$ atoms g^{-1}, and $8951x10^{-15} \pm 2501x10^{-15}$ respectively. Yosemite Creek samples during snowmelt had the lowest Cl^- concentrations (between 0.09 and 0.39 mgL^{-1}) and the highest $^{36}Cl/Cl$ ratios in the basin (~$9000\text{-}13000x10^{-15}$). Fifty one groundwater and spring samples had Cl, ^{36}Cl, and $^{36}Cl/Cl$ averaging 3.2 ± 5.4 mgL^{-1}, $6.0x10^4 \pm 3.69x10^4$ atoms g^{-1}, and $3093x10^{-15} \pm 3035x10^{-15}$ respectively. The highest Cl^- values were 32.74 and 17.47 mgL^{-1} at Happy Isles Spring and El Portal Well #2, which results in $^{36}Cl/Cl$ ratios of $71x10^{-15}$ at Happy Isles Spring and $537x10^{-15}$ at El Portal Well #2.

Table 2.1: Water Chemistry for precipitation, surface water, and groundwater (including springs) in the Merced River basin. There are a total of 123 samples

Sample Type statisitics	**$d^{18}O$**	**dD**	**^{222}Rn** (cpm)	**Cond** (mS cm^{-1})	**Na^{+}** (mgL^{-1})	**Ca^{2+}** (mgL^{-1})	**Cl^{-}** (mgL^{-1})	**$^{36}Cl/Cl$** ($x10^{15}$)	**^{36}Cl** (atoms g^{-1})
Snow									
Total of five samples									
Mean	NM	NM	NM	NM	NM	NM	0.1	441.8	2.98E+02
Standard Deviation	NM	NM	NM	NM	NM	NM	0.03	71.6	7.22E+01
Minimum	NM	NM	NM	NM	NM	NM	0.07	367.7	2.20E+02
Maximum	NM	NM	NM	NM	NM	NM	0.14	510.6	4.01E+02
Merced River									
Total of forty three samples									
Mean	-13.3	-98.4	976.1	24.7	3.4	**3.2**	1.9	1855.0	3.28E+04
Standard Deviation	1.0	6.9	1186.5	11.9	5.9	3.3	1.5	1522.7	1.56E+04
Minimum	-14.8	-110.0	11.9	8.1	0.4	0.7	0.2	376.6	9.58E+03
Maximum	-9.5	-75.4	6161.1	48.8	27.2	16.1	5.5	6566.0	6.09E+04
Tributaries									
Total of twenty four samples									
Mean	-12.1	-87.6	587.6	21.9	4.2	2.5	0.3	8951.1	4.30E+04
Standard Deviation	1.5	8.4	1432.2	15.8	8.4	1.9	0.2	2501.5	2.50E+04
Minimum	-14.1	-100.2	0.0	6.9	0.5	0.7	0.1	3578.2	1.49E+04
Maximum	-7.8	-67.6	4560.2	52.7	40.1	6.0	1.0	13232.0	1.13E+05
Groundwater									
Total of fifty one samples									
Mean	-12.0	-87.1	23318.4	87.1	**5.3**	10.0	3.2	3092.7	6.02E+04
Standard Deviation	0.8	6.3	15639.2	54.5	2.6	7.6	5.4	3034.7	3.69E+04
Minimum	-13.1	-96.7	1550.5	20.3	1.8	2.2	0.3	70.6	1.53E+04
Maximum	-9.3	-65.0	91541.2	234.6	14.0	28.2	32.7	12640.0	1.74E+05
Happy Isles Bridge	**Mean**	**Std. Dev.**	**Minimum**	**Maximum**					
(m3s-1)	10.8	19.1	0.1	124.6					
Pohono Bridge Flow	**Mean**	**Std. Dev.**	**Minimum**	**Maximum**					
(m3s-1)	20.2	34.7	0.4	229.5					

NOTEChemical Data is for a total of 123 samples.
NM = not measured

Yosemite Valley Well #1 had the lowest Cl^- concentrations (~0.3 mgL^{-1}) and highest $^{36}Cl/Cl$ ratios (10000-12000x10^{-15}) in groundwater. Chloride in snow samples ranged between 0.07 and 0.14 mgL^{-1}, while ^{36}Cl concentrations ranged between 368 and 511 atoms g^{-1}. This produces $^{36}Cl/Cl$ ratios between ~200 and ~400x10^{-15}. Although ratios were measured for all five snow samples, chloride concentrations are unavailable for two of the samples. Cl^- values in snow were similar to the low concentration river and tributary values, the $^{36}Cl/Cl$ ratios in snow were much lower than most other values in the watershed.

Conductivity, and Na^+, and Ca^{2+} concentrations were also measured in surface water and groundwater (Table 2.1). The mean value for conductivity in the Merced River and tributaries are 24.7 ± 11.9 and 21.9 ± 15.8 μScm^{-1} respectively. The mean Na^+ values for the Merced River and tributaries are 3.4 ± 5.9 and 4.2 ± 8.4 mgL^{-1} respectively, and the mean Ca^{2+} values for the Merced River and tributaries are 3.2 ± 3.3 and 2.5 ± 1.9 mgL^{-1}. These tracers are slightly elevated in groundwater and springs in comparison to surface water, with mean conductivity of 87.1 ± 54.5 μScm^{-1}, mean Na^+ of 5.3 ± 2.6 mgL^{-1}, and mean Ca^{2+} of 10.0 ± 7.6 mgL^{-1}.

Mean ^{222}Rn activity in the Merced River and tributaries were 976.1 ± 1186.5 and 587.6 ± 1432.2 counts per minute (cpm) respectively (Table 2.1). Mean ^{222}Rn activity in groundwater was 23318 ± 15639.2 cpm. The large standard deviations in the Merced River reflect the seasonal variations of ^{222}Rn activity; whereas, the variation of ^{222}Rn activity in groundwater primarily represents spatial differences in the subsurface. The mean $\delta^{18}O$ and δD values

were -13.3 ± 1.0 and -98.4 ± 6.9in the Merced River, -12.1 ± 1.5 and -87.6 ± 8.4 in tributaries, and -12.0 ± 0.8 and -87.1 ± 6.3 in groundwater. During the course of this study, the Merced River flow rates ranged between 0.1 to 124 m^3s^{-1} at Happy Isles, and 0.4 to 230 m^3s^{-1} at Pohono Bridge. Average flows at Happy Isles and Pohono Bridge were 10.8 m^3s^{-1} and 20 m^3s^{-1} respectively.

Seasonal/Temporal Variations

Seasonal variations of Cl^-, ^{36}Cl, and $^{36}Cl/Cl$ correlate closely with flow rates in the Merced River (Figure 2.3). From baseflow to snowmelt, Cl^- concentrations decrease from ~5 to ~0.25 mgL^{-1}; whereas, ^{36}Cl concentrations decrease around $5x10^4$ to $1x10^4$ atoms/g as a result of the inflow of meltwater with low concentrations. Concentrations are elevated during baseflow (September-November), which is attributed to mixing of groundwater that has undergone more chemical interactions with rock. From baseflow to snowmelt, conductivity decreases from ~45 to 10 $mScm^{-1}$, Ca^{2+} decreases from ~4.5 to 1 mgL^{-1}, and Na^+ also decreases from ~4.5 to 0.7 mgL^{-1}. All of these parameters have a dilution factor of 4.5 to 6 during snowmelt except Cl^-, which has a dilution factor of ~15. Previous studies also show similar seasonal fluctuations of major ions in the Merced River basin, and attribute the increase in concentrations during baseflow to mixing with subsurface water (Clow et al., 1996; Peterson et al., 2005).

The increased contribution of groundwater to the Merced River is also correlated with temporal variations of ^{222}Rn (Figure 2.3). During baseflow ^{222}Rn activity is above 2000 cpm; whereas, ^{222}Rn activity is less than 200 cpm during

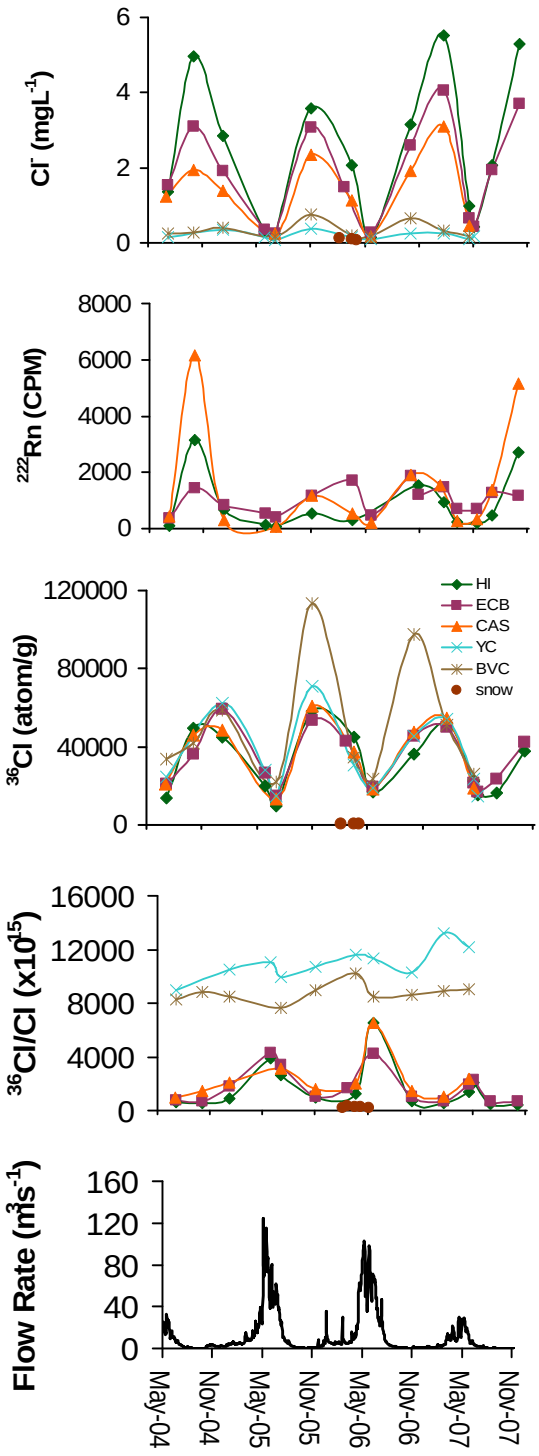

Figure 2.3: Temporal variations in (a) Cl^- (mgL^{-1}), (b) ^{222}Rn [counts per minute (cpm)], (c) ^{36}Cl (atoms/g), (d) $^{36}Cl/Cl$ ($x10^{-15}$), and (e) flow in the Merced River at Pohono Bridge (m^3s^{-1}). Water chemistry samples are measured in the Merced River at Happy Isles (HI), El Capitan Bridge (ECB), and Cascade Picnic Area (CAS), Yosemite Creek, Bridalveil Creek, and snow. Flow data are provided from the USGS.

snowmelt. Snow has non-detect values of ^{222}Rn, while groundwater incorporates ^{222}Rn due to subsurface production within the U-Th decay series (Cecil & Green, 2000).

Stable isotope values in the Merced River during baseflow are above -13.5 ‰ and -97.0 ‰ for $\delta^{18}O$ and δD respectively, and snowmelt $\delta^{18}O$ and δD values are below -14.2 ‰ and -103.0 ‰ respectively (Figure 2.3). The depleted stable isotope values in the Merced River during snowmelt (relative to baseflow values) can be attributed to increased orographic fractionation, precipitation at cooler temperatures, and/or a lower level of evaporation.

If chemical variations in the Merced River reflected mixing with snow during snowmelt, the $^{36}Cl/Cl$ ratios should decrease due to the low snow $^{36}Cl/Cl$ ratios. Instead, $^{36}Cl/Cl$ ratios significantly increase during snowmelt, suggesting increased incorporation of $^{36}Cl_{BP}$. However, given the shear volume of water that flushes through the river, the decreased (snow-like) major ion concentrations, and the lack of an increase in ^{222}Rn during snowmelt, it appears unlikely that the elevated $^{36}Cl/Cl$ ratios are the result of the incorporation of large quantities of ~50 year old water.

Discussion

Source Water Identification

Characterization of water sources to the Merced River, processes controlling source water chemistry, and water mixing in the Merced River basin can be addressed by examining the variations of Cl^- and $^{36}Cl/Cl$ for all surface

water and groundwater samples (Figure 2.4). All water samples, with the exception of precipitation, plot in a triangular shaped field indicating that three major chemical components exist in the watershed; samples with intermediate compositions suggest water mixing. Precipitation, although certainly one of the major water components in the basin, does not represent one of these chemical components. In this paper, the components which are characterized by the Cl^- and $^{36}Cl/Cl$ values of the corners of the triangle, will be referred to as endmembers 1-3 (EM 1-3), and they are characterized as follows:

EM 1. High $^{36}Cl/Cl$ ratios (up to 10,000 $x10^{-15}$) and low Cl- concentrations (less than 0.25 mgL^{-1}); most characteristic of Yosemite Creek during snowmelt.

EM 2. High $^{36}Cl/Cl$ ratios (>10,000$x10^{-15}$) and relatively low Cl- concentrations (0.35-1 mg/L); characteristic of Yosemite Valley Well #1 and Yosemite Creek samples collected during baseflow.

EM 3. Low $^{36}Cl/Cl$ ratios (<500 $x10^{-15}$) and high Cl- concentrations (>12 mgL^{-1}); most characteristic at El Portal Well 2 and Happy Isles Spring.

Processes Controlling Source Water Geochemistry

The arrows shown in Figure 2.4 illustrate processes acting on incoming water, and how the initial Cl^- and $^{36}Cl/Cl$ values of incoming water to the system can obtain the values of the three endmembers (Davis et al., 1998). The primary processes controlling chloride in water in the Merced River basin include 1)

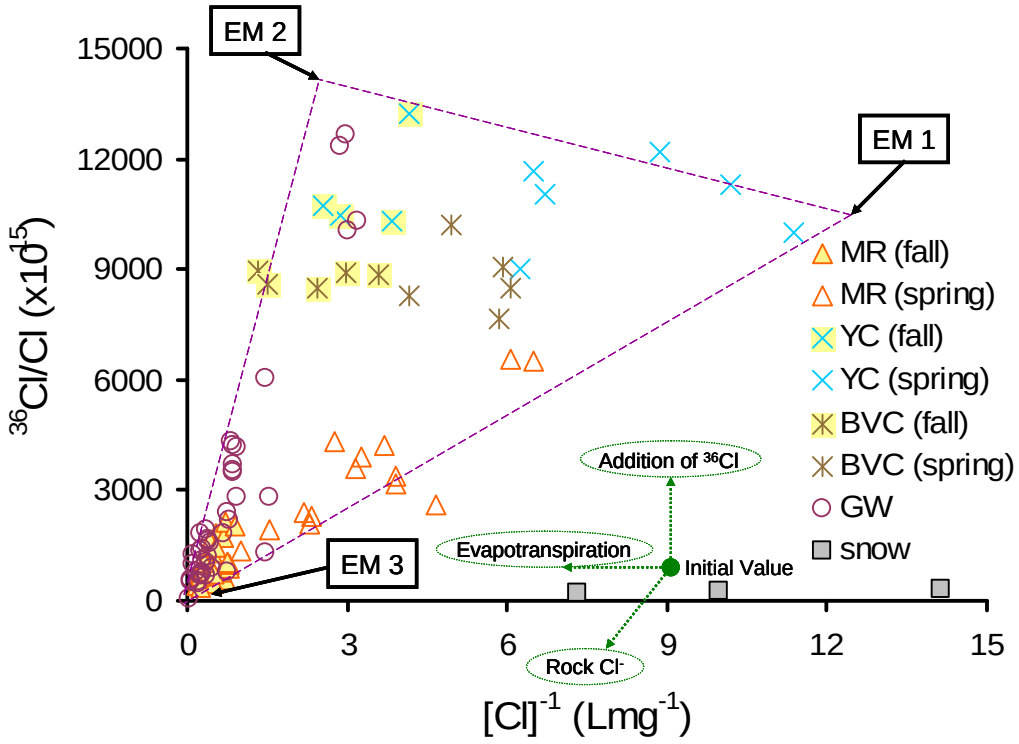

Figure 2.4: Reciprocal Cl^- concentrations (mgL^{-1}) vs. $^{36}Cl/Cl$ ($x10^{15}$) are plotted for the Merced River (MR), Yosemite Creek (YC), Bridalveil Creek (BVC), Crane Creek (CC), groundwater (GW), and snow. Arrows showing the direction water chemistry would move under various processes occurring within the basin, starting with the initial value (precipitation).

addition of ^{36}Cl, 2) addition of rock chloride, and 3) evapotranspiration. The major source of water to the system is snow, but none of the endmembers have similar chemical compositions as near snow. In order for melting snow to obtain similar compositions as EM 1, a significant amount of ^{36}Cl must be incorporated to snowmelt. The extreme elevation of the $^{36}Cl/Cl$ ratio of EM 1, the quantity of water containing this signature, and its appearance only during snowmelt, suggests incorporation of $^{36}Cl_{BP}$ into recent meltwater. The volume of water represented by EM 1 makes it implausible that it is water recharged during the 1950s or 1960s. This suggests that Cl^- has not behaved conservatively in the basin, resulting in rapid retention of $^{36}Cl_{BP}$ during the short period of nuclear fallout deposition (the majority of ^{36}Cl fallout was deposited in about 7 years) and slow release of $^{36}Cl_{BP}$ since that time. Other studies have observed retention of $^{36}Cl_{BP}$, but not to the degree of retention that must be necessary to observe EM 1 during snowmelt (Cornett et al., 1997; Milton et al., 1997; Blinov et al., 2000; Lee et al., 2001; Moysey et al., 2003; Corcho Alvarado et al., 2005).

EM 2 has $^{36}Cl/Cl$ ratios similar to EM 1, but Cl^- concentrations are ~4 times higher, suggesting that EM 2 has resulted from evapotranspiration of water containing the EM 1 component. Baseflow tributary samples and groundwater from Valley Well #1 are most characteristic of EM 2, and it is unclear whether the evapotranspired endmember detected in tributary samples is from evaporation acting on tributaries, which later recharge Yosemite Valley alluvium, or from mixing between EM 1-tributary water and an evapotranspired EM 2-subsurface-water.

Stable isotopes indicate that some of the baseflow tributary samples have undergone evaporation (Figure 2.5), but $^{36}Cl/Cl$ and Cl^- values suggest that evapotranspiration has occurred in on other samples which do not show evaporation δ D and $\delta^{18}O$ signals (Figure 2.4). One limitation with stable isotopes is the inability to identify transpiration by plotting the local meteoric water line (LMWL). If EM 2 is a subsurface endmember that mixes with tributaries above the water falls flowing to Yosemite Valley, then the increased Cl^- concentration either comes from transpiration of infiltrating groundwater, or it comes from infiltrating water incorporating salts remaining from previously evaporated infiltrating water.

The Cl^- and $^{36}Cl/Cl$ values of EM 3 probably reflect addition of Cl^- derived from rock, which contains relatively little ^{36}Cl ($^{36}Cl/Cl < 50x10^{-15}$). Addition of rock Cl^- would lower the $^{36}Cl/Cl$ ratio of EM 1 or EM 2 waters without significantly changing their ^{36}Cl concentrations. Most EM 3 samples have ^{36}Cl values similar to other groundwater and surface water samples (e.g., $3.92x10^4$ atoms/g at Happy Isles Spring and $1.59x10^5$ atoms/g at El Portal #2), but much higher Cl^- concentrations (32.74 mgL^{-1} at Happy Isles Spring and 17.47 mgL^{-1} at El Portal Well #2). Because the $^{36}Cl/Cl$ ratio of the EM 3 component is similar to background, non-bomb-pulse meteoric values, it is possible that the EM 3 waters have undergone high amounts of evapotranspiration, which would increase Cl^- concentrations in the remaining water but not affect $^{36}Cl/Cl$ ratios. High degrees of evaporation alone, however, are not indicated by their $\delta^{18}O$ and δD values.

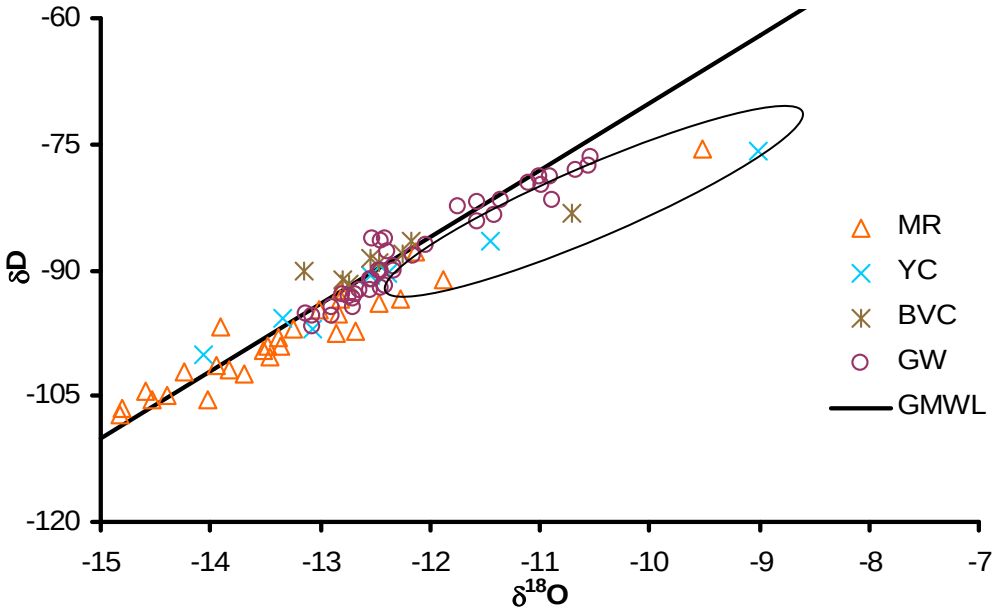

Figure 2.5: Local meteoric water line for stable isotopes in the Merced River basin for Yosemite Creek (YC), Bridalveil Creek (BVC), the Merced River (MR), groundwater (GW), and springs. All samples are compared with the global meteoric water line (GMWL). Major deviations are circled, which includes three tributary samples during late autumn, and one Merced River sample collected after significant rain events in the spring of 2006.

Mixing Between Source Waters

Chloride and $^{36}Cl/Cl$ ratios in the Merced River seem to be mostly controlled by EM 1 and EM 3 endmembers (Figure 2.4). During snowmelt, the Merced River is more characteristic of EM 1, and it is more characteristic of EM 3 during baseflow. The Merced River water trends toward the EM 3 endmember during baseflow probably because of a greater influence from high Cl^- EM 3 springs discharging above Happy Isles (Clow et al., 1996). Increased groundwater discharge percentages are indicated by elevated ^{222}Rn activity during the same time period. The amount of rock Cl^- added to the river samples is dependant upon the degree of mixing between these two endmembers, and Cl^- concentrations are sufficiently elevated so that the EM 3 component dominates the system during low flow periods, even if the total groundwater contribution is a small fraction of total flow.

Many groundwater samples and some baseflow Merced River samples also appear to be mixtures between EM 2 and EM 3 endmembers (Figure 2.4). Four Groundwater samples collected at Yosemite Valley Well #1 (shallowest Yosemite Valley well) between June 21, 2005 and October 24, 2007 also have similar Cl^- and $^{36}Cl/Cl$ as baseflow Yosemite Creek water. Valley Well #1 is set in coarse-grained alluvium ~150 m deep and could be receiving significant recharge from tributaries entering the Valley or from fractures discharging directly to the valley alluvium. The mixed EM 2 and EM 3 samples measured in the Merced River during baseflow may represent either direct EM 2 tributary

inflow or EM 2 groundwater discharge to the river. The significant increase in ^{222}Rn activity in the Merced River from snowmelt to baseflow suggests that the mixed EM 2 and EM 3 samples in the Merced River occur from inflow of groundwater. Furthermore, all tributaries except Bridalveil Creek completely dry during baseflow.

It is important to note that while Cl^- and ^{36}Cl elucidate three major endmembers, which probably reflect three separate physical compartments, other chemical species indicate a more complex system. For example, plotting Ca/Cl and Na/Cl ratios with time indicates that during snowmelt either the amount of Ca^{2+} and Na^+ increases significantly in comparison to Cl^-, or that there is a larger availability of Cl^- in comparison to Ca^{2+} and Na^+ during baseflow (Figure 2.6). There may be a higher rate of release of Na^+ and Ca^{2+} from minerals during snowmelt, or there may be more sorption of Na^+ and Ca^{2+} to mineral surfaces during baseflow. The later could be due to longer flow paths and contact time of baseflow water. The Na^+ and Ca^{2+} data suggest that there may be several sub-compartments within the system, each with different processes, or there may be a variety of chemical processes occurring within each of the three major Cl^- and ^{36}Cl compartments.

Endmember Mixing Analysis

In order to determine the fractions of each endmember mixing in the Merced River during the course of the year, an endmember mixing analysis (EMMA) was conducted using Cl^- and ^{36}Cl concentrations (Christopherson et al., 1990; Hooper et al., 1990; Genereux, 1998; Rice and Hornberger, 1998; Liu et al.,

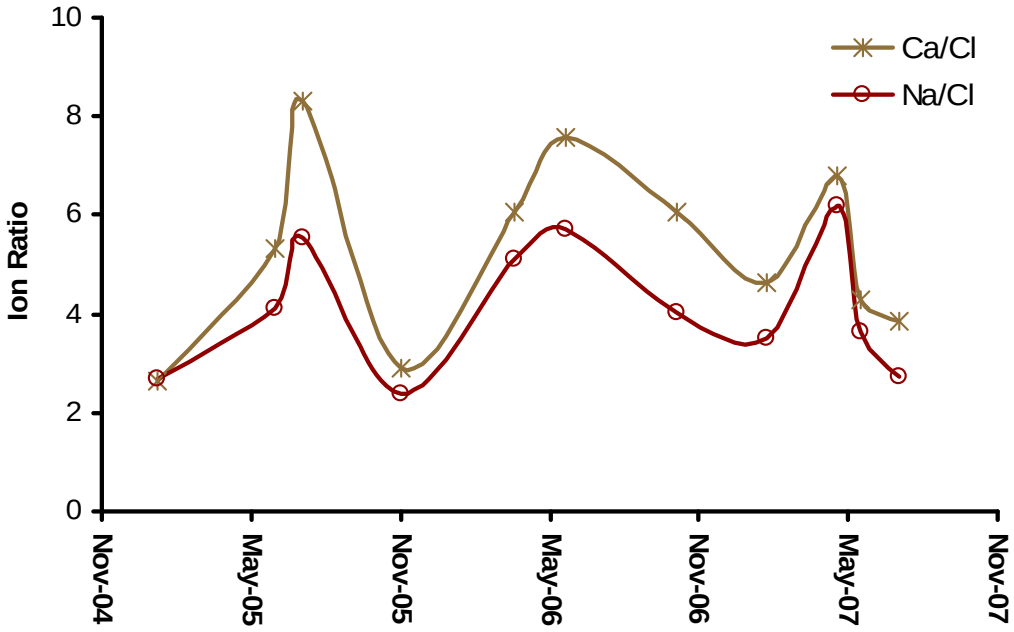

Figure 2.6: Ca/Cl and Na/Cl ratios in Yosemite Creek drainage from July 2004 to October 2007.

2004; Liu et al., 2008). Endmember compositions were assumed to be those at the corners of the triangle in Figure 2.4. Because Cl^- and ^{36}Cl were the only tracers used, this model is simplified into the major compartment mixing, and ignores sub-compartments. Fractions of total flow are shown for Yosemite and Bridalveil Creeks and at Happy Isles, El Capitan Bridge, and Cascade Picnic Area for the Merced River locations (Figure 2.7). As would be expected, all Merced River locations show mixing between the three endmembers with the highest fractions of near-surface water (EM 1) occurring throughout the basin during snowmelt, and the highest fractions of groundwater (EM 2 and EM 3) occurring during baseflow. EM 2 water mixes in higher fractions downstream of Happy Isles during baseflow. The fraction of EM 2 water is also always higher than EM 3. The fractions at Yosemite Creek and Bridalveil Creeks only show mixing between EM 1 water and EM 2 water.

The endmember mixing analysis can be tested for validation by multiplying the estimated fractions of each endmember by the conductivity of the endmember and summing the products. These calculated conductivities are then compared with observed conductivity values for each location (Figure 2.8). The R^2 values and the slope of the lines (which should be 1:1) indicate that the model has some error, but is generally valid in the Merced River at Happy Isles, El Capitan Bridge, and Cascade Picnic Area.

Hydrographs for the three endmembers are separated at Happy Isles by combining the EMMA results with gauged flows. The total discharge of all endmembers to the Merced River increases during snowmelt and decreases during

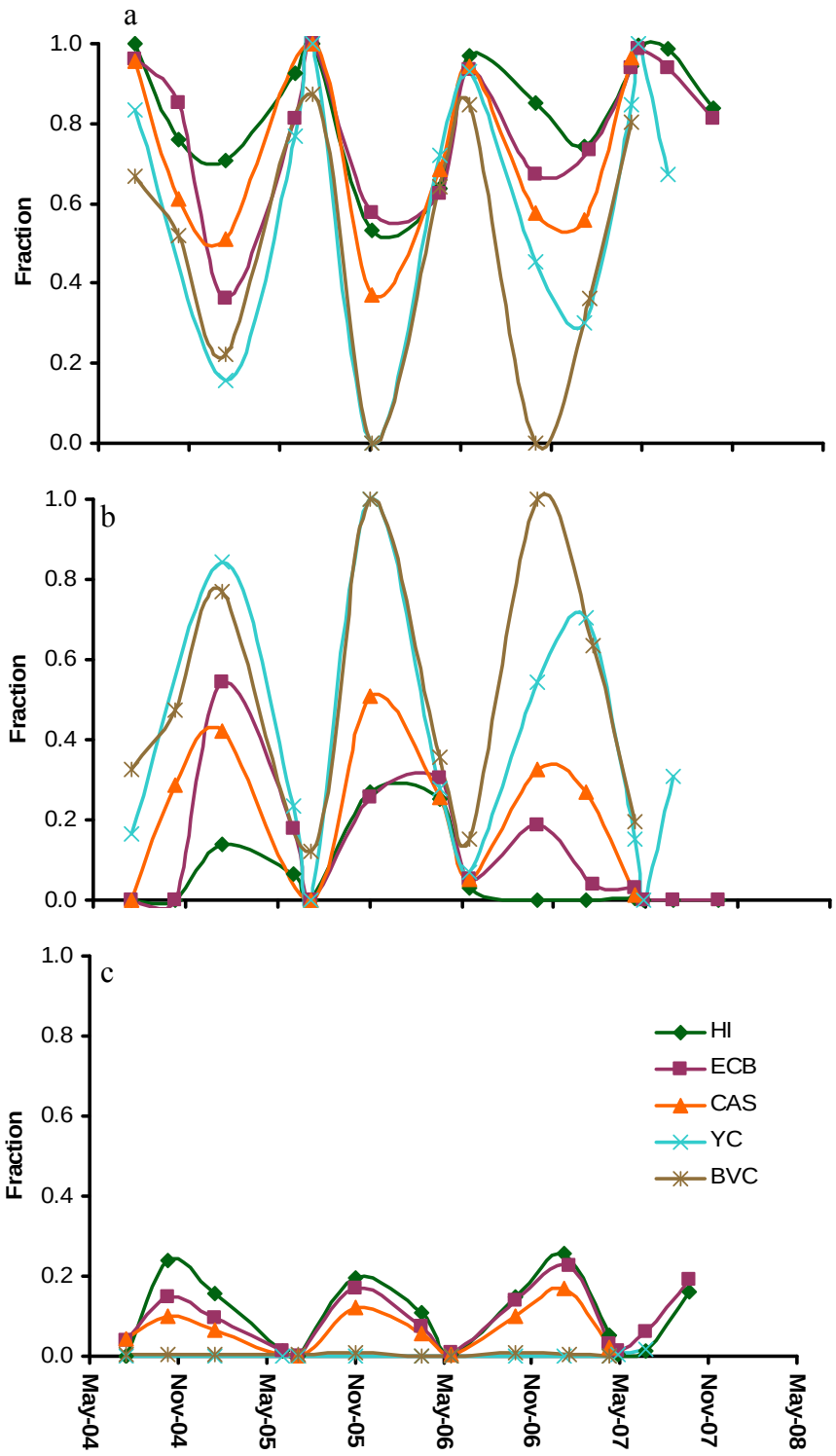

Figure 2.7: Fraction of total flow in the Merced River basin at Happy Isles (HIB), El Capitan Bridge (ECB), Cascade Picnic Area (CAS), Yosemite Creek (YC), and Bridalveil Creek (BVC) for a) near-surface water, b) low-Cl^- groundwater, and c) high-Cl^- groundwater. Fractions are determined using an endmember mixing analysis (EMMA). All symbols represent calculated values, and the lines connect the symbols.

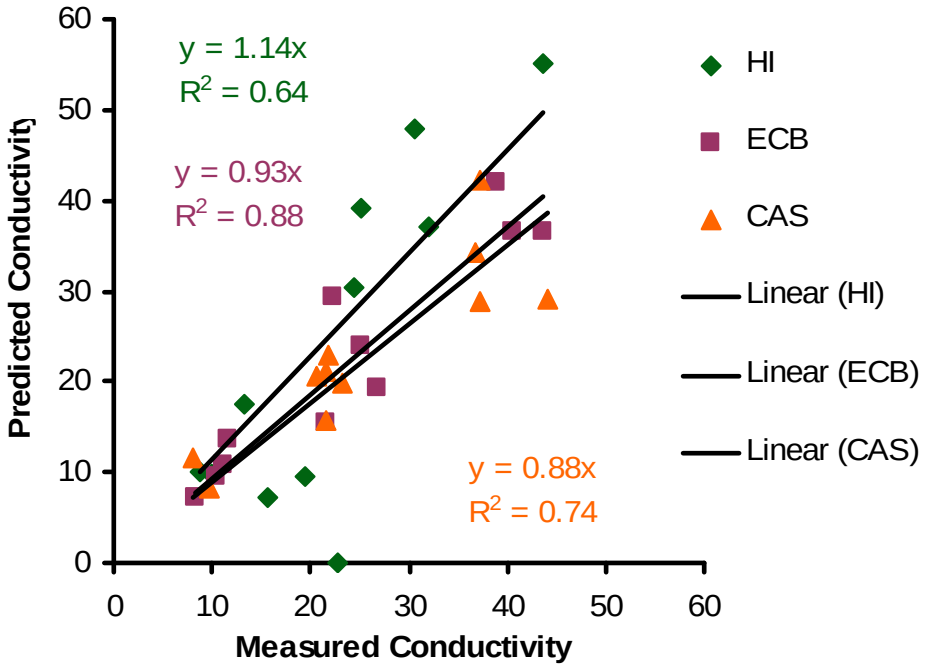

Figure 2.8: Measured electrical conductivity vs. predicted electrical conductivity based on EMMA results from the Merced River basin at Happy Isles (HI), El Capitan Bridge (ECB), and Cascade Picnic Area (CAS). The equation to the lines and R^2 values are given for each location at HI (green text), ECB (orange text), and CAS Area (purple text).

baseflow, but the fractions of the total flows, and the relative increases in flow, vary during the year (Figure 2.9). The flow of EM 3 water remains the most steady, with flow rates always less than 1 m^3s^{-1}; whereas, EM 2 water fluctuates between 0 to ~3 m^3s^{-1}. EM 2 stops discharging to the Merced River during baseflow for the two dry years (2004 and 2007). EM 1 also fluctuates from 0.08 m^3s^{-1} during baseflow to 40 m^3s^{-1} during snowmelt.

Locations of the three water compartments

Because of the high flow rates, high fractions of flow in the Merced River, and the similarity of major ion chemistry to snow, EM 1 water is most likely recent meltwater with short residence times. The elevated $^{36}Cl/Cl$ indicates that EM 1 water interacts with soil, and the quick response to snowmelt indicates that this interaction occurs near surface without deep infiltration.

EM 2 is located in both tributaries during baseflow and in the unconfined alluvium in Yosemite Valley. During snowmelt, the EM 2 water flow rates to the Merced River increase, but tributary water discharging to the Merced River is similar characteristic of EM 1 water. This suggests that that EM 2 water mixing with the Merced River is subsurface flow. This endmember may also occur in the shallow fractures in the subbasins above Yosemite Valley. EM 2 water has similar chloride concentrations and $^{36}Cl/Cl$ ratios as shallow fractured groundwater in Wawona (Borchers, 1996; Nimz, 1998), and recharge to fractures in these subbasins has been observed during snowmelt (Flint et al., 2008).

The high Cl^- concentrations and low $^{36}Cl/Cl$ ratios of the EM 3 water could be derived from prolonged interaction with local granitic rocks.

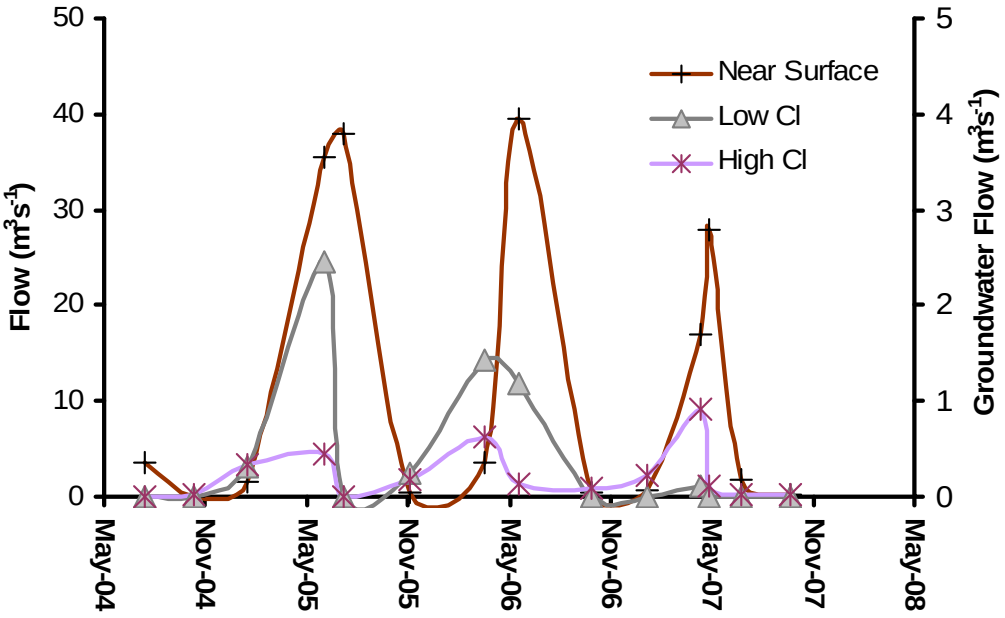

Figure 2.9: Fraction of flow converted to flow rates at Happy Isles. Other locations are not gauged. The green diamonds are near-surface water flows with values on the left Y-axis, while the purple squares and orange triangles are low-Cl^- and high-Cl^- groundwater respectively. Groundwater flow rates appear on the right Y-axis.

Groundwater in fractured granitic rock between 100 and 400 m deep in Wawona had higher Cl^- concentrations and lower $^{36}Cl/Cl$ ratios and could actually be the EM 3 component. If this is the case, then Happy Isles Spring and El Portal Well 2 would actually be a mixture of EM 3 and EM 2 water.

Elevated $^{36}Cl/Cl$

The mechanism by which snowmelt incorporates $^{36}Cl_{BP}$ is not well understood, but several studies have identified instances in which $^{36}Cl_{BP}$ appears to be retained or recycled in the hydrologic system (Cornett et al., 1997; Milton et al., 1997; Blinov et al., 2000; Phillips, 2000; Lee et al., 2001; Moysey et al., 2003; Corcho Alvarado et al., 2005). The apparent mechanism in these studies is chloride uptake into organic matter, that perhaps results in the formation of organochlorines, with later $^{36}Cl_{BP}$ release due to mineralization of organochlorines (Cl_{org}) to Cl^- (Myneni, 2002; Öberg, 2002; Öberg, 2003; Reina et al., 2004; Öberg and Sanden, 2005; Bastviken et al., 2007; Svensson et al., 2007). These processes occur at multiple timescales, and seem to be controlled mostly by vegetation, fungi, bacteria other biological reservoirs which retains organochlorines in soil organic matter.

Several studies in recent years focused on the occurrence of Cl_{org} in soils. These studies indicate that, 1) Cl^- input to soils can be converted to Cl_{org} within a matter weeks to months, 2) that >50% of chlorine in the top 40 cm of soil can exist as Cl_{org} and, 3) Cl_{org} may be stable in soils for at least decades. These studies will be discussed in the following paragraphs.

^{36}Cl and ^{3}H-spiked water was injected at the shallow groundwater surface (5 cm) and at 30 cm below ground surface in a till soil in Gardsjon, Sweden (Nyberg et

al., 1999). 78% of the injected ^{3}H was recovered, but only 47% of the ^{36}Cl was recovered six months after injection. More than 85% of both ^{3}H and ^{36}Cl was recovered from the deeper injection. Export of Cl^- from the Hubbard Brook Experimental Watershed, New Hampshire, remained relatively constant from 1964 to 2000, even though annual deposition of Cl^- was higher in the 1960s and 1970s than during the 1980s and 1990s (Lovett et al., 2005). These records support that retention of Cl^- was occurring in the catchment while inputs were elevated, and Cl^- was being released from the catchment when precipitation inputs were lower. ^{36}Cl-spiked water was also used in laboratory soil lysimeters using soil from the Stubbetorp catchment, Sweden (Bastviken et al., 2007). Roughly 24% of the incoming ^{36}Cl in pore spaces was retained but later released within the first month of the study as microbial populations decreased.

Fifteen centimeter deep topsoil samples from the Stubbetorp catchment, Sweden were collected and used in laboratory lysimeter studies, where artificial precipitation (with similar major ion concentrations as meteoric water) was applied to the samples for four months (Öberg and Sanden, 2005). Cl_{org} was 3-10 times higher than Cl^- in the samples, and over the duration of four months ~50% of the chlorine leaving the soil lysimeters was Cl_{org}. Bastviken et al., (2007) determined that the Cl_{org} deposition rate to soil in was 0.1 g $m^{-2}yr^{-1}$ in the same catchment. This deposition rate correlates to roughly 25% of incoming Cl^- being retained as Cl_{org}. Other estimates combining inputs, outputs of Cl^- and Cl_{org} from the Stubbetorp, and catchments, resulted in a Cl_{org} deposition rate of 0.2 g $m^{-1}yr^{-1}$ (Öberg et al., 2005). Lovett et al. (2005) also estimated that ~35% of the annual deposition of Cl^- was retained in the Hubbard Brook catchment during the 1960s and 1970s.

The retention time of Cl_{org} is the most uncertain parameter. Most of the studies previously discussed were conducted over short time periods (i.e. <1 yr), and there is no conclusive way of estimating retention timescales for Cl_{org} retained in these soils. Long-term monitoring and abrupt change in atmospheric Cl^- deposition (around 1980) at the Hubbard Brook catchment provides the most information regarding retention of Cl_{org}. One interpretation for the constant Cl^- export rate from the watershed includes slow release of retained Cl_{org} since 1980, which correlates to residence times ~20 years or greater.

These studies show that up to 50% of incoming Cl^- may be retained in a catchment, mostly by conversion of Cl^- to Cl_{org}, and the release of the Cl^- may occur much later. Although the actual timescales and specific mechanisms of retention are still not well understood (Myneni 2002; Öberg, 2002; Öberg, 2003**;** Öberg and Sanden, 2005; Bastviken et al., 2007), the results from the studies mentioned above provide a mechanism for retaining and later releasing $^{36}Cl_{BP}$ so that current runoff would be elevated in $^{36}Cl/Cl$. Retention of $^{36}Cl_{BP}$ apparently occurred on a larger scale than has been previously identified. Dye-3 ice cores indicate that $^{36}Cl_{BP}$ could be detected as late as 1985, but 98% of it had been deposited by 1970 (Elmore et al., 1982; Synal et al., 1990). This indicates that the mechanisms for retaining $^{36}Cl_{BP}$ in the Merced basin are highly efficient. Release must be slow because bomb-pulse $^{36}Cl/Cl$ ratios of similar magnitude to 2004-2007 samples were observed in the Merced River basin in 1992 and 1995 (Table 2.2). Five water samples collected at Happy Isles and Yosemite Creek had $^{36}Cl/Cl$ ratios almost identical to those in the samples we collected between 2004 and 2007. Based on knowledge of the ^{36}Cl bomb pulse and the observation made in the

Table 2.2: Cl^- and $^{36}Cl/Cl$ collected at Happy Isles and Yosemite Creek between 1992 and 1995 compared with values in 2005.

Location/date	Cl^- (mgL^{-1})	$^{36}Cl/Cl$ ($x10^{15}$)
Yosemite Cr.		
Jun-92	0.15	12000
Jun-95	0.15	94000
Jun-05	0.15	11059
Happy Isles		
Jun-92	0.15	8600
Jun-05	0.32	3889

Merced River basin, retention time of $^{36}Cl_{BP}$ is on the order of decades (40-50 years), which is similar to turnover rates of organic matter in the Stubbetorp catchment (Öberg and Sanden, 2005) and the Sagehen Basin (Blumhagen and Clark, 2008).

Conclusions

The identification of near-surface water, low-Cl^- evapotranspired water, and high-Cl^- groundwater in the Merced River basin helps provide information about surface water and groundwater flow paths and fluxes in a montane granitic catchment. This information can be used to assess water resources for communities depending on water from mountain systems. An understanding of these water resources is also crucial for understanding how water will respond to earlier snowmelt, increased summer lengths, and changes in precipitation type and timing as climate shifts.

The use of ^{36}Cl elucidates processes that would not have been observed if only physical methods or standard tracers had been used (e.g. major ion chemistry and stable isotopes). In particular the occurrence of bomb-pulse ^{36}Cl in surface water during snowmelt suggests that Cl^- is rapidly retained in significant quantities, and slowly released. The retention and release of $^{36}Cl_{BP}$ also elucidates that all runoff pathways interact with soils before entering surface water.

Future work related to the retention of chlorine may focus on determining environmental factors controlling chlorine biogeochemistry. More specifically, the following questions might be addressed when considering chlorine biogeochemistry. What environmental factors make Cl^- more or less conservative? How might these factors influence study sites where injected or

natural halides are used as tracers to understand water flow paths? What extent do these factors control chlorine-related contaminants, such as PCBs, perchlorate, fluorocarbons, etc.?, and How do these factors effect the fate of these contaminants?

References

Balderer, W. H. A., Synal, and J. Deak, Application of the chlorine-36 method for the delineation of groundwater infiltration of large river systems: example of the Danube River in western Hungary (Szigetkoz area), *Environmental Geology*, 46, 755-762, 2004.

Bales, R. C., N. P. Molotch, T. H. Painter, M. D. Dettinger, R. Rice, and J. Dozier, Mountain hydrology of the Western United States, *Water Resources Research*, 42, W08432, 2006.

Bastviken, D., F. Thomsen, T Svensson, S. Karlsson, P. Sanden, G. Shaw, M. Matucha, and G. Öberg, Chloride retention in forest soil by microbial uptake and by natural chlorination of organic matter, *Geochimica et Cosmochimica Acta*, 71, 3182-3192, 2007.

Bateman, P. C., Plutonism in the central part of the Sierra Nevada batholith, *U. S. Geological Survey Professional Paper 1483*, 186 pp., 1992.

Bentley, H. W., F. M. Phillips, S. N. Davis, S. Gifford, D. Elmore, L. E. Tubbs, and H. E. Gove, Thermonuclear ^{36}Cl pulse in natural water, *Letters to Nature*, 300, 737-740, 1982.

Bentley, H. W., F. M. Phillips, and S. N. Davis, Chlorine-36 in the terrestrial environment, In *Handbook of Environmental Isotope Geochemistry*, Vol. 2, eds. P. Fritz and J. C. Fontes, pp. 427-480, Elsevier, Amsterdam, 1986.

Blumhagen, E. D., and J. F. Clark, Carbon sources and signals through time in an alpine groundwater basin, Sagehen, California, *Applied Geochemistry*, 23, 2284-2291, 2008

Borchers, James, W., Ground-water resources and water-supply alternatives in the Wawona area of Yosemite National Park, California, *U.S. Geological Survey Water-Resources Investigations Report 95-4229*, pp 77, 1996.

Blinov, A., S. Massonet, H. Sachsenhauser, C. Stan-Sion, V. Lazarev, J. Beer, H.A. Synal, M. Kaba, J. Masarik, and E. Nolte, An excess of ^{36}Cl in modern atmospheric precipitation, *Nuclear Instruments and Methods in Physics Research B*, 172, 537-544, 2000.

Cecil, L. D., and J. R. Green, Radon-222, in *Environmental Tracers in Subsurface Hydrology*, edited by P. Cook and A. L. Herczeg, Kluwer Academic Publishers, Boston, 175-194, 2000.

Christopherson, N., C. Neal, R. P. Hooper, R. D. Vogt, and S. Anderson, Modeling stream water chemistry as a mixture of soil water end-members—A step towards second-generation acidification models, *Journal of Hydrology*, 116, 307-320, 1990.

Clow, David W., M. Alisa Mast, and Donald H. Campbell, Controls on surface water chemistry in the upper Merced River Basin, Yosemite National Park, California, *Hydrological Processes*, 10, 727-746, 1996.

Cook, P. G., I. D. Jolly, F. W. Leaney, G. R. Walker, G. L. Allen, L. K. Fifield, and G. B. Allison, Unsaturated zone tritium and chlorine 36 profiles from southern Australia: Their use as tracers of soil water movement, *Water Resources Research*, 30, 1709-1719, 1994.

Constantz, J., Interaction between stream temperature, stream flow, and groundwater exchanges in alpine streams, *Water Resources Research*, 34, 1609-1616, 1998.

Corcho Alvarado, J. A., R. Purtschert, K. Hinsby, L. Troldborg, M. Hofer, R. Kipfer, W. Aeschbach-Hertig, and H. Arno-Synal, ^{36}Cl in modern groundwater dated by a multi-tracer approach ($^{3}H/^{3}He$, SF_6, CFC-12, and ^{85}Kr); a case study in quaternary sand aquifers in the Odense Pilot River Basin, Denmark, *Applied Geochemistry*, 20, 599-609, 2005.

Cornett R. J., H. R. Andrews, L. A. Chant, W. G. Davies, B F. Greiner, Y. Imahori, V. T. Koslowsky, T. Kotzer, J. C. D. Milton, G. M. Milton, Is ^{36}Cl from weapons' test fallout still cycling in the atmosphere?, *Nuclear Instruments and Methods in Physics Research B*, 123, 378-381, 1997.

Davis, S. N., D. Cecil, M. Zreda, and P. Sharma, Chlorine-36 and the initial value problem, *Hydrogeology Journal*, 6, 104-114, 1998.

Davis, S. N., J. Fabryka-Martin, L. Wolfsberg, S. Moysey, R. Shaver, E. C. Alexander Jr., and N. Krothe, Chlorine-36 in ground water containing low chloride concentrations, *Ground Water*, 38, 912-921, 2000.

Davis, S. N., S. Moysey, L. D. Cecil, and M. Zreda, Chlorine-36 in groundwater of the United States: empirical data, *Hydrogeology Journal*, 11, 217-227, 2003.

Dettinger, M. D., D. R. Cayan, M. K. Meyer, and A. E. Jeton, Simulated hydrologic response to climate variations and change in the Merced, Carson, and American River Basins, Sierra Nevada, California, *Climate Change*, 62, 283-317, 2004.

Elmore, D. L. E. Tubbs, D. Newman, X. Z. Ma, R. Finkel, K. Nishiizumi, J. Beer, H. Oeschger, and M. Andree, ^{36}Cl bomb pulse measured in a shallow ice core from Dye 3, Greenland, *Letters to Nature*, 300, 735-737, 1982.

Ericson, K., P. Migon, and M. Olvmo, Fractures and drainage in the granite mountainous area—a study from Sierra Nevada, USA, *Geomorphology*, 64 (1-2), 97-116, 2005.

Flint, A. L., L. E. Flint, and M. D. Dettinger, Modeling soil moisture processes and recharge under a melting snowpack, *Vadose Zone Journal*, 7, 350-357, 2008.

Genereux, D., Quantifying uncertainty in tracer-based hydrograph separations, *Water Resources Research*, 34(4): 915-919, 1998.

Gutenberg, B., J. P. Buwalda, and P. Sharp, Seismic explorations on the floor of Yosemite Valley, California, *Bulletin of the Geological Society of America*, 67, 1051-1078, 1956.

Hainsworth, L. J., A. C. Mignerey, G. R. Helz, P. Sharma, and W. Kubik, Modern chlorine-36 deposition in southern Maryland, U.S.A. *Nuclear Instruments and Methods in Physics Research B*, 92, 345-349, 1994.

Hooper, R. P., N. Christophersen, and N. E. Peters (1990), Modeling stream water chemistry as a mixture of soil water end-members – an application to the Panola mountain catchment, Georgia, U.S.A., *Journal of Hydrology*, 116: 321-343.

Jahns, R. H., Sheet structure in granites: its origin and use as a measure of glacial erosion in New England, *Journal of Geology*, 11 (2), 71-98, 1943.

Knowles, N., M. D. Dettinger, and D. R. Cayan, Trends in snowfall vs. rainfall in the Western United States, *Journal of Climate*, 119, 4545-4559, 2006.

Lee, R. T., G. Shaw, P. Wadey, X. Wang, Specific association of ^{36}Cl with low molecular weight humic substances in soils, *Chemosphere*, 43, 1063-1070, 2001.

Lehmann, B. E., A. Love, R. Purtschert, P. Collon, H. H. Loosli, W. Kutschera, U. Beyerle, W. Aeschbach-Hertig, R. Kipfer, S. K. Frape, A. Herczeg, J. Moran, I. N. Tolstikhin, and M. Groning, A comparison of groundwater dating with ^{81}Kr, ^{36}Cl, and ^{4}He in four wells of the Great Artesian Basin, Australia, *Earth and Planetary Science Letters*, 211, 237-250, 2003.

Liu, F., M. W. Williams, and N. Caine, Source waters and flow paths in an alpine catchment, Colorado Front Range, United States, *Water Resources Research*, 40, W09401, 2004.

Liu, F., R. Parmenter, P.D. Brooks, M. H. Conklin, and R. C. Bales, Seasonal and interannual variation of streamflow pathways and biogeochemical implications in semi-arid, forested catchments in Valles Caldera, New Mexico, *Ecohydrology*, 1, 239-252, 2008.

Lovett, G. M., G. E. Likens, D. C. Buso, C. T. Driscoll, and S. W. Bailey, The biogeochemistry of chlorine at Hubbard Brook, New Hampshire, USA, *Biogeochemistry*, 72, 191-232, 2005.

Maloszewski, P. W., A. Zuber, Determining the turnover time of groundwater systems with the aid of environmental tracers. 1. models and their applicability, *Journal of Hydrology*, 57, 207-231, 1982.

Maloszewski, P, W. Rauert, W. Stichler, and A. Herrmann, Application of Flow Models in an Alpine Catchment Area Using Tritium and Deuterium Data, *Journal of Hydrology*, 66, 319-330, 1983.

Manning, A. H., J. S. Caine, Groundwater noble gas, age, and temperature signatures in an alpine watershed: Valuable tools in conceptual model development, *Water Resources Research*, 43, WO4404, 2007.

Martinec, J, H. Oeschger, U. Schotterer, and U. Siegenthaler, Snowmelt and groundwater storage in an alpine basin, in hydrological aspects of alpine and high-mountain areas *IAHS Publication No. 138, Proceedings of a Symposium at the First Scientific General Assembly of the IAHS*, July 19-30, 1982, England, 169-175, 1982.

Mattle, N., W. Kinzelbach, U. Beyerle, P. Huggenberger, H. H. Loosli, Exploring an aquifer system by integrating hydraulic, hydrogeologic and environmental tracer data in a three-dimensional hydrodynamic transport model, *Journal of Hydrology*, 242, 183-196, 2001.

Maurer, D. K., Geohydrology and Simulated Response to Ground-Water Pumpage in Carson Valley, a River-Dominated Basin in Douglas County, Nevada , and Alpine County, California, *U. S. Geological Survey Water Resources Investigations Report 86-4328*, pp109, 1986.

Maurer, D.K., Ground-Water flow and numerical simulation of recharge from stream flow infiltration near Pine Nut Creek, Douglas County, Nevada, *U.S. Geological Survey Water Resources Invesigations Report 02-4145 Carson City, Nevada*, pp. 45, 2002.

Metcalfe, R., M. B. Crawford, A. H. Bath, A. K. Littleboy, P. J. Degnan, and H. G. Richards, Characteristics fo deep groundwater flow in a basin marginal setting at Sellafield, Northwest England: ^{36}Cl and halide evidence, *Applied Geochemistry*, 22, 128-151, 2007.

Milton, J. C. D., G. M. Milton, H. R. Andrews, L. A. Chant, R. J. J. Cornett, W. G. Davies, B. F. Greiner, Y. Imahori, V. T. Koslowsky, T. Kotzer, S. J. Kramer, J. W. McKay, A new interpretation of the distribution of bomb-produced chlorine-36 in the environment, with special reference to the Laurentian Great Lakes, *Nuclear Instruments and Methods in Physics Research B*, 123, 382-386, 1997.

Moline, G. R., M. R. Schreiber, J. M. Bahr, Representative ground water monitoring in fractured porous systems, *Journal of Environmental Engineering*, 124 (6), 530-538, 1998.

Moran, J. E., T. P. Rose, A chlorine-36 study of regional groundwater flow and vertical transport in southern Nevada, *Environmental Geology*, 43, 592-605, 2003.

Moysey, S., S. N. Davis, M. Zreda, L. D. Cecil, The distribution of meteoric ^{36}Cl/Cl in the United States: A comparison of models, *Hydrogeology Journal*, 11, 615-627, 2003.

Myneni, S. C. B., Formation of stable chlorinated hydrocarbons in weathering plant material, *Science*, 295, 1039-1041, 2002.

Nimz, G., Lithogenic and cosmogenic tracers in catchment hydrology, in *Isotope Tracers in Catchment Hydrology*, edited by K. Kendall and J. J.McDonnell, 1, Elsevier, New York, 291-318, 1998.

Nyberg, Lars, A Rodhe, K. Bishop, Water transit times and flow paths from two line injections of ^{3}H and ^{36}Cl in a microcatchment at Gardjon, Sweden, *Hydrologic Processes*, 13 (11), 1557-1575, 1999.

Öberg, G, The natural chlorine cycle—fitting the scattered pieces, *Applied Microbiology and Biotechnology*, 58, 565-581, 2002.

Öberg, G., The biogeochemistry of chlorine in soil, *The Handbook of Environmental Chemistry*, 3, 43-62, 2003.

Öberg, G., and P. Sanden, Retention of chloride in soil and cycling of organic matter-bound chlorine, *Hydrological Processes*, 19 (11), 2123-2136, 2005.

Peterson, D. H., R. Smith, S. Hager, J. Hicke, M. Dettinger, and K. Huber, River Chemistry as a monitor of Yosemite Park mountain hydroclimates, *EOS, Transactions, American Geophysical Union*, 86 (31), 285-288, 2005.

Phillips, F. M., Chlorine-36, in *Environmental Tracers in Subsurface Hydrology*, edited by P. Cook and A. L. Herczeg, Kluwer Academic Publishers, Boston, 299-348, 2000.

Phillips, F. M., H. W. Bentley, and D. Elmore, ^{36}Cl dating of old groundwater in sedimentary basins, In: Hydrogeology of Sedimentary Basins: Application to Exploitation. *Proceedings of the 3rd Canadian/American Conference on Hydrogeology Alberta Research Council, National Water Wells Association*, 143-150, 1986.

Rademacher, L. K., J. F. Clark, G. B. Hudson, D. C. Erman, and N. A. Erman, Chemical evolution of shallow groundwater as recorded by springs, Sagehen Basin; Nevada County, California, *Chemical Geology*, 179, 37-51, 2001.

Reina, R. G., A. C. Leri, S. C. B. Myneni, Cl K-edge X-ray spectroscopic investigation of enzymatic formation of organochlorines in weathering plant material, *Environmental Science and Technology*, 38, 783-789, 2004.

Rice, K. C. and G. M. Hornberger, Comparison of hydrochemical tracers to estimate source contributions to peak flow in a small, forested, headwater catchment, *Water Resources Research*, 34(7), 1755-1766, 1998.

Segall, P., E. H., McKee, S. J. Martel, and B. D. Turrin, Late Cretaceous age of fractures in the Sierra-Nevada Batholith, California, *Geology*, 18(12), 1248-1251, 1990.

Sueker, J. K., J. N. Ryan, C. Kendall, and R. D. Jarrett, Determination of Hydrologic Pathways during snowmelt for alpine/subalpine basins, Rocky Mountain National Park, Colorado, *Water Resources Research*, 36 (1), 63-75, 2000.

Svensson, T., P. Sanden, D. Bastviken, G. Oberg, Chlorine transport in a small catchment in southeast Sweden during two years, *Biogeochemistry*, 82, 181-199, 2007.

Synal, H. A., J. Beer, G. Bonani, M. Suter, and W. Wolfli, Atmospheric transport of bomb-produced ^{36}Cl, *Nuclear Instruments and Methods in Physics Research B*, 52, 483-488, 1990.

Tosaki, Y., N. Tase, G. Massmann, Y. Nagashima, R. Seki, T Takahashi, K. Sasa, K. Sueki, T. Matsuhiro, T. Miura, K. Bessho, H. Matsumura, and M., He, Application of ^{36}Cl as a dating tool for modern groundwater, *Nuclear Instruments and Methods in Physics Research B*, 259, 479-485, 2007.

Wakabayashi, J., and T. L. Sawyer, Stream incision, tectonics, uplift, and evolution of topography of the Sierra Nevada, California, *Journal of Geology*, 109, pp539, 2001.

Warhaftig, C., Stepped topography of the Southern Sierra Nevada, California, *Geological Society of America Bulletin*, 76, 1165-1190, 1965.

Wilson, J. L., and H. Guan, Mountain-block hydrology and mountain-front recharge, in *Groundwater Recharge in a Desert Environment: The Southwestern United States*, edited by F. M. Phillips, J. H. Hogan, and B. Scanlon, AGU, Washington, DC, 2004.

CHAPTER 3

GROUNDWATER RESIDENCE TIMES IN THE MERCED RIVER BASIN, CALIFORNIA FROM ANALYSES OF TRITIUM AND NOBLE GASES

Abstract

The resiliency of lower order montane streams to climate change depends on the residence times of discharging groundwater. Noble gases (^{3}He, ^{4}He, Ne, Ar, Kr, Xe) and ^{3}H were collected and analyzed in twelve groundwater wells and two springs in the Merced River basin between Happy Isles and El Portal to determine mean groundwater residence times within a granitic montane catchment. Ten of the wells are placed in alluvium close to the Merced River, and two of the wells are placed in fractured granite below meadow alluvium. At least two distinct groundwater types exist; namely, low-Cl^- groundwater ($Cl^- < 1.5$ mgL^{-1}) and a high-Cl^- groundwater ($Cl^- > 8.0$ mgL^{-1}). The high-Cl^- groundwater is characterized by $^3H/^3He$ ages between 23 to 49 yrs, greater than 75% premodern water, and $^4He_{RAD}$ ranging between $6.7x10^{-7}$ and $1.6x10^{-6}$ $cm^3(STP)g^{-1}$. Low-Cl^- groundwater has $^3H/^3He$ ages between 7 and 28 yrs, 0-50% premodern water, and $^4He_{RAD}$ ranging between $1.0x10^{-8}$ to $5.7x10^{-8}$ cm^3 $(STP)g^{-1}$. ^3H and $^4He_{RAD}$ results suggest that most samples consist of a mixture of both modern and premodern

water. Nine seasonal helium isotope ratios (R/R_A) at Fern Spring, a low-Cl^- spring, between July 2004 and December 2006 show a relative age correlation with the Merced River hydrograph. R/R_A values at Fern Spring decrease during baseflow and increase during snowmelt, indicating that the groundwater age increased during baseflow. A comparison of $^3H/^3He$ ages collected wells during snowmelt and baseflow shows that groundwater ages increase up to 21 years. Rapid seasonal responses in apparent recharge ages suggest that groundwater in the catchment, as a whole, may be vulnerable to long term-perturbations, such as climate change. However, the high fraction of premodern water and greater residence times in high-Cl^- groundwater, suggests that a small fraction of the groundwater may be less vulnerable to long-term perturbations on the groundwater system.

Introduction

Water resources captured and stored in arid and semi-arid mountain regions depend heavily on precipitation in mountains (Bales, et al., 2006; Viviroli, et al., 2007). However, surface and subsurface water fluxes are not well understood, and these fluxes are expected to change as climate warms. Recent studies indicate that throughout the American West snowmelt occurs earlier and the average snowpack is declining because of increased temperatures (Knowles et al., 2006; Rauscher et al., 2008). The increased temperatures result in changes in type and timing of precipitation. Most mountain watersheds store water throughout the winter as snow, which is later released to the watershed. Much of the recently melted snowpack is released directly to surface water as overland or

near surface flow, but some of the melted snow infiltrates into alluvium and fractures in bedrock as groundwater recharge (Hood et al., 2006; Flint et al., 2008).

Current understanding of groundwater in mountain systems is limited, and an improved understanding is needed to more fully assess hydrology above the mountain front (Wilson and Guan, 2004). Complications arise because of the complexity of steep terrain with numerous faults, folds, and fractures (Maloszewski and Zuber, 1982; Moline et al., 1998; Manning and Caine, 2007). An improved understanding of groundwater within a mountain block is becoming increasingly important because of potential decreases in groundwater recharge as climate changes (Earman et al., 2006).

The primary focus of this study is to establish groundwater residence times in the Merced River basin in Yosemite National Park (a representative southern Sierra Nevada watershed). Noble gas and tritium analyses are appropriate for investigating groundwater residence times in montane systems (Plummer et al., 2001; Rademacher et al., 2001; Rademacher et al., 2005; Manning and Solomon, 2003; Manning and Solomon, 2005; Manning et al., 2005; Manning and Caine, 2007). Apparent $^{3}H/^{3}He$ ages can be used to estimate groundwater ages for water that recharged within the past 50 yrs (modern water), and tritium concentrations can be combined with ages to estimate the fraction of water that recharge more than 50 yrs ago (premodern water).

Other work in the Merced River basin shows three types of water with distinct endmember compositions mixing within the Merced River basin; namely,

near-surface soil water, low-Cl^- groundwater and high-Cl^- groundwater (see Chapter 2). Based on the dominance of near-surface water released to the catchment during snowmelt (mid-march through mid-June), it is hypothesized that it is mostly 'new' water (recharged < 1 yr ago). Both low and high-Cl^- groundwater are elevated during baseflow (late august to mid November), and it is hypothesized that they have longer residence times than near-surface soil water. The low-Cl^- groundwater discharges into the Merced River in proportions of ~2-10 times greater than the high-Cl^- groundwater depending on location and time of year, and the high-Cl^- groundwater has incorporated substantial rock Cl^- in comparison to the Low-Cl^- groundwater . Based on these two observations, it is hypothesized that the residence time of high-Cl^- groundwater is significantly greater than the low-Cl^- groundwater.

Establishing groundwater residence times will provide timescales for the circulation of unique groundwater bodies mixing within the montane catchment. Furthermore, groundwater residence times, coupled with understanding of groundwater fluxes, provide the initial framework for characterizing groundwater response to perturbations such as groundwater overdraft, or climate change. The following questions are addressed in this study: What are the mean residence times for different groundwater bodies in the Merced River basin? What do these residence times reveal about flow paths and groundwater mixing within the mountain block? How can combining $^3H/^3He$ ages and $^4He_{RAD}$ ages help understand residence times in a complex montane watershed? What are the seasonal responses in residence times? What do residence times imply regarding

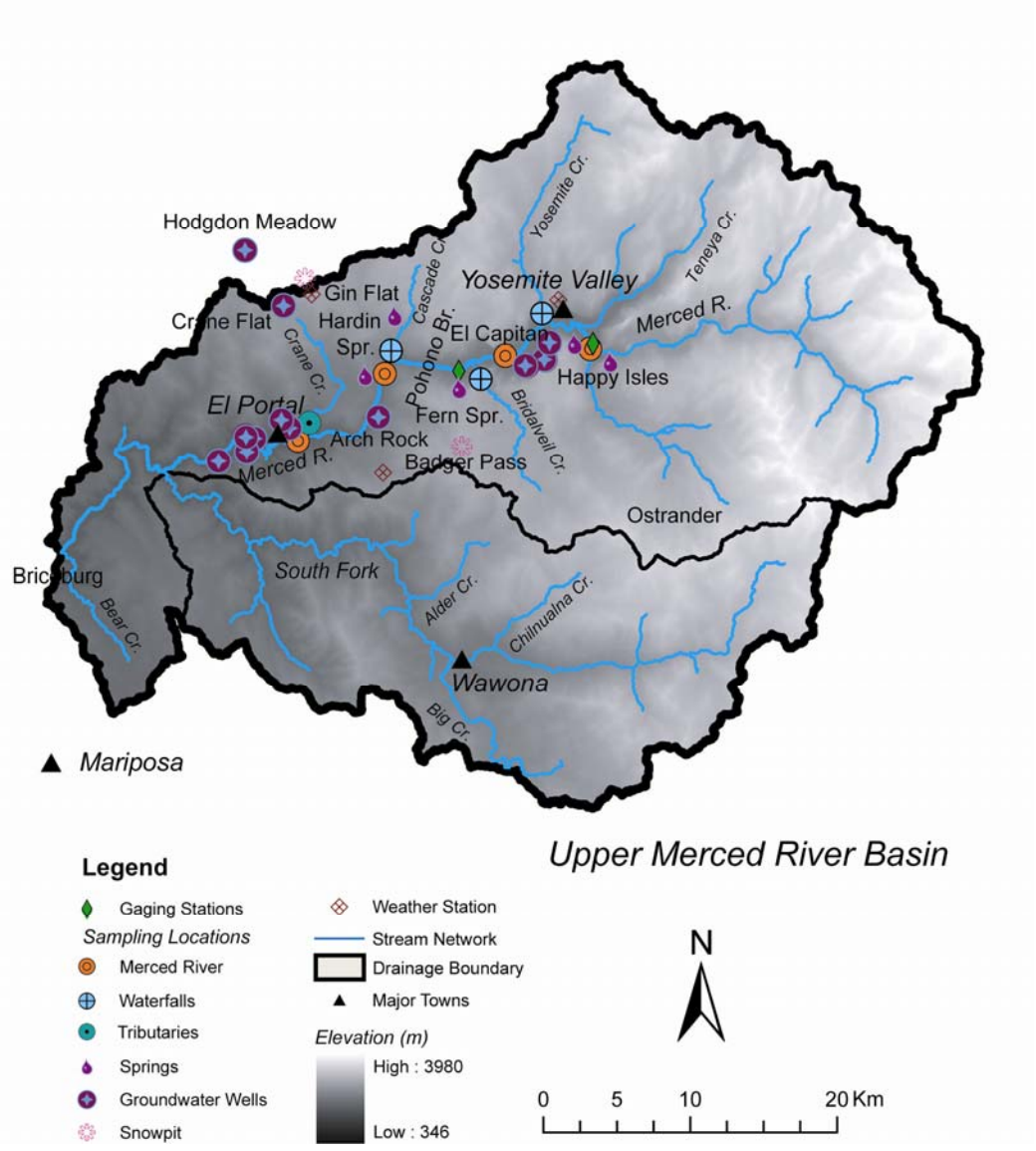

Figure 3.1: The Upper Merced River Watershed, with water sampling locations.

groundwater responses to perturbations such as climate change in mountain systems?

Field Area

The Merced River basin is on the western slopes of the Sierra Nevada Mountains with headwater elevations as high as 4000 meters above sea level (m.a.s.l.) at Mt Lyell. The study site consists of a 40 km reach of the Merced River beginning at Happy Isles, which is the upper end of Yosemite Valley at 1,224 m.a.s.l., and ending at El Portal with an elevation of 540 m a.s.l. (Figure 3.1). Twelve drinking water wells are located in the basin. Three wells (Yosemite Valley Wells 1, 2, and 4) located near Yosemite Creek range in depths from 159 to 244 m. Meadows at Crane Flat and Hodgdon Meadow each have one well set in bedrock below alluvium at depths of 112 and 63 m respectively (Table 3.1**)**. Arch Rock Well is set 28 m in river alluvium near the west entrance of Yosemite National Park, and six wells are set between 17 to 21 m near the bedrock-river alluvium interface near El Portal (El Portal Wells 2-7).

The terrain is mountainous with steep slopes and cliffs on both sides of the river basin, and consists of a complex network of fractures and faults throughout the system with multiple uplifts having occurred (Bateman and Wahrhaftig, 1966; Clow et al., 1996; Wakabayashi and Sawyer, 2001). The majority of the basin is underlain by 70 to 210 Ma granitic intrusions from the Sierra Nevada batholith (Bateman, 1992). Downstream of the Yosemite National Park boundary, bedrock is primarily metasedimentary and metavolcanic, and there are outcrops of metamorphic rock located at the upper end of the basin above the sampling sites (Bateman, 1992).

Table 3.1: Physical characteristics of wells sampled in the Merced River basin.

Well Location	Well Elevation (m)	Well Depth (m)	Depth of Borehole (m)	Depth to Bedrock (m)	Screened Interval (m)
Valley Well 1	1205	159	309	309	130-139
					144-159
Valley Well 2	1205	216	296	296	152-158
					170-177
					196-202
					207-213
Valley Well 4	1205	244	265		110-140
					165-177
					189-195
					226-238
Arch Rock	875	28	28		22-28
Crane Flat	1922	112	0	18	
Hodgdon's Meadow	1412	63	122	27	
El Portal Well 2	539	17	32	17	14-17
El Portal Well 3	526	20	27	25	15-20
El Portal Well 4	616	21	23	20	13-21
El Portal Well 5	546	20	23	19	12-20
El Portal Well 6	539	20	21	20	15-20
El Portal Well 7	526	21	24	15	8-10
					12-13
					19-20
Springs					
Happy Isles Spring	1260	na	na	na	na
Fern Spring	1193	na	na	na	na

Fractures are numerous, and range from microscopic to kilometers in length (Bateman and Wahrhaftig, 1966; Segall et al., 1990; Wakabayashi, and Sawyer, 2001; Ericson et al., 2005). Groundwater flow through fractures is largely controlled by fracture aperture (Brace, 1975; Park et al. 1997). Fractured bedrock porosity can be as low as 0.00001 (Snow, 1968), but typical fracture porosity ranges from 0.005 to 0.01 in groundwater producing aquifers in fractured bedrock (Aquilina et al., 2004). Many of the fractures in granitic systems are comprised of numerous well-connected exfoliation fractures, which have three perpendicular orientations, average 10s of m deep, and are spaced ~1-4 m apart (Jahns, 1943; Warhaftig, 1965). Gruss formation in granitic rocks may result in decreased permeability with fracture depth (Warhaftig, 1965).

Although much of the basin consists of exposed basement rock, there are numerous surficial deposits scattered throughout the basin, but the extent and depths are still widely unknown. Within the Yosemite National Park boundary surficial deposits are primarily glacial tills that occur in the valley bottoms as lateral and recessional moraines. Downstream of the Park boundary surficial deposits are generally thin with no glacial debris. Glacial tongues cut into pre-Pleistocene valleys and caused "further deepening and form change" (Ericson et al., 2005). The extent of glaciation, and the ages of glaciation in Yosemite have not been thoroughly deciphered, but Yosemite Valley alluvium consists primarily of glacial till and has a maximum thickness of 600 m (mean depth ~300 m). Yosemite Valley has three distinct layers of alluvium; each layer is ~100 m thick (Gutenberg et al., 1956). The upper layer consists of mostly sands and gravels, the intermediate layer is primarily

glacial flour with alternating layers of sands and gravels, and basal layer is dominantly sands and gravels with cobbles and boulders.

The climate in the Merced River basin is typically dry in the late spring through early fall, and wet from mid fall to mid spring. The dominant form of precipitation occurs as snow above ~2000 m (Rice et al., 2007). The dominant release of water to the watershed occurs during snowmelt. During this study, Merced River flows recorded at Happy Isles were as high as 125 $m^3 s^{-1}$ during peak snowmelt and as low as 0.1 $m^3 s^{-1}$ during baseflow (California Data Exchange Center, cdec.water.ca.gov). As snow melts, water either evaporates, runs overland to creeks and rivers, or infiltrates into shallow soil. Some of the recharged soil water flows along the bedrock soil boundary and later discharges to surface water bodies as soil through flow (Flint et al., 2008). Another component of the soil water recharges into the fractured bedrock (Flint et al., 2008).

Sampling and Laboratory Methods

Samples for dissolved noble gases (^{3}He, ^{4}He, Ne, Ar, Kr, and Xe) and ^{3}H were collected at 12 groundwater production wells located within the Merced River Basin on June 21, 2005; they were sampled again between May 31 and June 1, 2006 (Table 3.1). Arch Rock and El Portal Well 2 were also sampled on November 2 and 6, 2006, respectively. Two perennial springs were also sampled. One that discharges near Happy Isles, which will be referred to as Happy Isles Spring, was sampled on May 30, 2006, while nine samples were collected at Fern Spring between July 2004 and December 2006. Fern Spring, which discharges from an alluvium covered fracture zone (determined from topographic maps and

visual observations), was sampled frequently because the flow rates increase significantly during snowmelt (determined from visual observations). The two wells were sampled during baseflow because groundwater wells in the basin are artesian during snowmelt and non-artesian during baseflow (observed during sampling; and well operators verified that this pattern occurs annually). It was anticipated that seasonal patterns in flow rates may result in changes in groundwater residence times.

^{3}H samples were collected in 1 L glass bottles between July 2004 and July 2005, and 1 L HDPE plastic bottles, with PERAFILM sealing the cap, were used for collection of ^{3}H after July 2005. Samples were stored at room temperature. Dissolved noble gases were collected in two clamped 3/8" copper tubes. Noble gases (^{3}He, ^{4}He, Ne, Ar, Kr, and Xe) and tritium were analyzed using a quadropole mass spectrometer or VG 5400 mass spectrometer which is described in Hudson et al. (2002). In order to determine ^{3}H inputs to the watershed, five samples were taken directly from the Merced River, primarily during high flow periods.

The $^{3}H/^{3}He$ age-dating technique (Solomon, 2000a) was used to estimates modern groundwater. Premodern water fractions were also estimated by comparing decay-corrected ^{3}H values from the $^{3}H/^{3}He$ ages and comparing decay-corrected values with atmospheric ^{3}H fallout for corresponding recharge years. Radiogenic helium ($^{4}He_{RAD}$) ages, which are derived from assumed accumulation rates of radiogenic ^{4}He, were also estimated using methods described by Solomon (2000b).

Stream temperature measurements were recorded every 30 minutes at Bridalveil and Yosemite Creeks, in Yosemite Valley, and at Crane Creek, in El Portal, using Solinst 3001 Levelogger Gold. Measurements were recorded from January 2007 to December 2007 to infer information about recharge temperatures from high and low elevation catchment meltwater.

Conductivity measurements were collected at sampling locations using a YSI 30 EC probe, and radon activity was measured at the confluence of Cold Creek Canyon, in El Portal, to investigate how continuous groundwater discharge to the River is.

^{222}Rn was sampled at the confluence of Cold Canyon Creek and the Merced River to determine if fractured groundwater flow discharges to the Merced River. It was analyzed by mixing 20 ml of mineral oil scintillation cocktail with 1 L of water in a glass volumetric flask. Samples were shaken for 10 minutes, and mineral oil was extracted and placed in 20 ml scintillation vials. Samples were analyzed using a Beckman Coulter LS 6500 Multipurpose Scintillation Counter within three days after field collection.

Chloride samples for major ion chemistry were collected in 125 HDPE plastic bottles, stored at 4 C°, and filtered before analyzing. The analyses were completed using a Dionex ICS 2000 in the Sierra Nevada Research Institute (SNRI) Laboratory at the University of California, Merced (UC Merced).

Results and Data Analysis

Measured Results

Tritium in groundwater and surface water samples ranges between 6.7 and 20.4 $pCiL^{-1}$, which is well above the detection limit, and these values indicates some fraction of modern water mixes in each well or spring (Table 3.2). The river values ranged between 9.4 to 11.9 pCi L^{-1} (Table 3.3).

$^{3}He/^{4}He$ ratios in groundwater is normalized to atmospheric equilibrated $^{3}He/^{4}He$ ratios, and expressed as R/R_A. These values range between 1.42 and 0.15, with a mean value of 0.68 ±0.37. Virtually all groundwater sampled except for Valley Well 1, Crane Flat Well, Hodgdon Meadow, and El Portal Well 3 show depressed R/R_A values (less than 0.9). R/R_A values were also measured directly from the Merced River at the confluence of Cold Creek Canyon on July, 2004, and measured 0.82.

Radiogenic ^{4}He concentrations vary between $8.9x10^{-10}$ to $1.6x10^{-6}$ cm^3 (STP) g^{-1} and the mean value is $2.14x10^{-7}$ ±$3.97x10^{-7}$ cm^3 (STP) g^{-1}. These values are comparable to systems with mixtures of modern and premodern water (Beyerle et al., 1999; Aeschbach et al., 2000; Manning et al., 2005; Castro et al., 2007; Manning and Caine, 2007). Some of these studies also include water from high elevation catchments. Ninety six samples taken from a high-elevation catchment in the Rocky Mountains, or Salt Lake Valley wells receiving mountain block recharge, had $^{4}He_{RAD}$ values ranging between $6.45x10^{-11}$ and $1.77x10^{-6}$ cm^3 (STP) g^{-1} (Manning et al., 2005; Manning and Caine, 2007).

Table 2: Noble gas parameters measured and calculated from the Merced River basin.

Sample ID	collection date	Altitude (m)	Conductivity ($\mu S\ cm^{-1}$)	T_{sample} (^oC)	Cl^- (mgL^{-1})	Ne_{excess} ($cm^3STP\ g^{-1}$)	$T_{recharge}$ (^oC)	$T_{recharge}$ (^oC)	^3H ($pCi\ L^{-1}$)	$^3He/^4He$ R/R_A	^4He rad ($cm^3STP\ g^{-1}$)	$^3H/^3He$ age (yr)	initial ^3H ($pCi\ L^{-1}$)	% Premodern Fraction	$^4He_{rad}$ age (yr)
Groundwater Wells							Minimum	Maximum							
Valley Well 1	6/21/2005	1205	40.2	8.5	0.3	0.0044	7.1	1.2	17.95	0.98	3.94E-08	26	75.1	50%	166
	5/31/2006		44.0	8.9	0.3	0.0046	7.3	1.5	17.95	0.98	4.81E-08	28	87.8	38%	202
Valley Well 2	6/21/2005	1205	52.8	12.7	2.4	0.0036	8.1	2.3	15.20	0.27	3.65E-07	26	63.8	38%	1537
	5/31/2006		52.9	15.7	2.3	0.0047	8.7	2.9	15.20	0.29	2.67E-07	17	39.7	0%	1123
Valley Well #4	5/31/2006	1205	42.4	9.2	5.1	0.0051	8.2	2.5	13.65	0.37	1.55E-07	10	24.5	0%	653
Arch Rock	6/21/2005	875	74.2	12.8	1.1	0.0017	11.5	6.3	19.65	0.76	3.55E-08	13	40.1	0%	149
	11/02/2006		55.0	10.3	1.2	0.0022	13.9	8.6	19.65	0.71	3.60E-08	10	33.5	0%	152
Crane Flat	6/21/2005	1922	84.4	7.2	0.6	0.0038	6.9	6.2	18.78	1.42	9.17E-10	20	57.0	0%	4
	5/31/2006		100.0	10.7	2.8	0.0065	6.8	6.1	18.78	1.44	8.88E-10	23	66.6	0%	4
Hodgdon's Meadow	6/21/2005	1412	91.0	15.4	1.3	0.0027	9.5	7.5	20.44	1.14	4.61E-09	11	38.3	0%	19
	5/31/2006		87.0	12.4	0.7	0.0044	10.0	8.0	9.22	1.14	2.06E-09	17	23.4	38%	9
Well 2 El Portal	6/21/2005	539	199.0	16.3	8.2	0.0036	15.6	10.7	17.94	0.19	6.21E-07	23	63.0	7%	2613
	6/1/2006		209.8	16.0	8.5	0.0044	15.8	10.9	9.22	0.19	6.45E-07	31	51.5	75%	2714
	11/06/2006		206.5	16.3	15.1	0.0025	16.9	12.0	9.22	0.16	1.601E-06	42	183.6	96%	6736
Well 3 El Portal	6/21/2005	526	153.0	15.6	1.1	0.0054	14.2	9.4	14.39	0.90	5.36E-09	0	8.7	0%	23
	6/1/2006		157.8	14.2	1.2	0.0049	12.6	7.8	7.53	0.90	5.00E-09	0	1.1	na	21
Well 4 El Portal	6/21/2005	616	177.7	14.2	3.7	0.0042	13.0	8.1	15.81	0.30	1.70E-07	0	14.6	0%	716
	6/1/2006		127.8	14.2	3.8	0.0059	13.3	8.5	15.8	0.32	2.28E-07	12	30.5	0%	959
Well 5 El Portal	6/21/2005	546	130.2	17.4		0.0041	14.9	10.1	13.92	0.25	2.38E-07	1	14.9	0%	1003
	6/1/2006		124.5	17.2	2.6	0.0043	14.7	9.8	13.9	0.24	2.68E-07	0	8.5	na	1129
Well 6 El Portal	6/21/2005	539	92.6	18.5	3.8	0.0037	12.8	8.0	12.78	0.33	1.66E-07	11	23.9	0%	698
	6/1/2006		98.1	15.5	4.0	0.0040	14.1	9.3	12.8	0.35	1.33E-07	0	10.0	na	561
Well 7 El Portal	6/21/2005	526	80.7	16.3		0.0043	12.0	7.2	15.04	0.74	2.35E-08	0	14.1	0%	99
	6/1/2006		82.5	15.3	1.5	0.0042	12.2	7.4	15.0	0.73	2.66E-08	0	15.3	0%	112
Springs															
Happy Isle Spring	5/30/2006	1260	226.9	10.5	32.7	0.0030	11.0	6.1	6.7	0.15	1.32E-06	49	102.3	100%	5570
Fern Spring	7/21/2004	1193	25.5	9.3		0.0041	7.3	4.2	15.9	0.76	2.51E-08	15	102.1	0%	106
Fern Spring	1/17/2005	1193	36.4	8.0	0.4	0.0042	7.7	4.6	16.2	0.70	5.69E-08	19	45.7	0%	239
Fern Spring	7/13/2005	1193	28.1	7.7	0.3		10.0	6.9	12.8	1.00					
Fern Spring	11/11/2005	1198	33.5	8.1	0.4	0.0059	9.0	5.9	14.8	0.79	2.85E-08	8	23.7	0%	120
Fern Spring	3/30/2006	1193	27.4	7.5	0.3	0.0045	7.9	4.8	10.7	1.00		0	8.0		0
Fern Spring	5/30/2006	1193	20.3	8.8	0.3	0.0039	8.5	5.5	8.4	1.03		1	9.0		0
Fern Spring	10/12/2006	1193	32.9		0.3	0.0037	9.3	6.2		0.82	1.568E-08				66
Fern Spring	11/20/2006	1193		7.3		0.0030	9.7	6.6		0.81	1.213E-08				51
Fern Spring	12/12/2006	1193	22.0	7.4		0.0038	9.3	6.2		0.77	1.045E-08				44
Drive Point Sampler															
MP-El Capitan Bridge	7/13/2005	1198				0.0056	11.5		15.3	0.89	1.55E-08	6.3	21.8	2%	65
Average		1002	93	12.3	4.4	0.0041	10.9		14.1	0.68	2.14E-07	12.2	42.4	14%	902
Standard Deviation		386	64	3.7	8	0.0010	3.0		3.9	0.37	3.97E-07	16.9	38.7	33%	1669
Minimum		526	20	7.2	0.3	0.002	6.8		6.7	0.15	8.88E-10	-34.9	1.1	0	0
Maximum		1922	227	18.5	33	0.007	16.9		20.4	1.44	1.60E-06	48.9	183.6	1.0	6736

*Values for % premodern water reflect smoothed averages of 3H measured in precipitation, and a value of 0% may actually have some premodern water.

Table 3.3: Tritium measurements collected from surface water in the Merced River basin.

Location	Date	^{3}H ($pC\ L^{-1}$)
El Capitan Bridge	5/30/2006	9.4
Cascade Creek	10/14/2004	11.7
Bridalveil Creek	1/18/2005	11.3
Cascade Creek	1/18/2005	11.9
Happy Isles	3/30/2006	10.1

Noble gas concentrations in groundwater typically exceed noble gas solubilities, and it is important to calculate the amount of "excess" air before estimating groundwater ages (Stute and Schlosser, 2000). It is thought that excess air is caused by trapping air bubbles during rapid recharge, or from fluctuations of the water table. In this study, excess air is expressed as excess neon because neon only has an atmospheric source. Excess neon in the Merced River basin ranges between $2x10^{-3}$ and $7x10^{-3}$ cm^3 (STP) g^{-1} (Table 3.2). These values border on the low-end of typical excess air measurements in mountain groundwater (Manning and Caine, 2007). Significantly higher excess air between $2x10^{-3}$ and $7x10^{-3}$ cm^3 (STP) g^{-1} (Table 3.2). These values border on the low-end of typical excess air measurements in mountain groundwater (Manning and Caine, 2007). Significantly higher excess air is even more common in non-mountainous regions (Visser et al., 2007: Cey et al., 2008). The low excess air found in the Merced River basin decreases uncertainty estimating groundwater ages and recharge temperatures.

^{222}Rn activity was also measured at Cold Creek Canyon to determine is if groundwater discharge occurs continuously to the Merced River (Table 3.4). Activity ranges between 46 counts per minute (cpm) during snowmelt 2006 to 3843 cpm during baseflow 2007.

Groundwater temperatures at the time of sampling ranged between 7.2 to 18.5 °C with mean temperatures and standard deviations of 12.3 and 3.6 °C respectively.

Table 3.4: ^{222}Rn activity (counts per minute) in the Merced River near Cold Creek Canyon.

Date	^{222}Rn (cpm)	Error (cpm)
7/20/2004	675	34
10/15/2004	3322	166
1/25/2005	260	13
7/14/2005	79	4
11/11/2005	2735	137
3/30/2006	46	2
5/30/2006	105	5
10/12/2006	2862	143
1/31/2007	2913	146
5/24/2007	253	13
7/12/2007	2868	143
10/10/2007	3843	192

Groundwater conductivity values in wells and springs ranged between 20 to 227 μS cm^{-1} with mean temperatures and standard deviations of 93 and 64 μS cm^{-1} respectively (Figure 3.2). Conductivity measured directly from the Merced River at the confluence of Cascade Creek and the Merced River ranged between 9.5 and 44 μS cm^{-1}, with the highest values occurring during baseflow, and the lowest values occurring during snowmelt (Figure 3. 2). Baseflow conductivities values are approximately 3-5 μS cm^{-1} lower during baseflow proceeding wet years (i. e. 2003, 2005, and 2006), and when snowpacks are lower (i.e. 2004 and 2007), the baseflow conductivities are higher.

Temperature corrected conductivity was also measured upstream Cold Creek Canyon and at Cold Creek Canyon on July 2004 to investigate the possibility of groundwater discharge to the river. Just upstream of Cold Creek Canyon, the conductivity was 24 μScm-1 and it was 36 μScm^{-1} at the confluence with Cold Creek Canyon. Conductivity was also collected seasonally at Cascade Picnic Area from November 2003 to October 2007. Values of conductivity at Cascade Picnic area averaged 22.3 ±12.1 μS cm^{-1}, and the maximum and minimum values ranged between 8.4 and 44.0 μS cm^{-1}.

Calculating Recharge Temperatures

Recharge temperature calculations are dependant on the pressure of recharging groundwater (recharge elevations) and the amount of excess air. Once the excess air component is subtracted from the measured noble gas concentrations the atmospheric equilibrium noble gas concentrations can be determined if temperature and pressure is known (Stute and Schlosser, 2000). In

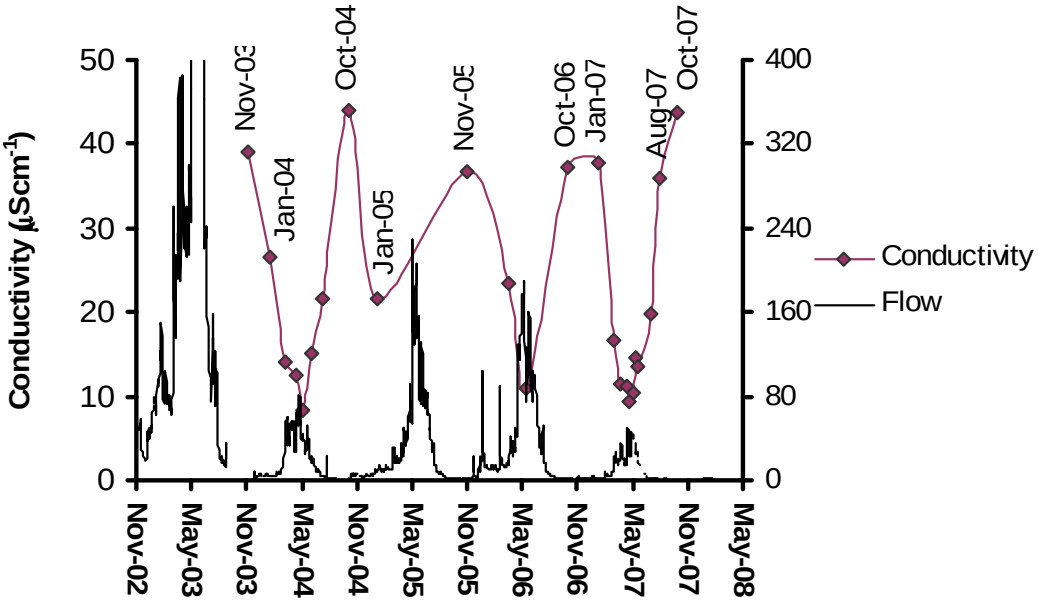

Figure 3.2: Temporal variations of electrical conductivity (µS cm^{-1}) and flow (m^3s^{-1}) in the Merced River. Flows are measured at Pohono Bridge, and conductivity measurements are taken at the confluence of Cascade Creek and the Merced River.

order to determine recharge temperature, a recharge elevation must be known or assumed. Xenon is the most temperature dependent, and the solubility constants for Xe are used for estimating recharge temperatures by the following equation:

$$T_R = A(Xe_{Sol})^3 + B(Xe_{Sol})^2 + C(Xe_{Sol}) + D \quad (1)$$

Where T_R is the recharge temperature, Xe_{Sol} is the air-equilibrated Xe concentration for a given temperature, and A-D are Xe solubility constants (A = -9.04×10^{24}, B = 4.92×10^{17}, C = -1.04×10^{10}, and D = 82.3) (Hudson et al., 2002).

Rice et al. (2007) combines remote sensing data from MODIS and ground data to show that ~50-60% of snowpack occurs between 2100-3000 m. a. s. l., and ~35% of snowpack occurs above 3100 m in the Merced and Tuolumne River basins. However, location of snowmelt does not necessarily correlate with location of groundwater recharge. Because of the large variability in possible recharge elevations in the Merced River basin, recharge temperatures are estimated iteratively using dissolved noble gas concentrations and by assuming the recharge elevations occur at 1) the well or spring elevation and 2) a maximum local recharge elevation based on topography and location of the well (Table 3.2). These elevations bracket the minimum and maximum recharge elevations, and they are compared with temperature measurements during snowmelt in 2007. Recharge temperatures vary between 7.3 to 17.7 °C when well elevations are used, 1.2 to 12.0 °C when maximum elevations are used as the recharge elevation. Recharge temperatures often reflect the mean annual ground temperature at the water table, which is typically ~1 °C higher than mean annual air temperatures,

but deserts and mountain systems can deviate from these values (Stute and Schlosser, 2000). Recharge temperatures in Salt Lake Valley wells and Wasatch Mountain springs receiving groundwater from high elevation mountains were ~2 °C cooler than the mean annual air temperature (Manning and Solomon, 2003; Manning et al., 2005). Typical mean annual air temperatures in the Sierra Nevada range between 4-15 °C (Riebe et al., 2001). Atmospheric lapse rates at high elevations in the Merced and Tuolumne River basins were estimated to be -0.68 °C per 100 m (Lundquist and Cayan, 2007). However, mean annual air temperatures taken at several locations near the Merced River basin, with elevations ranging between 30 to 2884 m, correlate to an atmospheric lapse rate of -0.45 °C per 100 m elevation gain (Table 3.5). These values correlate much closer to the temperatures ranges observed by Reibe et al, (2001). Maximum and minimum recharge temperatures are plotted with the respective recharge elevations, and compared with the atmospheric lapse rate (Figure 3.3).

Groundwater temperatures at the time of sampling are elevated in comparison to groundwater recharge temperatures at most locations, which indicates warming during subsurface transport (Figure 3.3). Increasing groundwater temperatures during subsurface transport has been observed in other mountain systems (Plummer et al., 2001; Manning et al., 2005). Mean annual ground temperatures typically increase 3 °C per 100 m depth due to geothermal heat flow (Stute and Schlosser, 2000), and increased well sample temperatures may reflect the depth of groundwater circulation. The increased temperatures may

Table 3.5: Mean annual air temperatures recorded at locations with various elevations in or nearby the Merced River basin. Mean annual air temperatures with WRCC codes were taken from the Western Regional Climate Center (www.wrcc.dri.edu). Hourly measurements were averaged at El Portal using a Levelogger Gold, and Tuolumne meadows mean annual air temperatures were recorded and presented by Lundquist and Cayan (2007).

Location	Source of Data	WRCC Code	recorded time period (year start-year end)	Temp (C)	Elevation (m)
Merced	WRCC	45532	1899-2008	16.2	30
Auburn Dam	WRCC	40385	1972-1984	14.5	400
El Portal	Levelogger		2006-2007	14.1	580
Groveland	WRCC	49065	1905-1954	12	869
Yosemite Valley	WRCC	49855	1905-2008	11	1280
Tuolumne Meadows	Lundquist & Cayan (2007)		2002-2004	3.3	2600
Gem Lake	WRCC	43369	1924-2004	5.3	2790
Ellery Lake	WRCC	42756	1924-2005	2.7	2884

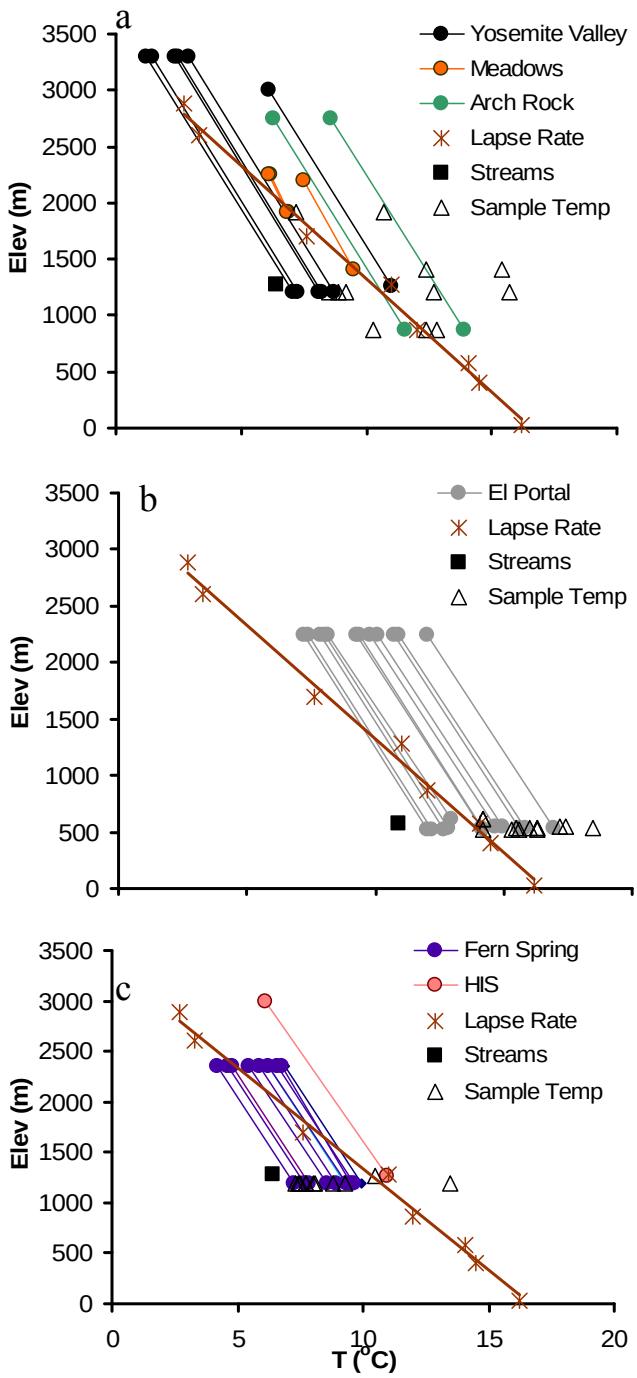

Figure 3.3: Filled circles represent recharge temperatures and Recharge elevations for all groundwater well samples in a) Yosemite National Park b) El Portal, and c) springs. Lines connecting the filled circles connect individual sample locations using the recharge elevations at the maximum local recharge elevation (top circles) and the sample elevation (bottom circles). The atmospheric lapse rate is -0.45 °C per 100 m, determined from mean annual air temperatures (Table 3.5). Hollow triangles represent the temperatures at the time of sampling, and the black squares represent mean tributary temperatures in the respective reaches of the river channel measured during snowmelt.

suggest some deep circulation (e.g. even local recharge in Yosemite Valley needs to circulate ~150-300 m to reach Valley wells.

To determine the most likely recharge elevations, the predicted recharge temperatures are compared to the mean annual air temperature for their elevation. Examining figure 3.3, one observes the recharge temperatures maximum local recharge elevations are greater than the mean annual air temperatures.

The two meadow wells above Yosemite Valley have minimum recharge temperatures near the mean annual air temperatures. This suggests that some meadow may provide recharge to underlying fractures, rather than the underlying fractures receiving groundwater from higher elevations.

If recharge occurs at well elevations from recharging waterfalls and tributaries, then recharge should reflect surface water temperatures during snowmelt, when flows are highest and recharge the greatest. During snowmelt, between March 15 and May 31, 2007, when groundwater recharge is assumed to be greatest, average stream temperatures for major tributaries at the confluence with the Merced River were 10.9 ± 3.6 °C at Crane Creek (in El Portal), 6.8 ± 3.3 °C at Bridalveil Creek below the falls, and 6.4 ± 3.1 °C at Yosemite Creek below the falls (Figure 3.3). The Yosemite and Bridalveil Creek temperatures are very similar to the lowest recharge temperatures occurring in Yosemite Valley (assuming recharge at well elevations), and the Crane Creek temperatures are also very similar to the lowest local recharge temperatures estimated at El Portal (Figure 3.3).

Yosemite Valley wells and springs have recharge temperatures at or below the mean annual air temperature when the well elevation is the assumed recharge elevation, which results in a larger degree of uncertainty for determining recharge locations. Recharge may reasonably occur 1) at well elevations or 2) between the maximum local recharge elevation and the well elevation. If recharge occurs at the well elevations, then the lowest Yosemite Valley well is ~5 °C less than the mean annual air temperature, which is actually a reasonable deviation from below the mean annual air temperatures (Manning and Solomon, 2003).

Most recharge temperatures in shallow river alluvium (i.e. El Portal and Arch Rock) have recharge temperatures near the mean annual air temperature, and in some cases recharge temperatures are even greater than the mean annual air temperatures (Figure 3.3). These recharge temperatures suggest that the dominant form of recharge to these wells may be from soil or surface water recharging river alluvium. The baseflow samples at Arch Rock and at El Portal Well 2 have the warmest recharge temperatures, suggesting that some of the flow paths may have recharged since snowmelt when surface waters are warmer.

Stream temperature and groundwater recharge temperature data combined with the mean annual air temperature strengthen the argument that the majority of recharge to valley and river alluvium occurs locally, but higher elevation recharge cannot be ruled out. Conceptually is make sense for large amounts of water from waterfalls and tributaries flowing to the Merced River to served as the primary source of recharge to alluvium. Yosemite Valley is the most uncertain, and possibly consists of the most complex groundwater flow paths. Recharge

temperatures can still be interpreted as a significant fraction of recharge occurring between the maximum and minimum recharge elevations. This would primarily be groundwater flow from fractures discharging to downstream locations. The presence of Happy Isles Spring and Fern Spring alone, suggests that higher elevation recharge to Yosemite Valley enters the valley as groundwater flow through fractures.

$^3H/^3He$ ages

Groundwater residence times can provide information about recharge locations and timing which will vary with climate change. Determining groundwater residence times through traditional well hydraulics depends on estimates of hydraulic conductivity, which varies over thirteen orders of magnitude in natural geologic material (Freeze and Cherry, 1979). Combining noble gases with tritium can provide estimates for groundwater residence times that are not dependent on determination of hydraulic conductivity.

Apparent groundwater ages can be determined using the $^3H/^3He$ age-dating method (Solomon, 2000a), using the following equation:

$$t = \lambda^{-1} \ln\left(\frac{^3H}{^3He^*} + 1\right) \quad (2)$$

Where $\lambda = 0.0556\ yr^{-1}$ is the tritium decay constant, ^3H and $^3He^*$ are the concentrations of tritium and tritiogenic ^3He in atoms/g. $^3He^*$ can be determined from the following:

$$^{3}He^{*} = {}^{3}He_{total} - {}^{3}He_{Sol} - {}^{3}He_{EA} - {}^{3}He_{RAD} - {}^{3}He_{Mantle} \quad (3)$$

$^{3}He_{total}$ is the total measured ^{3}He, $^{3}He_{Sol}$ is the equilibrium solubility component of ^{3}He, $^{3}He_{EA}$ is the ^{3}He from excess air, $^{3}He_{RAD}$ is the radiogenic ^{3}He, and $^{3}He_{Mantle}$ is ^{3}He from mantle degassing. In the Merced River basin, $^{3}He_{Mantle}$ is negligible because typical mantle $^{3}He/^{4}He$ values are on the order of 10^{-5}, which is much higher than observed $^{3}He/^{4}He$ (Seta et al., 2001). The Radiogenic $^{3}He/^{4}He$ ratio ($^{3}He/^{4}He_{RAD}$) is necessary to determine so that $^{3}He_{RAD}$ can be subtracted from $^{3}He_{total}$. Using methods described by Aeschbach-Hertig et al. (2000), $^{3}He/^{4}He_{RAD}$ was estimated to be $1.1x10^{-7}$. Analytical uncertainty is ±1 year; however, greater uncertainty in the estimate of mean age is associated with groundwater with a mixture over a range of ages. These measurements only provide an integrated mean residence time for the modern component of groundwater, and they are not influenced by the presence or absence of premodern water.

Values for $^{3}H/^{3}He$ ages range between recently recharged water and 49 years (Table 3.2). While most meadow and Yosemite Valley groundwater some detectable ages associated with them, the majority of El Portal groundwater samples consist of recently recharged groundwater (<1 yr).

Fraction Premodern Water

The occurrence of both modern (recharged <50 yrs ago) and premodern (recharged >50 yrs ago) water in individual samples has been observed previously in montane catchments, suggesting that groundwater in the Merced River basin originates from several flow paths with a wide range of residence times (Beyerle

et al., 1999; Manning et al., 2005; Manning and Caine, 2007). Because of this occurrence, there are at least two dominant processes occurring, and techniques for de-convoluting premodern and modern water fractions within a single sample have been developed by Manning (2002). This is done by comparing groundwater ^{3}H values at the time of recharge with atmospheric fallout for the corresponding recharge year, but the method must be developed for specific study locations.

Figure 3.4 shows the ^{3}H atmospheric fallout recorded at Santa Maria, CA, Portland, OR, and Ottawa, ON from 1960 to 2000. The Merced River samples were also included to extrapolate fallout values beyond 2000. Santa Maria is included because it is the nearest location with ^{3}H, and it is assumed that these values are closest to fallout that occurred in the Merced River basin. However, this dataset is the most incomplete, only ranging between 1963 and 1976. Portland Oregon ^{3}H values are included because they are the next closest physical location, and Ottawa is typically included because it has the most complete ^{3}H record. ^{3}H decay-corrected groundwater samples are also included in Figure 3.4, and if there is no mixing with premodern water, these should plot near atmospheric fallout values. However, there is large variation in the tritium fallout, and incoming fallout measurements should be smoothed to determine fraction of premodern water.

Tritium concentrations were smoothed to determine the mean concentrations (Figure 3.5). This is done by taking the dataset nearest the Merced River basin, and averaging each measurement by the previous and proceeding year of measurements (Figure 3.5). Because Santa Maria data ends after 1976, ^{3}H

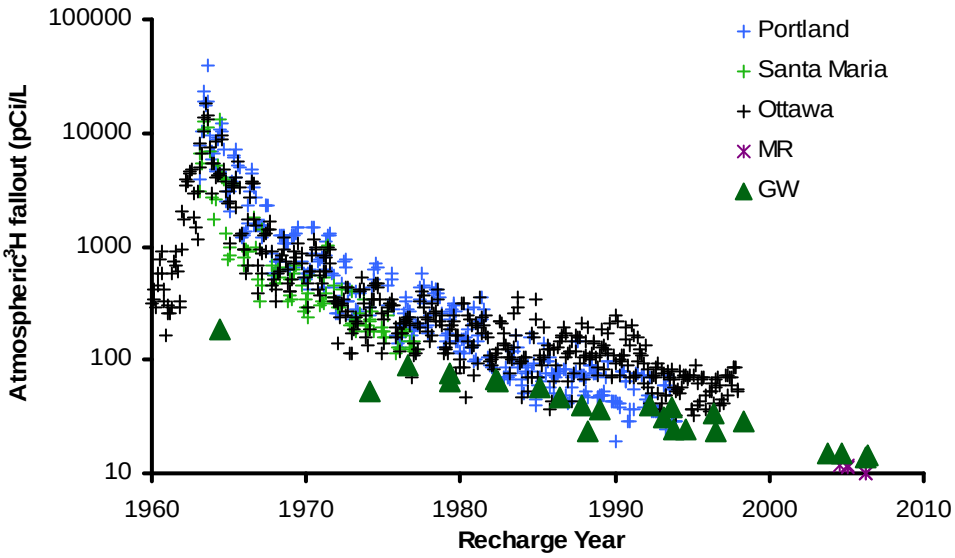

Figure 3.4: Tritium levels measured in precipitation at several locations (Data from IAEA). Decay-corrected tritium in groundwater is also plotted using recharge years corresponding to the estimated $^{3}H/^{3}He$ ages.

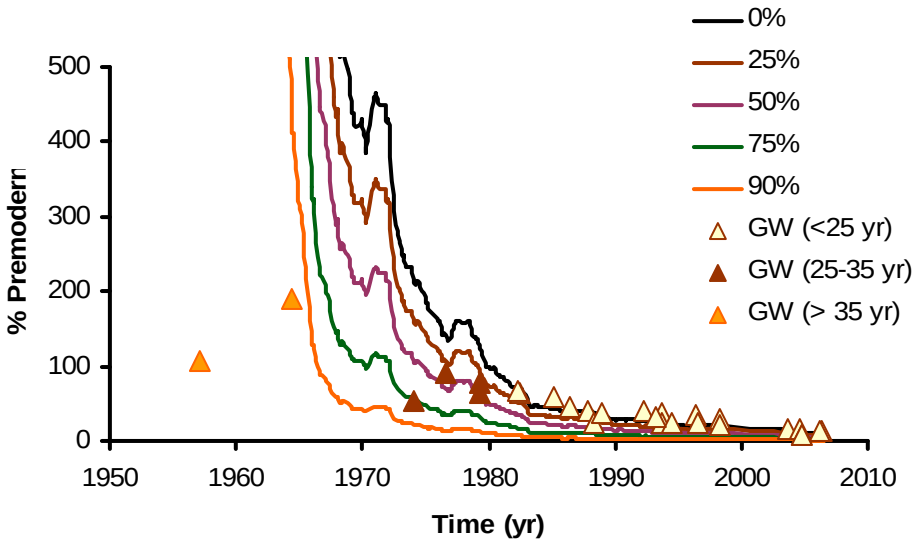

Figure 3.5: Decay corrected ^{3}H in groundwater (based on $^{3}H/^{3}He$ ages) are plotted to the corresponding recharge years, and plot near mixing lines representing the percent premodern groundwater mixed with individual samples (0%, 25%, 50%, 75%, and 90%). Atmospheric ^{3}H fallout was smoothed and plotted verses time (0% line). Atmospheric ^{3}H is based on measurements collected at Santa Maria, CA between 1963 and 1976. Tritium fallout measured at Portland, OR between 1976 and 1993, and Ottawa, ON between 1993 and1997 is scaled to Santa Maria. Merced River ^{3}H values taken during snowmelt between 2004 and 2006 were used as precipitation values occurring after 2000.

values measured in Portland are used between 1976 and 1993, and ^{3}H values measured in Ottawa are used between 1993 and 1997. Both Portland and Ottawa values had to additionally be scaled to assumed Santa Maria values. Merced River samples were also used, and they were assumed to represent fallout between 2004 to 2006. Four additional lines are plotted, which are used to determine the fraction of premodern water. These lines are 25%, 50%, 75%, and 90% less than the estimated mean fallout values. ^{3}H decay corrected groundwater samples plotting nearest these lines indicates the amount of premodern water.

Using the fraction of premodern water only provides a general understanding of how much water is modern, and how much is premodern. The error associated with this method tends to increase with increased $^{3}H/^{3}He$ ages (Manning 2000). Manning showed that for Salt Lake Valley groundwater wells, the error was <10% for apparent groundwater ages 0-10 yrs, < 20% for apparent groundwater ages ranging between 10-20 yrs, < 30% for apparent groundwater ages between 20-30 yrs, and >30% for apparent groundwater ages greater than 30 yrs because of dispersion effects from mixing with the ^{3}H bomb-pulse.

None of the groundwater samples with apparent recharge years less than 25 yrs have significant or detectable premodern water associated with them (Figure 3.5; Table 3.2). Groundwater with apparent ages between 25-35 yrs have approximately 50-75% premodern water, and groundwater with apparent ages greater 35 yrs have greater than 90% premodern water. It is not surprising that the El Portal wells with recently recharged groundwater have no premodern fraction associated with them.

$^4He_{RAD}$ Ages

Radiogenic ^4He ages can also be used as another alternative for estimating groundwater ages. However, this method is typically associated with groundwater with significant ages 100s to 10000 years. In order to make these estimates the helium release rate to water needs to be known in the aquifer, and the residence time is determined by the following equation:

$$\tau = \frac{^4He_{RAD}}{G\left(\frac{1}{n} - 1\right)} \quad (4)$$

Where τ is the residence time, G is the $^4He_{RAD}$ accumulation rate per unit volume of solids per unit time, and n is the porosity (Solomon, 2000b). Radiogenic ^4He is determined by the following equation:

$$^4He_{RAD} = {}^4He_{total} - {}^4He_{Sol} - {}^4He_{EA} - {}^4He_{Mantle} \quad (5)$$

Where $^4He_{total}$ is the total measured ^4He, $^4He_{Sol}$ is the equilibrium solubility ^4He component, $^4He_{EA}$ is the excess air component of ^4He, and $^4He_{Mantle}$ is any mantle component of ^4He. G is dependent on the density and on the ^{238}U, ^{235}U, and ^{232}Th concentrations of the aquifer material, and G typically ranges between 0.28 and 2.4 μcm^3 (STP)$m^{-3}yr^{-1}$. U and Th concentrations in the Sierra Nevada batholith are typically elevated in comparison to other non-granitic locations (Turekian and Wedepohl, 1961; Sawka and Chappell, 1988; House et al., 1997; Coleman et al., 2004; Brady et al., 2005). Based on this observation, G is assumed to be 2.4 μcm^3

(STP)$m^{-3}yr^{-1}$, but it is possible for groundwater ages to be greater if G is much smaller.

$^4He_{RAD}$ ages are also subject to uncertainty due to the large variation and difficulty of determining porosity and heterogeneity of median. Porosity in unconsolidated alluvium typically ranges from 0.2 to 0.5 (Freeze and Cherry, 1979), but groundwater transport time through river alluvium may be too short to incorporate sufficient $^4He_{RAD}$. It is assumed that the source for groundwater, with ages great enough to be detected by the $^4He_{RAD}$ method originates from groundwater flow through fractures, which later discharges into river alluvium where many of the wells are screened. A porosity of 0.01 is used to determine $^4He_{RAD}$ ages, which is a reasonable estimate for the dominantly shallow fractures that are probably interacting with the Merced River alluvium.

One possible area uncertainty for estimating $^4He_{RAD}$ ages is from rapidly releasing $^4He_{RAD}$ from sediment to groundwater. This has been observed in some North American continental glaciated terrain where bedrock with significant $^4He_{RAD}$ build up is eroded and later deposited as alluvium (Torgerson and Clarke, 1985; Solomon et al., 1996; Beyerle et al., 1999; Van der Hoven et al., 2005). The $^4He_{RAD}$ release rate from rock to water can increase significantly because it becomes controlled by diffusion rates rather than U-Th decay rates. In these systems, the $^4He_{RAD}$ age dating method described in equation 2 would significantly overestimate groundwater recharge ages. Although parts of the Merced River basin has been glaciated, and tills have been deposited, this scenario is unlikely for the following reasons: 1) so far, this process has only been

observed in rocks that are Paleozoic or older (>245 ma), and the Sierra Nevada batholith is Mesozoic, and 2) The locations with the most significant build up of $^{4}He_{RAD}$ either occur where there has been no glaciation (e.g. El Portal Well # 2) or directly from springs from fractured rock (e.g. Happy Isles Spring).

Assuming residence times are only controlled by equation (4) and assuming the above values for n and G, $^{4}He_{RAD}$ ages in the Merced River basin range between 0 and 6736 years (Table 3.2). Even if the porosity is under or over estimated, the pattern of $^{4}He_{RAD}$ ages is consistent.

Discussion

Residence Times and Water Chemistry

Cl^- concentrations in groundwater have a positive linear correlation with $^{4}He_{RAD}$ ages, suggesting that groundwater mixes between two endmembers in the Merced River basin (Figure 3.6). The endmember mixing line established from this relationship is essentially the same groundwater mixing line established when $[Cl^-]^{-1}$ is plotted verses $^{36}Cl/Cl$ (Figure 2.4). The low-Cl^- groundwater consists of mostly modern water, while the high-Cl^- groundwater shows high premodern water and $^{4}He_{RAD}$ ages up to 7000 yrs old.

One noticeable deviation from this mixing line is at Happy Isles Spring where Cl^- concentrations are greater than the expected $^{4}He_{RAD}$ age. It still has significantly higher residence times than most samples, but the age is under-predicted relative to the slope of the line. One explanation for this deviation could be that degassing of the spring sample during sampling resulted in an

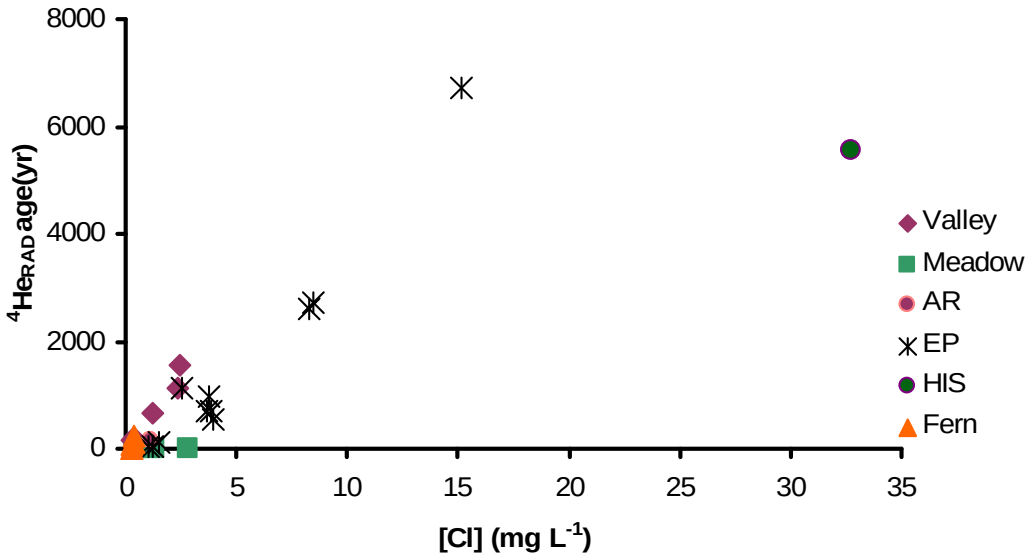

Figure 3.6: Chloride concentration verse $^4He_{RAD}$ ages in groundwater in the Merced River basin.

underestimation of the age. An alternative explanation may also be that the source of elevated Cl^- in these samples is different. The El Portal Wells are located in fractured metasedimentary rock surrounding the Sierra Nevada batholith, while Happy Isles Spring discharges in granitic rocks. Clow et al. (1996) reported elevated Cl^- in the Merced River and springs above Happy Isles closer to the headwaters of the Merced River. The source of Cl^- is not entirely known, but they speculated that it may originate from metasedimentary roof pendants that were once oceanic sediments. Regardless of the source of Cl^- there is at least a relative correlation between age and Cl^- concentrations in the Merced River basin.

The differences between the Cl^- verses $^4He_{RAD}$ ages can be further broken into different reaches of the Merced River basin. The trend is steeper in Yosemite Valley than in El Portal (Figure 3.6). The oldest Yosemite Valley wells are drawing water from below an apparent confining (or semi-confining) layer of glacial flour (Gutenberg et al., 1956). The steeper trend suggests that there may be a source of older groundwater mixing in greater fractions than locations downstream of Yosemite Valley. One explanation for this could be that there is a higher fraction of groundwater from fractured bedrock mixing with the valley alluvium. Recharge temperatures in Yosemite Valley also suggest that more groundwater recharge to these wells occurs from higher elevations than at El Portal, which is likely due to groundwater flowing through fractures in higher quantities in Yosemite Valley. Groundwater flow from fractures has been observed previously in the Merced River basin, including wells in Wawona (Borchers, 1996), and recharge studies at Gin Flat (Flint et al., 2008). The

meadow wells sampled in this study are set in fractured bedrock, and Fern Spring and Happy Isles Spring indicate that groundwater discharges from fractures near the Merced River.

Seasonal Groundwater Age Variations

Locations with samples collected seasonally show temporal variations in $^{3}H/^{3}He$ and $^{4}He_{RAD}$ ages. The most complete data set is the R/R_A values measured at Fern Spring. The R/R_A values at Fern Spring are superimposed on a graph of Merced River flow rates measured at Pohono Bridge (Figure 3.7). Fern Spring was not gauged, but the spring flow rates visually increase with increased flow in the Merced River. During baseflow, the R/R_A ratios are lowest, and they are nearly equilibrated with the atmosphere during snowmelt. The primary mechanism for decreasing R/R_A ratios is incorporation of $^{4}He_{RAD}$ from water flow paths with significant residence times. Samples with R/R_A values near 1 can be interpreted as water with relatively short flow paths and low residence times. $^{3}H/^{3}He$ and $^{4}He_{RAD}$ ages also correlate with R/R_A values. Cl^- values in Fern Spring also increase during baseflow and decrease during snowmelt.

El Portal Well 2 was the only well location where seasonal samples were collected (Figure 3.8). The apparent $^{3}H/^{3}He$ ages increase from ~25-30 yrs to ~40 yrs from snowmelt to baseflow, and the apparent He age increases from ~2600 yrs to ~6700 yrs from snowmelt to baseflow. Cl^- values at El Portal Well 2 also increase by ~7 mg L^{-1} during baseflow (Table 3.2). The R/R_A values did not change significantly because these values were already more than 80% less than atmospherically equilibrated values. High-Cl^- groundwater and low-Cl^-

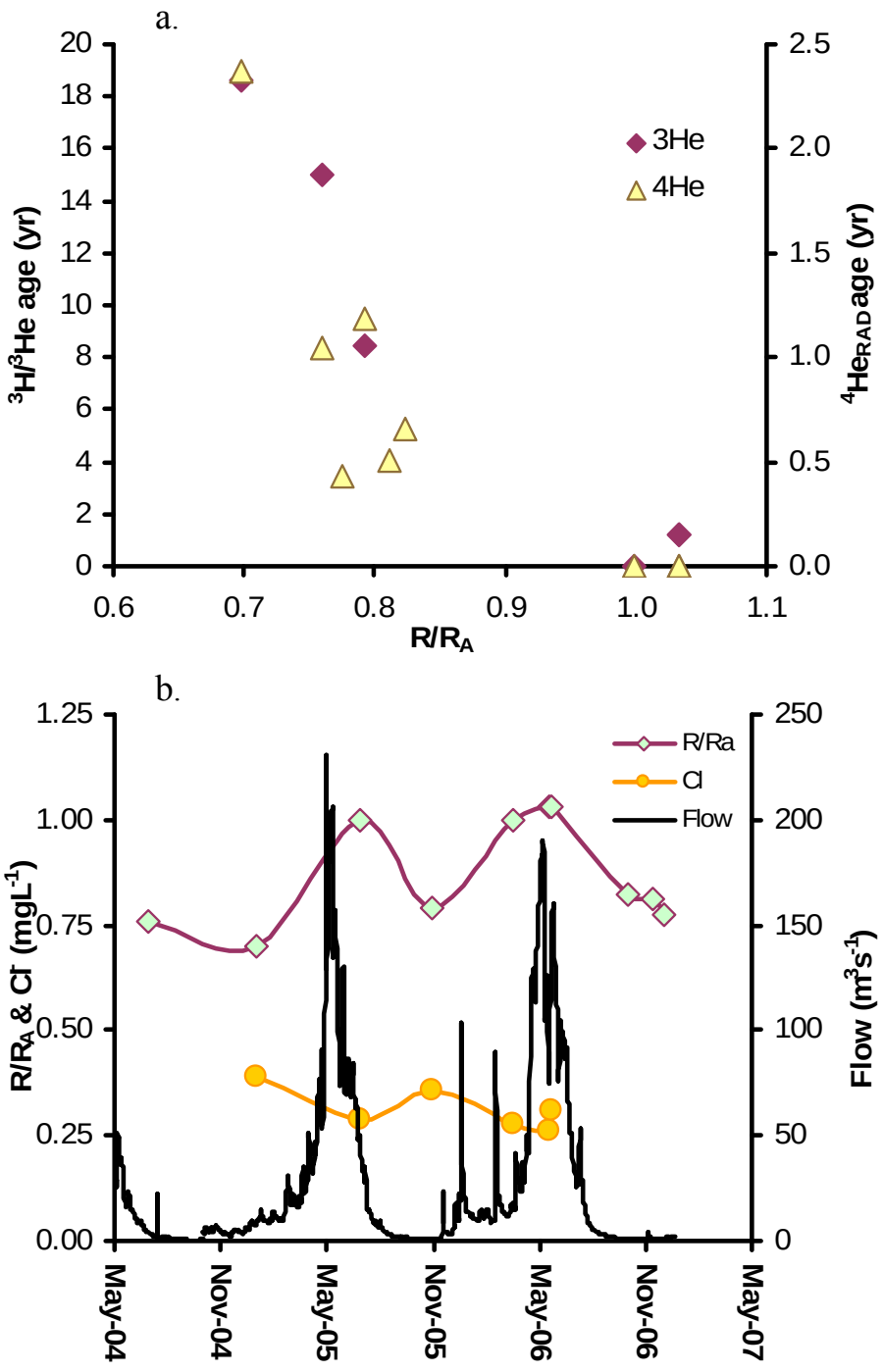

Figure 3.7: Temporal variations at Fern Spring comparing a) $^{3}He/^{4}He$ R/R_A verses $^{3}H/^{3}He$ and $^{4}He_{RAD}$ ages, and b) time verses R/R_A, Cl^-, and flow at Pohono Bridge (flow data come from the California Data Exchange Center, www.cdec.water.ca.gov).

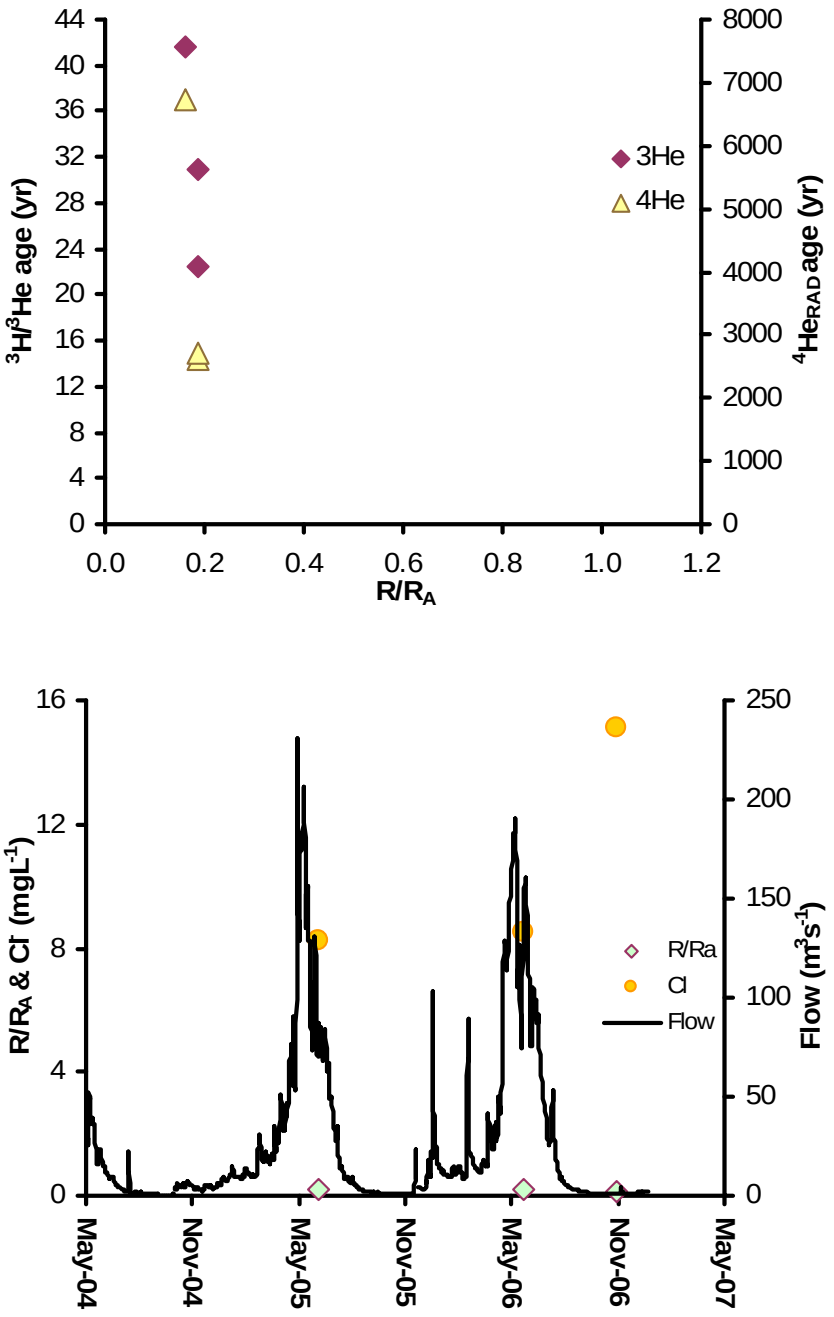

Figure 3.8: Temporal variations at El Portal Well 2 comparing a) $^{3}He/^{4}He$ R/R_A verses $^{3}H/^{3}He$ and $^{4}He_{RAD}$ ages, and b) time verses R/R_A, Cl^-, and flow at Pohono Bridge (Flow data come from the California Data Exchange Center, www.cdec.water.ca.gov).

groundwater mixes in different proportions is subject to seasonal variations within the Merced River (see Chapter 2).

We hypothesize that the seasonality in residence times is associated with a shifting between water sources. Fern Spring and El Portal Well 2 have different geochemical signatures, are located in different reaches along the Merced River, and have differences in residence times, but the seasonal fluctuations observed in both locations suggest that all groundwater sources are subject to some seasonality.

Mixing between source waters, including seasonal fluctuations may be connected to different characteristics of water observed in two vertically stratified groundwater aquifers near Wawona, each with unique geochemistry and apparent residence times (Borchers, 1996; Nimz, 1998). The shallow aquifer is less than 100 m deep, has low ion concentrations, and has ^{3}H and $^{36}Cl/Cl$ ratios indicating recharge after above-ground thermonuclear weapons testing (anthropogenic). The deeper aquifer is below 100 m deep, has elevated ion concentrations, and has pre-anthropogenic ^{3}H and $^{36}Cl/Cl$. Deep groundwater in Wawona has $^{36}Cl/Cl$ ratios $<30x10^{-15}$ (Nimz, 1998), which is significantly lower than the secular equilibrium $^{36}Cl/Cl$ ratio of host rocks (Nimz, et al., 1993; Nimz et al., 1997). This may suggest groundwater residence times higher than $^{4}He_{RAD}$ ages measured in the Merced River wells. The water in Wawona was sampled from fractured bedrock, and there is limited mixing between the deep and shallow groundwater (Borchers, 1996; Nimz 1998). The only wells with apparent mixing occur near 100 m, near the boundary between the two aquifers. The mixed wells in Wawona actually

have similar Cl^- concentrations (chloride concentrations of 31.5 mg L-1) as the high-Cl^- groundwater observed mixing with the Merced River (see Chapter 2). The median Cl^- concentrations in the shallow Wawona aquifer (0.8 mg L^{-1}) are similar to the low-Cl^- groundwater observed mixing with the Merced River (see Chapter 2). The deep Wawona groundwater has median Cl^-, and 100 mg L^{-1}, which is significantly elevated in comparison to any groundwater samples near the Merced River (Borchers 1996).

The groundwater chemistry and $^4He_{RAD}$ ages of the high-Cl^- groundwater mixing with the Merced River is similar to water samples that are a mixture of the deep and shallow groundwater observed in Wawona. This suggests that sources similar to Wawona may be mixing with the Merced River; furthermore, the temporal variations in groundwater endmember fractions are likely controlling the temporal age variations in the Merced River.

Evidence of Old Water

The groundwater ages and fraction of premodern water estimated cannot be sufficiently correlated with the lateral or vertical relationship between water entering wells throughout the catchment. Instead, the variations seem to depend on the physical characteristics of aquifers providing water to the wells. El Portal is perhaps the most anomalous reach of the watershed because high $^4He_{RAD}$ ages are the highest, but $^3H/^3He$ ages and fraction premodern water are typically the lowest in the watershed (Table 3.2). The majority of groundwater in El Portal has close to no apparent $^3H/^3He$ ages and ~0% premodern water. Furthermore the recharge elevations indicate that the primary source of recharge occurs locally near the well

elevations. One explanation could be that the majority of water in this stretch of the river is recently recharged river water, but there is a small fraction of very old groundwater discharging to the river alluvium as well.

Evidence of premodern groundwater flow to the river alluvium in El Portal is strengthened by comparing the $^{3}He/^{4}He$ ratios of surface water where the ratio is significantly lower than air-equilibrated ratios. In July, 2004 R/R_A was also measured along with conductivity Merced River near the confluence with Cold Creek (which was dry). The elevated ^{222}Rn at this location suggests that there is an input of groundwater from fractures discharging to the river (Table 3.4). R/R_A decreased from 1.0 upstream the fracture zone to 0.82 near the confluence with Cold Creek. Approximately 80% of the helium comes from equilibration with air-derived helium—probably from river water contact time with the atmosphere. If this component is subtracted from the $^{3}He/^{4}He$ ratio, then a ratio of $2.0x10^{-7}$ g cm^{-3}_STP results, which is nearly identical to $^{3}He/^{4}He_{RAD}$ estimated in the basin. The most plausible explanation for this is the absence of ^{3}He from tritium decay because the majority of the discharging groundwater is premodern water. This is corroborated by an increase in conductivity from 24 μScm^{-1} to 36 μScm^{-1} at the confluence of Cold Creek. It is likely that these observations are from high-Cl^- groundwater with premodern residence times discharging to the Merced River.

The placement of wells in El Portal also suggests that wells nearest fracture zones have the highest $^{4}He_{RAD}$ ages. Figure 3.9 shows that wells placed upstream of El Portal Well 2 have the lowest groundwater ages, while El Portal

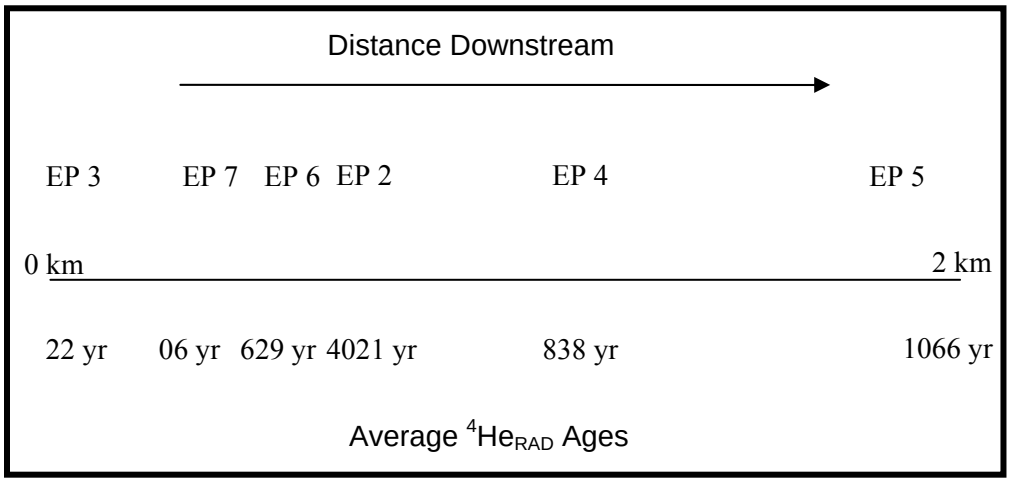

Figure 3.9: A schematic of El Portal Wells, indicating approximate distances downstream and $^4He_{RAD}$ ages averaged for each sampling event.

Well 2 has the highest groundwater age. Wells downstream progressively decrease in apparent ages. This pattern suggests that there may be groundwater discharging from fractures near El Portal Well 2, while there are no groundwater inputs directly upstream El Portal Well 2. The decrease in ages downstream of El Portal Well 2 suggests either dilution from younger water recharging river alluvium, or less fractured groundwater discharge than at El Portal Well 2.

Vulnerability to Climate Change

The increased apparent ages associated with high-Cl^- groundwater suggest that this endmember may be less vulnerable to perturbations such as climate change. The increase in conductivity observed in the Merced River during baseflow proceeding dry water years shows that near-surface water and the low-Cl^- groundwater is more vulnerable to seasonal perturbations (Figure 3.2). This suggests that if snowmelt occurs earlier and the dry season is lengthened, then the high-Cl^- groundwater may be critical for providing baseflow to the Merced River. As a result, a longer term increase in conductivity may be observed during baseflow as climate changes.

One result of decreased snowpack, earlier snowmelt, and increased baseflow seasons could be a decrease in hydrostatic pressure during snowmelt. Wells throughout the basin are artesian during snowmelt, but they are not artesian during baseflow. Furthermore, flow pulses such as at Fern Spring also indicate the importance of hydrostatic pressure to flow rate. If the decrease in hydrostatic pressure were significant enough, it may result in less groundwater discharge to the system, and possibly "shut off" flow of high-Cl^- groundwater to surface water

seasonally. Current observations of conductivity with time indicate that this is not occurring in the Merced River basin (Figure 3.2). Even ^{222}Rn activity at cold creek canyon indicates that groundwater continues to discharge during baseflow even during dry years (Table 3.3).

Conclusions

In the American West, snowmelt is occurring earlier and average snowpack is declining due to increased temperatures. As climate warms, the amount of precipitation may not fluctuate as much as the timing and type of precipitation. The impact on mountain groundwater is not well understood, and establishing an understanding of spatial and temporal groundwater residence time trends provides an important step in characterizing the response of groundwater to climate change. The estimated residence times between the different groundwater bodies provide the framework for understanding how vulnerable groundwater is toward major perturbations, such as response to climate change. The apparent young age of low-Cl^- groundwater, and the nearly instantaneous response to snowmelt suggests that this groundwater body may be the most vulnerable to climate change. The greater residence times of contributions of high-Cl^- groundwater might damp out climate perturbations.

References

Aeschbach-Hertig, W., F. Peeters, U. Beyerle, and R. Kipfer, Paleotemperature reconstruction from noble gases in ground water taking into account equilibration with entrapped air, *Nature*, 405, 1040-1044, 2000

Aquilina, L., J. W. de Dreuzy, O. Bour, and P. Davy, Porosity and fluid velocity in the upper continental crust (2-4 km) inferred from injection tests at the Soultz-sous-Forêts geothermal site, *Geochimica et Cosmochimica Acta*, 68, 2405-2415, 2004.

Bales, R. C., N. P. Molotch, T. H. Painter, M. D. Dettinger, R. Rice, and J. Dozier, Mountain hydrology of the western United States, *Water Resources Research*, 42, W08432, 2006.

Bateman, P. C., Plutonism in the central part of the Sierra Nevada batholith, *U. S. Geological Survey Professional Paper 1483*, 186 pp., 1992.

Bateman, P. C., and C, Wahrhiftig, Geology of the Sierra Nevada, In Bailey, E, H., ed. *Geology of Northern California, California Division of Mines and Geology Bulletin*, 190: 107-172, 1966.

Beyerle, U., W. Aeschbach-Hertig, M. Hofer, D. M. Imboden, H. Baur, and R. Kipfer, Infiltration of river water to a shallow aquifer investigated with $^{3}H/^{3}He$, noble gases, and CFCs, *Journal of Hydrology*, 220, 169-185, 1999.

Borchers, James, W., Ground-water resources and water-supply alternatives in the Wawona area of Yosemite National Park, California, *U.S. Geological Survey Water-Resources Investigations Report 95-4229*, pp 77, 1996.

Brace, W. F., Dilantancy-related electrical resistivity changes in rocks, *Pure and Applied Geophysics*, 113, 207-217, 1975.

Brady, R. J., M. N. Ducea, S. B. Kidder, and J. B. Saleeby, The distribution of radiogenic heat production as a function of depth in the Sierra Nevada batholith, California, *Lithosphere*, 86, 229-244, 2005.

Castro, M. C., C. M. Hall, D. Patriarche, P. Goblet, and B. R. Ellis, A new noble gas paleoclimated record in Texas—basic assumptions revisited, *Earth and Planetary Science Letters*, 257, 170-187, 2007.

Cey, B. D., G. B. Hudson, J. E. Moran, and B. R. Scanlon, Impact of artificial recharge on dissolved noble gases in groundwater in California, *Environmental Science and Technology*, 42, 1017-1023, 2008.

Clow, D. W., M. A. Mast, and D. H. Campbell, Controls on surface water chemistry in the upper Merced River Basin, Yosemite National Park, California, *Hydrological Processes*, 10, 727-746, 1996.

Coleman, D. S., A. F. Glazner, J. S. Miller, K. J. Bradford, T. P. Frost, J. L. Joye, C. A. Bachl, Exposure of a late Cretaceous layered mafic-felsic magma system in the Central Sierra Nevada batholith, California, *Contributions to Mineralogy and Petrology*, 120, 129-136, 2004.

Earman, S. A. R. Campbell, B. D. Newman, and F. M. Phillips, Isotopic exchange between snow and atmospheric water vapor: Estimation of the snowmelt component of groundwater recharge in the southwestern United States, *Journal of Geophysical Research*, 111, D09302, doi: 10.1029/2005JD006470, 2006.

Ericson, K., P. Migon, and M. Olvmo, Fractures and drainage in the granite mountainous area—a study from Sierra Nevada, USA, *Geomorphology*, 64 (1-2), 97-116, 2005.

Flint, A. L., L. E. Flint, and M. D. Dettinger, Modeling soil moisture processes and recharge under a melting snowpack, *Vadose Zone Journal*, 7, 350-357, 2008.

Freeze, R. A., and J. A. Cherry, *Groundwater*, Prentice Hall, Englewood Cliffs, NJ, 604 pp., 1979.

Gutenberg, B., J. P. Buwalda, and P. Sharp, Seismic explorations on the floor of Yosemite Valley, California, *Bulletin of the Geological Society of America*, 67, 1051-1078, 1956.

Hood, J. L., J. W. Roy, and M. Hayashi, Importance of groundwater in the water balance of an alpine headwater lake, *Geophysical Research Letters*, 33, L13405, 2006.

House, M. A., B. P. Wernicke, K. A. Farley, and T. A. Dumitru, Cenozoic thermal evolution of the Central Sierra Nevada, California, from (U-Th)/He thermochronometry, *Earth and Planetary Science Letters*, 151, 167-179, 1997.

Hudson, G.B. J. E. Moran, G. F. Eaton, Interpretation of Tritium-3Helium Groundwater Ages and Associated Dissolved Noble Gas Results from Public Supply Wells in the Los Angeles Physiographic Basin: *Report to California State Water Resources Control Board, Lawrence Livermore National Laboratory*, 59 pp., 2002. http://www.llnl.gov/tid/lof/documents/pdf/245359.pdf

Jahns, R. H., Sheet structure in granites: its origin and use as a measure of glacial erosion in New England, *Journal of Geology*, 11 (2), 71-98, 1943.

Knowles, N., M. D. Dettinger, and D. R. Cayan, Trends in snowfall vs. rainfall in the Western United States, *Journal of Climate*, 119, 4545-4559, 2006.

Lundquist, J. D., and D. R. Cayan, Surface temperature patterns in complex terrain: daily variations and long-term change in the central Sierra Nevada, California, *Journal of Geophysical Research*, 112, D11124, 2007.

Maloszewski, P. W., A. Zuber, Determining the turnover time of groundwater systems with the aid of environmental tracers. 1. models and their applicability, *Journal of Hydrology*, 57, 207-231, 1982.

Manning, A. H., J. S. Caine, Groundwater noble gas, age, and temperature signatures in an alpine watershed: Valuable tools in conceptual model development, *Water Resources Research*, 43, WO4404, 2007.

Manning, A. H., and D. K. Solomon, Using noble gases to investigate mountain-front recharge, *Journal of Hydrology*, 275, 194-207, 2003.

Manning, A. H., D. K. Solomon, and S. Thiros, On the utility of 3H/3He age data in assessment of well susceptibility, *Ground Water*, 43, 353-367, 2005.

Manning A. H., and D. K. Solomon, An integrated environmental tracer approach to characterizing groundwater circulation in a mountain block, *Water Resources Research*, 41, W12412, 2005.

Manning, A. H., Using noble gas tracers to investigate mountain-block recharge to an intermountain basin, *Ph.D. Dissertation, University of Utah*, 187 pp., 2002.

Moline, G. R., M. R. Schreiber, J. M. Bahr, Representative ground water monitoring in fractured porous systems, *Journal of Environmental Engineering*, 124 (6), 530-538, 1998.

Nimz, G., Lithogenic and cosmogenic tracers in catchment hydrology, in *Isotope Tracers in Catchment Hydrology*, edited by K. Kendall and J. J. McDonnell, 1, Elsevier, New York, 291-318, 1998.

Nimz, G. J., M. W. Caffee, and J. W. Borchers, Extremely low $^{36}Cl/Cl$ values in deep groundwater at Wawona, Yosemite National Park, California: evidence for rapid upwelling of deep crustal waters? *EOS, Transactions American Geophysical Union*, 74, 582, 1993.

Nimz, G. J., Moore, J. N., and P. W. Kasameyer, $^{36}Cl/Cl$ ratios in geothermal systems: preliminary measurements from the Coso Field, *Geothermal Resources Council Transactions*, 21, 211-217, 1997.

Park, C. K., T. T. Vandergraaf, D. J. Drew, and P. S. Hahn, Analysis of the migration of nonsorbing tracers in a natural fracture in granite using a variable aperture channel model, *Journal of Contaminant Hydrology*, 26, 97-108, 1997.

Plummer, L. N., E. Busenberg, J. K. Böhlke, R. L. Michel, and P. Schlosser, Groundwater residence times in Shenendoah National Park, Blue Ridge Mountains, Virginia, USA: a multi-tracer approach, *Chemical Geology*, 179, 93-111, 2001.

Rademacher, L. K., J. F. Clark, G. B. Hudson, D. C. Erman, and N. A. Erman, Chemical evolution of shallow groundwater as recorded by springs, Sagehen basin; Nevada County, California, *Chemical Geology*, 179, 37-51, 2001.

Rademacher, L. K., J. F. Clark, D. W. Clow, and G. B. Hudson, Old groundwater influence on stream hydrochemistry and catchment response times in a small Sierra Nevada catchment: Sagehen Creek, California, *Water Resources Research*, 41, W02004, 2005.

Rauscher, S. A., J. S. Pal, N. S. Diffenbaugh, and M. M. Benedetti, Future changes in snowmelt-driven runoff timing over the western US, *Geophysical Research Letters*, 35, L16703, 2008.

Rice, R. R. Bales, T. H. Painter, and J. Dozier, Snowcover along elevation gradients in the Upper Merced and Tuolumne River basins of the Sierra Nevada of California from MODIS and blended ground data, *Proceedings from 75th Annual Western Snow Conference*, 3-14, 2007.

Riebe, C. S., J. W. Kirchner, D. E. Granger, and R. C. Finkel, Minimal climate control on erosion rates in the Sierra Nevada, California, *Geology*, 29, 447-450, 2001.

Sawka, W. N., and B. W. Chappell, Fractionation of uranium, thorium, and rare earth elements in a vertically zoned granodiorite: Implications for heat production distributions in the Sierra Nevada batholith, California, U.S.A., *Geochimica et Cosmochimica Acta*, 52, 1131-1143, 1988.

Segall, P., E. H., McKee, S. J. Martel, and B. D. Turrin, Late Cretaceous age of fractures in the Sierra-Nevada Batholith, California, *Geology*, 18(12), 1248-1251, 1990.

Seta, Akihiro, Takuya Matsumoto, and Jun-ichi Matsuda, Concurrent evolution of $^{3}He/^{4}He$ ratio in the Earth's mantle reservoirs for the first 2 Ga, *Earth and Planetary Science Letters*, 281 (1-2), 211-219, 2001.

Solomon, D. K., and P. G. Cook, ^{3}H and ^{3}He, in *Environmental Tracers in Subsurface Hydrology*, P. G. Cook and A. L. Herczeg, eds., Kluwer Academic Press, 397-424, 2000a.

Solomon, D. K., 4He in Groundwater, in *Environmental Tracers in Subsurface Hydrology*, P. G. Cook and A. L. Herczeg, eds., Kluwer Academic Press, 425-439, 2000b

Solomon, D. K., A. Hunt, and R. J. Poreda, Source of radiogenic ^{4}He in shallow aquifers: Implications for dating young groundwater, *Water Resources Research*, 32, 1805-1813, 1996.

Snow, D. T., Rock fracture spacings, openings, and porosities, Proceedings from the American Society of Civil Engineers, *Journal of Soil Mechanics Foundation Division*, 94, 73-91, 1968.

Stute, M., and P. Schlosser, Atmospheric Noble Gases, in *Environmental Tracers in Subsurface Hydrology*, P. G. Cook and A. L. Herczeg, eds., Kluwer Academic Press, 349-377, 2000.

Torgerson, T., and W. B. Clarke, Helium accumulation in groundwater, I: An evaluation of sources and the continental flux of crustal ^{4}He in the Great Artesian Basin, Australia, *Geochimica et Cosmochimica Acta*, 49, 1211-1218, 1985.

Turekian, K. K., and K. H. Wedepohl, Distribution of the elements in some major units of the Earth's crust, *Geological Society of America Bulletin*, 72, 175-192, 1961.

Van der Hoven, S. J., R. E. Wright, D. A. Carstens, and K. C. Hackley, Radiogenic ^{4}He as a conservative tracer in buried-valley aquifers, *Water Resources Research*, 41, W11414, 2005.

Visser, A., H. P. Broers, and M. F. P. Bierkens, Dating degassed groundwater with $^{3}H/^{3}He$, *Water Resources Research*, 43, W10434, doi:10.1029/2006WR005847, 2007.

Viviroli, D., H. H. Durr, B. Messerli, M. Meybeck, Mountains of the world, water towers for humanity: typology, mapping, and global significance, *Water Resources Research*, 43, W07447, 2007.

Wakabayashi, J., and T. L. Sawyer, Stream incision, tectonics, uplift, and evolution of topography of the Sierra Nevada, California, *Journal of Geology*, 109, pp539, 2001.

Warhaftig, C., Stepped topography of the Southern Sierra Nevada, California, *Geological Society of America Bulletin*, 76, 1165-1190, 1965.

Wilson, J. L., and H. Guan, Mountain-block hydrology and mountain-front recharge, in *Groundwater Recharge in a Desert Environment: The Southwestern United States*, edited by F. M. Phillips, J. H. Hogan, and B. Scanlon, AGU, Washington, DC, 2004.

CHAPTER 4

LOCAL GROUNDWATER DISCHARGE TO SURFACE WATER IN THE MERCED RIVER BASIN: COMPARING GLACIAL AND RIVER-CUT REACHES USING ^{222}Rn AND ^{3}He/^{4}He

Abstract

Dissolved ^{222}Rn and ^{3}He/^{4}He (expressed as R/R_A) were measured in surface water, springs, and groundwater in the upper Merced River basin, starting in the glacially carved Yosemite Valley and ending in the river-cut reaches in the foothills of the Sierra Nevada. Box models were used to estimate the spatial and temporal groundwater fractions and groundwater fluxes in locations where groundwater enters the Merced River. The fluxes of groundwater are higher in Yosemite Valley, a U-shaped valley consisting of alluvium ~300 m thick and ~1000m wide. Groundwater discharge in the glacially carved valley reaches occurs as spatially continuous groundwater fluxes to surface water, whereas groundwater discharge in the river-cut valley downstream occurs at discrete fracture zones. Groundwater discharge to the river is also higher near tributary catchments with higher elevations suggesting that more recharge occurs where snowpack is largest. Groundwater discharges in higher fractions throughout the

watershed during baseflow than during snowmelt. R/R_A in surface water also decreases during baseflow, suggesting substantial enough residence times to build up radiogenic helium in the discharging groundwater.

Introduction

Recent advances in hydrology stress the importance of groundwater interactions with surface water within a mountain block (Liu et al., 2004; Hood et al., 2006). Groundwater plays an important role in controlling surface water chemistry, which in turn plays an important role in ecohydrology (Clow and Sueker, 2000; Williams et al., 2005; Liu et al., 2008). Water originating within a mountain block provides downstream communities with water for power generation, agriculture, and drinking water (Bales, et al., 2006). Understanding of the groundwater flow paths and how they interact with surface water provides information for assessing these resources. The need for characterizing water resources in mountains is even more essential because of potential changes in mountain water fluxes stemming from climate change (Bales et al., 2006; Earman et al., 2006).

Box models are appropriate for determining groundwater fluxes to surface water bodies with groundwater inputs (Genereux & Hemond, 1990; Wanninkof et al., 1990; Genereux et al., 1993; Folger et al., 1996; Hamada, 1999; Cecil & Green, 2000; Cook et al., 2003; Hofmann, 2004; Wu & Zhang, 2004). In order to characterize groundwater and surface water interactions, many studies use physical flow and hydraulic head information combined with numerical simulations, or they use environmental tracers that are essentially conservative in

combination with mixing models such as endmember mixing analyses (Martinec et al., 1982; Maloszewski et al., 1982; Maloszewski et al., 1983; Maurer, 1986; Constanz, 1998; Sueker et al., 2000; Mattle, 2001; Maurer, 2002; Liu et al., 2004). Typical tracers include major ions (SO_4^{2-}, F^-, Cl^-, Ca^{2+}, Mg^{2+}, Na^+, and K^+) and stable isotopes (^{18}O and ^{2}H), but several other tracers can also be used. Using conservative tracers generally results in characterizing groundwater quantities that occur within the entire basin above sampling locations. Dissolved gases in groundwater discharging to surface water may provide a method for identifying groundwater and surface water interactions within a watershed (Genereux and Hemond, 1992; Choi et al., 1998; Rathbun, 1998). Although degassing may complicate the use of dissolved gases for quantifying groundwater flow occurring in the entire basin, dissolved gases can be used to quantify groundwater discharge to surface water at point locations. ^{222}Rn is ideal for this application and has been used extensively to track subsurface discharge to surface water bodies (Rogers, 1958; Hoen & Von Gunten, 1989; Genereux & Hemond, 1990; Wanninkof et al., 1990; Genereux et al., 1993; Folger et al., 1996; Hamada, 1999; Cecil & Green, 2000; Cook et al., 2003; Hofmann, 2004; Wu & Zhang, 2004).

The purpose of the research presented in this chapter was to use dissolved gases (^{222}Rn and $^{3}He/^{4}He$) to investigate point locations where groundwater interacts with surface water within a glaciated reach and a stream-cut reach of the Merced River basin, California. It was hypothesized that the spatial variations at point locations would elucidate groundwater discharge processes occurring within the watershed, and that combining point locations would allow further characterization of

controls on groundwater interactions with surface water. Additionally, it was hypothesized that the spatial controls would be different between Yosemite Valley, which has large glacial till deposits, and the area downstream of Yosemite Valley, which has relatively thin river alluvium deposits. ^{222}Rn, and ^{3}He and ^{4}He were used to investigate these processes.

The questions addressed in this chapter are, 1) What processes control groundwater discharge to the Merced River within glacially-cut reaches and stream-cut reaches of the Merced River basin? and 2) What are the implications for groundwater recharge throughout the basin?

Background

^{222}Rn is a daughter product of the U-decay sequence; therefore, dissolved ^{222}Rn activity is a function of U and Th abundance in the surrounding bedrock or soil that groundwater flows through (Brooklin, 1991; Szabo & Zapecza, 1991; Cecil and Green, 2000; Isam et al., 2002). The half life of ^{222}Rn is 3.8 days, which typically limits its use to determining locations and fluxes where groundwater discharges. If radon flows through the watershed for approximately one month in soil or bedrock with a uniform ^{222}Rn emission rate, an equilibrium radon activity will be reached in the subsurface (Krishnaswami & Seidemann, 1988; Wanty et al., 1991; Torgerson et al., 1992; Cecil & Green, 2000). In locations where subsurface water discharges to surface water, ^{222}Rn activity is high, but it degasses downstream of these discharge locations. In mountain streams, gas exchange is typically rapid (Wanninkof et al., 1990; Genereux and Hemond, 1992), so locations where ^{222}Rn activity is elevated may only represent a small reach of the river where the measured radon entered the

stream. These local influences can be used to understand groundwater discharge processes both temporally and spatially.

As U and Th decays in the subsurface, emitted alpha particles are also released, and they are sometimes released to subsurface water (Solomon, 2000). The $^{3}He/^{4}He$ R/R_A values can also be used to identify locations where groundwater discharge occurs, and to determine relative ages of groundwater discharging to surface water.

Modeling

Radon box models are used in this study to estimate groundwater fluxes to the Merced River. The first approach is to use a mass fraction model that provides a fraction of groundwater mixing with surface water, and the second approach is to use a mass balance approach where fluxes can be quantified in some locations where groundwater enters the river.

Mass Fraction approach

The percent groundwater can be estimated at sampling locations in surface water by the determined at a given location by the following equation:

$$f_G = \frac{Q_G}{Q_S}100\% = \frac{C_S - C_b}{C_G - C_b}100\% \qquad (4.1)$$

where f_{gw} is the fraction of groundwater (%), Q_G is the flow of groundwater discharge ($m^3\ s^{-1}$), Q_S is the surface water in the location of measurement ($m^3\ s^{-1}$), C_S is the surface water concentration of ^{222}Rn (cpm), and C_G is the groundwater

concentration of ^{222}Rn (cpm), and C_b is the background ^{222}Rn activity (cpm) (Hamada., 1999; Wu & Zhang, 2004). C_b is any residual ^{222}Rn activity originating from upstream the sampling locations (i.e. ^{222}Rn that is not entirely degassed), because surface water in equilibrium with the atmosphere has ~0 ^{222}Rn activity.

Gas exchange in the Merced River is rapid because surface water is typically swift, shallow, and turbulent. Based on the gas exchange velocities estimated in the Merced River, it is likely that the estimated groundwater fractions of groundwater represent only a short reach of river where groundwater may have entered the system. Because of the high gas exchange, C_b is assumed to be negligible, and equation 4.1 simplifies to:

$$f_G = \frac{C_S}{C_G} 100\% \qquad (4.2)$$

Mass Balance Approach

A mass balance approach can be used to describe inputs and outputs of ^{222}Rn into as a one-dimensional, steady-state, box model with no storage or inflows (Figure 4.1). At the upstream end of the box model the inflow of ^{222}Rn is determined by the gas flux that enters the box model at the upstream cross-sectional area of the stream (F_{in}) is defined as:

$$F_{in} = QC_i \qquad (4.3)$$

where Q is the surface water flow rate ($m^3\ s^{-1}$) into the box, and C_i (cpm m^{-3}) is background ^{222}Rn that has not degassed before entering the box.

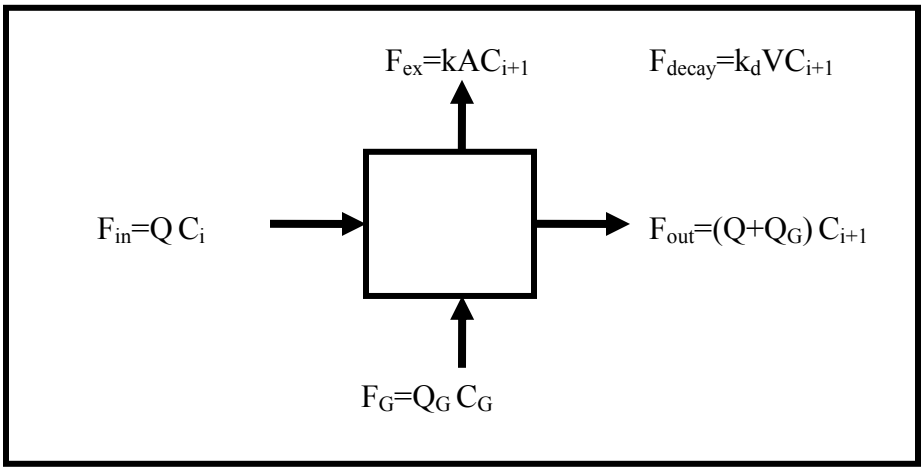

Figure 4.1: This figure shows a control volume, assuming a plug flow model, and it represents a portion of a river with inputs and outputs of ^{222}Rn.

The inflow of radon in groundwater (F_G) is also expressed as:

$$F_G = Q_G C_G \tag{4.4}$$

where Q_G (m^3 s^{-1}) is the groundwater flow rate into the box.

The outflowing ^{222}Rn (F_{out}) can be described as:

$$F_{out} = (Q + Q_G)C_{i+1} \tag{4.5}$$

where C_{i+1} (cpm) is ^{222}Rn activity of water flowing out of the box model. Degassing is described as:

$$F_{ex} = kAC_{i+1} \tag{4.6}$$

where k is the gas exchange velocity (m s^{-1}), and A (m^2) is the area of the river reach that exchange occurs over.

Radioactive decay of ^{222}Rn is described as:

$$F_{decay} = k_d VC_{i+1} \tag{4.7}$$

where k_d is the radon decay coefficient (2.08×10^{-6} s^{-1}), and V (m^3) is the river volume of the reach where decay occurs.

Combining all the outflows and inflows and taking into account radioactive decay of Rn results in the following:

$$0 = QC_i + Q_G C_G - kAC_{i+1} - k_d VC_{i+1} - (Q + Q_G)C_{i+1} \tag{4.8}$$

In order to solve for the downstream ^{222}Rn activity, Equations 4.15 can be rearranged to:

$$C_{i+1} = \frac{\left[QC_i + Q_G C_G\right]}{\left[kA + k_d V + Q + Q_G\right]} \tag{4.9}$$

Gas Exchange

Degassing must be quantified in order to determine groundwater fluxes using equation 4.9. Radon is a compound with chemical and physical properties allowing it to move freely between the water and air phases, and understanding the gas exchange velocity of radon is essential in understanding its fate and transport in streams (Genereaux & Hemond, 1992; Rathbun, 1998). Gas exchange is a first-order process in which the rate of the reaction is directly proportional to the concentration of the species. The rate of the exchange is described as

$$\frac{dC}{dt} = \lambda(C - C_{ATM}) \tag{4.10}$$

where C (cpm) is the concentration of the gas in the water, t (s) is the time, λ (s^{-1}) is the gas exchange coefficient, C_{ATM} (cpm) is what the gas concentration would be if fully equilibrated with the atmospheric concentration (Clark et al., 1992; Wanninkhof, 1992; Rathbun 1998). However, in the case of ^{222}Rn in most surface water bodies, C_{ATM} is negligible and equation 11 becomes:

$$\frac{dC}{dt} = \lambda C \tag{4.11}$$

The relationship between the gas exchange coefficient and the gas exchange velocity (k) can be developed by considering the mass flux, N [MLT^{-1}] defined as:

$$N = b\frac{dC}{dt} \tag{4.12}$$

where b is the average stream depth (m). The mass flux can also be defined as

$$N = k(C - C_{ATM}). \tag{4.13}$$

By setting equations 4.12 and 4.13 equal, and dividing it into equation 4.10 the following relationship is found:

$$k = \lambda b \tag{4.14}$$

According to the "Two-Film Model", both the water phase and the air phase are assumed to be uniformly mixed, but are separated by two films of air and water in which the rate of mass transfer is only by molecular diffusion (Lewis & Whitman, 1924; Rathbun, 1998). The exchange outside of these two films is believed to be fast, and therefore most of the concentration gradient only exists in the two films. It is also assumed that the interface between the air and the water films has no resistance to gas exchange. Although the exchange occurs mostly in the air and water films, it is difficult to determine concentrations in these two films, and thus it is necessary to assume that the overall concentration in the

stream and the overall concentration in the air constitute the driving force in the air-water exchange.

Gas exchange increases as the stream velocity increases (Wanninkhof et al., 1990; Genereaux & Hemnond, 1992; Rathbun, 1998). As the velocity increases, more turbulence occurs in the water phase, thus reducing the water film thickness and increasing the gas exchange coefficient and velocity. This creates a higher rate of gas exchange. Smooth or laminar flow allows a thicker water film thickness which decreases the gas exchange velocity.

If the two-film model is appropriate for a stream, then gas exchange occurs mostly at the air-water interface, and the exchange rate is highly dependent on the aqueous diffusion coefficients (D) [L^2T^{-1}], where the gas exchange velocity can be described as

$$k = \frac{D}{\delta} \tag{4.15}$$

where δ [L] is the thickness of the water film (Genereaux & Hemond, 1992; Rathbun, 1998). Wanninkhof (1992) says that the gas exchange velocity is not just a function of the gas diffusion coefficient, but the ratio of gas diffusion coefficient to kinematic fluid viscosity (μ) [L^2T^{-1}]. The ratio of (D/μ) is defined as the Schmidt number (Sc), and λ is proportional to $(Sc)^{-2/3}$ for a smooth liquid interface (Deacon, 1977), and λ is proportional to $(Sc)^{-1/2}$ for a more turbulent liquid interface (Ledwell, 1984; Coantic, 1986).

With cascades, waterfalls, and other irregularities in a stream, air bubbles can get trapped in the stream and strip dissolved gases out as the air bubbles rise to the surface of the stream (Hayduk, 1982; Genereaux & Hemond, 1992). If ebullition is a major process of gas exchange, the gas exchange coefficient may be more closely related to the Henry's law constant rather than the aqueous diffusion coefficient.

Gas exchange velocities vary widely in surface water bodies. Clark et al. (1992, 1995) estimated exchange velocities between 2-4 cm hr^{-1} for CFCs in the Hudson Estuary. A tropical lowland river in Australia also had CFC exchange estimated at 4 cm hr^{-1}. Genereaux & Hemond (1992) predicted exchange velocities of ~42 cm/hr for propane and ~49 cm hr^{-1} for ethane from a continuous injection test in a small mountain stream draining the west fork of Walker Branch Watershed Tennessee. Gas exchange velocities in Little Cottonwood Creek, Utah in the Wasatch Mountains were estimated to be 90 cm hr^{-1} and 223 cm hr^{-1} for CFC-12 and ^{4}He respectively (Shaw, 2000). Choi et al. (1998) show that propane gas exchange coefficients in Pinal Creek, in Central Arizona range between 1.7 to 6.9 hr^{-1} (Little Cottonwood Creek ranges between 5.0 and 12.4 hr^{-1}). Furthermore Genereux and Hemond estimate gas exchange coefficients of 1.6 hr^{-1} in Bickford watershed in Massachussetts. Look up Wanningkof exchange rates and comparison between SF_6, propane and ^{222}Rn. These exchange coefficients are on the same order of magnitude as many of the small mountain creek exchange velocities. Top et al. (2001) show that air-sea exchange velocities are 3.5 cm hr^{-1}.

Degassing in locations where no groundwater with elevated ^{222}Rn enters surface water can be described by separating and integrating equation 4.10 as:

$$C_d = C_u e^{-\lambda t} \tag{4.16}$$

where C_d is the surface water concentration at the downstream measuring location, C_u is the surface water concentration at the upstream measuring location, λ is the radon degassing coefficient, and t is the time. This equation can be rewritten as:

$$C_d = C_u^{\frac{-kxw}{Q}} \tag{4.17}$$

where x is the length of the control volume (m), w is the width of the control volume (m), and Q is the flow rate of the control volume (m^3).

The gas exchange velocity can then be solved by rearranging equation 4.17 as follows:

$$k = -\left(\frac{Q}{xw}\right)\ln\left(\frac{F_{ex}}{C}\right) \tag{4.18}$$

Field Area

The Merced River basin is on the western slopes of the Sierra Nevada with headwater elevations as high as 4000 meters above sea level (m a.s.l.) at Mt. Lyell. The study site consists of a 70 km reach of the Merced River beginning at Happy Isles, which is the upper end of Yosemite Valley at 1,224 m a.s.l., and ending at Briceburg with an elevation of 365 m a.s.l. (Figure 4.2). Fourteen

locations along the Merced River, nine tributary locations, four springs, and twelve groundwater locations were investigated.

The terrain is mountainous, with steep slopes and cliffs on both sides of the river basin. A complex network of fractures and faults runs throughout the system, multiple uplifts having occurred (Bateman and Wahrhaftig, 1966; Clow et al., 1996; Wakabayashi and Sawyer, 2001). The majority of the basin is underlain by 70 to 210 Ma granitic intrusions from the Sierra Nevada batholith (Bateman, 1992). Downstream, at the Yosemite National Park boundary, bedrock is primarily metasedimentary and metavolcanic, and there are small outcrops of metamorphic rock located at the upper end of the basin above the sampling sites (Bateman, 1992).

The upper reach of the study area includes Yosemite Valley, which is a glacially carved, alluvium-filled basin approximately 15 km long and 1 km wide (Ericson et al., 2005). The alluvium is mostly coarse-grained glacial material with an average depth of ~300 m and a maximum depth of ~600 m (Gutenberg et al., 1956). Well logs for three production wells, ranging in depths from 159 to 244 m, are all placed in alluvium.

Downstream from Yosemite Valley, the river flows through a V-shaped valley with steep canyon walls and little alluvial extent perpendicular to the river. Well logs for a well located at the west entrance to Yosemite (Arch Rock Well) and six wells set in El Portal (El Portal Wells 2-7) indicate that the alluvium consists of coarse-grained sand, gravel and cobble, with some boulders. Depth to bedrock is typically ~20 m in El Portal, and the Arch Rock well was set in alluvium at >30 m.

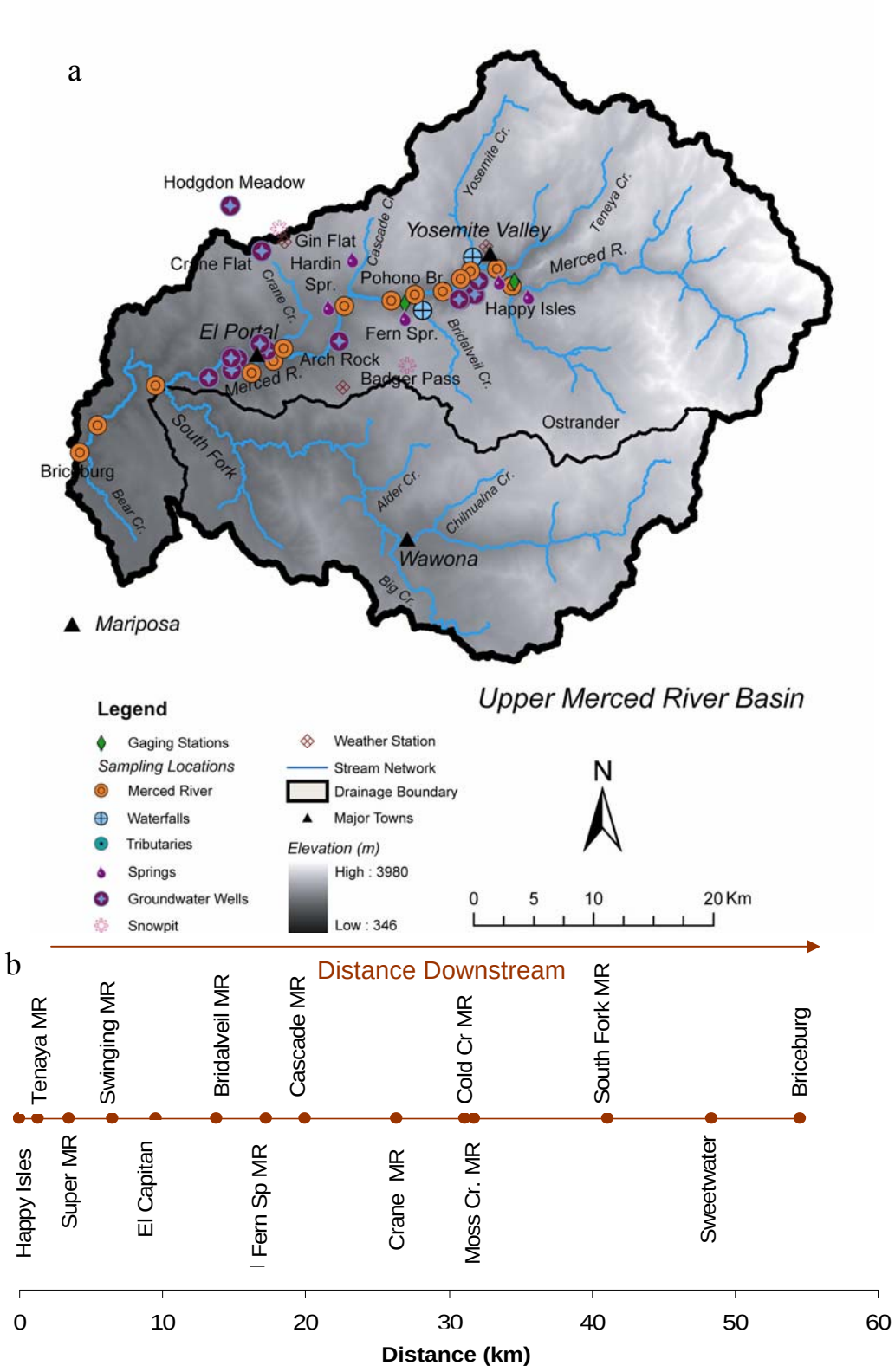

Figure 4.2: Sampling locations in the Merced River basin; (a) shows a map of the area with locations, and (b) shows the Merced River sampling locations with respect to distance downstream.

Two wells are set in granitic fractures underlying meadows (Crane Flat and Hodgdon Meadow Wells). Several wells in Wawona also indicate that there is a groundwater system in fractured bedrock (Borchers, 1996).

Sampling and Analytical Methods

Samples were collected seasonally from November 2003 to July 2008, consisting of a total of 215 groundwater, surface water, spring, and drive point samples (Table 4.1). From November 2003 until July 2004 conductivity and temperature were measured in the Merced River. After visual assessments of geomorphology and interpreting initial conductivity and temperature measurements, ^{222}Rn and R/R_A sampling locations were determined based on locations where groundwater discharge to surface water was anticipated (i.e. at the confluence of sub-basins with the Merced River).

From July 2004 to October 2006 R/R_A measurements were collected 5 to 6 times at Happy Isles, El Capitan, Cascade MR, and Cold Cr. MR.

^{222}Rn was sampled at ten locations from July 2004 to July 2005. Merced River samples included Happy Isles, El Capitan, Cascade MR, Cold Cr. MR, South Fork MR, and Briceburg (Figure 4.2). Tributaries included Yosemite Creek and Bridalveil Creek near the falls, and Crane Creek. Spring samples included Fern Spring.

Cascade MR and Cold Cr MR were also sampled for ^{222}Rn and R/R_A downstream of Yosemite Valley on a finer spatial scale. Eight samples were collected between a 1.6 km reach to spatially determine where groundwater from fractures occurs.

Table 4.1: ^{222}Rn activity in the upper Merced River basin.

Location	# samples	Minimum (cpm)	Minimum Sample Date	Maximum (cpm)	Maximum Sample Date	Average (cpm)	Standard Deviation (cpm)
Merced River							
Happy Isles*	13	50	7/13/2005	3143	10/14/2004	849	1011
Tenaya MR	4	1006	1/31/2007	2320	7/12/2007	1403	616
Super MR	10	321	7/14/2005	2937	10/10/2007	1504	876
Swinging MR	6	326	7/14/2005	2709	10/10/2007	1616	867
El Capitan	15	362	7/21/2004	1858	10/12/2006	1020	484
Bridalveil MR	8	412	7/14/2005	1205	10/10/2007	828	310
Fern Spring MR	9	812	5/24/2007	2930	10/10/2007	1640	762
Cascade MR	13	73	7/13/2005	6161	10/14/2004	1495	1945
Crane Creek MR	4	49	7/13/2005	335	10/10/2007	155	125
Cold Creek MR	12	46	3/30/2006	3843	10/10/2007	1663	1525
Moss Creek MR	2	213	11/11/2005	77	7/13/2005	145	96
South Fork MR	5	108	10/10/2007	23	1/17/2005	57	44
Sweetwater MR	3	37	7/13/2005	107	11/11/2005	67	36
Briceburg	6	65	3/30/2006	229	10/12/2006	121	66
Tributaries							
Illuette Creek (upstream)	1	na**		na		118	na
Tenaya Creek	1	na		na		6600	na
Yosemite Creek (base of falls)	4	5	1/17/2005	78	6/9/2005	35	32
Yosemite Creek (confluence)	1	na		na		4560	na
Bridalveil Creek (base of falls)	16	0	10/14/2004	1050	7/21/2004	83	457
Bridalveil Creek (confluence)	7	6039	7/24/2008	12460	7/24/2008	8780	2801
Cascade Creek	4	0	10/14/2004	590	7/12/2007	250	290
Crane Creek	2	64	7/12/2007	152	10/10/2007	108	62
Pidgeon Creek	1	na		na		45	na
upper South Fork	1	na		na		107	na
South Fork	1	na		na		90	na
Springs							
Happy Isle Spring	2	57055	5/30/2006	91541	4/6/2006	74298	24386
Fern Spring	15	11776	7/21/2004	44299	11/2/2006	31398	10837
Cascade Spring	1	na		na		32108	na
Groundwater Wells							
Valley Well 1	4	7168	5/31/2006	10675	11/2/2006	8488	1662
Valley Well 2	4	5417	5/31/2006	8467	11/2/2006	6960	1255
Valley Well 4	4	9860	10/24/2007	5475	6/21/2005	8038	1941
Arch Rock	4	19217	10/24/2007	31354	11/2/2006	26163	5186
Crane Flat	4	2807	11/2/2006	15570	6/21/2005	10658	5480
Hodgdons Meadow	4	22711	6/21/2005	55298	10/24/2007	36666	15176
EP Well 2	4	28116	6/21/2005	34964	10/30/2007	31634	3197
EP Well 3	4	7628	11/6/2006	18498	10/30/2007	13652	4588
EP Well 4	4	22269	11/6/2006	21393	10/30/2007	34826	10136
EP Well 5	4	14406	11/6/2006	21393	10/30/2007	18012	2858
EP Well 6	4	26526	6/21/2005	47260	10/30/2007	37086	8671
EP Well 7	4	26624	6/1/2006	36849	6/21/2005	31490	4253

*Underlined locations are in Yosemite Valley.

**na-not applicable because there is only one sample.

From July 2005 to July 2008 twenty additional locations for ^{222}Rn were added to the sampling plan to increase the spatial and temporal variations of groundwater discharge to surface water. Merced River samples include Tenaya Creek MR, Super MR, Swinging MR, Fern Sp MR, Crane MR, Moss Cr. MR, and Sweetwater (Figure 4.2). Tributaries include Illilouette Creek, Tenaya Creek, Yosemite Creek (at the confluence) Bridalveil Creek (at the confluence), Cascade Creek, Pidgeon Creek, and the Upper South Fork (Table 4.1). Springs include Happy Isles Spring and Cascade Spring. Many of the tributaries that were sampled only once or twice had low ^{222}Rn activity, so these sites were discontinued from the study.

Twelve groundwater wells were sampled four times for ^{222}Rn and R/R_A between June 2005 and October 2007.

Electrical conductivity and temperature was recorded using a hand held YSI EC 30 meter.

^{222}Rn was analyzed by mixing 20 ml of mineral oil scintillation cocktail with 1 L of water in a glass volumetric flask. Samples were shaken for 10 minutes, and mineral oil was extracted and placed in 20 ml scintillation vials. Samples were analyzed using a Beckman Coulter LS 6500 Multipurpose Scintillation Counter within three days after field collection.

Helium samples were collected in 3/8 inch copper tubes, and the helium isotopic ratio $^{3}He/^{4}He$ isotopes were analyzed using a quadropole mass spectrometer at Lawrence Livermore National Laboratory as referenced by

Hudson et al. (2002). The measured $^{3}He/^{4}He$ ratio is compared to the air-equilibrated $^{3}He/^{4}He$ ratio and expressed as R/R_A.

Results and Data Analysis

Measured Results

Temperature ranged between 0.5 and 27.8 °C, and electrical conductivity ranged between 6.9 and 260.9 μS cm^{-1}. Average groundwater temperature was 11.3 ±3.5 °C, mean Merced River conductivity was 11.1 ±5.4 °C, and mean tributary conductivity was 10.8 ±4.9 °C. Average groundwater conductivity was 90.0 ± 60.3 μS cm^{-1}, mean Merced River conductivity was 32.6 ± 20.3 μS cm^{-1}, and mean tributary conductivity was 27.8 ±18.6 μS cm^{-1}.

In the Merced River, temperature and electrical conductivity vary seasonally, with high temperatures and conductivity occurring during baseflow and low temperatures and conductivities occurring during snowmelt (Figure 4.3). Spatially the temperatures and conductivities remain relatively constant in Yosemite Valley, and they increase downstream of Yosemite Valley. Some of measurements show step-like increases downstream of Yosemite Valley. Cascade MR shows a 2.5 °C increase in November 2003 and a 1.3 °C increase in January 2004 from the previous sampling location near Fern Spring. Conductivity at Cold Creek MR increases by 9.5 μS cm^{-1} during November 2003 and 7.6 μS cm^{-1} during March 2004. The South Fork MR also increases in conductivity by 10.1 μS cm^{-1} during November 2003. All of the increases mentioned above are much greater than typical increases (Figure 4.3). All of these increases occur near the

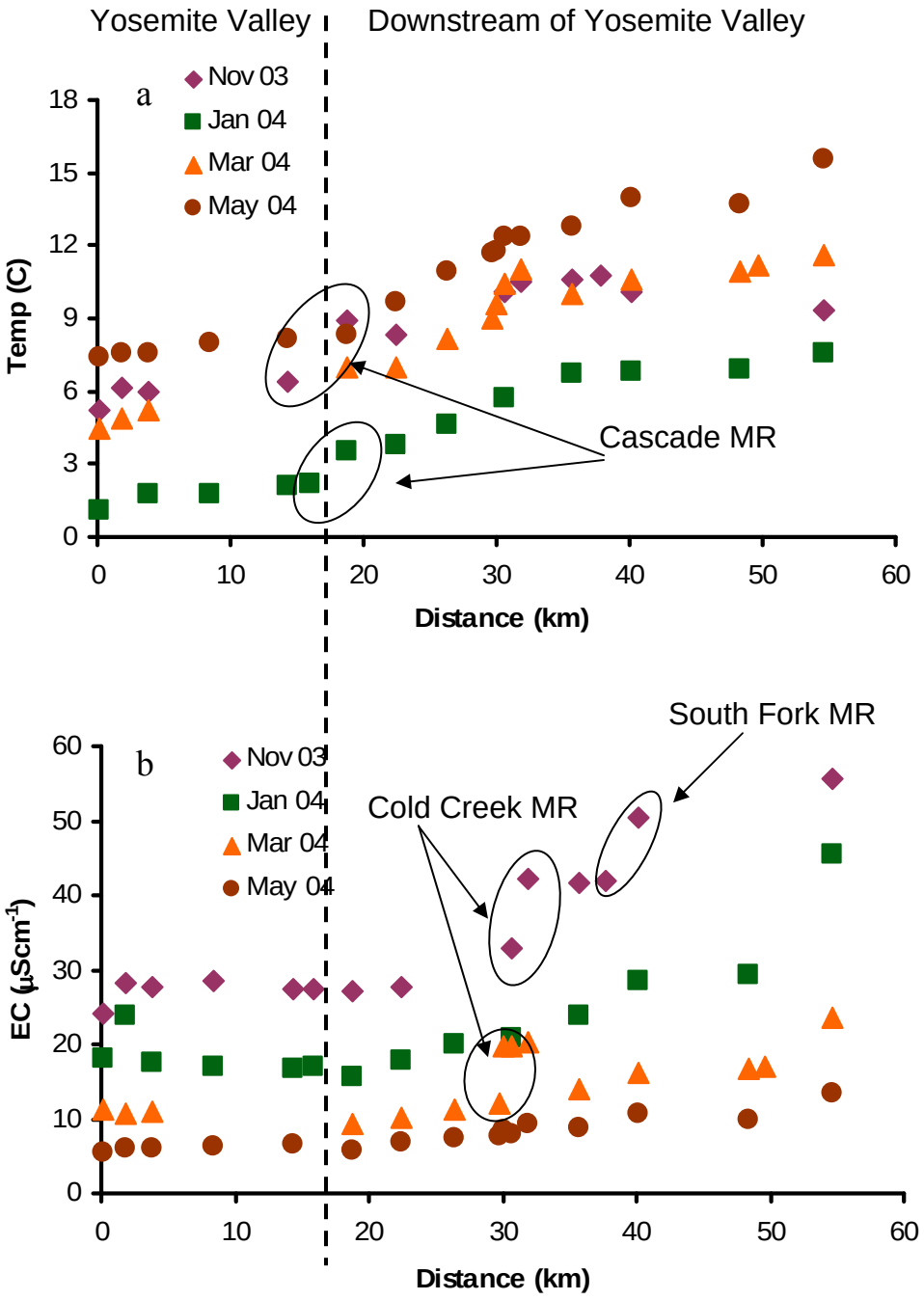

Figure 4.3: Temperature and electrical conductivity measurements collected in the Merced River between November 2003 and May 2004. Cascade MR, Cold Creek MR, and the South Fork MR show step increases in comparison to the upstream measurements, indicating a source of conductivity and temperature occurs to the river during lower flows.

confluence of a sub-basin, but the other sub-basins do not show significant increases in temperature and conductivity.

^{222}Rn activity in all Merced River samples range between 0 and 6161 cpm. Average ^{222}Rn activity is 914±1119 cpm, and the median value is 412 cpm (Table 4.1). ^{222}Rn activity in the Merced River is highest in Yosemite Valley (Table 4.1). The only locations downstream of Yosemite Valley with comparable ^{222}Rn are at Cascade MR and at Cold Creek MR.

^{222}Rn activity in tributary samples range between 0 and 6600 cpm. Average ^{222}Rn activity is 669±1683 cpm, and the median value is 75 cpm (Table 4.1). The highest ^{222}Rn activity in tributaries was measured at the confluence of the Merced River in Yosemite Valley. All other sampled tributaries had little to no ^{222}Rn activity (i.e. downstream of Yosemite Valley and near the canyon walls of Yosemite Valley) (Table 4.1). Low ^{222}Rn activity at the tributaries does not indicate that there is no mixing with groundwater in these tributaries; only an absence of significant groundwater inputs at these locations.

^{222}Rn activity in all groundwater wells and springs range between 2807 and 91541 cpm. Average ^{222}Rn activity is 25875±15819 cpm, and the median value is 26272 cpm (Table 4.1). The lowest activity in groundwater was sampled at Crane Flat on November 2006, and it is anomalously low compared to the other three times it was sampled. The average values of Yosemite Valley wells are the lowest ^{222}Rn activity (Table 4.1).

The R/R_A and ^{222}Rn values measured on a fine scale at Cascade MR and Cold Creek MR show low activity at the upstream end of sampling, low activity

at the downstream end of sampling, elevated activity between (Figure 4.4) Cascade MR has ~600 m stretch, and Cold Creek MR has a <400 m where ^{222}Rn activity is elevated and R/R_A is depressed.

R/R_A values taken spatially along the entire Merced River reach decrease during baseflow, and most locations have nearly air-equilibrated values during snowmelt (Figure 4.5). Rn activity also increases during baseflow as does temperature and conductivity (Figure 2.3; Figure 4.3).

Percent Groundwater

In order to successfully use the model in equation 4.2 and equation 4.9, C_G needs to be estimated. ^{222}Rn activity in groundwater varies over an order of magnitude, so care must be taken to determine what activity to use at different sections of the river. Similar variations of ^{222}Rn activity were also observed in 15 wells sampled previously near Wawona (Borchers, 1996). These wells had values ranging between 1,200 to 12,000 piC/L, which is similar to the wells sampled in this study (assuming that 1 piC/L is equal to 3 cpm).

In order to determine C_G, it is necessary to divide the basin into reaches, and assign separate values for C_G to these reaches. The most noticeable difference in ^{222}Rn activity in groundwater is at Yosemite Valley, which includes samples from three wells ranging in depth from 159 to 244 m (Table 4.1). The mean activity for Yosemite Valley groundwater is 7948±1631 cpm, which is assumed to as C_G throughout Yosemite Valley.

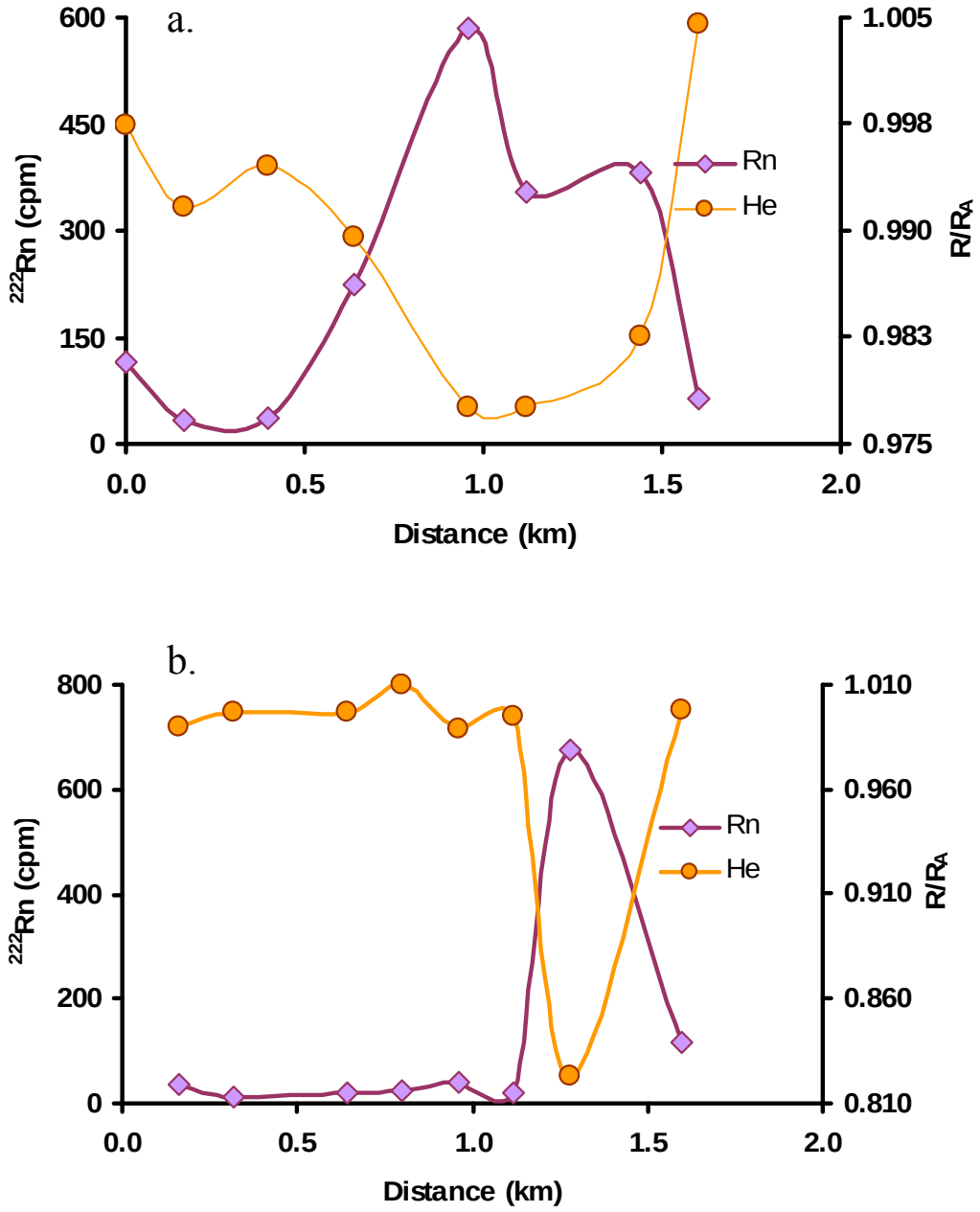

Figure 4.4: ^{222}Rn and R/R$_A$ collected on a fine scale at a) Cascade MR, and b) Cold Creek MR. Depressed R/R$_A$ suggest a source of dissolved gases to the river.

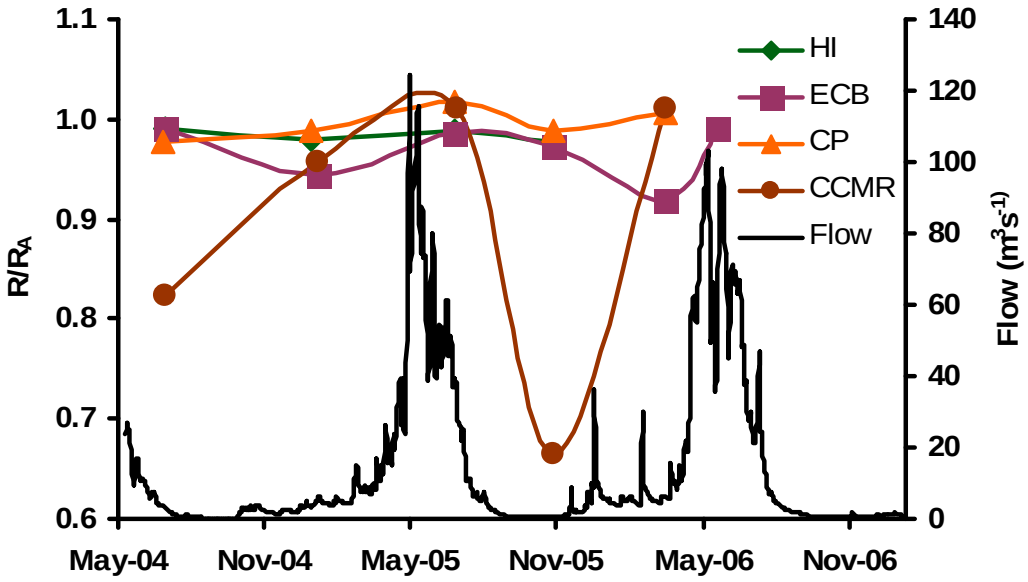

Figure 4.5: R/R_A values at Happy Isles (HI), El Capitan Bridge (ECB), Cascade MR (CP), Cold Creek MR (CCMR) compared with the Merced River flows at Pohono Bridge. Flow data are from the California Data Exchange Center (www.cdec.water.ca.gov).

Wells and springs in other granitic locations outside of Yosemite Valley have mean ^{222}Rn activity of 32560±16761 cpm. This value is assumed to represent C_G interacting with the Merced River between Yosemite Valley and the Park boundary.

The six El Portal wells discharge in or near metamorphic rock and have a mean ^{222}Rn activity of 27783±10521 cpm. This value is used as C_G for all samples located downstream of the Yosemite National Park boundary.

Using equation 4.2 and respective values for C_G, the fraction of groundwater is estimated at several key locations and time periods (Figure 4.6). The percent groundwater varies from ~0% to 30%.

^{222}Rn Mass Balance

Using equation 4.18, the gas exchange velocity was determined at Cascade MR where exchange was elevated and then reduces to significantly lower activity within 160 m (Figure 4.4). These locations were measured on July 18, 2004, October 14, 2004, January 20, 2005, and July 14, 2005. Using a stream width of 20 m, gas exchange velocities ranged between 188 and 3866 cm hr^{-1}. Exchange velocities increase with river flow rates (Figure 4.7). During July 2005, when flow rates were significantly higher than compared to other sampling times, the estimated exchange velocity deviates slightly from the other samples. These changes are probably associated with nonlinear changes in stream depth, velocity, and turbulence, which controls gas exchange rates (Wanninkhof et al. 1990; Genereaux & Hemond, 1992; and Rathbun, 1998).

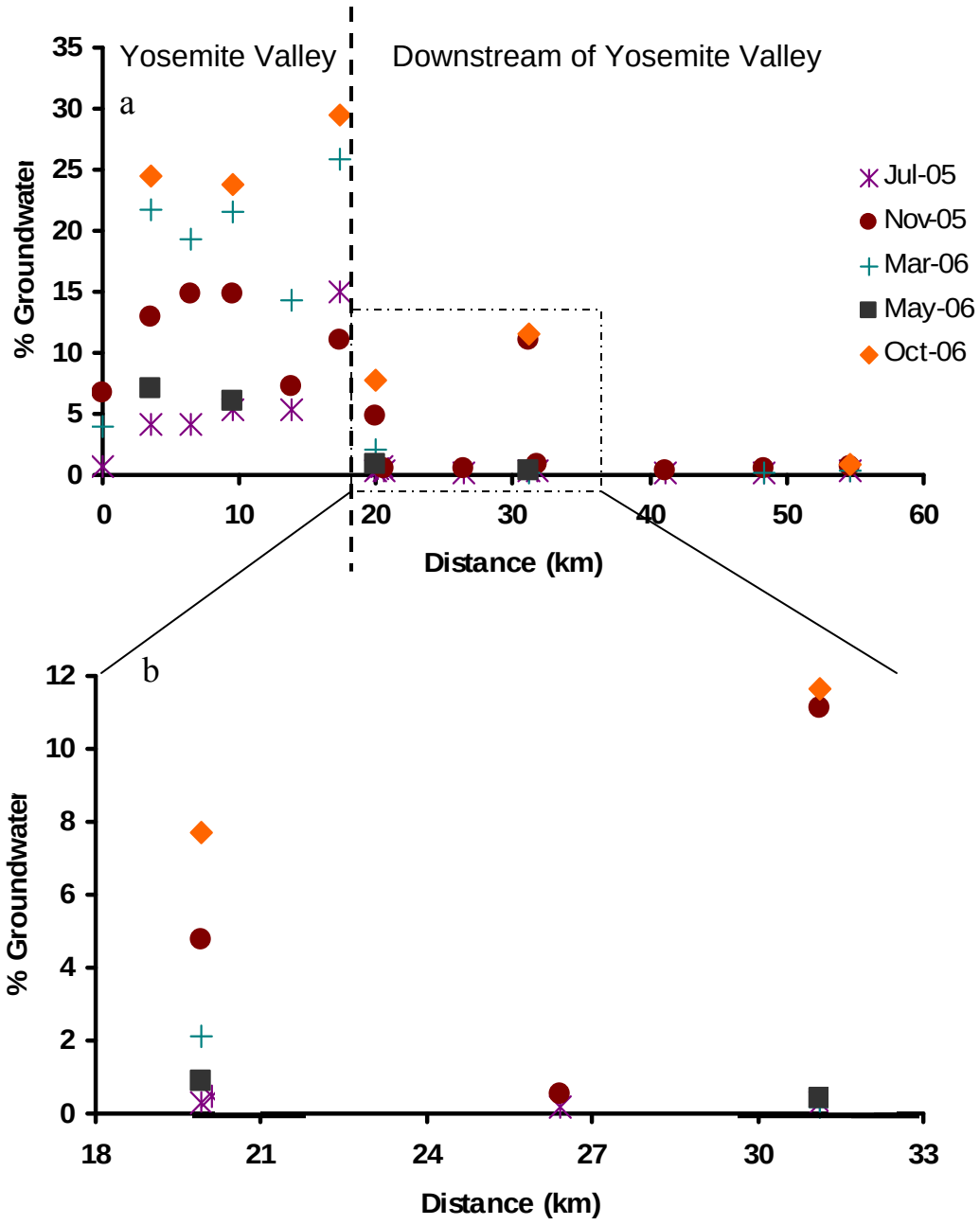

Figure 4.6: Fraction of groundwater flow based on ^{222}Rn measurements in the Merced River basin for a) the entire reach of the Merced River sampled, and b) Cascade MR to Cold Creek MR.

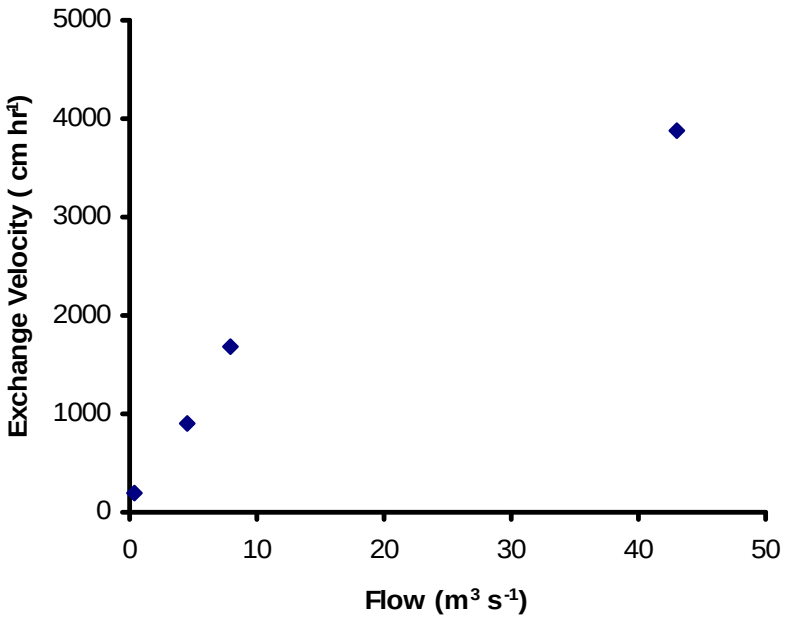

Figure 4.7: Flow measurements at Pohono Bridge in the Merced River and estimated gas exchange velocities at Cascade MR Flow measurements come from the California Data Exchange Center (www.cdec.water.ca.gov).

When equation 4.9 is used to model groundwater fluxes within Yosemite Valley, the amount of groundwater discharge is overestimated ~10 to 100 times higher than the total increase in gauged flows between Happy Isles and Pohono Bridge. A reasonable explanation for the over estimate of groundwater discharge could be overestimating the gas exchange velocity. Several locations along Yosemite Creek are more placid than other locations in the entire catchment. The relatively uniform ^{222}Rn activity through the valley makes estimates of gas exchange difficult.

Using equation 4.9, the amount of groundwater discharging at Cascade MR and Cold Creek MR were determined. The control volume was modeled in 10 m segments. At Cascade MR the model was conducted in two ways. Model 1 varies the groundwater flux to match observed sampling points, and model 2 assumes a constant groundwater flux throughout the entire reach. Both models result in identical groundwater inputs (Figure 4.8a). Cold Creek MR was modeled assuming a constant groundwater flux (Figure 4.8b). Groundwater fluxes estimated at Cascade MR show a 9 % increase in groundwater inputs, correlating to 0.41 $m^3 s^{-1}$, and Cold Creek MR increases in flow by 3.8%, or 0.19 $m^3 s^{-1}$.

Discussion

Groundwater fraction model shows that, 1) the percent groundwater discharge is spatially uniform within Yosemite Valley, 2) the percent groundwater varies downstream from Yosemite Valley, 3) groundwater discharge is always higher in Yosemite Valley than downstream from Yosemite Valley, and 4) the percent groundwater discharge is much higher during baseflow than during

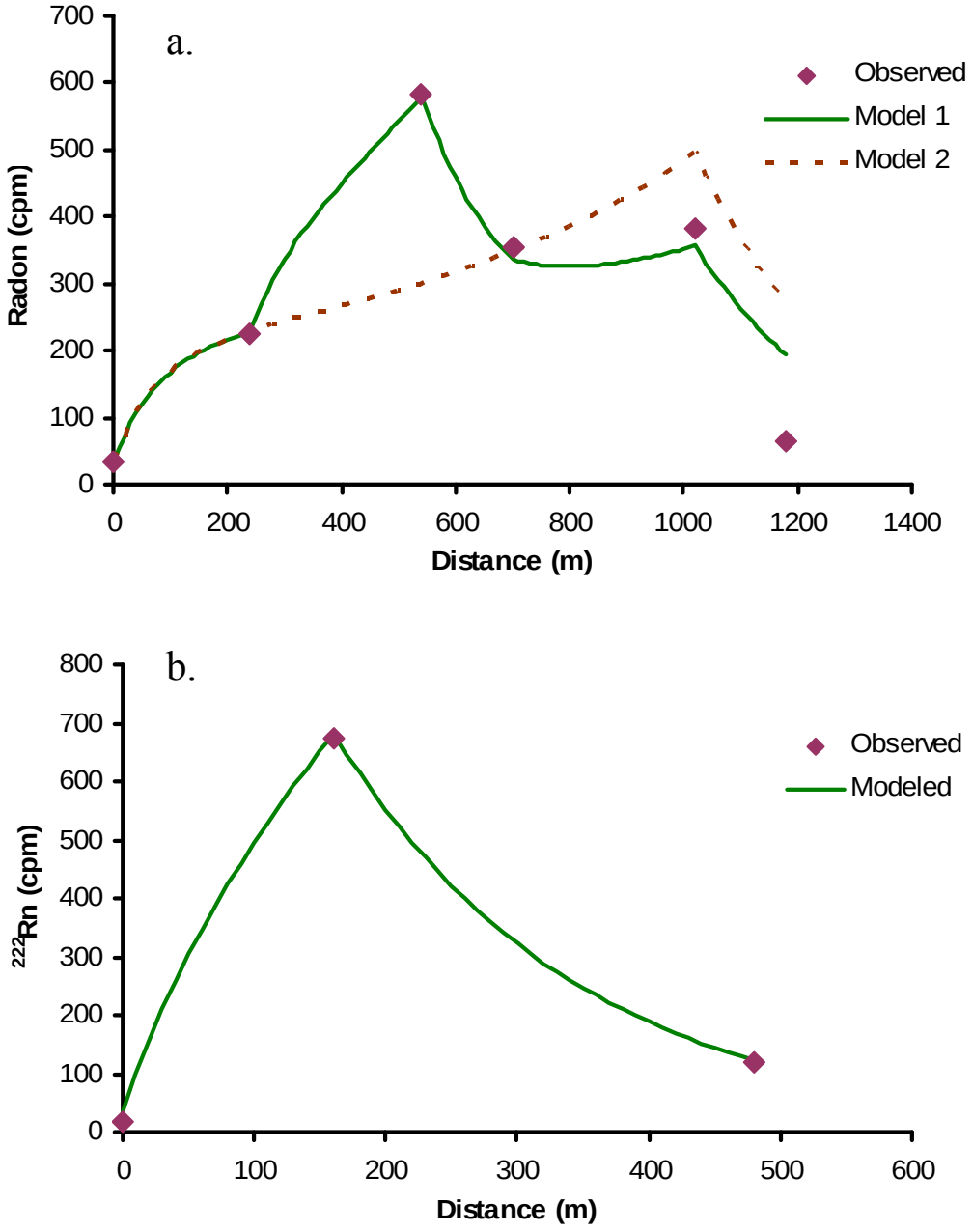

Figure 4.8 Modeled and observed ^{222}Rn activity at a) Cascade MR, and b) Cold Creek MR. Model 1 varies groundwater fluxes between observed points, and model 2 assumes a constant groundwater flux.

snowmelt (Figure 4.6). These observations may be attributed to the differences between the geomorphology of the river reaches (i.e. deep and wide alluvium deposits in Yosemite Valley, and narrow and thin alluvium deposits downstream of Yosemite Valley). Additionally, the elevation differences of the tributary catchments adjacent to these two reaches and the relative fluxes base may also control the amount of groundwater discharge to the Merced River (based on amount of snowmelt and inferred groundwater recharge).

Groundwater Discharge in a Glacial Reach

The volume of water discharging per unit length of river appears to be spatially uniform throughout Yosemite Valley from Happy Isles to Pohono Bridge (Figure 4.6). Temporally, the flux through Yosemite Valley varies with the highest percent groundwater occurring during baseflow or winter prior to snowmelt, and the lowest percent groundwater occurring during snowmelt or during the recession limb of the hydrograph while there is still significant snowmelt occurring.

A closer look at groundwater fractions within Yosemite Valley shows that Happy Isles and Bridalveil MR have the lowest groundwater fractions. One possible explanation for the lower estimated groundwater fractions is that the Merced River is more turbulent in these two locations than the other Yosemite Valley locations, and the decreases may actually represent higher gas exchange, resulting in readings of lower activity (Rathbun, 1998).

The percent groundwater is always elevated at Fern Spring MR compared with other Yosemite Valley locations. One explanation could be that springs

similar to Fern Spring are also discharging directly to the Merced River. ^{222}Rn at Fern Spring is ~3-4 times higher in comparison to groundwater in Yosemite Valley alluvium. The alluvial material and canyon walls are much narrower at Fern Spring than at other locations in the valley, and it would be reasonable for a local increase in ^{222}Rn activity to occur in this location if there were additional springs along the fracture zone near Fern Spring.

The uniform fraction of groundwater in Yosemite Valley suggests that the groundwater flux out of Yosemite Valley alluvium to the Merced River is spatially continuous. Merced River temperature and electrical conductivity measurements collected during the 2003 water year in Yosemite Valley vary seasonally, but remain spatially constant, complimenting the uniform ^{222}Rn activity (Figure 4.3).

The water inputs to Yosemite Valley alluvium may not be spatially continuous. Most likely, they occur at discrete locations such as groundwater discharge from fractures to the alluvium, or from waterfalls and tributaries recharging Yosemite Valley alluvium between the canyon walls and the confluences with the Merced River. Fracture flow to Yosemite Valley is plausible because Happy Isles Spring and Fern Spring both discharge along fractures within Yosemite Valley. Recharging tributaries is also possible because ^{222}Rn activity is absent at Yosemite and Bridalveil Creeks near the waterfalls, which suggests these are losing reaches with groundwater recharging alluvium. ^{222}Rn activity in Yosemite and Bridalveil Creeks increase significantly near the confluence of the Merced River, suggesting that local recharge in the upstream reaches may be

forced back to surface water prior to discharging to the Merced River (Table 4.1). Water inputs to Yosemite Valley alluvium are apparently separated enough from the Merced River that discharge to the river is not manifested at discrete locations. Rather, the hydrostatic pressure along the outer boundaries of the alluvium increase enough to force uniform fluxes of groundwater to the River.

Groundwater Discharge in a Stream-Cut Reach

Elevated ^{222}Rn activity at Cascade MR and Cold Creek MR show that there are short reaches downstream of Yosemite Valley where groundwater discharges to the Merced River, and groundwater discharge is not spatially continuous (Figure 4.4; Figure 4.6). There may be other locations with elevated ^{222}Rn activity, but they were not identified in this study. Based on the geomorphology, the elevated conductivity or temperature (Figure 4.3), the increased ^{222}Rn activity, and the depressed R/R_A ratios at these locations, it is likely that groundwater from fractures enters the river.

^{222}Rn activity has been observed in fractured bedrock in numerous other studies. It was observed in groundwater discharging from fractures in a tunnel below Roseland Lake in the French Alps (Pili et al., 2004; Provost et al., 2004). Fracture discharge to surface water has been observed in the Heihe River in northwestern China along the mountain-arid basin transition (Wu et al., 2004), and in a tropical lowland river in the Northern Territory of Australia (Cook et al., 2003). Wu et al. (2003) use radon to isolate groundwater flow from fractures at ~30 locations in four separate reaches (120-250 m long) in a hill stream in the Guanyinyan Study Area, China. Even continuous Cl^- tracer tests in Little

Cottonwood Creek, UT, show that groundwater input occurs at discrete fracture locations (Kimball et al., 2004). These studies combined with observations in the Merced River basin suggest that the abrupt increases in ^{222}Rn and R/R_A can be attributed to groundwater discharge from fractures where surface deposits are thin and the river corridor is narrow.

None of the previously mentioned studies take into account R/R_A measurements in surface water. The depressed R/R_A observed at Cascade MR and Cold Creek MR also suggest that groundwater residence times are sufficient to incorporate substantial $^4He_{RAD}$ discharges to the Merced River (Figure 4.4). The mass balance model shows that there is less groundwater discharge at Cold Creek MR than at Cascade MR, but the R/R_A values are much lower at Cold Creek MR. The lower groundwater flux and R/R_A at Cold Creek MR suggests that groundwater is significantly older at Cold Creek MR.

Implications for Groundwater Recharge and Discharge

A conceptual model for explaining the amounts of water and the differences between the glacially carved and stream-cut reaches of the catchment can be explained. The deep alluvium in Yosemite Valley may operate as a large reservoir for rapidly recharging groundwater from the many tributaries flowing over Yosemite Valley alluvium. High-infiltrating groundwater during snowmelt may result in the higher fractions of groundwater in the Merced River in Yosemite Valley. The tributaries discharging to the Merced River downstream Yosemite Valley have very little contact time with river alluvium before entering the river because of the lack of alluvium. This likely prevents large quantities of

tributary water recharging into the river alluvium, and that may result in lower overall groundwater fluxes to the river. River alluvium is also narrow enough that fracture flow to river alluvium is only observed locally rather than as one spatially continuous flux along the river.

The basin topography and characteristics is such that the groundwater fractions and fluxes seem to not just be controlled by the extent of alluvium in the catchment, but there also appears to be an elevation effect on the amount of groundwater discharge. Higher elevation catchments leading to the Merced River have the most groundwater discharge to the Merced River. The percent groundwater in the Merced River ranges from 5 to 25% at Yosemite Valley, and from < 1 to 10% downstream of Yosemite Valley, depending on the time of year (Figure 4.6). Roughly 85-90% of snowmelt occurs above the rain-snow transition, which is between 1500-1800 m (Rice et al., 2007). The headwater catchments for tributaries entering Yosemite Valley receive meltwater from elevations well above the snowline. Yosemite Creek, Bridalveil Creek, and Tenaya Creek all have headwater catchments ~3500 m, ~3000 m, and ~2700 m respectively.

Tributaries with headwater catchments near the rain-snow transition are more variable in the amount of groundwater input to the Merced River. Cascade Creek and Cold Creek have tributary headwater catchments of ~2500 m and ~1800 m respectively, and Cascade Creek basin has more groundwater discharge to the Merced River. Crane Creek and Moss Creek also have headwater catchments of around 2000 m, but neither shows any evidence of groundwater discharge to the Merced River. Crane Creek and Moss Creek are both perennial

streams but they have south facing slopes, while Cold Creek is ephemeral and has a north facing slope. All three have similar headwater catchment elevations, but there may be some process controlling groundwater recharge. The north facing slope may result in slower snowmelt, which may recharge groundwater in higher fractions.

Tributaries below Cold Creek have much lower catchments and appear to have less significant groundwater. The two that were sampled were Sweetwater Creek Bear Creek discharges at Briceburg. These tributaries have headwater catchments at ~1200 m and ~1000 m respectively.

The elevation gradient suggests that catchments with more snowpack have higher rates of groundwater recharge to fractures, but catchments near the rain-snow transition may depend on more variables such as the aspect of the catchment.

Comparison of Dissolved Gases and Conservative Tracers

In addition to the conceptual model, the groundwater fractions estimated from ^{222}Rn can be compared with the groundwater fractions determined from endmember mixing analyses by using Cl^- and ^{36}Cl (Figure 2.7). This comparison can be made at Happy Isles and El Capitan Bridge for Yosemite Valley, and at Cascade MR for the stream-cut reaches of the Merced River (Figure 4.9). The majority of the fractions of groundwater estimated using ^{222}Rn are lower than the groundwater fractions estimated from the endmember mixing analyses (EMMA), which emphasizes the effects of degassing. Five samples during snowmelt were less than 5% higher groundwater fractions during snowmelt. The October 2004

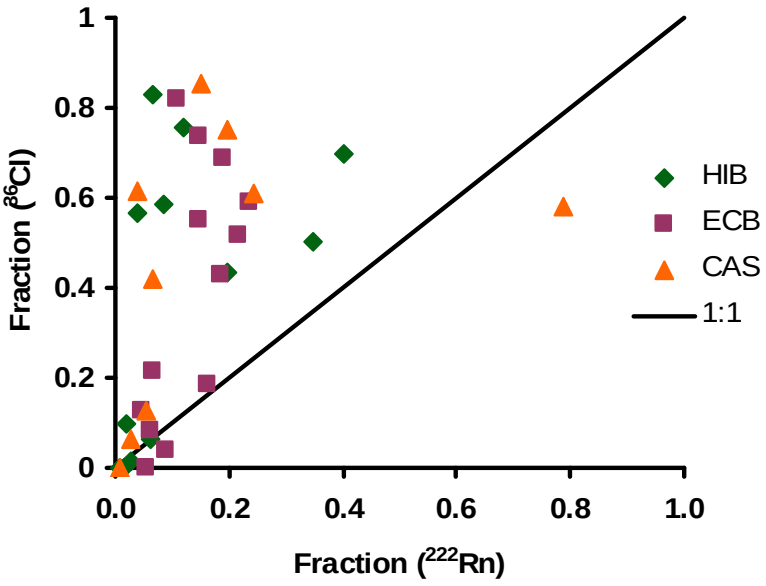

Figure 4.9: Comparison between the ^{222}Rn estimated fraction of groundwater flow and the ^{36}Cl and Cl^- EMMA fractions of flow. Both low-Cl^- and high-Cl^- groundwater fractions are combined for the EMMA results in this figure.

Cascade MR sample showed about 20% higher groundwater fractions from the ^{222}Rn method. In general, the effects of degassing may be used advantageously to identify local processes occurring with groundwater discharge to surface water. But local effects (mostly during snowmelt) may indicate that the ^{222}Rn method slightly overestimates groundwater discharge.

Conclusions

^{222}Rn and R/R_A were successfully used to determine spatial and temporal trends of groundwater discharge to surface water in the Merced River basin, a high elevation montane watershed separated by glacially carved reaches with thick and wide alluvium and river-cut reaches with thin and narrow alluvium. ^{222}Rn and R/R_A measurements in surface water provides a new combination of techniques that provide information on processes controlling groundwater discharge to surface water and even relative information on residence times.

It is concluded that glacially-carved reaches with extensive alluvium function as reservoirs for groundwater storage, with discharge to rivers occurring as a spatially uniform flux. Stream-cut reaches where alluvium is thin and narrow have point discharge locations to surface water from fractured groundwater flow to the alluvium or rivers. The river reaches with the highest elevation tributary catchments have higher rates of groundwater recharge and enough hydrostatic pressure to force higher groundwater fluxes to surface water. Furthermore, dissolved gases reflect more local groundwater discharge to surface water, where mixing models using conservative tracers provide discharge estimates for the entire basin.

References

Bales, R. C., N. P. Molotch, T. H. Painter, M. D. Dettinger, R. Rice, and J. Dozier, Mountain hydrology of the Western United States, *Water Resources Research*, 42, W08432, 2006.

Bateman, P. C., and C, Wahrhiftig, Geology of the Sierra Nevada, In Bailey, E, H., ed. *Geology of Northern California, California Division of Mines and Geology Bulletin*, 190: 107-172, 1966.

Bateman, P. C., Plutonism in the central part of the Sierra Nevada batholith, *U. S. Geological Survey Professional Paper 1483*, 186 pp., 1992.

Borchers, James, W., Ground-water resources and water-supply alternatives in the Wawona area of Yosemite National Park, California, *U.S. Geological Survey Water-Resources Investigations Report 95-4229*, pp 77, 1996.

Brooklins, D. G., Correlation of soil radon and uranium with indoor radon in Albuquerque, New Mexico area, *Environmental Geology*, 17: 209-217, 1991

Cecil. L. D., and J. R. Green, Radon-222, in *Environmental Tracers in Subsurface Hydrology*, eds. P. Cook and A. L. Herczeg, Kluwer Academic Publishers, 175-194, 2000.

Choi, J., S. M. Hulseapple, M. H. Conklin, and J. W. Harvey, Modeling CO_2 degassing and pH in a stream-aquifer system, *Journal of Hydrology*, 209, 297-310, 1998.

Clow, D. W., J. K. Sueker, Relations between basin characteristics and stream water chemistry in alpine/subalpine basin in Rocky Mountain National Park, *Water Resources Research*, 36, 49-61, 2000.

Clow, D. W., M. A. Mast, and D. H. Campbell, Controls on surface water chemistry in the upper Merced River Basin, Yosemite National Park, California, *Hydrological Processes*, 10, 727-746, 1996.

Constantz, J., Interaction between stream temperature, stream flow, and groundwater exchanges in alpine streams, *Water Resources Research*, 34, 1609-1616, 1998.

Cook, P.G., G. Favreau, J. C. Dighton, S. Tickell, Determining natural groundwater influx to a tropical river using radon, chlorofluorocarbons and ionic environmental tracers, *Journal of Hydrology*, 277, 74-88, 2003.

Earman, S. A. R. Campbell, B. D. Newman, and F. M. Phillips, Isotopic exchange between snow and atmospheric water vapor: Estimation of the snowmelt component of groundwater recharge in the southwestern United States, *Journal of Geophysical Research*, 111, D09302, doi: 10.1029/2005JD006470, 2006.

Ericson, K., P. Migon, and M. Olvmo, Fractures and drainage in the granite mountainous area—a study from Sierra Nevada, USA, *Geomorphology*, 64 (1-2), 97-116, 2005.

Folger, P. F., E. Poeter, R. B. Wanty, D. Frishman, and W. Day, Controls on radon-222 variations in a fractured crystalline rock aquifer evaluated using aquifer tests and geophysical logging, *Ground Water*, 34, 250-261, 1996.

Genereaux, D. P., and H. F. Hemond, Determination of gas exchange rate constants for a small stream on Walker Branch Watershed, Tennessee, *Water Resources Research,* 28, 2365-2374, 1992.

Genereux, D. P., and H. F. Hemond, Naturally occurring Radon-222 as a tracer for stream flow generation: steady state methodology and field example, *Water Resources Research*, 26, 3065-3075, 1990.

Genereux, D. P., H. F. Hemond, and P. J. Mulholland, Use of radon –222 and calcium as tracers in a three-end-member mixing model for stream flow generation on the west fork of Walker Branch watershed, *Journal of Hydrology*, 142, 167-211, 1993.

Gutenberg, B., J. P. Buwalda, and P. Sharp, Seismic explorations on the floor of Yosemite Valley, California, *Bulletin of the Geological Society of America*, 67, 1051-1078, 1956.

Hamada, H., Analysis of the interaction between surface water and groundwater using Radon-222, *Japan Agricultural Research Quarterly*, 33 (3), 1999.

Hoen, E., and H. R. Von Gunten, Radon in groundwater: a tool to assess infiltration from surface waters to aquifers, *Water Resources Research*, 25, 1795-1803, 1989.

Hofmann, H., A. Kies, Z. Tosheva, L. Hoffmann, and L. Pfister, Hydrograph separation in micro basins using ^{222}Rn and ^{18}O, *Geophysical Research Abstracts*, European Geoscience Union, Vol 6, 07281, 2004.

Hood, J. L., J. W. Roy, and M. Hayashi, Importance of groundwater in the water balance of an alpine headwater lake, *Geophysical Research Letters*, 33, L13405, 2006.

Hudson, G.B. J. E. Moran, G. F. Eaton, Interpretation of Tritium-3Helium Groundwater Ages and Associated Dissolved Noble Gas Results from Public Supply Wells in the Los Angeles Physiographic Basin: *Report to California State Water Resources Control Board, Lawrence Livermore National Laboratory*, 59 pp., 2002. http://www.llnl.gov/tid/lof/documents/pdf/245359.pdf

Isam, S. M., H. B. L. Pettersson, A. Siverton, and E. Lund, Spatial correlation between radon (^{222}Rn) in groundwater and bedrock uranium (^{238}U): GIS and geostatistical analyses, *Journal of Spatial Hydrology*, 2, 2002.

Kimball, B. A., R. L. Runkel, and L. J. Gerner, Quantification of mine-drainage inflows to Little Cottonwood Creek, Utah, using a tracer-injection and synoptic-sampling study, *Environmental Geology*, 40, 1390-1404.

Krishnaswami S., and D. E. Seidemann, Comparative study of Rn-222, Ar-40, and Ar-37 leakage from rocks and minerals: implications for the role of nanopores in gas transport through natural silicates, *Geochimica Cosmochimica Acta*, 52, 655-658, 1988.

Liu, F., M. W. Williams, and N. Caine, Source waters and flow paths in an alpine catchment, Colorado Front Range, United States, *Water Resources Research*, 40, W09401, 2004.

Liu, F. R. Parmenter, P. D. Brooks, M. H. Conklin, and R. C. Bales, Seasonal and interannual variation of streamflow pathways and biogeochemical implications in semi-arid, forested catchments in Valles Caldera, New Mexico, *Ecohydrology*, 1, 239-252, 2008.

Maloszewski, P. W., A. Zuber, Determining the turnover time of groundwater systems with the aid of environmental tracers. 1. models and their applicability, *Journal of Hydrology*, 57, 207-231, 1982.

Maloszewski, P, W. Rauert, W. Stichler, and A. Herrmann, Application of Flow Models in an Alpine Catchment Area Using Tritium and Deuterium Data, *Journal of Hydrology*, 66, 319-330, 1983.

Martinec, J, H. Oeschger, U. Schotterer, and U. Siegenthaler, Snowmelt and groundwater storage in an alpine basin, in hydrological aspects of alpine and high-mountain areas *IAHS Publication No. 138, Proceedings of a Symposium at the First Scientific General Assembly of the IAHS*, July 19-30, 1982, England, 169-175, 1982.

Mattle, N., W. Kinzelbach, U. Beyerle, P. Huggenberger, H. H. Loosli, Exploring an aquifer system by integrating hydraulic, hydrogeologic and environmental tracer data in a three-dimensional hydrodynamic transport model, *Journal of Hydrology*, 242, 183-196, 2001.

Maurer, D. K., Geohydrology and Simulated Response to Ground-Water Pumpage in Carson Valley, a River-Dominated Basin in Douglas County, Nevada , and Alpine County, California, *U. S. Geological Survey Water Resources Investigations Report 86-4328*, pp109, 1986.

Maurer, D.K., Ground-Water flow and numerical simulation of recharge from stream flow infiltration near Pine Nut Creek, Douglas County, Nevada, *U.S. Geological Survey Water Resources Invesigations Report 02-4145 Carson City, Nevada*, pp. 45, 2002.

Pili, E., F. Perrier, and P. Richon, Dual porosity mechanism for transient groundwater and gas anomalies induced by external forcing, *Earth and Planetary Science Letters*, 227, 473-480, 2004.

Provost, A. S., P. Richon, E. Pili, F. Perrier, and S. Bureau, Fractured porous media under influence: the Roseland experiment, *EOS*, 85, 113-119, 2004.

Rathbun, R. E. Transport, behavior, and fate of volatile organic compounds in streams, *U.S. Geological Survey, Professional Paper, 1589*, 151 pp., 1998.

Rice, R. R. Bales, T. H. Painter, and J. Dozier, Snowcover along elevation gradients in the Upper Merced and Tuolumne River basins of the Sierra Nevada of California from MODIS and blended ground data, *Proceedings from 75th Annual Western Snow Conference*, 3-14, 2007.

Rogers, A. S., Physical behavior and geologic control of radon in mountain streams, *U.S. Geological Survey Bulletin, 1052-E*, 187-211, 1958.

Solomon, D. K., 4He in Groundwater, in *Environmental Tracers in Subsurface Hydrology*, P. G. Cook and A. L. Herczeg, eds., Kluwer Academic Press, 425-439, 2000.

Sueker, J. K., J. N. Ryan, C. Kendall, and R. D. Jarrett, Determination of Hydrologic Pathways during snowmelt for alpine/subalpine basins, Rocky Mountain National Park, Colorado, *Water Resources Research*, 36 (1), 63-75, 2000.

Szabo, Z., and O. S. Zapecza, Geologic and geochemical factors controlling uranium, radium-226, and radon-222 in groundwater, Newark Basin, New Jersey, in *Field Studies of Radon in Rocks, Soils, and Water*, eds. L.C.S. Gundersen and R. B. Wanty, C.K. Smoley, pp. 243-265, 1991.

Torgerson, T., J. Benoit, and D. Mackie, Lithological control of groundwater ^{222}Rn concentrations in fractured rock media, In *Isotopes of Noble Gases as Tracers in Environmental Studies*, IAEA, Vienna, 263-287, 1992.

Wakabayashi, J., and T. L. Sawyer, Stream incision, tectonics, uplift, and evolution of topography of the Sierra Nevada, California, *Journal of Geology*, 109, pp539, 2001.

Wanninkof, R., P. J. Mulholland, and J. W. Elwood, Gas exchange rates for a first-order stream determined with deliberate and natural tracers. *Water Resources Research*, 26, 1621-1630, 1990.

Wanty, R. B., E. P. Lawrence, and L. C. S. Gundersen, A theoretical model for the flux of radon-222 from rock to groundwater, In Geologic Controls on Radon, eds. A. E. Gates and L. C. S. Gunderson, *Geological Society of America Special Paper 271*, 73-78, 1991.

Williams, M. W., A. D. Brown, and J. M. Melack, Geochemical and hydrologic controls on the composition of surface water in a high-elevation basin, Sierra Nevada, California, *Limnology and Oceanography*, 38, 775-797, 2005.

Wu, Y., X. Wen, and Y. Zhang, Analysis of the exchange of groundwater and river water by using Radon-222 in the middle Heihe Basin of northwestern China, *Environmental Geology*, 45, 647-653, 2004.

Wu, Y, W. Wang, Y. Xu, H. Liu, X. Zhou, L. Wang, and R. Titus, Radon concentration: A tool for assessing the fracture network at Guanyinyan study area, China, Water SA, 29, 49-53, 2003.

CHAPTER 5

WHY IS NEAR-SURFACE $^{36}Cl/Cl$ ELEVATED IN THE MERCED RIVER BASIN: A CLOSER LOOK AT CHLORINE BIOGEOCHEMISTRY

Introduction

Chloride is generally assumed to behave conservatively in surface water and groundwater with only a small amount of uptake by plants (Lovett, et al., 2005). Because of the assumed conservative nature of Cl^-, it has been hypothesized that the ^{36}Cl bomb pulse ($^{36}Cl_{BP}$), released from above-ground thermonuclear weapons testing, could be detected in groundwater and used as an age-indicating tracer for groundwater (Bentley et al., 1982; Elmore et al., 1982; Phillips, 2000). However, these studies are rare and have only been done semi-successfully in a few select locations (Cook et al., 1994; Balderer et al, 2004; Tosaki et al., 2007). It has been more common to encounter difficulties in using $^{36}Cl_{BP}$ for determining groundwater residence times because of possible biogeochemical retention, retardation, and/or recycling of the $^{36}Cl_{BP}$ (Cornett et al., 1997; Milton et al., 1997; Nyberg et al., 1999; Blinov et al., 2000; Davis et al., 2001; Lee et al., 2001; Shaw et al., 2004; Corcho Alvarado et al., 2005).

Between 1991 and 2007, $^{36}Cl/Cl$ ratios were elevated in the Merced River basin, especially during peak snowmelt when the majority of the watershed

consists of recently released meltwater. Tributaries discharging to Yosemite Valley typically have $^{36}Cl/Cl$ ratios around $10000x10^{-15}$, and $^{36}Cl/Cl$ in the Merced River had ratios as high as $\sim 6500x10^{-15}$ during snowmelt (see Chapter 2). However, $^{36}Cl/Cl$ ratios measured in the snowpack are at natural background levels of $220\text{-}401x10^{-15}$. One explanation for the elevated $^{36}Cl/Cl$ is through incorporation of $^{36}Cl_{BP}$ derived through interaction with soil into recent meltwater. In order for this to have occurred there must be a mechanism responsible for rapidly retaining significant amounts of $^{36}Cl_{BP}$ in soils.

Several recent studies show that chlorine undergoes a complex biogeochemical cycle occurring between soil, water, and the biological components, and cycling is occurring at rates much greater and faster than previously assumed (Öberg, 1998; Heraty et al., 1999; Casey, 2002; Myneni 2002; Öberg 2002; Öberg, 2003; Rodstedth et al., 2003; Öberg et al., 2005; Öberg and Sanden, 2005; Bastviken et al., 2007; Svensson et al., 2007). These studies show that biological processes can convert Cl^- to organochlorines (Cl_{org}), and Cl_{org} is later mineralized back to Cl^-. The majority of these studies imply pathways and mechanisms for retaining and releasing Cl^- within a watershed, but most lack isotopic or long term observations to accurately determine timescales, quantities, and mechanisms for retention and release Cl^-.

A few studies have injected ^{36}Cl-spiked water into laboratory lysimeters or piezometers in shallow groundwater, but these studies are generally conducted for less than 6 months (Nyberg et al., 1999; Bastviken et al., 2007). The Merced

River, on the other hand, provides a natural laboratory that may have evidence of >50 yr old $^{36}Cl_{BP}$ still cycling.

This chapter uses 1) ^{36}Cl information from the Merced River basin, 2) information about $^{36}Cl_{BP}$, and 3) information about chlorine biogeochemistry to establish the following hypothesis: Large quantities of $^{36}Cl_{BP}$ were rapidly retained in organic matter in soil and small amounts of $^{36}Cl_{BP}$ are released from soil annually. The following questions are addressed in this chapter; i) Could the source of the elevated $^{36}Cl/Cl$ be from $^{36}Cl_{BP}$? ii) How much $^{36}Cl_{BP}$ would have been retained in the watershed to match observed ^{36}Cl export in the Merced River? iii) What role could Cl biogeochemistry play in controlling retention of $^{36}Cl_{BP}$? and iv) How much more $^{36}Cl_{BP}$ could still be retained?

Background

Occurrence of organochlorines

Over 1500 naturally occurring chlorinated compounds have been identified, and thousands of organisms are known to produce Cl_{org} in the form of alkenes, terpenes, steroids, fatty acids, glycopeptides, among other complex organic molecules (Öberg, 2002; Öberg, 2003). Several plant species, algae, terrestrial fungi, bacteria, and lichens are known to produce Cl_{org} from Cl^-.

One common pathway for Cl^- is for vegetation to incorporate Cl^- from surface and subsurface water (Sheppard et al., 1993). Over 80 known plants produce chlorometabolites, including mosses and grasses, and chlorine is concentrated in leaves in comparison to woody material (Öberg 2003). Using

near-edge x-ray absorption fine structure (NEXAFS) and extended x-ray absorption fine structure (EXAFS) spectroscopy on roots, stem, bark, and leaves taken from different plant species in redwood and pine forests in California, New Jersey, and Puerto Rico, it was determined that the majority of chlorine in plants is in the form of inorganic chloride and doesn't convert to Cl_{org} until humification of the plant material (Myneni, 2002). Chlorine in young and partly yellow colored leaves were almost entirely inorganic Cl^-, but over 70% of chlorine was Cl_{org} in reddish brown and humified leaves. Reina et al. (2004) use K-edge X-ray spectroscopy to show that reactions of Cl^- in Sequoia semperviren (Redwood) needles with chloroperoxidase enzymes released from common fungi in the environment react to convert Cl_{org} in plant material. They claim that this reaction is one plausible mechanism for the transformation of Cl^- to Cl_{org} in plant material. As leaves and needles are further humified, Cl_{org} derived from decaying plant material is thereby incorporated into soil. Cl_{org} concentrations in soil are also highest near trees (Öberg, 2003).

Soils play a major role in biogeochemical cycling of nutrients, especially carbon. There is more C storage in soil than there is in the atmosphere and in vegetation (Dahlgren, et al., 1997). Organochlorines tend to be associated with organic matter (Lee et al., 2001; Myneni, 2002; Reina et al., 2004). Myneni (2002) determined that the dominant form of chorine in topsoil from forests in California, New Jersey, and Puerto Rico is Cl_{org}. Cl_{org} can later mineralize in the form of Cl^- as organic matter degrades (Öberg, 2003) because decomposing Cl_{org}

bound organic matter releases Cl^-, which indicates that sometimes soil is a sink for retaining chlorine and other times it's a source by releasing chlorine.

Once deposited in the terrestrial environment, chlorine can be volatilized and later redeposited as precipitation or dry deposition. The presence of low levels of DDT, PCBs and other persistent organochlorines that are often present in precipitation suggest volatilization of chorine is another mechanism in the chlorine biogeochemical cycle (Öberg, 2002 and 2003). Chlorine is incorporated to the terrestrial environment through both dry and wet deposition. Cl_{org} in precipitation typically ranges between 1-30 μgL^{-1} which is up to 1000 times lower typical meteoric Cl^- concentrations (Öberg, 2003). Total amounts of Cl^- entering catchments as both dry and wet deposition are assumed to be roughly equal, but the amount of Cl_{org} deposited as dry deposition is not well known. Volatilization and deposition of low-molecular weight Cl_{org} was discussed as a possible mechanism for apparent recycling of $^{36}Cl_{BP}$ in the Experimental Lakes Observatory in Canada because i) $^{36}Cl/Cl$ ratios in precipitation were elevated in comparison to small lakes and streams, and ii) groundwater samples with no measurable ^3H had lower $^{36}Cl/Cl$ than precipitation. (Cornett et al., 1997; Milton et al., 1997).

Quantities of Cl_{org} in Soils

Cl_{org} appears to be associated with organic matter because Cl_{org} concentrations are typically highest in the upper layers of soil where organic carbon is highest (Öberg, 2003; Svensson et al., 2007). Cl_{org} in the top 15 cm of soil collected in three catchments in Sweden ranged between 212-309 $\mu g\ Cl_{org}\ g^{-1}$

soil dry weight, but Cl^- only measured 68 μg Cl^- g^{-1} soil dry weight (Öberg, 2003). In the Stubbetorp catchment, Sweden, soil samples collected to depth of 40 cm (or less if bedrock was encountered) had an average of 87 μg Cl_{org} g^{-1} soil (dry weight), while the average Cl^- concentrations were only 40 μg Cl_{org} g^{-1} soil dry weight (Svensson et al., 2007). Cl_{org} measured in a 60 cm soil profile in Denmark was only 43 μg Cl_{org} g^{-1} soil dry weight. The lower amount of Cl_{org} in the deeper soil columns (i.e. the 40 and 60 cm columns) suggests that Cl_{org} concentrations decrease with soil depth. Öberg and Sanden (2005) collected 15 cm deep soil cores from the Stubbetorp catchment. The soil cores were taken to a laboratory and set up as lysimeters where deionized water was applied to the samples. Cl^- and Cl_{org} concentrations were determined in the soil, and in out-flowing water from the lysimeters. The outflowing water samples suggest that the concentration of leachable Cl_{org} in the topsoil was 3-10 times higher than Cl^- in the samples, and up to 50% of the chlorine leached from the soil was Cl_{org} during a 4 month period.

Timescale for Retention of Chlorine

Information regarding timescales for retention of chlorine is sparse, but there are a few tracer studies which provide some information on relatively short timescales. Nyberg et al. (1999) injected ^{36}Cl and ^{3}H into shallow groundwater in a small till soil catchment in Gardsjon, Sweden, where the groundwater table is 5 cm below the ground surface. When injections (~1000 times background) were conducted in eight holes at the groundwater table, only 47% of the ^{36}Cl was recovered compared to 78% of the ^{3}H. An additional injection of ^{36}Cl and ^{3}H-spiked water 30 cm below ground surface resulted in 83% of the ^{36}Cl and 96% of

the ^{3}H being recovered. Each injection was followed by sprinkling of ~144 mm of water over the injection site for four months. The results from these injections suggest that topsoil has the capacity to retain up to 50% of incoming Cl^-, and less Cl^- retention occurs below the topsoil.

^{36}Cl-spiked water was also used in laboratory soil lysimeters using soil from the Stubbetorp catchment in Sweden (Bastviken et al., 2007). Roughly 24% of the inflowing ^{36}Cl was retained but later released within the first month of the study as microbial populations decreased in the lysimeters. Over a period of four months, the amount of retained ^{36}Cl was used to determine a Cl_{org} deposition rate that correlates to roughly 25% of incoming Cl^- being retained in organic matter (Bastviken et al., 2007).

Myneni (2002) also showed that on the order of 3-4 months the majority of Cl^- in fresh leaf litter had converted to Cl_{org}. The three previously mentioned studies suggest rapid retention of Cl occurs, but they lack information on chlorine retention time in soil.

The Hubbard Brook Experimental Watershed provides evidence for longer term retention of chloride. Export of Cl^- from the Hubbard Brook Experimental Watershed was monitored and has remained relatively constant from 1964 to 2000, but the 1960s and 1970s annual deposition of Cl^- was higher than during the 1980s and 1990s because of pollution inputs (Lovett et al., 2005). Early records support the occurrence of Cl^- retention, while later records suggest that release of Cl^- was occurring because of the large differences between atmospheric deposition and no change in Cl^- export. Lovett et al. (2005) attribute this

observation to vegetative uptake of Cl^- and slow release from vegetation or litter after the decrease of annual deposition of Cl^- since the 1980s, and they estimate that ~35% of the annual deposition of Cl^- was retained in the catchment during the 1960s and 1970s. Because the atmospheric deposition of Cl^- has decreased since ~1980 and Cl^- export has remained constant until at least 2000, it suggests that there may be slow release of Cl^- from Cl_{org} with minimum timescales of ~20 years. The relative magnitudes and processes that may be occurring on soil pore water are illustrated in Figure 5.1.

^{36}Cl Budget and Environmental Sources

Natural Background and Terrestrial Sources of ^{36}Cl

Natural background levels of ^{36}Cl are produced from cosmogenic interactions with atmospheric gases, which are later released to catchments as dry or wet deposition, and measured ^{36}Cl/Cl in snow in the Merced River basin match predicted background levels (Bentley et al., 1986; Hainsworth et al., 1994; Philips, 2000; Moysey et al., 2003). The mean ^{36}Cl concentration and flow rate, in the Merced River, between January 2004 and December 2007 is 4.75×10^4 atoms g^{-1} and 20.9 $m^3 s^{-1}$ respectively. Flow was measured at the Pohono Bridge gauging station, which correlates to a watershed area of 8.31×10^8 m^2. Mean flow rates (L yr^{-1}) multiplied by the average annual ^{36}Cl concentration (atoms L^{-1}) results in an average annual export of 3.13×10^{19} ^{36}Cl atoms yr^{-1} in the Merced River. It is therefore necessary to investigate natural production rates of ^{36}Cl to investigate potential sources for the current export rates observed in the Merced River basin.

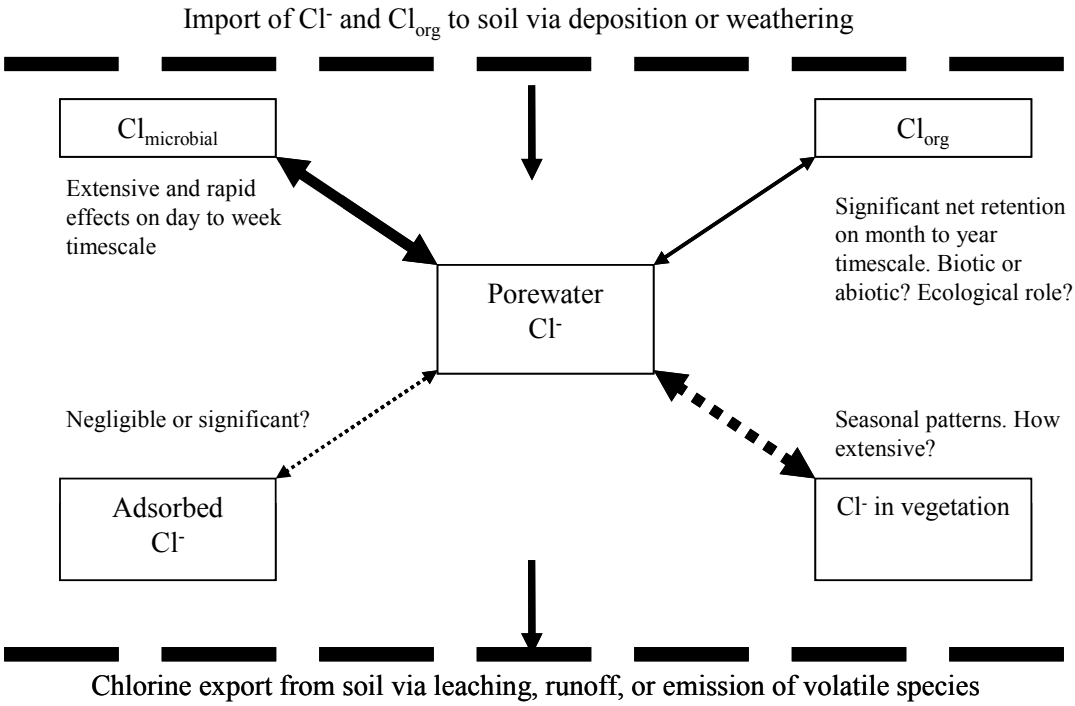

Figure 5.1: Conceptual illustration describing some of the Cl biogeochemical processes occurring (modified from Bastviken et al., 2007).

Subsurface production of ^{36}Cl from the U-Th decay series occurs on timescales too long to explain the elevated ^{36}Cl in the watershed, and the actual nucleogenic ratio of $^{36}Cl/Cl$ in equilibrium with granitic rocks is actually much lower than background $^{36}Cl/Cl$ (i.e. $20\text{-}40 \times 10^{-15}$; Phillips, 2000).

Surface production of ^{36}Cl on exposed granitic rocks cannot explain the ^{36}Cl budget in the Merced River. The majority of the basement rock in the Merced River where ^{36}Cl is elevated is granitic. Typical weight percent of K^+ and Ca^{2+} in granitic rocks is ~5.5%, and a reasonable density for granite is ~2.65 g cm^{-3} (Krauskopf and Bird, 1995). A reasonable, but somewhat high estimate of surface production of ^{36}Cl on granitic boulders in the foothills of the Rocky Mountains in Colorado is 154 ^{36}Cl atoms g^{-1} yr^{-1} (Brugger, 2007). If 100% of the K^+ and Ca^{2+} to a depth of 100 cm is converted to ^{36}Cl and released to the Merced River, it would correlate to $\sim 2 \times 10^{16}$ ^{36}Cl atoms. This one time release is ~1000 times less than the annual export of ^{36}Cl in the Merced River, and it is impossible for 100% of all K^+ and Ca^{2+} to be converted to ^{36}Cl at these depths in this short time period. It is therefore concluded that there are no known naturally occurring processes that would result in the current Merced River ^{36}Cl budget, and leading to the inference that the source is from $^{36}Cl_{BP}$.

Anthropogenic Sources of ^{36}Cl

Synal et al. (1990) measured $^{36}Cl_{BP}$ deposition (atoms cm^{-2} yr^{-1}) and $^{36}Cl/Cl$ ratios in the Dye-3 Greenland Ice Core (Table 5.1; Figure 5.2). The total deposition of $^{36}Cl_{BP}$ measured between 1950 and 1985 is 2.45×10^{12} atoms m^{-2}, but the deposition rate needs to be scaled from the Dye-3 ice core site to the Merced

Table 5.1: $^{36}Cl/Cl$ ratios and ^{36}Cl deposition measured in the Dye-3 Greenland Ice Core (data from Synal et al., 1990).

Year	$^{36}Cl/Cl$ ($x10^{15}$)	^{36}Cl deposition (10^{3} atoms $cm^{-2}yr^{-1}$)
1985	38.1	44.4
1984	66.3	110
1983	117	226
1982	109	176
1981	114	167
1980	109	170
1978	92	162
1977	159	245
1976	135	211
1974	520	749
1973	494	701
1972	558	796
1971	325	485
1970	874	1290
1969	975	1510
1968	1550	1990
1967	3110	4170
1966	1820	2580
1965	3570	5410
1964	4460	6330
1963	4870	7280
1962	8120	11900
1961	12100	20100
1960	20300	30700
1959	18900	27800
1958	18200	26000
1957	28600	39000
1956	17100	25000
1955	13100	18600
1954	5800	8210
1953	871	1220
1952	426	612
1951	145	204
1950	49.8	72.9
1949	44.0	66.1
1948	53.1	74.0
1947	55.9	84.2
1945	79.6	120

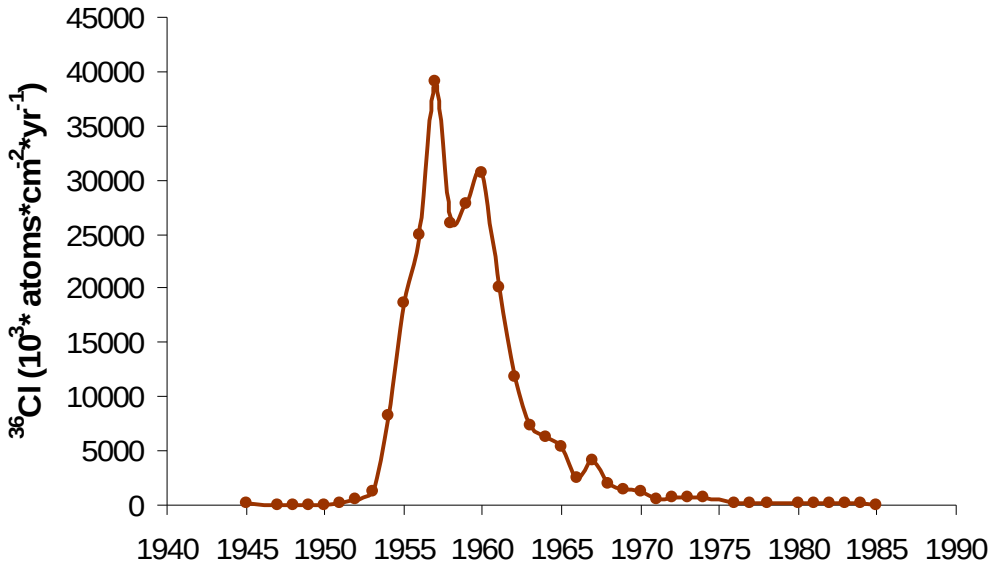

Figure 5.2: ^{36}Cl deposition measured from the Dye-3 Greenland Ice Core (data taken from Synal et al., 1990). The circles are measured values, and the smooth line is assumed ^{36}Cl fallout.

River basin in order to compare $^{36}Cl_{BP}$ with current ^{36}Cl export. Four studies, using observation of ^{36}Cl in surface water and groundwater, and correlating ^{36}Cl deposition to latitude and the amount of precipitation were compared to determine scaling factors from Dye-3 to the Merced River basin (Bentley et al., 1986; Hainsworth et al., 1994; Philips, 2000; Moysey et al., 2003). Scaling factors range between 1.5 to 2.5. Moysey et al. (2003) show that the 2.5 scaling factor from the Phillips (2000) model typically overestimates ^{36}Cl deposition, while the scaling factor of 1.5 from Bentley et al. (1986) underestimates ^{36}Cl deposition. Both the Moysey et al. (2003) and Hainsworth et al. (1994) studies indicate a scaling factor of 2 should be used from Dye-3 to Yosemite.

Using the range of estimated scaling factors, deposition of $^{36}Cl_{BP}$ in the Merced basin from 1950 to 1985 should range between 3.68×10^{12} and 6.13×10^{12} ^{36}Cl atoms m^{-2}, which correlates to a total of 3.05×10^{21} to 5.09×10^{21} ^{36}Cl atoms being deposited over the Merced River basin above Pohono Bridge (4.07×10^{21} atoms using the most probable scaling factor of 2). These results are ~2 orders of magnitude higher than annual ^{36}Cl export (i.e. 3.13×10^{19} atoms yr^{-1}) measured in the Merced River.

The elevated $^{36}Cl/Cl$ ratios in the Merced River basin during peak snowmelt were first noticed in samples collected between 1991 and 1995 (Table 5.2; Nimz, unpublished data). These ratios are similar to the ratios measured between 2004 and 2007 (see Chapter 2). Between 1992 and 1995, Yosemite and Chilnualna Creeks had $^{36}Cl/Cl$ ratios between 9400 and 12000×10^{-15} during

Table 5.2: Chloride (mg L^{-1}) and $^{36}Cl/Cl$ ratios ($x10^{15}$) measured in the Merced River basin between 1991 and 1995. These samples were analyzed at the Center For Accelerator Mass Spectrometry at Lawrence Livermore National Laboratory.

Location		Cl^- (mgL^{-1})	$^{36}Cl/Cl$ ($x10^{15}$)
Happy Isles	Mar-92	0.14	1300
Happy Isles	Jun-95	0.15	8600
Happy Isles	Nov-95	0.25	2380
Chilnualna Cr.	Mar-92	0.16	9900
Yosemite Creek	Mar-92	0.15	9800
Yosemite Creek	Jun-92	0.15	12000
Yosemite Creek	Nov-95	0.36	5480
Yosemite Creek	Jun-95	0.15	9400
South Fork MR	Sep-91	2.5	3110
South Fork MR	Mar-92	0.25	4800
South Fork MR	Mar-92	0.2	5570
South Fork MR	Nov-95	0.3	1740

snowmelt (Table 5.2). These ratios are similar to the ratios measured in Yosemite and Bridalveil Creeks between 2004 and 2007, which are two similar high-elevation catchments with elevations ranging between ~3000 m to 1200 m (see Chapter 2). Measurements at Happy Isles, between 1992 and 1995, were also similar to values measured between 2004 and 2007.

The consistency between $^{36}Cl/Cl$ ratios in multiple high elevation tributaries between 1991-1995 and 2004-2007 suggests that ^{36}Cl export has remained constant for the past 17 yrs. This correlates to export of $5.32x10^{20}$ ^{36}Cl atoms between 1991 and 2007, which is 10.5 to 17.4% of the total $^{36}Cl_{BP}$ deposited on the Merced River basin (13.1% of $^{36}Cl_{BP}$ using a scaling factor of 2). The amount of ^{36}Cl export from the Merced River basin between 1991 and 2007 is still within the total $^{36}Cl_{BP}$ budget, and $^{36}Cl/Cl$ measured during snowmelt are very similar to expected $^{36}Cl/Cl_{BP}$.

Discussion and Results

Several studies were discussed, which elucidate to role of chlorine biogeochemistry in the natural environment. These studies show that Cl_{org} may be widespread in soil, and possibly even as abundant as Cl^-. Some of these studies discuss the possibility of incoming Cl^- being converted to Cl_{org} and retained in soil organic matter for many years. As organic matter decays, some Cl_{org} may be converted back to Cl^- and released to surface water or groundwater. The following sections utilize the findings from these studies, and turn to implications for chlorine biogeochemistry in the Merced River basin as a mechanism to explain the rapid retention and slow release of $^{36}Cl_{BP}$.

Soil Distribution in the Merced Basin

All observations of elevated ^{36}Cl in the Merced River basin occur within Yosemite National Park, which has considerably steeper terrain and less soil cover in comparison to the study sites where chlorine biogeochemistry has been discussed (e.g. Sweden, Denmark, New Jersey, New Hampshire, and California Redwoods). The Merced basin headwater elevations reach as high as 4000 m above sea level (m. a. s. l.) at Mt Lyell, and it is underlain by mostly Mesozoic granitic basement rock (Bateman, 1992), but there are small outcrops of metavolcanic and metasedimentary rocks at the upper end of the basin. The terrain is mountainous with steep slopes and cliffs, and there is a complex network of joints, fractures, and faults (Bateman, 1992; Clow et al., 1996). Fractures range from regional fractures with spacing on the order of hundreds to thousands of m to numerous well-connected shallow exfoliation fractures with spacing on the order of 1-4 m. (Jahns, 1943; Warhaftig, 1965; Segall et al., 1990; Ericson et al., 2005; Wakabayashi & Sawyer, 2005). The slopes are primarily a series of steps with surficial deposits accumulating on the flats (Warhaftig, 1965).

Only 20% of the basin above Happy Isles (1224 m. a. s. l.) is covered by surficial deposits (Clow et al., 1996). Although most observations of elevated $^{36}Cl/Cl$ in the Merced River basin are taken from tributaries just below Happy Isles, the sub-basins most likely have a similar extent of surficial deposits. Most surface deposits above the river corridor are assumed to be thin (< 1m). At Gin Flat, a small forested region at 2149 m. a. s. l., has loamy sand on average of 72 cm thick (Flint et al., 2008), and Tuolumne meadows, in the Tuolumne drainage

basin, also has approximately 1 m of alluvium (Cooper et al., 2006). Well logs for two wells located in meadows at Hodgdon Meadow and Crane Flat have mostly coarse-grained alluvium 27 to 18 m deep, and well logs and seismic reflection and refraction studies in Yosemite Valley wells are filled with glacial till ~300 m thick (Gutenberg et al., 1956). Well logs for wells set in river alluvium downstream of Yosemite Valley indicate that alluvial fill is greater than 28 m thick near the west Yosemite National Park entrance, and alluvial fill ranges between 15 and 25 m thick in six El Portal well logs. Virtually all alluvium within the river corridor is primarily coarse-grained sands, gravels, cobbles, and boulders. Although no information is available concerning organic matter in soils in the Merced River basin, Tuolumne Meadow soils were studied and indicate that soil organic matter at the upper 20 cm of soil ranged between ~7-18% (Cooper et al., 2006).

The majority of the chlorine biogeochemistry study sites, discussed above, occur in heavily forested temperate regions including, Sweden, Denmark, Ontario, Canada, and New Hampshire, and New Jersey. However, samples from Myneni (2002) were also collected in Puerto Rico and Big Basin Redwood State Park, California (near the coast of California). All of these studies stress the importance of topsoil and the catchments are nearly 100% covered with surface deposits. Furthermore, these soils would likely have more continuous and deeper organic layers, and fine-grained sediments, than the Merced River basin. The studies discussed above depend on organic matter in topsoil, which is much less in the Merced River basin. If Cl^- is retained as organic matter in the Merced River

basin, it is likely that very little organic matter is necessary to retain a large amount of Cl^-.

Implications for Chlorine Storage in the Merced River Basin

One explanation for high $^{36}Cl/Cl$ ratios observed in the Upper Merced River and tributaries during snowmelt is that a large percentage of incoming Cl^- is retained in the near surface environment, and that it is still cycling through the basin. This retention implies a "reservoir" of ^{36}Cl in the biosphere. It is hypothesized that this reservoir is Cl_{org}. Assuming that there is no fractionation between ^{35}Cl, ^{36}Cl, and ^{37}Cl, at least 10.5 to 17.5% of Cl^- must have been retained during the bomb pulse in order to satisfy observed $^{36}Cl_{BP}$ export for the past 17 years. It is likely that a substantially higher percentage of $^{36}Cl_{BP}$ must have been retained, since discharge of $^{36}Cl_{BP}$ has probably occurred prior to 1991, and no sign of diminishing $^{36}Cl/Cl$ is evident in the near future. The studies discussed above indicate that retention of up to 50% of incoming Cl^- is possible in some locations, and that the likely method of retention is from conversion of Cl^- to Cl_{org} in soil and vegetation.

The presence of $^{36}Cl_{BP}$ in current snowmelt runoff also indicates a retention time of Cl_{org} on the order of decades. Approximately 98% of the bomb pulse was flushed from the atmosphere between 1950 and 1970, which would result in Cl_{org} residence times in the Merced basin of 21 to 57 years. These residence times would suggest that individual Cl_{org} compounds persist for decades, or that Cl^- released upon mineralization of Cl_{org} is quickly recaptured into Cl_{org}.

$^{36}Cl/Cl$ ratios measured in leachate from five different types of vegetation samples that were collected in the Merced River basin, ranged between $355x10^{-15}$ and $2000x10^{-15}$ (Table 5.3; Nimz unpublished data). The ratios are significantly lower than $^{36}Cl/Cl$ measured in near surface water, which suggests that most $^{36}Cl_{BP}$ is not still retained in vegetation. It is likely, however, that vegetation was part of the initial retention of ^{36}Cl, but that it has been released to the watershed, volatilized, or has been incorporated into Cl_{org} in soil (Myneni, 2002).

If current $^{36}Cl_{BP}$ measured in meltwater in the Merced River is derived from release of retained $^{36}Cl_{BP}$, then only a small quantity of soil is necessary to retain large amounts of Cl^-. There may be other mechanisms occurring in the watershed that might result in retention of $^{36}Cl_{BP}$, but these mechanisms have yet to be identified. The amount of $^{36}Cl_{BP}$ released since 1991, and the apparent residence times for Cl_{org}, suggests that $^{36}Cl_{BP}$ could be observed in the Merced River for another 3 to 4 decades, and it may provide a natural tracer for characterizing water flow paths in other mountain systems.

Theoretical Compartment Models

Two simple theoretical compartment models are used to evaluate the likeliness of chlorine biogeochemistry or any other terrestrial source of ^{36}Cl added to meltwater. These models are used to explain Cl^- and $^{36}Cl/Cl$ observations in tributaries such as Yosemite or Bridalveil Creeks, because they have little to no addition of rock Cl^-. They must provide explanations for, 1) the increase in $^{36}Cl/Cl$ ratios from fresh snow (~ $<400x10^{-15}$) to tributary water ($>10000x10^{-15}$), and 2) the change in Cl^- concentrations from spring runoff (~0.1 mgL^{-1}) to

Table 5.3: $^{36}Cl/Cl$ and ^{36}Cl in vegetation in the Merced River basin.

Vegetation type	$^{36}Cl/Cl$ ($x10^{15}$)
western Cedar leaves	355
doug Fir needles	1280
pine needle litter	504
whitebark pine needles	1522
grass	2002

baseflow (~0.5 mgL^{-1}) with little variation in the $^{36}Cl/Cl$ ratio. The initial compartment is incoming precipitation and the final compartment is tributary water. The first model is a three compartment model, and the second model is a four compartment model. The middle compartments may not necessarily represent physical locations, but they may represent physical, chemical, and/or biological processes occurring within the watershed.

The middle compartment in the three compartment model would have to have similar $^{36}Cl/Cl$ ratios as the tributary ratios. As meltwater transports between the snowpack and the tributaries, it picks up chloride from this compartment. The $^{36}Cl/Cl$ ratio would increase from snow ratios to ratios similar to the middle compartment after a four or five time increase in total Cl^-. This model would require a minimum snow Cl^- concentration of ~0.25 mg L^{-1} to result in the Cl^- concentrations of ~0.1 observed during snowmelt. It is likely that an alternative model occurs.

In a four compartment model, there would be one middle compartment with $^{36}Cl/Cl$ ratios above the observed tributary $^{36}Cl/Cl$ ratio and a second middle compartment with $^{36}Cl/Cl$ ratios equal to the tributary ratios (Figure 5.3). This model assumes that meltwater incorporates Cl^- from the second compartment until the $^{36}Cl/Cl$ ratios increase to the observed tributary ratios. The third compartment allows further incorporation of Cl^- while keeping the $^{36}Cl/Cl$ ratio constant. Interaction with the second compartment must be rapid enough to elevate $^{36}Cl/Cl$ ratios to the tributary levels—even during peak snowmelt. If precipitation had Cl^- concentrations of 0.05 mg L^{-1} chloride and $^{36}Cl/Cl$ ratios of $400x10^{-15}$, and the Cl^- concentrations only doubled

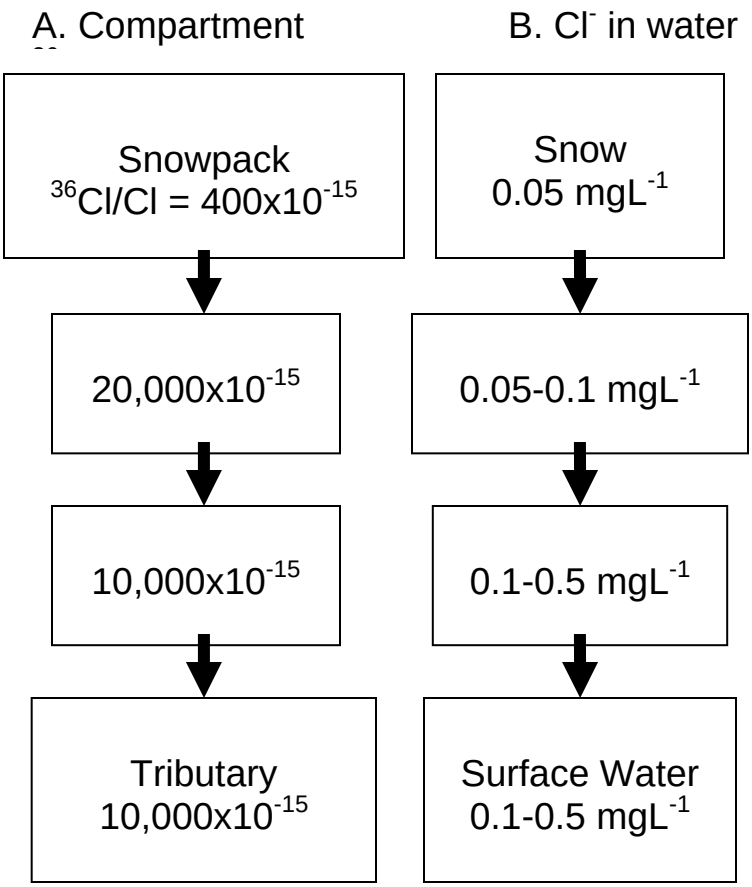

Figure 5.3: A four compartment box model showing a). compartments with there respective $^{36}Cl/Cl$ ratios, and b). evolution of water chloride concentrations flowing through each compartment.

to 0.1 ppm, then the $^{36}Cl/Cl$ ratio of second compartment would have to be $20{,}000 \times 10^{-15}$. The resulting water interacting with the second compartment would obtain ratios of $\sim 10{,}000 \times 10^{-15}$. Further incorporation of Cl^- in the third compartment would not change the $^{36}Cl/Cl$ ratio, but it would allow increases in Cl^- concentrations.

The four compartment model is the most reasonable model that provides a simple mechanism that can explain how $^{36}Cl/Cl$ ratios might rapidly increase from snow to tributary ratios while still preserving low Cl^- concentrations during peak snowmelt. The third compartment is necessary to explain the uniformity between snowmelt and baseflow $^{36}Cl/Cl$ even though Cl^- concentrations increase. Chlorine biogeochemical processes discussed in the beginning of this chapter may provide an explanation for the second compartment, while evapotranspiration of infiltrating water that has initially undergone similar biogeochemical processes may provide a reasonable explanation for the third compartment.

Conclusions and Future Work

Elevated $^{36}Cl/Cl$ has been observed in the Merced River basin during snowmelt between 1991 and 2007, but the snowpack has natural background $^{36}Cl/Cl$ ratios. There are no natural subsurface or surface sources of ^{36}Cl that can currently explain these observations, and the most reasonable source is from $^{36}Cl_{BP}$. However, $^{36}Cl_{BP}$ would have to be rapidly retained and slowly released to explain these observations. Several studies in temperate forest catchments suggest that a reasonable mechanism for $^{36}Cl_{BP}$ retention may be conversion of Cl^- to Cl_{org} in soil, and some of these studies suggest Cl^- retention may be as high as 50%.

The elevated $^{36}Cl/Cl$ suggests that the Merced River basin may provide a natural, large-scale laboratory for investigating the role of chlorine biogeochemistry. Future work may include expansion of ^{36}Cl sampling from groundwater and surface water to soil, vegetation, and other biological reservoirs. These analyses should also be coupled with an investigation of organochlorines in groundwater and surface water, soil, vegetation, and other biological reservoirs. Organochlorine analyses may be conducted similar to the soil studies presented from Scandanavia (Appendix B.5). If enough Cl_{org} and Cl^- are present in these reservoirs, then use of EXAFS may also elucidate processes and compartments where $^{36}Cl_{BP}$ may be stored. In situ lysimeter studies with ^{36}Cl-spiked water may also be injected in locations with significant topsoil. Because of the general lack of surficial deposits in high elevation montane catchments, clays and soil formed along weathered fracture surfaces may also be investigated for ^{36}Cl and Cl_{org}.

References

Balderer, W. H. A., Synal, and J. Deak, Application of the chlorine-36 method for the delineation of groundwater infiltration of large river systems: example of the Danube River in western Hungary (Szigetkoz area), *Environmental Geology*, 46, 755-762, 2004.

Bastviken, D., F. Thomsen, T Svensson, S. Karlsson, P. Sanden, G. Shaw, M. Matucha, and G. Öberg, Chloride retention in forest soil by microbial uptake and by natural chlorination of organic matter, *Geochimica et Cosmochimica Acta*, 71, 3182-3192, 2007.

Bateman, P. C., Plutonism in the central part of the Sierra Nevada batholith, *U. S. Geological Survey Professional Paper 1483*, 186 pp., 1992.

Bentley, H. W., F. M. Phillips, S. N. Davis, S. Gifford, D. Elmore, L. E. Tubbs, and H. E. Gove, Thermonuclear ^{36}Cl pulse in natural water, *Letters to Nature*, 300, 737-740, 1982.

Bentley, H. W., F. M. Phillips, and S. N. Davis, Chlorine-36 in the terrestrial environment, In *Handbook of Environmental Isotope Geochemistry*, Vol. 2, eds. P. Fritz and J. C. Fontes, Elsevier, Amsterdam, pp. 427-480, 1986.

Blinov, A., S. Massonet, H. Sachsenhauser, C. Stan-Sion, V. Lazarev, J. Beer, H.A. Synal, M. Kaba, J. Masarik, and E. Nolte, An excess of ^{36}Cl in modern atmospheric precipitation, *Nuclear Instruments and Methods in Physics Research B*, 172, 537-544, 2000.

Brugger, K. A., Cosmogenic ^{10}Be and ^{36}Cl ages from Late-Pleistocene terminal moraine complexes in the Taylor River drainage basin, Central, Colorado, USA, *Quaternary Science Reviews*, 494-499, 2007.

Casey, W. H., The fate of chlorine in soils, *Science*, 295, 985-986, 2002.

Clow, David W., M. Alisa Mast, and Donald H. Campbell, Controls on surface water chemistry in the upper Merced River Basin, Yosemite National Park, California, *Hydrological Processes*, 10, 727-746, 1996.

Cook, P.G., I.D. Jolly, F.W. Leaney, G.R. Walker, G.L. Allen, L.K. Fifield, and G.B. Allison, Unsaturated zone tritium and chlorine 36 profiles from Southern Australia: There use as tracers of soil water movement, *Water Resources Research*, 30 (6), 1709-1719, 1994.

Cooper, D. J., J. D. Lundquist, J. King, A. Flint, L. Flint, E. Wolf, F. C. Lott, and J. Roche, Effects of the Tioga Road on Hydrologic Processes and Lodgepole Pine Invasion into Tuolumne Meadows, Yosemite National Park, *report prepared for Yosemite National Park*, 146 pp., 2006.

Corcho Alvarado, J. A., R. Purtschert, K. Hinsby, L. Troldborg, M. Hofer, R. Kipfer, W. Aeschbach-Hertig, and H. Arno-Synal, ^{36}Cl in modern groundwater dated by a multi-tracer approach (^{3}H/^{3}He, SF_6, CFC-12, and ^{85}Kr); a case study in quaternary sand aquifers in the Odense Pilot River Basin, Denmark, *Applied Geochemistry*, 20, 599-609, 2005.

Cornett R. J., H. R. Andrews, L. A. Chant, W. G. Davies, B F. Greiner, Y. Imahori, V. T. Koslowsky, T. Kotzer, J. C. D. Milton, G. M. Milton, Is ^{36}Cl from weapons' test fallout still cycling in the atmosphere?, *Nuclear Instruments and Methods in Physics Research B*, 123, 378-381, 1997.

Dahlgren, R. A., J. L. Boettinger, G. L. Huntington, and R. G. Amundson, Soil development along an elevational transect in the western Sierra Nevada, California, *Geoderma*, 78, 207-236, 1997.

Davis, S. N., L. D. Cecil, M. Zreda, and S. Moysey, Chlorine-36, bromide, and the origin of spring water, *Chemical Geology*, 179, 3-16, 2001.

Elmore, D. L. E. Tubbs, D. Newman, X. Z. Ma, R. Finkel, K. Nishiizumi, J. Beer, H. Oeschger, and M. Andree, ^{36}Cl bomb pulse measured in a shallow ice core from Dye 3, Greenland, *Letters to Nature*, 300, 735-737, 1982.

Ericson, K., P. Migon, and M. Olvmo, Fractures and drainage in the granite mountainous area—a study from Sierra Nevada, USA, *Geomorphology*, 64 (1-2), 97-116, 2005.

Flint, A. L., L. E. Flint, and M. D. Dettinger, Modeling soil moisture processes and recharge under a melting snowpack, *Vadose Zone Journal*, 7, 350-357, 2008.

Gutenberg, B., J. P. Buwalda, and P. Sharp, Seismic explorations on the floor of Yosemite Valley, California, *Bulletin of the Geological Society of America*, 67, 1051-1078, 1956.

Hainsworth, L. J., A. C. Mignerey, and G. R. Helz, Modern chlorine-36 deposition in southern Maryland, U.S.A., *Nuclear Instruments and Methods in Physics Research B*, 92, 345-349, 1994.

Heraty, L. J., M. E. Fuller, L. Huang, T. Abrajano Jr., and N. C. Sturchio, Isotopic fractionation of carbon and chlorine by microbial degradation of dichloromethane, *Organic Geochemistry*, 30, 793-799, 1999.

Krauskopf, K. B., and D. K. Bird, *Introduction to Geochemistry*, 3rd Ed, McGraw-Hill, Inc., New York, 647 pp., 1995.

Jahns, R. H., Sheet structure in granites: its origin and use as a measure of glacial erosion in New England, *Journal of Geology*, 11 (2), 71-98, 1943.

Lee, R. T., G. Shaw, P. Wadey, X. Wang, Specific association of ^{36}Cl with low molecular weight humic substances in soils, *Chemosphere*, 43, 1063-1070, 2001.

Lovett, G. M., G. E. Likens, D. C. Buso, C. T. Driscoll, and S. W. Bailey, The biogeochemistry of chlorine at Hubbard Brook, New Hampshire, USA, *Biogeochemistry*, 72, 191-232, 2005.

Milton, J. C. D., G. M. Milton, H. R. Andrews, L. A. Chant, R. J. J. Cornett, W. G. Davies, B. F. Greiner, Y. Imahori, V. T. Koslowsky, T. Kotzer, S. J. Kramer, J. W. McKay, A new interpretation of the distribution of bomb-produced chlorine-36 in the environment, with special reference to the Laurentian Great Lakes, *Nuclear Instruments and Methods in Physics Research B*, 123, 382-386, 1997.

Moysey, S., S. N. Davis, M. Zreda, and L. D. Cecil, The distribution of meteoric $^{36}Cl/Cl$ in the United States: a comparison of models, *Hydrogeology Journal*, 11, 615-627, 2003.

Myneni, S. C. B., Formation of stable chlorinated hydrocarbons in weathering plant material, *Science*, 295, 1039-1041, 2002.

Nyberg, Lars, A Rodhe, K. Bishop, Water transit times and flow paths from two line injections of ^{3}H and ^{36}Cl in a microcatchment at Gardjon, Sweden, *Hydrologic Processes*, 13 (11), 1557-1575, 1999.

Oades, J. M., The retention of organic matter in soils, *Biogeochemistry*, 5, 35-70, 1988.

Öberg, G., Chloride and organic chlorine in soil, *Acta Hydrochimica et hydrobiologica*, 26, 137-144, 1998.

Öberg, G., The natural chlorine cycle-fitting the scattered pieces, *Applied Microbiology and biotechnology*, 58, 565-581, 2002.

Oberg, G., The biogeochemistry of chlorine in soil, *The Handbook of Environmental Chemistry*, 3, 43-62, 2003.

Öberg, G., M. Holm, P. Sanden, T. Svensson, and M. Parikka, The role of organic-matter-bound chlorine in the chlorine cycle: a case study of the Stubbetorp catchment, Sweden, *Biogeochemistry*, 75, 241-269, 2005.

Öberg, G., and P. Sanden, Retention of chloride in soil and cycling of organic matter-bound chlorine, *Hydrological Processes*, 19 (11), 2123-2136, 2005.

Phillips, F. M., Chlorine-36, In *Environmental Tracers in Subsurface Hydrology*, eds. P. G. Cook and A. L. Herczeg, Kluwer Academic Publishers, Boston, pp. 299-348, 2000.

Reina, R. G., A. C. Leri, S. C. B. Myneni, Cl K-edge X-ray spectroscopic investigation of enzymatic formation of organochlorines in weathering plant material, *Environmental Science and Technology*, 38, 783-789, 2004.

Rodstedth, M. C. Stahlberg, P. Sanden, and G. Öberg, Chloride imbalances in soil lysimeters, *Chemosphere*, 52, 381-389, 2003.

Segall, P., E. H., McKee, S. J. Martel, and B. D. Turrin, Late Cretaceous age of fractures in the Sierra-Nevada Batholith, California, *Geology*, 18(12), 1248-1251, 1990.

Shaw, G., P. Wadey, and J. N. B. Bell, Radionuclide transport above a near-surface water table: IV Vertical soil profile distributions and crop uptake of beta-emitting radionuclides (^{36}Cl and ^{99}Tc) during the period 1990 to 1993, *Journal of Environmental Quality*, 33, 2272-2280, 2004.

Sheppard, S. C., W. G. Evenden, and B. D. Amiro, Investigation of soil-to-plant pathway for I, Br, Cl, and F, *Journal of Environmental Radioactivity*, 21, 9-21, 1993.

Svensson, T., P. Sanden, D. Bastviken, G. Oberg, Chlorine transport in a small catchment in southeast Sweden during two years, *Biogeochemistry*, 82, 181-199, 2007.

Synal, H. A., J. Beer, G. Nonani, M. Suter, and W. Wolfli, Atmospheric transport of bomb-produced ^{36}Cl, *Nuclear Instruments and Methods in Physics Research B*, 52, 483-488, 1990.

Tosaki, Y., N. Tase, G. Massmann, Y. Nagashima, R. Seki, T Takahashi, K. Sasa, K. Sueki, T. Matsuhiro, T. Miura, K. Bessho, H. Matsumura, and M., He, Application of ^{36}Cl as a dating tool for modern groundwater, *Nuclear Instruments and Methods in Physics Research B*, 259, 479-485, 2007.

Wakabayashi, J., and T. L. Sawyer, Stream incision, tectonics, uplift, and evolution of topography of the Sierra Nevada, California, *Journal of Geology*, 109, pp539, 2001.

Warhaftig, C., Stepped topography of the Southern Sierra Nevada, California, *Geological Society of America Bulletin*, 76, 1165-1190, 1965.

CHAPTER 6

CONCLUSIONS

In order to characterize water resources available in Yosemite Valley and El Portal, a simple water balance can be assessed. Isotope and noble gas information from this dissertation can be coupled with this mass balance to help make assumptions or validate findings. Between January 1, 2004 to December 31, 2007, the average annual extraction of groundwater was 665022 m^3 yr^{-1} in Yosemite Valley, and 170864 m^3 yr^{-1} in El Portal (Yosemite National Park, unpublished data). Yosemite Valley and El Portal wells are screened in valley and river alluvium because water can be sustained at higher pumping rates than in fractured bedrock. Assuming that the alluvium in Yosemite Valley and El Portal is fully saturated with groundwater, the mean volume of water in each location can be estimated. Yosemite Valley groundwater aquifer is ~15 km long, 1 km wide, 300 m deep. Wells in El Portal are placed along a 2000 m length of the river, which has ~100 m width and 25 m depth of alluvium. Assuming that all river and valley alluvium has a porosity of 30%, this correlates to 1.35×10^9 m^3 of water stored in Yosemite Valley alluvium and 1.50×10^6 m^3 of water in the alluvium near El Portal (Table 6.1). Using the extraction rates mentioned below, annual water withdrawals correlate to removal of ~0.05% of Yosemite Valley

Table 6.1: Aquifer parameters and extraction rates for Yosemite National Park groundwater wells (extraction data, courtesy of Yosemite National Park).

Aquifer Parameters	Yosemite Valley	El Portal
Width (m)	1000	100
Length (m)	15000	2000
Thickness (m)	300	25
Porosity (%)	30	30
Total Water (m^3)	1350000000	1500000
Average Annual Extraction (m^3 yr^{-1})	665022	170864
Total aquifer volume extracted (% yr^{-1})	0.05	11.4

groundwater and ~11% of El Portal groundwater per year (Table 6.1).

Noble gas and isotope data suggest that a large fraction of recharge occurs from infiltrating tributaries, and a simple check can be conducted to estimate the likeliness of tributary recharge to alluvium balancing groundwater withdrawals. A reasonable, and possibly conservative, infiltration rate is assumed to be 25 mm yr^{-1} (Smedema et al., 2004). Tributary dimensions are typically ~3 m wide, and they flow approximately 500 m in Yosemite Valley and 50 m in El Portal discharging to the Merced River (Table 6.2). If infiltration occurs over this area, then the mean volume of annually infiltrated water from each tributary is $3.3x10^5$ m^3 yr^{-1} in Yosemite Valley and $3.3x10^4$ m^3 yr^{-1} in El Portal. This correlates to ~50% and ~20% of the total extracted groundwater being replenished from each tributary in Yosemite Valley and at El Portal respectively (Table 6.2).

Yosemite Valley has at least 10 tributaries spilling over the canyon walls and discharging to the Merced River during snowmelt and during the recession limb of snowmelt. Whereas, only three tributaries discharge to the Merced River in El Portal (Table 6.3). Based on these data, Yosemite Valley has the potential to recharge ~500% of the total annual extraction volume of water (Table 6.2), and El Portal only has the potential to recharge ~60% of the total extracted volume of water.

The highest monthly extraction rates occur after peak snowmelt (Figure 6.1). There may be times during baseflow when Extraction rates may actually be higher than infiltration rates. Because of the large aquifer volume and the large

Table 6.2: Infiltration parameters for tributaries in Yosemite Valley and El Portal. These parameters are used to determine the amount of extracted groundwater that is replenished from tributaries (extraction rates, courtesy of Yosemite National Park).

Tributary Infiltration Parameters	Yosemite Valley	El Portal
Length (m)	500	50
Width (m)	3	3
Infiltration rate (mm hr^{-1})	25	25
Volume Recharged [per trib]	328500	32850
recharged water/extracted water (% yr^{-1})	50	20
# Tribs in the area	10	3
recharged water/extracted water (% yr^{-1}) [For all tributaries]	500	60

Table 6.3: Merced River tributaries in Yosemite Valley and El Portal.

Yosemite Valley	El Portal
Illilouette Creek	Crane Creek
Tenaya Creek	Cold Creek
Royal Arch Cascade	Moss Creek
Staircase Creek	
Indian Canyon Creek	
Sentinal Creek	
Yosemite Creek	
Horse Tall Creek	
Ribbon Creek	
Bridalveil Creek	

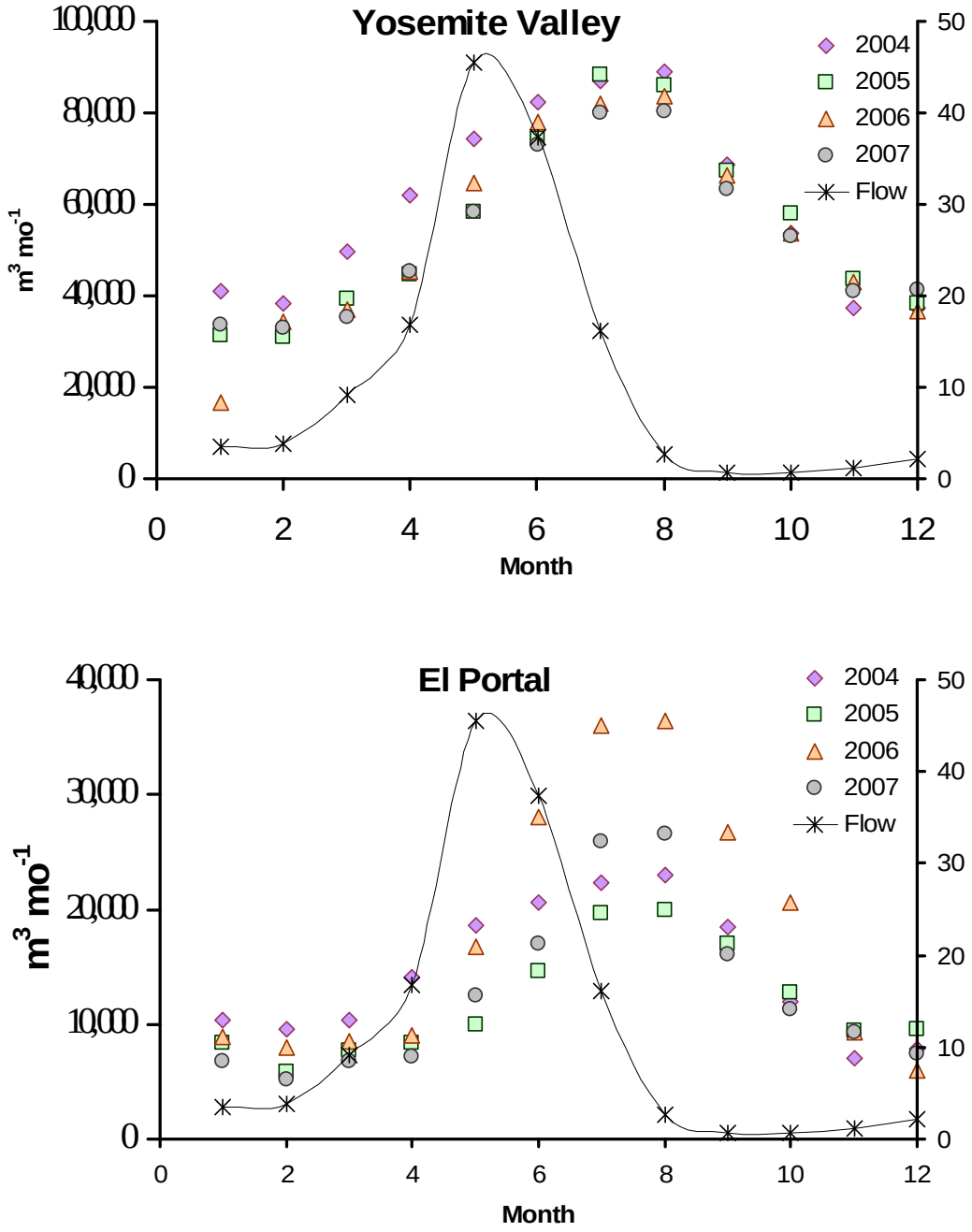

Figure 6.1: Monthly groundwater extraction rates averaged between January 1, 2004 to December 31, 2007 at a) Yosemite Valley and b) El Portal. Average monthly Merced River flow rates are averaged for the same time period.

number of tributaries with potential to recharge into alluvium, Yosemite Valley appears to have the most sustainable extraction rates even though total annual extraction is ~4 times higher than in El Portal. Furthermore, recharge temperatures and elevations, and the occurrence of springs in Yosemite Valley indicate that there is also more groundwater discharging to the valley alluvium through fractures than in El Portal. There is also no indication of a reversal of groundwater discharge to the Merced River to groundwater recharge from the Merced River due to high rates of groundwater extraction. Residence times also suggest relatively young water in Yosemite Valley.

In El Portal, there is still a 40% annual deficit in groundwater extraction to tributary recharge, so another source of water is necessary to balance recharge and discharge when groundwater pumping is occurring. ^{222}Rn and noble gases suggest existence of locations where groundwater flows through fractures to the river alluvium, but these locations are infrequent, and the total volume of this water may be minimal. The majority of the groundwater deficit is likely replenished from another source. The short residence times estimated from ^{3}H/^{3}He age dating suggests that this source is recently recharge water, and it is likely that it is from direct recharge of Merced River water to river alluvium.

Because recharge from Merced River water is required to balance inflows and outflows in the river alluvium aquifer in El Portal, this region is more susceptible to mining groundwater or negatively impacting surface water than in Yosemite Valley. During the high flow period, recharge is most likely significant enough to recharge any deficits in the river alluvium, but the threat to the system

most likely occurs during baseflow when groundwater extraction is still elevated and river and tributary flow rates are significantly reduced (Figure 6.1).

In addition to a potential groundwater deficit in El Portal is extracting more groundwater from fracture discharge than if there was no groundwater extraction. Noble gases show that bedrock groundwater in El Portal is mostly premodern, and the longer travel times suggest that this water is more difficult to replenish.

Foothill locations further downstream of El Portal may be the most vulnerable to mining water and impacting surface water. The city of Mariposa extracts some groundwater from river alluvium near Briceburg. This portion of the watershed has lower elevation tributary headwaters with very little snow in the catchments. The tributaries are perennial and smaller than in El Portal, and ^{222}Rn measurements showed no evidence of significant groundwater discharge to surface water from fractures.

This dissertation study shows that through the use of noble gas, ^{36}Cl, ^{3}H, and ^{222}Rn tracer techniques, valuable information can be obtained to characterize mountain source waters, fluxes, flow paths, and residence times. Each tracer elucidates different processes occurring in the watershed. ^{36}Cl with Cl^- can be used to identify source waters, and they can be incorporated into endmember-mixing analyses to characterize how source waters mix in the watershed. Noble gas tracers provide information about recharge temperatures, locations, and residence times, which results in a greater understanding of subsurface flow paths. ^{222}Rn can also be used to characterize locations of groundwater discharge to surface water, and processes controlling groundwater discharge. In combination, these tracers can be

used to better assess water distribution, timing, and fluxes to communities and regions depending on mountain water resources.

Near-surface water with very little subsurface residence time provides the largest volume of water export from the Merced River basin, but groundwater flow to surface water is critical for providing stream flow after snowmelt. The relatively small amount of groundwater discharging to surface water in the Merced River basin can be broken into a larger quantity of low-Cl^- groundwater consisting of mostly modern water, and a smaller quantity of high-Cl^- groundwater consisting of mostly premodern water. Increased discharge to surface water, and decreased residence times, during snowmelt suggest that low-Cl^- groundwater may be most vulnerable to changes in climate. The high-Cl^- groundwater may become increasingly more important during baseflow, and as a result, stream salinity may even increase in Sierran streams.

A general characterization for the vulnerability and response to climate change may also be inferred through characterizing source waters mixing and their residence times. The relatively small percentage of groundwater interacting with near-surface water suggests that the Merced River basin, or other Sierran watersheds, may be more vulnerable to climate change in comparison to mountain regions that have more groundwater resources (i.e. greater aquifer porosity and storage capacity). Examples of such may include the Cascade Mountains, Wasatch, and possibly the Colorado Rocky Mountains.

On a local scale, Yosemite Valley groundwater might not be as vulnerable to climate change, in comparison to other parts of the watershed, because of the presence of deep, coarse-grained alluvium. The constant uniform groundwater discharge along the Merced River within the valley appears to be from displacing

valley groundwater from recharging valley alluvium near the canyon walls. Changes in timing and type of precipitation might result in changes in amounts and timing of groundwater recharge and discharge, but it may not significantly change the overall annual recharge to the valley alluvium, providing a continued resource for Yosemite National Park.

Other tracers may also be used to identify and separate endmembers mixing in a watershed, but ^{36}Cl provides unique hydrologic and biogeochemical information. Specifically, the presence of $^{36}Cl_{BP}$ in near-surface water suggests that all endmembers exchange with soil, even though soil cover is typically sparse in high elevation mountain catchments. The presence of ^{36}Cl in recent snowmelt also suggests that a large portion of incoming $^{36}Cl_{BP}$ was rapidly retained in the near-surface and slowly released to surface and groundwater.

Estimates for retention of $^{36}Cl_{BP}$ may be >50 yrs, and the continued release of $^{36}Cl_{BP}$ may provide a useful tracer for studying hydrologic fluxes and flow paths of recent snowmelt in other locations in the Sierra Nevada, or even other mountain regions. $^{36}Cl_{BP}$ retained in the near-surface may also have the potential to advance understanding of chlorine biogeochemistry if retention of $^{36}Cl_{BP}$ occurred in the biosphere. Characterizing the fate and transport of Cl^- in the environment has implications for the utility of halides as conservative tracers. There may also be implications regarding how these processes control chlorine-related contaminants in the natural environment.

An obvious next step to this or similar studies is to combine observations from isotope tracers observations with other techniques such as using i) heat as a tracer (e.g. DTS cables or temperature probes), ii) geophysical methods (e.g. resistivity or ground penetrating radar), iii) geologic mapping (e.g. fracture mapping),

and/or iv) numerical modeling . These methods would provide additional information about groundwater recharge, water flow paths, and water travel times, which are necessary for assessing resources. In particular, isotope tracers in combination with numerical simulations of water flow and transport can be used to make quantitative predictions of water responses to climate change.

References

Smedema, L. K., W. F. Vlotman, D. W. Rycroft, Modern Land Drainage: Planning, Design and Management of Agricultural Drainage Systems, Science, London, 400 pp., 2004.

APPENDIX A

DATA TABLES

Table A.1. Chemistry and stable isotope data for the Merced River basin.

Location	Date Collected	^{18}O	D	EC (25 ^{o}C)	Na^{+}	K^{+}	Ca^{2+}	Mg^{2+}	Cl^{-}	SO_4^{2-}
MERCED RIVER	m/d/yr	(‰)	(‰)	($mScm^{-1}$)	(mgL^{-1})	(mgL^{-1})	(mgL^{-1})	(mgL^{-1})	(mgL^{-1})	(mgL^{-1})
Nevada Falls	6/9/2005	nm	nm	8.8	0.63	0.18	0.84	0.08	0.32	0.36
Happy Isles	7/18/2004	nm	nm	15.7	18.37	0.22	10.44	1.12	1.37	0.76
Happy Isles	10/14/2004	-12.86	-97.6	43.7	2.81	0.83	3.74	0.38	4.97	0.40
Happy Isles	1/18/2005	-13.74	nm	25.1	2.05	0.34	2.14	0.13	2.85	0.59
Happy Isles	6/9/2005	nm	-110.0	11.1	0.74	0.23	0.93	0.06	0.31	0.38
Happy Isles	7/13/2005	-14.80	-106.5	nm	0.45	0.13	0.69	0.04	0.21	0.41
Happy Isles	11/11/2005	-13.51	-99.6	30.6	2.45	0.44	2.77	0.19	3.58	0.41
Happy Isles	3/30/2006	-13.82	-101.8	24.4	4.57	0.38	2.98	0.19	2.07	0.57
Happy Isles	10/12/2006	-13.39	-97.96	32.0	2.42	0.48	3.15	0.24	3.16	0.45
Happy Isles	1/19/2007	-13.69	-102.43	22.8	3.31	0.48	3.79	0.29	nm	0.55
Happy Isles	4/27/2007	-14.03	-105.49	13.3	1.01	0.20	1.21	0.07	0.98	0.34
Happy Isles	5/24/2007	-14.60	-104.49	11.9	0.67	0.17	0.97	0.04	nm	0.30
Happy Isles	7/12/2007	-12.67	-97.17	19.4	1.41	0.26	1.95	0.10	2.06	0.52
Happy Isles	10/10/2007	-12.84	-95.28	nm	2.96	0.58	3.35	0.19	5.28	0.42
El Capitan Bridge	7/18/2004	nm	nm	21.5	31.50	0.57	16.57	0.41	1.55	0.93
El Capitan Bridge	10/14/2004	-12.46	-93.88	40.6	3.16	1.45	4.68	0.63	3.11	0.56
El Capitan Bridge	1/18/2005	-13.70	nm	22.4	1.67	0.44	2.12	0.22	1.92	0.42
El Capitan Bridge	6/9/2005	-14.39	-104.83	12.3	0.87	0.33	1.26	0.14	0.36	0.40
El Capitan Bridge	7/13/2005	-14.53	-105.56	nm	0.57	0.20	0.95	0.09	0.26	0.40
El Capitan Bridge	11/11/2005	-13.24	-96.96	38.8	2.63	0.85	3.59	0.43	3.08	0.56
El Capitan Bridge	3/30/2006	-13.47	-98.96	25.1	4.34	0.51	3.01	0.19	1.48	0.57
El Capitan Bridge	5/30/2006	-14.82	-107.20	10.4	2.84	0.42	1.60	0.09	0.27	0.62
El Capitan Bridge	10/12/2006	-13.02	-94.80	43.6	2.87	1.18	4.02	0.41	2.60	0.79
El Capitan Bridge	1/31/2007	-13.36	-99.00	nm	2.87	0.75	3.82	0.34	4.05	nm
El Capitan Bridge	4/27/2007	-13.94	-101.33	11.7	0.84	0.23	1.10	0.07	0.64	0.35
El Capitan Bridge	5/24/2007	-13.45	-100.45	13.5	0.74	0.21	1.13	0.05	nm	0.22
El Capitan Bridge	7/12/2007	-12.26	-93.48	26.7	1.72	0.67	2.62	0.20	1.94	0.55
El Capitan Bridge	10/10/2007	-11.88	-91.04	nm	2.94	1.45	4.07	0.33	3.72	0.84
Cascade-1	7/18/2004	nm	nm	20.7	14.28	0.50	8.56	0.90	1.27	0.67
Cascade-6	7/18/2004	nm	nm	21.6	30.08	0.47	16.27	0.22	1.24	0.91
Cascade-6	10/14/2004	nm	nm	44.1	2.94	1.12	4.78	0.63	1.95	0.86

Table A.1. Cont.

Location	Date Collected	^{18}O	D	EC (25 ^{o}C)	Na^{+}	K^{+}	Ca^{2+}	Mg^{2+}	Cl^{-}	SO_4^{2-}
MERCED RIVER	**m/d/yr**	**(‰)**	**(‰)**	**($mScm^{-1}$)**	**(mgL^{-1})**	**(mgL^{-1})**	**(mgL^{-1})**	**(mgL^{-1})**	**(mgL^{-1})**	**(mgL^{-1})**
Cascade-6	1/18/2005	-13.01	nm	21.7	1.73	0.50	2.19	0.26	1.38	0.41
Cascade-6	7/13/2005	-14.24	-102.18	nm	0.66	0.22	1.11	0.11	0.26	0.39
Cascade-6	11/11/2005	-12.81	-93.35	36.7	2.64	0.88	3.71	0.47	2.34	0.58
Cascade-6	3/30/2006	-9.52	-75.45	23.3	1.66	0.52	2.83	0.16	1.13	0.63
Cascade 6	5/30/2006	-12.13	-87.87	9.8	0.69	0.27	1.44	0.05	0.17	0.37
Cascade 6	10/12/2006	-12.82	-92.54	37.3	2.61	0.92	3.95	0.42	1.92	0.86
Cascade 6	4/27/2007	-13.91	-96.74	8.1	1.39	0.46	1.25	0.10	0.46	0.26
Cascade-10	7/18/2004	nm	nm	21.5	18.06	0.48	10.63	0.94	1.31	0.72
El Portal-1	7/18/2004	nm	nm	24.3	27.20	0.56	15.20	0.64	1.31	0.88
El Portal-8	10/14/2004	nm	nm	54.8	2.21	0.03	5.60	0.82	1.60	3.64
El Portal-8	7/13/2005	nm	nm	14.5	0.74	0.27	1.49	0.11	0.32	n.a.
El Portal-8	11/11/2005	nm	nm	82.6	3.55	0.04	10.29	1.38	3.43	8.03
TRIBUTARIES										
Yosemite Falls	7/18/2004	nm	nm	14.4	18.16	0.40	10.35	1.07	0.16	0.31
Yosemite Falls	1/18/2005	-12.84		9.5	0.92	0.25	0.92	0.06	0.35	0.26
Yosemite Falls	6/9/2005		-97.89	7.8	0.62	0.23	0.80	0.09	0.15	0.24
Yosemite Falls	7/13/2005	-12.54	-90.53	7.4	0.49	0.17	0.73	0.04	0.09	0.17
Yosemite Falls	11/11/2005	-11.44	-86.60	12.7	0.93	0.35	1.13	0.08	0.39	0.29
Yosemite Falls	3/30/2006	nm	nm	7.0	0.78	0.25	0.93	0.06	0.15	0.19
Yosemite Falls	5/30/2006	-14.06	-100.15	7.0	0.56	0.29	0.74	0.04	0.10	0.29
Yosemite Falls	10/12/2006	-9.01	-75.82	16.1	1.05	0.48	1.58	0.12	0.26	0.73
Yosemite Falls	1/19/2007	-13.07	-96.92	6.9	0.84	0.24	1.12	0.08	0.24	0.24
Yosemite Falls	4/27/2007	-13.35	-95.77	8	0.70	0.23	0.76	0.04	0.11	0.20
Yosemite Falls	5/12/2007	-12.39	-90.40	nm	0.68	0.21	0.80	0.04	0.19	0.18
Yosemite Creek	7/12/2007	-7.80	-67.65	20	1.35	0.74	1.91	0.13	0.50	0.29
Bridal Veil Falls	7/18/2004	nm	nm	39.5	40.09	0.96	20.97	0.04	0.24	0.60
Bridal Veil Falls	10/14/2004	-10.72	-83.18	51.1	3.32	0.78	5.96	0.84	0.28	0.42
Bridal Veil Falls	1/18/2005	-13.08	nm	21.8	1.53	0.74	2.47	0.36	0.41	0.32
Bridal Veil Falls	7/13/2005	-12.16	-86.59	22.4	1.61	0.36	2.57	0.33	0.17	0.13
Bridal Veil Falls	11/11/2005	-12.47	-89.16	38.0	2.59	0.69	4.28	0.61	0.74	0.29

Table A.1. Cont

Location	Date Collected	^{18}O	D	EC (25 ^{o}C)	Na^{+}	K^{+}	Ca^{2+}	Mg^{2+}	Cl^{-}	SO_4^{2-}
MERCED RIVER	m/d/yr	(‰)	(‰)	($mScm^{-1}$)	(mgL^{-1})	(mgL^{-1})	(mgL^{-1})	(mgL^{-1})	(mgL^{-1})	(mgL^{-1})
Bridal Veil Falls	3/30/2006	-12.79	-91.08	11.2	3.80	0.34	2.76	0.19	0.20	0.38
Bridal Veil Falls	5/30/2006	-12.54	-88.59	nm	3.91	0.32	2.23	0.13	0.17	0.30
Bridal Veil Falls	10/12/2006	-12.24	-87.99	48.6	3.04	0.75	5.77	0.76	0.67	0.30
Bridal Veil Falls	1/31/2007	-12.74	-91.77	19.8	2.50	0.53	4.30	0.51	0.34	nm
Bridal Veil Falls	4/27/2007	-13.14	-90.07	16.7	1.29	0.31	1.77	0.16	0.17	0.23
Crane Creek	3/30/2006	nm	-77.94	42.1	4.40	0.89	4.77	0.68	0.52	0.45
Crane Creek	10/12/2006	nm	-75.94	52.7	5.29	1.18	6.03	1.00	1.00	0.41
Crane Creek	10/10/2007	nm	nm	nm	5.83	1.22	6.55	1.03	0.84	0.66
MR South Fork	10/10/2007	nm	nm	nm	4.62	1.27	7.23	0.59	3.84	2.99
SPRINGS										
Happy Isle Spring	4/6/2006	-13.06	-96.74	184.1	13.98	1.29	21.58	0.62	32.74	1.36
Fern Spring	7/18/2004	nm	nm	36.3	28.23	0.76	16.35	1.00	0.43	0.79
Fern Spring	10/14/2004	-11.21	-89.65	36.0	2.58	0.77	3.93	0.53	0.39	0.74
Fern Spring	1/18/2005	-12.46	nm	36.4	2.58	0.77	3.96	0.54	0.39	0.69
Fern Spring	6/9/2005	nm	-86.72	23.4	1.78	0.61	2.22	0.31	0.41	0.35
Fern Spring	7/13/2005	-12.26	-86.09	28.4	1.95	0.64	2.88	0.40	0.29	0.31
Fern Spring	11/11/2005	-12.35	-87.40	33.5	2.35	0.71	3.48	0.47	0.36	0.58
Fern Spring	3/30/2006	-12.47	-87.88	27.4	4.25	0.58	3.19	0.14	0.28	0.36
Fern Spring	5/30/2006	-12.49	-87.58	20.3	4.78	0.54	2.81	0.17	0.26	0.44
Fern Spring	10/12/2006	-12.47	-87.33	32.9	2.24	0.66	3.32	0.38	0.31	0.49
Fern Spring	4/27/2007	-12.44	-85.24	29	2.11	0.70	3.35	0.36	0.30	0.34
Fern Spring	10/10/2007	nm	nm	nm	2.58	0.72	3.53	0.31	0.39	0.68
Hardin Spring	5/30/2006	-11.95	-83.78	55.0	8.41	1.11	5.69	0.42	0.42	0.43
Cascade Spring	1/18/2005	-11.30	nm	37.6	3.99	1.21	4.28	0.57	0.69	1.45
Drinking Fountain	4/6/2006	-9.31	-65.01	61.6	5.85	0.57	6.49	1.79	1.09	5.46
GROUNDWATER										
Valley Well 1	6/20/2005	-12.89	-95.56	40.4	2.36	2.02	3.52	0.73	0.31	0.66
Valley Well 1	5/31/2006	-12.69	-93.40	44.0	2.61	2.20	3.74	0.96	0.35	0.78
Valley Well 1	11/2/2006	-13.07	-95.44	43.6	2.53	2.16	3.75	0.92	0.33	0.70
Valley Well 1	10/24/2007	-12.40	-91.85	46.4	2.37	2.16	3.54	0.69	0.34	0.69
Valley Well 2	6/20/2005	-12.65	-92.51	52.8	4.39	2.11	4.42	0.61	2.45	1.31

Table A.1. Cont.

Location	Date Collected	^{18}O	D	EC (25 ^{o}C)	Na^{+}	K^{+}	Ca^{2+}	Mg^{2+}	Cl^{-}	SO_4^{2-}
MERCED RIVER	m/d/yr	(‰)	(‰)	($mScm^{-1}$)	(mgL^{-1})	(mgL^{-1})	(mgL^{-1})	(mgL^{-1})	(mgL^{-1})	(mgL^{-1})
Valley Well 2	5/31/2006	-12.54	-92.33	54.3	4.41	2.06	4.68	0.62	2.33	1.20
Valley Well 2	11/2/2006	-12.68	-93.06	57.6	5.33	2.15	4.92	0.60	3.51	1.52
Valley Well 2	10/24/2007	nm	nm	54.2	nm	2.23	nm	nm	4.59	1.54
Valley Well 4	6/20/2005	-12.73	-93.27	68.0	6.13	2.57	4.76	0.69	5.06	2.09
Valley Well 4	5/31/2006	-12.70	-94.51	42.4	3.11	1.73	3.83	0.48	1.27	0.79
Valley Well 4	11/2/2006	-12.89	-94.39	51.8	3.89	2.04	4.08	0.58	2.51	1.08
Valley Well 4	10/24/2007	-12.44	-92.09	43.6	3.02	1.76	3.35	0.36	1.34	0.70
Arch Rock	6/20/2005	-12.46	-90.03	74.2	5.96	1.46	6.94	1.36	1.14	1.94
Arch Rock	5/31/2006	-12.32	-90.07	76.4	6.11	1.45	7.33	1.51	1.17	1.76
Arch Rock	11/2/2006	-12.44	-90.25	55	6.04	1.47	7.04	1.46	1.17	1.78
Arch Rock	10/24/2007	-12.39	-87.82	88.1	7.35	1.20	8.00	1.37	1.21	0.88
Crane Flat	6/20/2005	-12.44	-86.56	86.8	4.72	1.03	9.95	1.74	0.65	1.07
Crane Flat	5/31/2006	-12.40	-86.28	100.0	6.23	1.04	10.47	1.83	2.79	1.59
Crane Flat	11/2/2006	-12.53	-86.26	86.2	5.51	0.97	9.83	1.97	2.21	1.08
Crane Flat	10/24/2007	nm	nm	99.3	5.09		12.34	1.58	0.68	1.33
Hodgdon's	5/31/2006	-11.56	-82.00	91.0	7.08	1.04	8.81	0.88	1.31	0.05
Hodgdon's	11/2/2006	-11.73	-82.50	87	6.18	1.00	8.23	0.82	0.68	0.08
Hodgdon's	10/24/2007	nm	nm	97.5	7.62	nm	10.30	0.88	0.67	1.79
EP Well 2	6/20/2005	-10.91	-78.95	198.1	9.84	1.47	25.22	4.19	8.24	7.73
EP Well 2	6/1/2006	-10.56	-77.68	209.8	9.84	1.48	26.07	4.40	8.50	8.38
EP Well 2	11/6/2006	-11.40	-83.45	206.5	10.21	1.29	26.58	3.54	15.12	9.42
EP Well 2	10/30/2007	-10.88	-81.62	234.6	12.29	1.57	28.15	3.40	17.47	7.96
EP Well 3	6/20/2005	-10.53	-76.69	151.2	5.66	1.60	21.19	2.95	1.07	8.77
EP Well 3	6/1/2006	-10.68	-78.14	157.8	6.08	1.62	21.96	3.14	1.18	7.81
EP Well 3	11/6/2006	-11.56	-84.36	140.8	5.50	1.37	19.50	2.05	2.75	6.61
EP Well 3	10/30/2007	-10.98	-79.90	173.1	7.01	1.89	24.70	2.52	4.10	7.71
EP Well 4	6/20/2005	-11.35	-81.62	118.3	7.05	1.04	15.64	1.19	3.66	6.93
EP Well 4	6/1/2006	-11.10	-79.69	127.8	7.26	1.06	16.70	1.26	3.78	6.97
EP Well 4	11/6/2006	-12.54	-91.15	118	6.54	0.83	15.30	0.75	5.61	3.97
EP Well 4	10/30/2007	nm	nm	101.5	6.97	0.96	12.55	0.63	7.53	0.19
EP Well 5	6/1/2006	-11.01	-78.88	124.5	5.00	1.22	14.76	2.97	2.57	14.71

Table A.1. Cont.

Location	Date Collected	^{18}O	D	EC (25 ^{o}C)	Na^{+}	K^{+}	Ca^{2+}	Mg^{2+}	Cl^{-}	SO_4^{2-}
MERCED RIVER	m/d/yr	(‰)	(‰)	($mScm^{-1}$)	(mgL^{-1})	(mgL^{-1})	(mgL^{-1})	(mgL^{-1})	(mgL^{-1})	(mgL^{-1})
EP Well 5	11/6/2006	-12.04	-87.15	109	4.36	0.96	13.24	1.89	2.85	10.67
EP Well 5	10/30/2007	nm	nm	105.5	4.76	1.07	12.04	1.63	2.67	1.50
EP Well 6	6/20/2005	-12.32	-89.61	94.0	4.49	1.19	11.76	1.51	3.83	2.38
EP Well 6	6/1/2006	-12.16	-88.38	98.1	4.56	1.23	12.61	1.63	3.97	3.02
EP Well 6	11/6/2006	-12.79	-92.89	82.6	4.07	1.10	10.39	1.38	3.59	2.82
EP Well 6	10/30/2007	nm	nm	77.5	4.00	1.10	9.33	0.81	3.34	0.32
EP Well 7	6/1/2006	-12.53	-91.11	82.5	3.71	1.05	10.92	1.48	1.47	3.19
EP Well 7	11/6/2006	-13.13	-95.20	77.7	3.66	0.99	9.45	1.18	4.52	2.03
EP Well 7	10/30/2007	-14.82	nm	79.0	3.16	1.04	8.10	0.66	3.38	0.43

nm = not measured

Table A.2. ^{36}Cl data for the Merced River basin.

Sample Name	Sample Date	Analysis Date	Cl- µg/g	36Cl/Cl ratio				[36Cl] (atoms/g)
				Bkgd&Carrier Corrected		(x1015)	(x1015)	
				ratio	±	ratio	±	
NeFa0605	6/9/2005	Dec-06	0.32	3.58E-12	1.19E-13	3578	119	1.92E+04
HI704	7/18/2004	Oct-04	1.37	5.94E-13	2.24E-14	594	22	1.38E+04
HI1004BN	10/14/2004	Aug-06	4.97	5.87E-13	6.31E-14	587	63	4.96E+04
HI0105BN	1/18/2005	Aug-06	2.85	9.34E-13	5.11E-14	934	51	4.52E+04
HI0605BN	6/9/2005	Aug-06	0.31	3.89E-12	4.42E-13	3889	442	2.01E+04
HI0705	7/14/2005	Dec-06	0.21	2.63E-12	1.14E-13	2630	114	9.58E+03
HI1105	11/11/2005	Jun-06	3.58	9.60E-13	1.10E-13	960	110	5.84E+04
HI0306	3/30/2006	Jun-06	2.07	1.28E-12	5.22E-14	1276	52	4.49E+04
HI 0506	5/30/2006	Jan-07	0.15	6.51E-12	3.16E-13	6505	316	1.70E+04
HI1006	10/12/2006	Dec-06	3.16	6.78E-13	2.90E-14	678	29	3.64E+04
HI 0107	1/30/2007	Sep-07	5.51	5.58E-13	2.11E-14	558	21	5.22E+04
HI 0407	4/27/2007	Sep-07	0.98	1.36E-12	5.40E-14	1361	54	2.26E+04
HI 0507	5/12/2007	Sep-07	0.44	2.08E-12	1.28E-13	2082	128	1.55E+04
HI0707	7/12/2007	Jan-08	2.06	4.75E-13	1.46E-14	475	15	1.66E+04
HI1007	10/12/2007	Jan-08	5.28	4.24E-13	1.55E-14	424	16	3.80E+04
ECB704	7/18/2004	Oct-04	1.55	7.89E-13	2.58E-14	789	26	2.08E+04
ECB1004BN	10/14/2004	Aug-06	3.11	6.85E-13	3.77E-14	685	38	3.62E+04
ECB0105	1/18/2005	Jun-06	1.92	1.82E-12	7.88E-14	1816	79	5.92E+04
ECB0605	6/9/2005	Dec-06	0.36	4.31E-12	1.84E-13	4312	184	2.66E+04
ECB0705BN	7/14/2005	Aug-06	0.26	3.38E-12	2.87E-13	3381	287	1.47E+04
ECB1105	11/11/2005	Jun-06	3.08	1.02E-12	4.09E-14	1024	41	5.35E+04
ECB0306BN	3/3/2006	Aug-06	1.48	1.70E-12	9.42E-14	1697	94	4.27E+04
ECB 0506	5/30/2006	Jan-07	0.27	4.21E-12	2.60E-13	4214	260	1.93E+04
ECB 1006	10/12/2006	Jan-07	2.60	1.03E-12	4.00E-14	1035	40	4.57E+04
ECB 0107	1/30/2007	Sep-07	4.05	7.25E-13	2.74E-14	725	27	4.99E+04
ECB 0407	4/27/2007	Sep-07	0.64	1.94E-12	6.46E-14	1940	65	2.12E+04
ECB 0507	5/12/2007	Sep-07	0.43	2.30E-12	9.43E-14	2297	94	1.67E+04
ECB0707	7/12/2007	Jan-08	1.94	7.14E-13	2.65E-14	714	27	2.36E+04
ECB1007	10/12/2007	Jan-08	3.72	6.71E-13	2.45E-14	671	24	4.23E+04
CC1704	7/14/2004	Oct-04	1.27	9.09E-13	2.67E-14	909	27	1.96E+04
CC6704	7/14/2004	Oct-04	1.24	9.96E-13	4.21E-14	996	42	2.10E+04

Table A.2. Cont.

Sample Name	Sample Date	Analysis Date	Cl- µg/g	36Cl/Cl ratio Bkgd&Carrier Corrected ratio	±	(x1015) ratio	(x1015) ±	[36Cl] (atoms/g)
C61004	10/14/2004	Dec-06	1.95	1.38E-12	3.77E-14	1463	38	4.57E+04
C60105	1/18/2005	Dec-06	1.38	2.06E-12	8.50E-14	2120	85	4.84E+04
C60705	7/14/2005	Dec-06	0.26	3.10E-12	1.65E-13	3153	165	1.34E+04
C61105	11/11/2005	Dec-06	2.34	1.53E-12	6.68E-14	1593	67	6.09E+04
C60306	3/30/2006	Dec-06	1.13	1.95E-12	7.42E-14	2025	74	3.74E+04
C6 0506	5/30/2006	Jan-07	0.17	6.57E-12	3.57E-13	6566	357	1.84E+04
C6 1006	10/12/2006	Jan-07	1.92	1.46E-12	5.59E-14	1456	56	4.75E+04
C6 0107	1/30/2007	Sep-07	3.10	1.03E-12	9.95E-14	1035	100	5.44E+04
C6 0407	4/27/2007	Sep-07	0.46	2.40E-12	1.00E-13	2398	100	1.86E+04
CC10704	7/18/2004	Oct-04	1.31	1.02E-12	3.36E-14	1025	34	2.28E+04
EP1704	7/18/2004	Oct-04	1.31	1.04E-12	2.78E-14	1045	28	2.32E+04
SF704	7/18/2004	Oct-04	3.94	3.77E-13	9.94E-15	377	10	2.52E+04
YC704	7/18/2004	Oct-04	0.16	8.99E-12	3.12E-13	8992	312	2.44E+04
YC0105	1/18/2005	Jun-06	0.35	1.05E-11	1.18E-12	10487	1178	6.23E+04
YC0605	6/9/2005	Dec-06	0.15	1.11E-11	4.22E-13	11059	422	2.79E+04
YC0705	7/14/2005	Jan-07	0.09	9.98E-12	4.44E-13	9976	444	1.49E+04
YC 1105	11/11/2005	Sep-07	0.39	1.07E-11	3.39E-13	10711	339	7.10E+04
YC0306	3/30/2006	Dec-06	0.15	1.16E-11	4.42E-13	11649	442	3.05E+04
YC 0506	5/30/2006	Jan-07	0.10	1.13E-11	5.94E-13	11312	594	1.88E+04
YC1006	10/12/2006	Dec-06	0.26	1.03E-11	3.94E-13	10305	394	4.55E+04
YC 0107	1/30/2007	Sep-07	0.24	1.32E-11	4.03E-13	13232	403	5.39E+04
YC 0407	4/27/2007	Sep-07	0.11	1.22E-11	3.95E-13	12181	395	2.34E+04
BV704	7/18/2004	Sep-04	0.24	8.27E-12	4.84E-13	8273	484	3.37E+04
BVF1004	10/14/2004	Jun-06	0.28	8.83E-12	3.58E-13	8834	358	4.20E+04
BVF 0105	1/18/2005	Sep-07	0.41	8.46E-12	3.72E-13	8464	372	5.89E+04
BVF 0705	7/14/2005	Jan-07	0.17	7.64E-12	4.45E-13	7642	445	2.22E+04
BVF1105	11/11/2005	Dec-06	0.74	8.96E-12	2.01E-13	8962	201	1.13E+05
BVF0306	3/30/2006	Dec-06	0.20	1.02E-11	2.19E-13	10194	219	3.50E+04
BVF 0506	5/30/2006	Jan-07	0.17	8.47E-12	3.43E-13	8466	343	2.37E+04
BVF 1006	10/12/2006	Jan-07	0.67	8.62E-12	3.18E-13	8620	318	9.78E+04

Table A.2. Cont.

Sample Name	Sample Date	Analysis Date	Cl- µg/g	36Cl/Cl ratio Bkgd&Carrier Corrected ratio	±	(x1015) ratio	±	[36Cl] (atoms/g)
BVF 0107	1/30/2007	Sep-07	0.34	8.92E-12	3.32E-13	8918	332	5.10E+04
BVF 0407	4/27/2007	Sep-07	0.17	9.07E-12	3.51E-13	9070	351	2.60E+04
CrCr0306	3/30/2006	Dec-06	0.52	5.01E-12	1.40E-13	5011	140	4.40E+04
CrCr1006	10/12/2006	Dec-06	1.00	3.58E-12	9.73E-14	3578	97	6.09E+04
Fern1004	10/14/2004	Jun-06	0.39	3.45E-12	1.52E-13	3455	152	2.29E+04
Fern0105	1/18/2005	Aug-06	0.39	3.64E-12	7.88E-14	3637	79	2.41E+04
Fern0605	6/9/2005	Jun-06	0.41	2.50E-12	5.46E-14	2497	55	1.74E+04
Fern0705	7/14/2005	Jun-06	0.29	3.54E-12	1.06E-13	3537	106	1.74E+04
Fern1105	11/11/2005	Jun-06	0.36	3.62E-12	1.24E-13	3621	124	2.21E+04
Fern0306	3/30/2006	Jun-06	0.28	4.02E-12	1.07E-13	4020	107	1.91E+04
Fern 0506	5/30/2006	Jan-07	0.26	6.77E-12	2.68E-13	6772	268	2.94E+04
Fern1006	10/12/2006	Dec-06	0.31	7.93E-12	2.19E-13	7930	219	4.20E+04
FS 0407	4/27/2007	Sep-07	0.30	6.90E-12	2.24E-13	6899	224	3.53E+04
HIS0406	4/6/2006	Aug-06	32.74	7.06E-14	6.34E-15	71	6	3.92E+04
Hard0606	5/31/2006	Aug-06	0.42	2.96E-12	1.46E-13	2956	146	2.10E+04
CaSp0105	1/25/2005	Dec-06	0.69	6.06E-12	2.10E-13	6060	210	7.08E+04
DF0406	4/6/2006	Aug-06	1.09	2.82E-12	1.03E-13	2816	103	5.20E+04
VW1 0605	6/21/2005	Jan-07	0.31	1.03E-11	3.89E-13	10322	389	5.49E+04
VW1 06	5/31/2006	Aug-06	0.35	1.24E-11	6.21E-13	12360	621	7.29E+04
VW11106	11/2/2006	Dec-06	0.33	1.01E-11	3.07E-13	10075	307	5.65E+04
VW1 1007	10/24/2007	Jan-08	0.34	1.26E-11	4.38E-13	12640	438	7.24E+04
VW2 0605	6/21/2005	Jan-07	2.45	1.61E-12	5.36E-14	1613	54	6.70E+04
VW2 06	5/31/2006	Aug-06	2.33	1.56E-12	5.27E-14	1560	53	6.16E+04
VW21106	11/2/2006	Dec-06	3.51	1.10E-12	4.12E-14	1100	41	6.56E+04
VW4 0605	6/21/2005	Jan-07	5.06	5.30E-13	2.07E-14	530	21	4.55E+04
VW4 06	5/31/2006	Aug-06	1.27	2.16E-12	7.16E-14	2164	72	4.66E+04
VW4 1106	11/2/2006	Jan-07	2.51	1.68E-12	6.34E-14	1685	63	7.18E+04
VW4 1007	10/24/2007	Jan-08	1.34	2.37E-12	7.15E-14	2373	71	5.41E+04
AR 0605	6/21/2005	Jan-07	1.14	3.68E-12	1.83E-13	3682	183	7.12E+04

Table A.2. Cont.

Sample Name	Sample Date	Analysis Date	Cl- µg/g	36Cl/Cl ratio Bkgd&Carrier Corrected ratio	±	(x1015) ratio	± (x1015)	[36Cl] (atoms/g)
AR 06	5/31/2006	Aug-06	1.17	4.20E-12	1.25E-13	4199	125	8.35E+04
AR 1106	11/2/2006	Jan-07	1.17	3.52E-12	1.44E-13	3523	144	7.01E+04
AR1007	10/24/2007	Jan-08	1.21	4.30E-12	1.56E-13	4298	156	8.86E+04
CF 0605	6/21/2005	Sep-07	0.65	2.79E-12	1.20E-13	2788	120	3.06E+04
CF 06	5/31/2006	Aug-06	2.79	6.69E-13	2.55E-14	669	26	3.16E+04
CF 1106	11/2/2006	Jan-07	2.21	8.64E-13	3.44E-14	864	34	3.24E+04
HM 06	5/31/2006	Aug-06	1.31	7.87E-13	6.04E-14	787	60	1.75E+04
HM1106	11/2/2006	Dec-06	0.68	1.33E-12	5.41E-14	1325	54	1.53E+04
EPW2 0605	6/21/2005	Jan-07	8.24	1.24E-12	4.60E-14	1243	46	1.74E+05
EP2 06	6/1/2006	Aug-06	8.50	1.01E-12	2.93E-14	1015	29	1.46E+05
EPW21106	11/6/2006	Dec-06	15.12	5.48E-13	1.66E-14	548	17	1.41E+05
EPW2 1007	10/30/2007	Jan-08	17.47	5.37E-13	1.97E-14	537	20	1.59E+05
EPW3 0605	6/21/2005	Jan-07	1.07	4.16E-12	1.55E-13	4158	155	7.57E+04
EP3 06	6/1/2006	Aug-06	1.18	3.49E-12	1.25E-13	3493	125	7.00E+04
EPW31106	11/6/2006	Dec-06	2.75	1.95E-12	5.87E-14	1947	59	9.08E+04
EPW3 1007	10/30/2007	Jan-08	4.10	1.84E-12	6.75E-14	1844	68	1.29E+05
EPW4 0605	6/21/2005	Sep-07	3.66	1.39E-12	5.15E-14	1391	52	8.64E+04
EP4 06	6/1/2006	Aug-06	3.78	1.34E-12	3.98E-14	1342	40	8.62E+04
EPW41106	11/6/2006	Dec-06	5.61	7.59E-13	2.06E-14	759	21	7.24E+04
EP5 06	6/1/2006	Aug-06	2.57	1.19E-12	3.90E-14	1194	39	5.22E+04
EPW5 1106	11/6/2006	Jan-07	2.85	1.02E-12	3.93E-14	1020	39	4.93E+04
EPW6 0605	6/21/2005	Sep-07	3.83	7.38E-13	2.80E-14	738	28	4.80E+04
EP6 06	6/1/2006	Aug-06	3.97	6.79E-13	2.69E-14	679	27	4.57E+04
EPW6 1106	11/6/2006	Jan-07	3.59	7.17E-13	2.31E-14	717	23	4.36E+04
EP7 06	6/1/2006	Aug-06	1.47	1.82E-12	8.02E-14	1823	80	4.56E+04
EPW7 1106	11/6/2006	Jan-07	4.52	4.49E-13	1.50E-14	449	15	3.45E+04
Gin Flat	2/15/2006	Aug-06	0.14	2.20E-13	2.46E-13	220	246	5.11E+02
Tioga Pass	4/15/2006	Aug-06	0.07	3.06E-13	5.06E-13	306	506	3.68E+02
TM	3/27/2006	Aug-06	0.10	2.63E-13	3.31E-13	263	331	4.47E+02
BP	3/1/2006	Aug-06	nm	3.62E-13	3.25E-14	362	33	9.38E+03

Table A.2. Cont.

Sample Name	Sample Date	Analysis Date	Cl- µg/g	36Cl/Cl ratio Bkgd&Carrier Corrected ratio	±	(x1015) ratio	(x1015) ±	[36Cl] (atoms/g)
BP replicate	3/1/2006	Aug-06	nm	4.01E-13	1.51E-14	401	15	9.65E+03
TM	5/15/2006	Aug-06	0.42	2.36E-13	4.03E-14	236	40	1.69E+03
Blk704 blank		Oct-04	---	1.6E-15	3.4E-16	1.6	0.34	-----
NaCl704 blank		Oct-04	---	1.6E-15	3.2E-16	1.6	0.32	-----
AGCL Blank	8/23/2006	Aug-06	---	1.0E-14	4.2E-15	10.1	4.17	-----
PB072506	7/25/2006	Aug-06	---	1.6E-14	1.5E-15	16.4	1.49	-----
PB072606	7/25/2006	Aug-06	---	1.9E-14	2.7E-15	19.2	2.73	-----
PB823-1	8/23/2006	Aug-06	---	1.4E-14	1.8E-15	14.1	1.76	-----
PB823-2	8/23/2006	Aug-06	---	1.1E-14	1.5E-15	11.1	1.54	-----
Blank12/06B	12/19/2006	Dec-06	-----	7.8E-15	7.3E-16	7.8	0.73	-----
Proc Blank#1	1/14/2008	Jan-08	1.69802E+19	5.5E-16	1.8E+00	0.6	-----	
Proc Blank#2	1/14/2008	Jan-08	1.39556E+19	1.8E-16	5.6E-01	0.2	-----	
PB1 0108	1/14/2008	Jan-08	1.69802E+19	5.1E-16	1.1E+00	0.5	-----	
PB2 0108	1/14/2008	Jan-08	1.69802E+19	7.1E-16	1.7E+00	0.7	-----	
UCM 100	9/16/2007	Sep-07	-----	1.0E-14	1.0E-15	10.3	1.05	
UCM 50	9/16/2007	Sep-07	-----	7.7E-15	9.5E-16	7.7	0.95	
UCM 25	9/16/2007	Sep-07	-----	5.3E-15	7.6E-16	5.3	0.76	
UCM 5	9/16/2007	Sep-07	-----	3.3E-15	6.0E-16	3.3	0.60	
PB 1	9/14/2007	Sep-07	-----	9.8E-15	2.0E-15	9.8	2.01	
PB 2	9/14/2007	Sep-07	-----	3.4E-15	6.3E-16	3.4	0.63	
PB1	1/12/2007	Jan-07	-----	9.5E-15	1.2E-15	9.5	1.21	
PB2	1/12/2007	Jan-07		1.5E-14	1.4E-15	14.5	1.43	

Table A.3. ^{222}Rn data for the Merced River basin.

Location MERCED RIVER	Date Collected (m/d/yr)	222Rn (cpm)	Conductivity (μScm^{-1})
Nevada Falls	6/9/2005	12	8.8
Happy Isles	7/18/2004	114	15.7
Happy Isles	10/14/2004	3143	43.7
Happy Isles	1/18/2005	662	25.1
Happy Isles	6/9/2005	148	11.1
Happy Isles	7/13/2005	50	nm
Happy Isles	11/11/2005	523	30.6
Happy Isles	3/30/2006	312	24.4
Happy Isles	11/6/2006	1528	39.0
Happy Isles	1/31/2007	922	nm
Happy Isles	3/16/2007	242	20.8
Happy Isles	5/24/2007	201	11.9
Happy Isles	7/12/2007	476	19.4
Happy Isles	10/10/2007	2721	nm
Tenaya Creek MR	7/12/2007	2320	nm
Super Bridge	7/13/2005	321	8.2
Super Bridge	11/11/2005	1008	31.3
Super Bridge	3/30/2006	1696	25.4
Super Bridge	5/30/2006	549	nm
Super Bridge	10/12/2006	1921	nm
Super Bridge	11/6/2006	2511	44.4
Super Bridge	1/31/2007	2012	nm
Super Bridge	5/12/2007	605	nm
Super Bridge	7/12/2007	1480	22
Super Bridge	10/10/2007	2937	nm
El Capitan Bridge	7/18/2004	362	21.5
El Capitan Bridge	10/14/2004	1456	40.6
El Capitan Bridge	1/18/2005	850	22.4
El Capitan Bridge	6/9/2005	529	12.3
El Capitan Bridge	7/13/2005	412	nm
El Capitan Bridge	11/11/2005	1162	38.8
El Capitan Bridge	3/30/2006	1692	25.1

Table A.3. Cont.

Location MERCED RIVER	Date Collected (m/d/yr)	222Rn (cpm)	Conductivity (μScm^{-1})
El Capitan Bridge	5/30/2006	478	10.4
El Capitan Bridge	10/12/2006	1858	43.6
El Capitan Bridge	11/6/2006	1217	45.5
El Capitan Bridge	1/31/2007	1484	nm
El Capitan Bridge	3/16/2007	694	16.6
El Capitan Bridge	5/24/2007	693	13.5
El Capitan Bridge	7/12/2007	1258	26.7
El Capitan Bridge	10/10/2007	1158	nm
Swinging Bridge	7/13/2005	326	8.4
Swinging Bridge	11/11/2005	1158	38.7
Swinging Bridge	3/30/2006	1514	22.7
Swinging Bridge	11/6/2006	2437	43.3
Swinging Bridge	7/12/2007	1553	24.2
Swinging Bridge	10/10/2007	2709	nm
Bridalveil MR	7/13/2005	412	nm
Bridalveil MR	11/11/2005	561	35.5
Bridalveil MR	3/30/2006	1117	nm
Bridalveil MR	11/6/2006	1062	nm
Bridalveil MR	1/31/2007	729	nm
Bridalveil MR	5/24/2007	515	nm
Bridalveil MR	7/12/2007	1026	26.1
Bridalveil MR	10/10/2007	1205	nm
Fern Spring MR	7/13/2005	1178	10.4
Fern Spring MR	11/11/2005	862	38.5
Fern Spring MR	3/30/2006	2029	nm
Fern Spring MR	10/12/2006	2302	nm
Fern Spring MR	11/6/2006	2289	nm
Fern Spring MR	1/31/2007	1318	nm
Fern Spring MR	5/24/2007	812	nm
Fern Spring MR	7/12/2007	1036	27.2
Fern Spring MR	10/10/2007	2930	nm
Cascade-1	7/18/2004	114	20.7

Table A.3. Cont.

Location MERCED RIVER	Date Collected (m/d/yr)	222Rn (cpm)	Conductivity (μScm^{-1})
Cascade-1	10/14/2004	687	42.9
Cascade-1	1/18/2005	154	25.2
Cascade-2	7/18/2004	33	20.8
Cascade-4	7/18/2004	35	20.7
Cascade-4	10/14/2004	271	nm
Cascade-4	1/18/2005	67	25.1
Cascade-5	7/18/2004	225	20.8
Cascade-5	10/14/2004	296	25.2
Cascade Picnic	7/18/2004	427	21.6
Cascade Picnic	10/14/2004	6161	44.1
Cascade Picnic	1/18/2005	297	21.7
Cascade Picnic	7/13/2005	73	nm
Cascade Picnic	11/11/2005	1172	36.7
Cascade Picnic	3/30/2006	526	23.3
Cascade Picnic	5/30/2006	217	9.8
Cascade Picnic	10/12/2006	1900	37.3
Cascade Picnic	1/19/2007	1531	37.3
Cascade Picnic	3/16/2007	266	16.6
Cascade Picnic	4/27/2007		8.1
Cascade Picnic	5/24/2007	340	14.6
Cascade Picnic	7/12/2007	1377	28.1
Cascade Picnic	10/10/2007	5148	nm
Cascade-7	7/18/2004	354	21.7
Cascade-7	1/18/2005	341	24.4
Cascade-7	7/13/2005	109	nm
Cascade-9	7/18/2004	382	21.6
Cascade-9	10/14/2004	5155	44.8
Cascade-9	1/18/2005	373	24.8
Cascade-9	7/13/2005	149	nm
Cascade-10	7/18/2004	65	21.5
Cascade-10	10/14/2004	225	43.8
Cascade-10	1/18/2005	57	24.9

Table A.3. Cont.

Location MERCED RIVER	Date Collected (m/d/yr)	222Rn (cpm)	Conductivity (μScm^{-1})
Cascade-10	7/13/2005	67	nm
Cascade-10	11/11/2005	120	nm
Crane Creek MR	7/12/2007	102	30.1
Crane Creek MR	10/10/2007	335	nm
El Portal-1	7/18/2004	37	24.3
El Portal-2	7/18/2004	12	24.9
El Portal-4	7/18/2004	20	26.5
El Portal-5	7/18/2004	23	25.1
El Portal-5	1/18/2005	47	27.5
El Portal-6	7/18/2004	39	24.8
El Portal-6	10/14/2004	2046	59.3
El Portal-6	1/18/2005	50	27.5
El Portal-7	7/18/2004	19	25.2
El Portal-8	7/18/2004	675	38.1
El Portal-8	10/14/2004	3322	54.8
El Portal-8	1/18/2005	260	45.6
El Portal-8	7/13/2005	79	14.5
El Portal-8	11/11/2005	2735	82.6
El Portal-8	3/30/2006	46	92.6
El Portal 8	5/30/2006	105	32.3
El Portal 8	10/12/2006	2862	55.5
El Portal-8	1/19/2007	2913	107.8
El Portal 8	5/24/2007	253	nm
El Portal 8	7/12/2007	2868	39.3
El Portal 8	10/10/2007	3843	nm
El Portal-10	7/18/2004	118	25.1
El Portal-10	10/14/2004	203	50.4
El Portal-10	1/18/2005	10	27.6
South Fork MR	7/18/2004	68	48.8
South Fork MR	10/14/2004	0	93.9
South Fork MR	1/18/2005	23	50.0
South Fork MR	7/13/2005	39	nm

Table A.3. Cont.

Location	Date Collected	222Rn	Conductivity
MERCED RIVER	**(m/d/yr)**	**(cpm)**	**(μScm^{-1})**
South Fork MR	11/11/2005	104	66.9
South Fork MR	10/10/2007	90	nm
Briceburg	7/13/2005	86	nm
Briceburg	11/11/2005	174	90.0
Briceburg	5/30/2006	65	17.3
Briceburg	10/12/2006	229	80.8
Briceburg	7/12/2007	81	48.5
Briceburg	10/10/2007	88	nm
TRIBUTARIES			
Illuette Creek	3/30/2006	118	23.1
Tenaya Creek	11/6/2006	1202	37
Tenaya Creek	1/31/2007	1006	32.5
Tenaya Creek	7/12/2007	6600	33.9
Teneya Creek	10/10/2007	1087	nm
Yosemite Falls	7/18/2004	17	14.4
Yosemite Falls	1/18/2005	5	9.5
Yosemite Falls	6/9/2005	78	7.8
Yosemite Falls	7/13/2005	40	7.4
Yosemite Falls	7/12/2007	4560	20
Bridal Veil Falls	7/18/2004	1050	39.5
Bridal Veil Falls	10/14/2004	0	51.1
Bridal Veil Falls	1/18/2005	0	21.8
Bridal Veil Falls	7/13/2005	51	22.4
Bridal Veil Falls	11/11/2005	75	38.0
Cascade Falls	10/14/2004	0	24.2
Cascade Falls	7/13/2005	18	11.1
Cascade Creek	11/11/2005	393	17.1
Cascade Creek	7/12/2007	590	19.8
Crane Creek	7/13/2005	49	nm
Crane Creek	11/11/2005	133	52.8
Crane Creek	7/12/2007	64	62.7
Crane Creek	10/10/2007	152	nm

Table A.3. Cont.

Location	Date Collected	222Rn	Conductivity
MERCED RIVER	**(m/d/yr)**	**(cpm)**	**(μScm^{-1})**
Pidgeon Creek	7/13/2005	45	nm
Moss Creek	7/13/2005	77	nm
Moss Creek	11/11/2005	213	51.8
upper South Fork	4/6/2006	107	27.3
South Fork	10/10/2007	108	nm
Sweetwater Creek	7/13/2005	37	nm
Sweetwater Creek	11/11/2005	107	nm
Sweetwater Creek	3/30/2006	57	83.2
SPRINGS			
Happy Isle Spring	4/6/2006	91541	184.1
Happy Isle Spring	5/19/2006	57055	226.6
Fern Spring	7/18/2004	11776	36.3
Fern Spri Check	7/18/2004	31999	nm
Fern Spring	10/14/2004	42466	36.0
Fern Spring	1/18/2005	40040	36.4
Fern Spring	6/9/2005	18701	23.4
Fern Spring	7/13/2005	27319	28.4
Fern Spring	11/11/2005	33985	33.5
Fern Spring	3/30/2006	26884	27.4
Fern Spring	5/30/2006	22897	20.3
Fern Spring	10/12/2006	42001	32.9
Fern Spring	11/6/2006	44299	31.7
Fern Spring	12/12/2006	14406	33
Fern Spring	1/31/2007	41070	30.3
Fern Spring	3/16/2007	42327	34.1
Fern Spring	4/27/2007		29
Fern Spring	5/24/2007	33389	37.5
Fern Spring	10/10/2007	30820	nm
Hardin Spring	5/30/2006		55.0
Hardin Spring	10/12/2006		**48.1**
Cascade Spring	1/18/2005	32108	37.6
Drinking Fountain	4/6/2006	1550	61.6

Table A.3 Cont.

Location	Date Collected	222Rn	Conductivity
MERCED RIVER	**(m/d/yr)**	**(cpm)**	**(μScm^{-1})**
Drinking Fountain	10/12/2006		**260.9**
Drive Point Samplers			
MP-Superintendent Bridge	7/13/2005	129	nm
MP-El Capitan Bridge	7/13/2005	9384	nm
MP-Cascade Picnic	7/13/2005	4194	nm
GROUNDWATER			
Valley Well 1	6/20/2005	7222	40.4
Valley Well 1	5/31/2006	7168	44.0
Valley Well 1	11/2/2006	10675	43.6
Valley Well 1	10/24/2007	8886	46.4
Valley Well 2	6/20/2005	7173	52.8
Valley Well 2	5/31/2006	5417	54.3
Valley Well 2	11/2/2006	8467	57.6
Valley Well 2	10/24/2007	6781	54.2
Valley Well 4	6/20/2005	5475	68.0
Valley Well 4	5/31/2006	7652	42.4
Valley Well 4	11/2/2006	9163	51.8
Valley Well 4	10/24/2007	9860	43.6
Arch Rock	6/20/2005	25638	74.2
Arch Rock	5/31/2006	28445	76.4
Arch Rock	11/2/2006	31354	55
Arch Rock	10/24/2007	19217	88.1
Crane Flat	6/20/2005	15570	86.8
Crane Flat	5/31/2006	12053	100.0
Crane Flat	11/2/2006	2807	86.2
Crane Flat	10/24/2007	12203	99.3
Hodgdon Meadow	6/20/2005	22711	180.9
Hodgdon Meadow	5/31/2006	26018	91.0
Hodgdon Meadow	11/2/2006	42637	87
Hodgdon Meadow	10/24/2007	55298	97.5
El Portal Well 2	6/20/2005	28116	198.1
El Portal Well 2	6/1/2006	29832	209.8

Table A.3. Cont.

Location MERCED RIVER	Date Collected (m/d/yr)	222Rn (cpm)	Conductivity (μScm^{-1})
El Portal Well 2	11/6/2006	33623	206.5
El Portal Well 2	10/30/2007	34964	234.6
El Portal Well 3	6/20/2005	13083	151.2
El Portal Well 3	6/1/2006	15400	157.8
El Portal Well 3	11/6/2006	7628	140.8
El Portal Well 3	10/30/2007	18498	173.1
El Portal Well 4	6/20/2005	31805	118.3
El Portal Well 4	6/1/2006	39448	127.8
El Portal Well 4	11/6/2006	22269	118
El Portal Well 4	10/30/2007	45781	101.5
El Portal Well 5	6/20/2005	18257	131.2
El Portal Well 5	6/1/2006	17991	124.5
El Portal Well 5	11/6/2006	14406	109
El Portal Well 5	10/30/2007	21393	105.5
El Portal Well 6	6/20/2005	36849	94.0
El Portal Well 6	6/1/2006	34992	98.1
El Portal Well 6	11/6/2006	39567	82.6
El Portal Well 6	10/30/2007	47260	77.5
El Portal Well 7	6/20/2005	26526	80.4
El Portal Well 7	6/1/2006	26624	82.5
El Portal Well 7	11/6/2006	32181	77.7
El Portal Well 7	10/30/2007	30306	79.0

Samples ending with MR are collected in the Merced River near the confluence of the
Yosemite Falls samples were collected at the base of the falls
Yosemite Creek samples were collected near the confluence with the Merced River
Upper South Fork was collected in Wawona
Samples starting with "MP" are drive point samples
Conductivity values are normalized at 25 ^{o}C
nm = not measured
cpm = counts per minute

Table A.4. ^{3}H and noble gas data for the Merced River basin.

Sample ID	Sample Date (m/d/yr)	Analysis Date (m/d/yr)	^{3}H (pCi/L)	$^{3}He/^{4}He$ (ratio)	+- (ratio)	^{4}He ($cm^{3}STP/g$)	+- ($cm^{3}STP/g$)	Ne ($cm^{3}STP/g$)	+- ($cm^{3}STP/g$)	Ar ($cm^{3}STP/g$)	+- ($cm^{3}STP/g$)	Kr ($cm^{3}STP/g$)	+- ($cm^{3}STP/g$)	Xe ($cm^{3}STP/g$)	+- ($cm^{3}STP/g$)
Merced River															
Happy Isles Bridge	7/20/2000		19.05	1.35E-06		3.98E-08		1.66E-07				6.91E-08		9.13E-09	
Happy Isles Bridge	10/13/2000		17.35	nm		nm		nm		nm		nm		nm	
Happy Isles Bridge	1/16/2001	4/12/2005	12.65	1.34E-06	1.00E-08	4.26E-08	8.52E-10	1.96E-07	3.92E-09	4.10E-04	8.20E-06	1.01E-07	3.03E-09	1.50E-08	4.50E-10
Happy Isles Bridge	7/12/2001	8/25/2005	14.50	1.35E-06	1.01E-08	3.73E-08	7.46E-10	1.69E-07	3.37E-09	2.79E-04	5.58E-06	6.51E-08	1.95E-09	8.76E-09	2.63E-10
Happy Isles Bridge	11/11/2005	12/14/2005	13.35	1.33E-06	1.04E-08	3.82E-08	7.63E-10	1.77E-07	3.54E-09	3.38E-04	6.76E-06	8.31E-08	2.49E-09	1.17E-08	3.52E-10
Happy Isles Bridge	3/30/2006	5/14/2006	10.12	nm		nm		nm		nm		nm		nm	
Tenaya Creek MR	11/6/2006		nm	1.32E-06		3.15E-08	6.30E-10	1.69E-07	3.38E-09	3.27E-04	6.54E-06	8.04E-08	2.41E-09	1.16E-08	3.49E-10
Superintendents Bridge	7/12/2001	9/1/2005	nm	1.34E-06	1.04E-08	3.81E-08	7.62E-10	1.68E-07	3.36E-09	2.97E-04	5.94E-06	7.01E-08	2.10E-09	9.65E-09	2.90E-10
Superintendents Bridge	11/11/2005	12/14/2005	nm	1.15E-06	1.04E-08	4.79E-08	9.58E-10	1.72E-07	3.43E-09	3.34E-04	6.68E-06	7.96E-08	2.39E-09	1.14E-08	3.42E-10
Superintendents Bridge	3/30/2006	5/14/2006	nm	1.18E-06	8.85E-09	4.68E-08	9.35E-10	1.85E-07	3.70E-09	3.82E-04	7.64E-06	9.55E-08	2.86E-09	1.39E-08	4.16E-10
Swinging Bridge	11/11/2005	12/14/2005	nm	1.24E-06	1.04E-08	4.22E-08	8.44E-10	1.67E-07	3.34E-09	3.32E-04	6.63E-06	8.02E-08	2.41E-09	1.15E-08	3.44E-10
Swinging Bridge	3/30/2006	5/14/2006	nm	1.26E-06	9.45E-09	4.44E-08	8.88E-10	1.92E-07	3.83E-09	3.88E-04	7.75E-06	9.43E-08	2.83E-09	1.44E-08	4.33E-10
Swinging Bridge	11/6/2006		nm	1.24E-06		4.23E-08	8.46E-10	1.68E-07	3.37E-09	3.27E-04	6.55E-06	7.69E-08	2.31E-09	1.14E-08	3.41E-10
El Capitan Bridge	7/21/2004		nm	1.35E-06		4.06E-08		1.64E-07				6.78E-08		9.46E-09	
El Capitan Bridge	10/14/2004		17.97	nm		nm		nm		nm		nm		nm	
El Capitan Bridge	1/25/2005	4/13/2005	15.09	1.29E-06	9.66E-09	4.36E-08	8.71E-10	1.88E-07	3.76E-09	3.85E-04	7.70E-06	9.42E-08	2.83E-09	1.36E-08	4.07E-10
El Capitan Bridge	7/13/2005	8/25/2005	nm	1.34E-06	1.01E-08	3.82E-08	7.64E-10	1.71E-07	3.42E-09	2.93E-04	5.87E-06	6.77E-08	2.03E-09	9.47E-09	2.84E-10
El Capitan Bridge	11/11/2005	12/14/2005	nm	1.33E-06	9.95E-09	3.97E-08	7.93E-10	1.89E-07	3.78E-09	3.35E-04	6.70E-06	7.82E-08	2.35E-09	1.15E-08	3.45E-10
El Capitan Bridge	3/30/2006	5/14/2006	nm	1.25E-06	9.57E-09	4.32E-08	8.64E-10	1.84E-07	3.67E-09	3.87E-04	7.74E-06	9.79E-08	2.94E-09	1.46E-08	4.39E-10
El Capitan Bridge	5/30/2006	5/14/2006	9.37	1.35E-06	1.01E-08	3.85E-08	7.70E-10	1.74E-07	3.48E-09	3.30E-04	6.60E-06	7.81E-08	2.34E-09	1.12E-08	3.37E-10
Bridalveil Falls MR	11/2/2006		nm	1.34E-06		4.40E-08	8.81E-10	1.86E-07	3.71E-09	3.30E-04	6.59E-06	7.68E-08	2.30E-09	1.14E-08	3.42E-10
Fern Spring MR	11/11/2005	12/14/2005	nm	1.38E-06	9.95E-09	3.81E-08	7.61E-10	1.77E-07	3.55E-09	3.29E-04	6.59E-06	7.78E-08	2.34E-09	1.08E-08	3.24E-10
Fern Spring MR	11/2/2006		nm	1.34E-06		2.64E-08	5.28E-10	1.64E-07	3.28E-09	3.17E-04	6.33E-06	7.62E-08	2.29E-09	1.09E-08	3.26E-10
Cascade 1	7/21/2004		15.88	1.36E-06		4.02E-08		1.66E-07				6.47E-08		8.59E-09	
Cascade 1	1/18/2005	4/12/2005	nm	1.35E-06	1.01E-08	4.20E-08	8.41E-10	1.92E-07	3.84E-09	4.02E-04	8.04E-06	9.85E-08	2.95E-09	1.45E-08	4.34E-10
Cascade 2	7/21/2004		nm	1.35E-06		3.97E-08		1.65E-07				6.48E-08		8.70E-09	
Cascade 4	7/21/2004		nm	1.36E-06		3.94E-08		1.60E-07				6.31E-08		8.14E-09	
Cascade 4	1/18/2005	4/11/2005	nm	1.38E-06	1.03E-08	4.16E-08	8.31E-10	1.93E-07	3.87E-09	4.01E-04	8.02E-06	9.79E-08	2.94E-09	1.43E-08	4.28E-10
Cascade 5	7/21/2004		nm	1.35E-06		3.98E-08		1.68E-07				6.31E-08		8.60E-09	
Cascade 5	1/18/2005	4/12/2005	nm	1.33E-06	1.00E-08	4.23E-08	8.46E-10	1.91E-07	3.82E-09	3.98E-04	7.96E-06	9.75E-08	2.93E-09	1.39E-08	4.16E-10
Cascade Picnic	7/19/2004		16.32	1.33E-06		4.07E-08		1.59E-07				6.37E-08		8.38E-09	
Cascade Picnic	1/18/2005	4/12/2005	11.89	1.35E-06	1.01E-08	4.23E-08	8.46E-10	1.90E-07	3.80E-09	4.02E-04	8.05E-06	9.87E-08	2.96E-09	1.44E-08	4.31E-10
Cascade Picnic	7/13/2005	8/25/2005	nm	1.39E-06	1.04E-08	3.86E-08	7.71E-10	1.78E-07	3.56E-09	2.94E-04	5.87E-06	6.66E-08	2.00E-09	9.24E-09	2.77E-10
Cascade Picnic	7/21/2004		nm	1.33E-06		4.15E-08		1.69E-07				6.54E-08		8.91E-09	
Cascade Picnic	11/11/2005	12/14/2005	nm	1.35E-06	1.01E-08	4.42E-08	8.83E-10	1.83E-07	3.66E-09	3.39E-04	6.79E-06	7.87E-08	2.36E-09	1.16E-08	3.47E-10
Cascade Picnic	3/30/2006	5/14/2006	nm	1.37E-06	1.03E-08	3.99E-08	7.99E-10	1.80E-07	3.60E-09	3.69E-04	7.39E-06	8.94E-08	2.68E-09	1.31E-08	3.92E-10
Cascade 7	1/18/2005	4/11/2005	nm	1.36E-06	1.02E-08	4.24E-08	8.49E-10	1.97E-07	3.94E-09	4.02E-04	8.05E-06	9.88E-08	2.96E-09	1.44E-08	4.33E-10
Cascade 9	7/21/2004		nm	1.34E-06		4.12E-08		1.67E-07				6.50E-08		8.77E-09	
Cascade 9	1/18/2005	4/8/2005	nm	1.33E-06	9.98E-09	4.15E-08	8.31E-10	1.89E-07	3.78E-09	3.93E-04	7.86E-06	9.75E-08	2.93E-09	1.42E-08	4.25E-10
Cascade 10	7/19/2004		15.88	1.37E-06		4.63E-08		1.91E-07				6.81E-08		8.91E-09	
Cascade 10	1/18/2005	4/8/2005	nm	1.37E-06	1.03E-08	4.40E-08	8.80E-10	1.99E-07	3.97E-09	4.13E-04	8.26E-06	1.02E-07	3.05E-09	1.47E-08	4.41E-10
El Portal 1	7/21/2004		nm	1.35E-06		4.20E-08		1.78E-07				6.74E-08		9.10E-09	
El Portal 2	7/21/2004		nm	1.36E-06		4.12E-08		1.68E-07				6.24E-08		8.03E-09	
El Portal 4	7/21/2004		nm	1.36E-06		4.18E-08		1.71E-07				6.32E-08		9.11E-09	

Table A.4. Cont.

Sample ID	Sample Date (m/d/yr)	Analysis Date (m/d/yr)	^{3}H (pCi/L)	$^{3}He/^{4}He$ (ratio)	+- (ratio)	^{4}He ($cm^{3}STP/g$)	+- ($cm^{3}STP/g$)	Ne ($cm^{3}STP/g$)	+- (cm3STP/g)	Ar ($cm^{3}STP/g$)	+- ($cm^{3}STP/g$)	Kr ($cm^{3}STP/g$)	+- ($cm^{3}STP/g$)	Xe ($cm^{3}STP/g$)	+- ($cm^{3}STP/g$)
El Portal 5	7/21/2004		nm	1.38E-06		4.11E-08		1.71E-07				6.22E-08		8.33E-09	
El Portal 5	1/25/2005	4/15/2005	nm	1.36E-06	1.02E-08	4.40E-08	8.79E-10	1.92E-07	3.83E-09	3.92E-04	7.85E-06	9.46E-08	2.84E-09	1.35E-08	4.05E-10
El Portal 6	7/21/2004		nm	1.35E-06		4.26E-08		1.72E-07				6.67E-08		8.86E-09	
El Portal 6	1/25/2005	4/8/2005	nm	1.35E-06	1.01E-08	4.46E-08	8.92E-10	2.00E-07	4.00E-09	3.94E-04	7.88E-06	9.51E-08	2.85E-09	1.38E-08	4.14E-10
El Portal 7	7/21/2004		nm	1.36E-06		4.13E-08		1.78E-07				6.43E-08		8.08E-09	
El Portal-8	7/21/2004		nm	1.12E-06		5.21E-08		1.71E-07				6.49E-08		8.52E-09	
El Portal-8	1/25/2005	4/14/2005	nm	1.30E-06	9.78E-09	4.66E-08	9.33E-10	1.97E-07	3.94E-09	3.88E-04	7.76E-06	9.37E-08	2.81E-09	1.33E-08	4.00E-10
El Portal-8	7/13/2005	9/1/2005	nm	1.38E-06	1.04E-08	4.72E-08	9.44E-10	1.99E-07	3.98E-09	3.04E-04	6.08E-06	6.81E-08	2.04E-09	9.10E-09	2.73E-10
El Portal-8	11/11/2005	12/14/2005	nm	9.08E-07	1.01E-08	6.48E-08	1.30E-09	1.81E-07	3.62E-09	3.26E-04	6.52E-06	7.66E-08	2.30E-09	1.04E-08	3.13E-10
El Portal-8	3/30/2006	5/14/2006	nm	1.38E-06	1.03E-08	4.15E-08	8.31E-10	1.90E-07	3.80E-09	3.52E-04	7.05E-06	8.33E-08	2.50E-09	1.18E-08	3.53E-10
El Portal 10	7/19/2004		16.10	1.36E-06		nm		nm				nm		nm	
El Portal 10	1/25/2005	4/14/2005	nm	1.38E-06	1.03E-08	4.38E-08	8.75E-10	1.91E-07	3.82E-09	3.93E-04	7.86E-06	9.48E-08	2.84E-09	1.35E-08	4.06E-10
South Fork MR	7/19/2004		nm	1.37E-06		4.12E-08		1.66E-07				5.62E-08		7.72E-09	
South Fork MR	1/17/2005	4/12/2005	nm	1.36E-06	1.02E-08	4.46E-08	8.92E-10	2.02E-07	4.03E-09	4.01E-04	8.01E-06	9.72E-08	2.91E-09	1.38E-08	4.15E-10
South Fork MR	7/13/2005	12/14/2005	nm	nm		nm		nm		nm		nm		nm	
South Fork MR	11/11/2005	12/14/2005	13.21	nm		nm		nm		nm		nm		nm	
Tributaries															
Yosemite Falls	7/21/2004		nm	1.36E-06		3.84E-08		1.62E-07				6.77E-08		9.03E-09	
Yosemite Falls	1/17/2005		13.96	nm		nm		nm		nm		nm		nm	
Bridalveil Falls	7/21/2004		nm	1.37E-06		3.92E-08		1.66E-07				6.91E-08		9.83E-09	
Bridalveil Falls	10/14/2004		14.39	nm		nm		nm		nm		nm		nm	
Bridalveil Falls	1/16/2001	4/11/2005	11.31	1.39E-06	1.04E-08	4.09E-08	8.18E-10	1.88E-07	3.76E-09	3.86E-04	7.72E-06	9.35E-08	2.81E-09	1.35E-08	4.06E-10
Cascade Falls	10/15/2004		11.70	nm		nm		nm		nm		nm		nm	
Springs															
Happy Isle Spring	5/31/2002	6/9/2006	6.68	1.96E-07	1.47E-09	1.37E-06	2.74E-08	1.90E-07	3.80E-09	3.32E-04	6.63E-06	7.69E-08	2.31E-09	1.09E-08	3.26E-10
Fern Spring	7/20/2000		15.90	1.02E-06		9.70E-08		2.34E-07		nm		9.00E-08		1.28E-08	
Fern Spring	10/13/2000		19.80	nm		nm		nm		nm		nm		nm	
Fern Spring	1/16/2001	4/11/2005	16.16	9.33E-07	7.00E-09	1.13E-07	2.25E-09	2.32E-07	4.63E-09	3.89E-04	7.79E-06	9.04E-08	2.71E-09	1.26E-08	3.78E-10
Fern Spring	7/12/2001	8/29/2005	12.78	1.33E-06	9.98E-09	5.32E-08	1.06E-09	2.20E-07	4.41E-09	3.52E-04	7.04E-06	8.37E-08	2.51E-09	1.15E-08	3.46E-10
Fern Spring	11/10/2001	12/19/2005	14.79	1.06E-06	7.94E-09	9.39E-08	1.88E-09	2.62E-07	5.24E-09	3.83E-04	7.67E-06	8.24E-08	2.47E-09	1.23E-08	3.68E-10
Fern Spring	3/29/2002	5/17/2006	10.70	1.33E-06	1.00E-08	5.46E-08	1.09E-09	2.31E-07	4.61E-09	3.74E-04	7.49E-06	8.86E-08	2.66E-09	1.25E-08	3.76E-10
Fern Spring	5/31/2002	6/22/2006	8.41	1.38E-06	1.04E-08	5.21E-08	1.04E-09	2.25E-07	4.51E-09	3.57E-04	7.15E-06	8.52E-08	2.56E-09	1.22E-08	3.65E-10
Fern Spring	06/01/2006	6/22/2006	8.41	1.38E-06		5.21E-08	1.04E-09	2.25E-07	4.51E-09	3.57E-04	7.15E-06	8.52E-08	2.56E-09	1.22E-08	3.65E-10
Fern Spring	10/12/2006		nm	1.10E-06		7.10E-08	1.42E-09	2.27E-07	4.53E-09	3.61E-04	7.22E-06	8.28E-08	2.48E-09	1.19E-08	3.56E-10
Fern Spring	11/20/2006		nm	1.08E-06		6.40E-08	1.28E-09	2.14E-07	4.28E-09	3.52E-04	7.03E-06	8.33E-08	2.50E-09	1.16E-08	3.49E-10
Fern Spring	12/12/2006		nm	1.04E-06		6.62E-08	1.32E-09	2.27E-07	4.55E-09	3.58E-04	7.17E-06	8.29E-08	2.49E-09	1.19E-08	3.56E-10
Cascade Spring	1/17/2001	4/15/2005	9.17	1.34E-06	1.01E-08	4.08E-08	8.15E-10	1.94E-07	3.87E-09	3.94E-04	7.89E-06	8.88E-08	2.67E-09	1.15E-08	3.46E-10
Drive Point Sampler															
MP-Superintendents Bridge	7/12/2001	8/25/2005	12.83	1.35E-06	1.01E-08	3.90E-08	7.79E-10	1.67E-07	3.33E-09	2.90E-04	5.79E-06	6.74E-08	2.02E-09	9.17E-09	2.75E-10
MP-El Capitan Bridge	7/12/2001	8/27/2005	15.34	1.19E-06	8.89E-09	7.89E-08	1.58E-09	2.57E-07	5.13E-09	3.92E-04	7.84E-06	8.36E-08	2.51E-09	1.13E-08	3.40E-10
MP-Cascade-6	7/12/2001	8/25/2005	10.89	1.37E-06	1.04E-08	5.75E-08	1.15E-09	2.50E-07	4.99E-09	4.45E-04	8.89E-06	8.94E-08	2.68E-09	1.32E-08	3.97E-10
Groundwater Wells															
Valley Well 1	6/21/2005	8/14/2005	17.95	1.31E-06	9.85E-09	9.45E-08	1.89E-09	2.28E-07	4.55E-09	3.76E-04	7.52E-06	8.94E-08	2.68E-09	1.29E-08	3.86E-10
Valley Well 1	5/31/2006	6/9/2006	17.95	1.31E-06	9.79E-09	1.04E-07	2.08E-09	2.30E-07	4.59E-09	3.75E-04	7.51E-06	8.75E-08	2.63E-09	1.28E-08	3.83E-10
Valley Well 2	6/21/2005	8/14/2005	15.20	3.57E-07	2.68E-09	4.21E-07	8.41E-09	2.29E-07	4.59E-09	3.80E-04	7.60E-06	8.78E-08	2.63E-09	1.24E-08	3.71E-10

Table A.4. Cont.

Sample ID	Sample Date (m/d/yr)	Analysis Date (m/d/yr)	^3H (pCi/L)	$^3He/^4He$ (ratio)	+- (ratio)	^4He (cm^3STP/g)	+- (cm^3STP/g)	Ne (cm^3STP/g)	+- (cm3STP/g)	Ar (cm^3STP/g)	+- (cm^3STP/g)	Kr (cm^3STP/g)	+- (cm^3STP/g)	Xe (cm^3STP/g)	+- (cm^3STP/g)
Valley Well 2	5/31/2006	6/9/2006	15.20	3.83E-07	2.87E-09	3.24E-07	6.49E-09	2.36E-07	4.73E-09	3.80E-04	7.61E-06	8.70E-08	2.61E-09	1.22E-08	3.65E-10
Valley Well 4	6/21/2005	8/14/2005	13.65	3.08E-07	2.31E-09	2.16E-06	4.32E-08	1.33E-06	2.67E-08	8.92E-04	1.78E-05	1.64E-07	4.93E-09	1.85E-08	5.54E-10
Valley Well 4	5/31/2006	6/9/2006	13.65	4.89E-07	3.67E-09	2.14E-07	4.29E-09	2.42E-07	4.84E-09	3.80E-04	7.61E-06	8.86E-08	2.66E-09	1.24E-08	3.72E-10
Arch Rock	6/21/2005	8/14/2005	19.65	1.02E-06	7.66E-09	8.37E-08	1.67E-09	2.02E-07	4.04E-09	3.48E-04	6.97E-06	8.18E-08	2.45E-09	1.12E-08	3.36E-10
Arch Rock	5/31/2006	6/9/2006	19.65	9.35E-07	7.01E-09	9.04E-08	1.81E-09	2.21E-07	4.42E-09	3.49E-04	6.97E-06	7.84E-08	2.35E-09	5.54E-09	1.66E-10
Arch Rock	6/1/2006	6/9/2006	19.60	9.49E-07		8.41E-08	1.68E-09	1.99E-07	3.98E-09	3.30E-04	6.61E-06	7.64E-08	2.29E-09	1.03E-08	3.09E-10
Crane Flat	6/21/2005	8/14/2005	18.78	1.89E-06	1.42E-08	5.49E-08	1.10E-09	2.25E-07	4.50E-09	3.83E-04	7.66E-06	8.80E-08	2.64E-09	1.20E-08	3.59E-10
Crane Flat	5/31/2006	6/9/2006	18.78	1.92E-06	1.44E-08	6.59E-08	1.32E-09	2.70E-07	5.39E-09	4.06E-04	8.12E-06	9.11E-08	2.73E-09	1.23E-08	3.70E-10
Hodgdon Meadow	6/21/2005	8/14/2005	20.44	1.52E-06	1.14E-08	5.41E-08	1.08E-09	2.08E-07	4.17E-09	3.67E-04	7.35E-06	8.54E-08	2.56E-09	1.14E-08	3.41E-10
Hodgdon Meadow	5/31/2006	6/9/2006	9.22	1.52E-06	1.14E-08	5.77E-08	1.15E-09	2.28E-07	4.57E-09	3.68E-04	7.36E-06	8.35E-08	2.50E-09	1.13E-08	3.40E-10
El Portal Well 2	6/21/2005	8/14/2005	17.94	2.52E-07	1.89E-09	6.74E-07	1.35E-08	2.18E-07	4.36E-09	3.48E-04	6.95E-06	7.85E-08	2.36E-09	1.02E-08	3.07E-10
El Portal Well 2	6/1/2006	6/9/2006	9.22	2.53E-07	1.89E-09	7.04E-07	1.41E-08	2.37E-07	4.74E-09	3.55E-04	7.10E-06	7.95E-08	2.39E-09	1.03E-08	3.10E-10
El Portal Well 2	11/06/2006	6/9/2006	18.00	2.16E-07		1.65E-06	3.30E-08	2.05E-07	4.10E-09	3.27E-04	6.54E-06	7.32E-08	2.20E-09	9.74E-09	2.92E-10
El Portal Well 3	6/21/2005	8/14/2005	14.39	1.20E-06	9.04E-09	6.65E-08	1.33E-09	2.47E-07	4.93E-09	3.70E-04	7.39E-06	8.19E-08	2.46E-09	1.09E-08	3.28E-10
El Portal Well 3	6/1/2006	6/9/2006	7.53	1.20E-06	9.02E-09	6.73E-08	1.35E-09	2.51E-07	5.02E-09	3.75E-04	7.50E-06	8.12E-08	2.44E-09	1.15E-08	3.45E-10
El Portal Well 4	6/21/2005	8/14/2005	15.81	4.05E-07	3.04E-09	2.25E-07	4.50E-09	2.25E-07	4.49E-09	3.59E-04	7.18E-06	8.22E-08	2.47E-09	1.12E-08	3.36E-10
El Portal Well 4	6/1/2006	6/9/2006	15.81	4.24E-07	3.18E-09	2.94E-07	5.88E-09	2.65E-07	5.29E-09	3.78E-04	7.56E-06	8.20E-08	2.46E-09	1.14E-08	3.41E-10
El Portal Well 5	6/21/2005	8/14/2005	13.92	3.38E-07	2.54E-09	2.93E-07	5.85E-09	2.22E-07	4.45E-09	3.51E-04	7.03E-06	7.74E-08	2.32E-09	1.05E-08	3.15E-10
El Portal Well 5	6/1/2006	6/9/2006	13.92	3.19E-07	2.39E-09	3.28E-07	6.57E-09	2.42E-07	4.83E-09	3.55E-04	7.10E-06	7.66E-08	2.30E-09	1.07E-08	3.22E-10
El Portal Well 6	6/21/2005	8/14/2005	12.78	4.45E-07	3.34E-09	2.19E-07	4.37E-09	2.17E-07	4.33E-09	3.50E-04	6.99E-06	8.06E-08	2.42E-09	1.12E-08	3.36E-10
El Portal Well 6	6/1/2006	6/9/2006	12.78	4.68E-07	3.51E-09	1.90E-07	3.81E-09	2.31E-07	4.61E-09	3.49E-04	6.99E-06	7.50E-08	2.25E-09	1.08E-08	3.25E-10
El Portal Well 7	6/21/2005	8/14/2005	15.04	9.82E-07	7.37E-09	7.88E-08	1.58E-09	2.27E-07	4.54E-09	3.65E-04	7.30E-06	8.21E-08	2.46E-09	1.16E-08	3.48E-10
El Portal Well 7	6/1/2006	6/9/2006	15.04	9.69E-07	7.27E-09	8.39E-08	1.68E-09	2.34E-07	4.69E-09	3.71E-04	7.43E-06	8.48E-08	2.54E-09	1.16E-08	3.47E-10

Samples ending with MR are collected in the Merced River near the confluence of the identified creek
Samples starting with "MP" are drive point samples
nm = not measured

Table A.5. Merced River flows (provided on CD)

Table A.6. Temperature Data for tributaries in the Merced River Basin (provided on CD).

APPENDIX B

SUPPLEMENTAL INFORMATION

B.1 Supplemental Material for ^{36}Cl

An alternative method for characterizing processes controlling ^{36}Cl and Cl^- is to plot the $^{36}Cl/Cl$ ratio verse the ^{36}Cl concentrations. The following figures (Figure B.1 to Figure B.3) elucidate similar processes that are determined from plotting $[Cl^-]^{-1}$ verses $^{36}Cl/Cl$ (Figure 2.4). Some of the figures refer to EM 2 and EM 3, which are two subsurface endmembers mixing in the watershed, and their description is in Chapter 2.

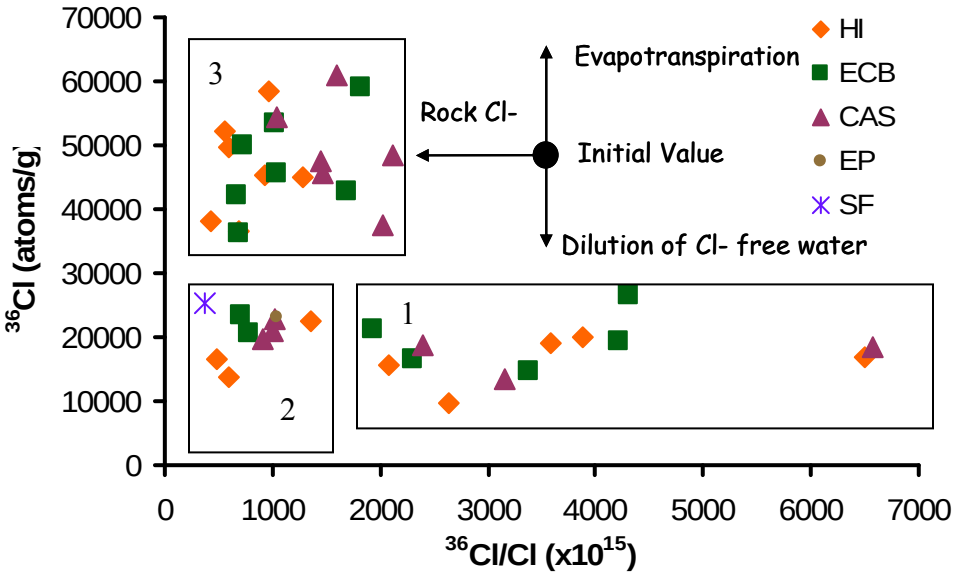

Figure B.1: $^{36}Cl/Cl$ verses ^{36}Cl for Merced River samples. The samples fall into three groups. Group 1 consists of all spring samples, group 2 consists of all summer samples, and group 3 consists of all autumn samples. Samples include Happy Isles (HI), El Capitan Bridge (ECB), Cascade Picnic area (CAS), El Portal (EP), and the South Fork of the Merced River (SF). This figure suggests that source waters feeding the Merced River during snowelt are diluted with Cl^- free water, or that source waters during baseflow have undergone evapotranspiration and have incorporated rock Cl^-.

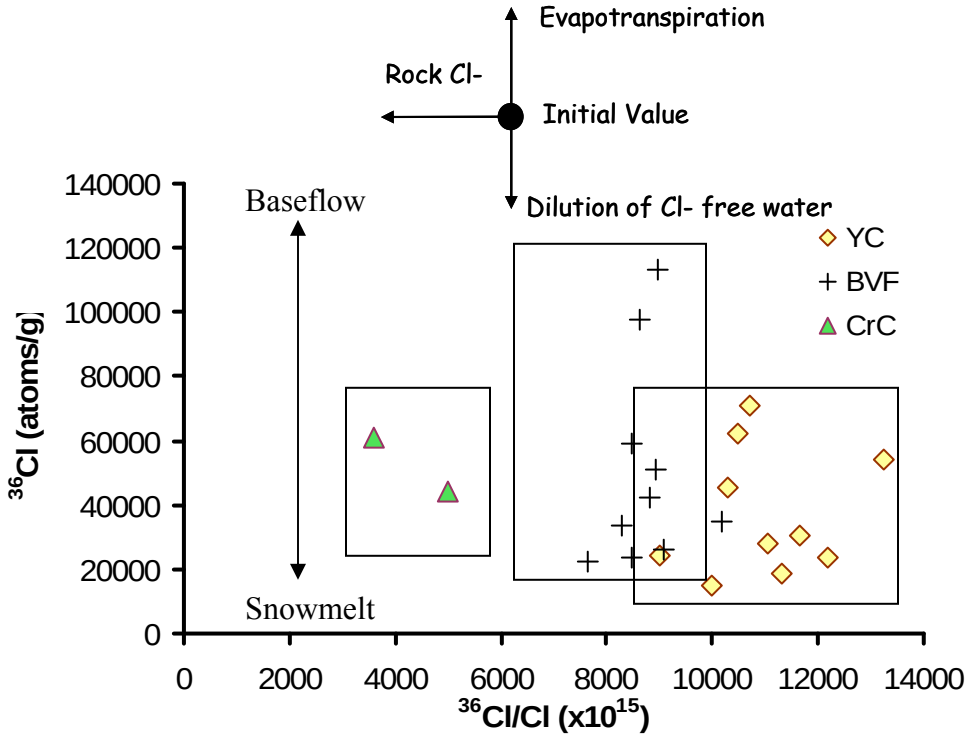

Figure B.2: $^{36}Cl/Cl$ verses ^{36}Cl for tributary samples. The samples are for Yosemite Creek (YC), Bridalveil Creek (BVF), and Crane Creek (CrC). Each tributary has a narrow $^{36}Cl/Cl$ range, but the ^{36}Cl concentrations increase during baseflow, and the lowest concentrations occurring during snowmelt. This figure indicates that Crane Creek source waters have more rock Cl^-, and that the baseflow samples have undergone higher evapotranspiration, and the snowmelt samples are diluted with Cl^- free water.

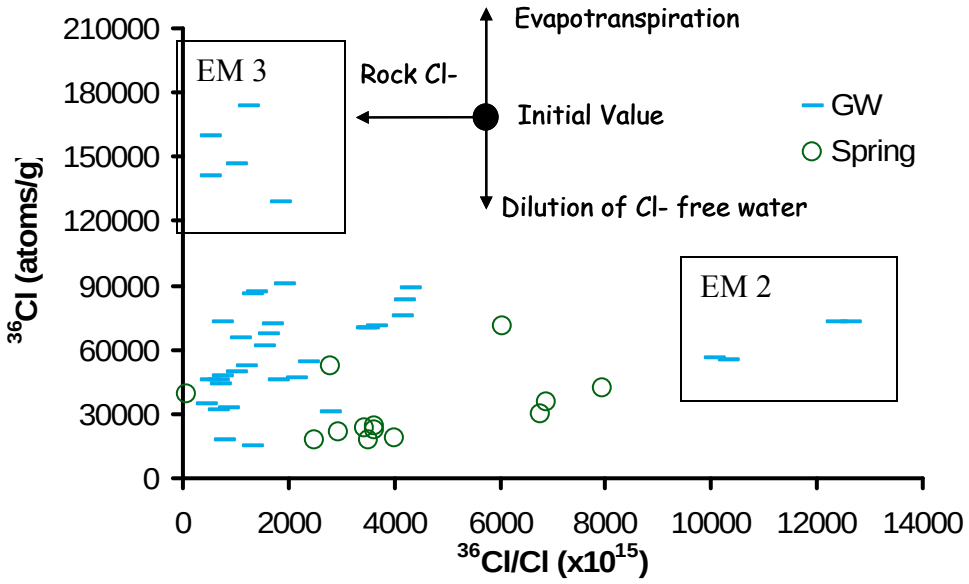

Figure B.3: $^{36}Cl/Cl$ verses ^{36}Cl for all groundwater samples. EM 2 is more diluted with Cl^- free water, and it has less rock Cl^-. EM 3 water has the most rock Cl^-, and has undergone the highest amount of evapotranspiration. All other groundwater samples appear to be mixtures of EM 2 and EM 3 water.

B.2 Supplemental Material for Noble Gas and ^3H

Noble Gas and Tritium Analytical Methods

Reactive gases are removed with a SAES Ti-Al getter operated at 400C. Argon, Kr and Xe are collected on activated charcoal using liquid nitrogen, and He and Ne is analyzed using a quadrupole mass spectrometer (Hudson et al., 2002). The remaining He and Ne are then collected at 15K on activated charcoal. The low temperature charcoal trap is then warmed to 35K and the He is released and admitted to the VG 5400 mass spectrometer. The mass spectrometer uses a conventional 17-stage electron multiplier and a SR400 pulse counting system for measuring ^3He. Helium-4 is measured using a faraday cup with a 10^{11} Ohm feedback resistor. The Ar abundance is determined by measuring its total pressure using a high-sensitivity capacitive manometer. The Kr and Xe abundances are determined using the quadrupole mass spectrometer.

For tritium determinations, 500g samples are loaded into stainless-steel bottles and attached to a multiport gas-handling manifold (Hudson et al., 2002). The samples are chilled with an ice water bath and headspace gases are pumped away. Samples are then heated with valves closed to re-equilibrate the water and the headspace void. Samples are then re-chilled and headspace gases are pumped away. In each cycle, approximately 99% of the He is removed. After five cycles, virtually no ^3He remains (< 100 atoms). The ^3He from tritium decay is allowed to accumulate for about 10-20 days. The samples are heated and then frozen (dry ice, -77C) and headspace gases are analyzed to determine the amount ^3He in-growth. The procedure is calibrated using a NIST-4361-B tritium standard

Background on Excess Air

Low excess air is sometimes interpreted as resulting from minimal fluctuation in the water table (Plummer et al., 2001, Cey et al., 2008). Holocher et al. (2002) show that incorporation of excess air results dominantly from a combination of the hydrostatic pressure and capillary pressure exerted on entrapped air. In the case of groundwater wells and springs in the Merced River basin, low excess air does not necessarily correlate strictly small variations in the water table, or even small increases in hydrostatic pressure. All wells sampled are artesian during the snowmelt season, and they are not artesian during the baseflow season, which indicates variations of hydrostatic pressure throughout the watershed. Groundwater wells in the Merced River watershed draw a combination of alluvial groundwater and fractured bedrock groundwater. Much of the aquifer alluvium consists of coarse-grained material, and if the majority of fracture apertures are wide enough, the capillary pressure may be minimized such that air can escape before becoming entrapped. Other factors that may cause low excess air are a more horizontal flow regime (not likely in mountainous terrain), small volumes of initially entrapped air, and increased size of entrapped air bubbles (Holocher et al., 2002). It is also possible that some combination of these other variables may control the low excess air component. Because the excess air component is so low, there is less uncertainty in $^{3}H/^{3}He$ age determination, and in the overall understanding the noble gas geochemistry of the system.

Determining $^3He/^4He_{RAD}$

In order to calculate the residence times of groundwater samples, it is important to determine the radiogenic $^3He/^4He$ ($^3He/^4He_{RAD}$), so that the amount of radiogenic ^3He can be separated from tritiogenic ^3He ($^3He_{trit}$). Average crustal radiogenic $^3He/^4He$ ratios are typically 10^{-8} to 10^{-7} (Oxbergh and O'Nions, 1987; Xu et al., 1996). In order to determine more accurately $^3He/^4He_{RAD}$, the measured Ne/He is plotted against the measured $^3He/^4He$ in all groundwater and spring samples. The Y-intercept is a measure of the $^3He/^4He_{RAD}$ (Aeschbach-Hertig et al., 2000). In the Merced River basin, $^3He/^4He_{RAD}$ is $1.1x10^{-7}$(Figure B.4).

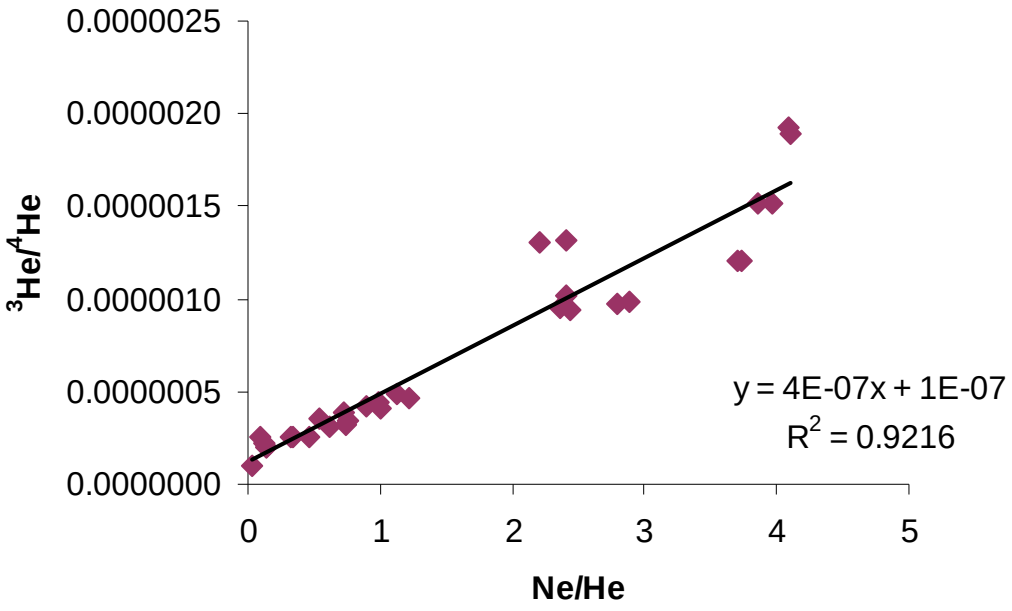

Figure B.4: Determination of radiogenic $^3He/^4He$.

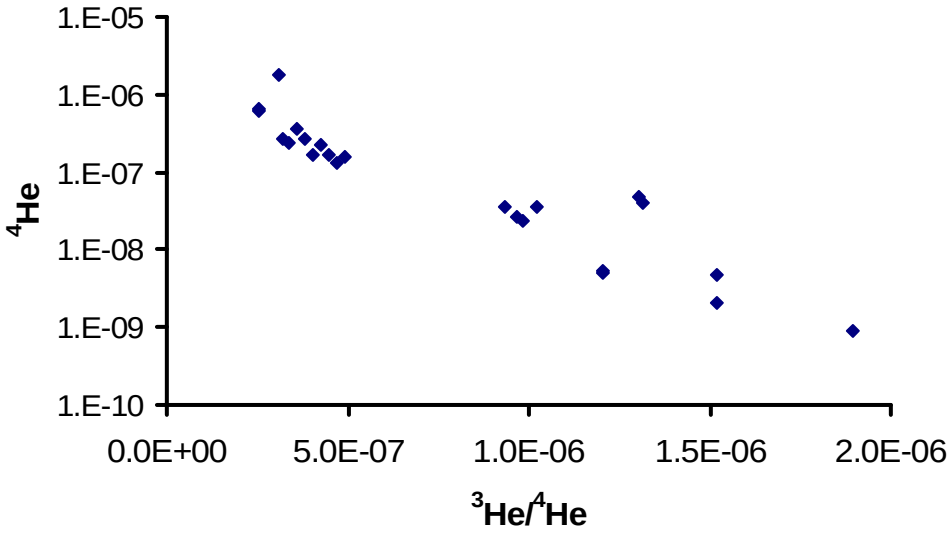

Figure B.6: This figure indicates that there is a relationship between $^{4}He_{RAD}$ and the $^{3}He/^{4}He$ ratios in the Merced River basin.

References

Aeschbach-Hertig, W., F. Peeters, U. Beyerle, and R. Kipfer, Paleotemperature reconstruction from noble gases in ground water taking into account equilibration with entrapped air, *Nature*, 405, 1040-1044, 2000

Cey, B. D., G. B. Hudson, J. E. Moran, and B. R. Scanlon, Impact of artificial recharge on dissolved noble gases in groundwater in California, *Environmental Science and Technology*, 42, 1017-1023, 2008.

Holocher, J., F. Peeters, W. Aeschbach-Hertig, M. Hofer, M. Brenwald, and R. Kipfer, Experimental investigations on the formation of excess air in quasi-saturated porous media, *Geochimica et Cosmochimica Acta*, 66, 4103-4117, 2002.

Hudson, G.B. J. E. Moran, G. F. Eaton, Interpretation of Tritium-3Helium Groundwater Ages and Associated Dissolved Noble Gas Results from Public Supply Wells in the Los Angeles Physiographic Basin: *Report to California State Water Resources Control Board, Lawrence Livermore National Laboratory*, 59 pp., 2002. http://www.llnl.gov/tid/lof/documents/pdf/245359.pdf

Manning, A. H., J. S. Caine, Groundwater noble gas, age, and temperature signatures in an alpine watershed: Valuable tools in conceptual model development, *Water Resources Research*, 43, WO4404, 2007.

Oxburgh, E. R., and R. K. O'Nions, Helium loss, tectonics, and the terrestrial heat budget, *Science*, 237, 1583-1588, 1987.

Plummer, L. N., E. Busenberg, J. K. Böhlke, R. L. Michel, and P. Schlosser, Groundwater residence times in Shenendoah National Park, Blue Ridge Mountains, Virginia, USA: a multi-tracer approach, *Chemical Geology*, 179, 93-111, 2001.

Visser, A., H. P. Broers, and M. F. P. Bierkens, Dating degassed groundwater with $^{3}H/^{3}He$, *Water Resources Research*, 43, W10434, doi:10.1029/2006WR005847, 2007.

Xu, Yongchang, Wenhui Liu, Ping Shen, and Mingxin Tao, *Geochemistry of Noble Gases in Natural Gases*, Science Press, Beijing, China, pp. 276, 1996.

B.3 Comparison of Water Chemistry and Residence Times

Water Chemistry and Noble Gases

Groundwater in the Merced River basin mixes between a high-Cl^- and low-Cl^- end member (see Chapter 2), and dissolved gas concentrations and age estimates help elucidate differences between these two end members. Chloride and $^4He_{RAD}$ ages show a linear positive correlation, but $^3H/^3He$ ages and fraction premodern water do not. The relationship between water chemistry and age is only observed if samples are placed in groups of low-Cl^- groundwater (<1.5 mgL^{-1} Cl^-), mixed-Cl^- groundwater (1.5 to 8 mg L^{-1} Cl^-), and high-Cl^- groundwater (>8 mg L^{-1} Cl^-). Additionally, samples with $^3H/^3He$ ages less than 1 yr are assumed to be invalid because they may be drawing recently recharged river water with elevated Cl^- (e.g. many wells in El Portal). Using these categories, there is a group relationship between noble gases and water chemistry (Figure C.2).

The low-Cl^- groundwater have average $^3H/^3He$ ages of 13±9 yrs, 11 ±19% premodern water, and $^4He_{RAD}$ ages of 82±79 years. The mixed-Cl^- groundwater has average $^3H/^3He$ ages of 18±8 yrs, 13 ±22% premodern water, and $^4He_{RAD}$ ages of 1105±442 years. The high-Cl^- groundwater on average has $^3H/^3He$ ages of 36±12 yrs, 70 ±44% premodern water, and $^4He_{RAD}$ ages of 4408±2071 years (Figure B.6). These data indicate that there is a general increase in residence times with increasing Cl^- concentrations.

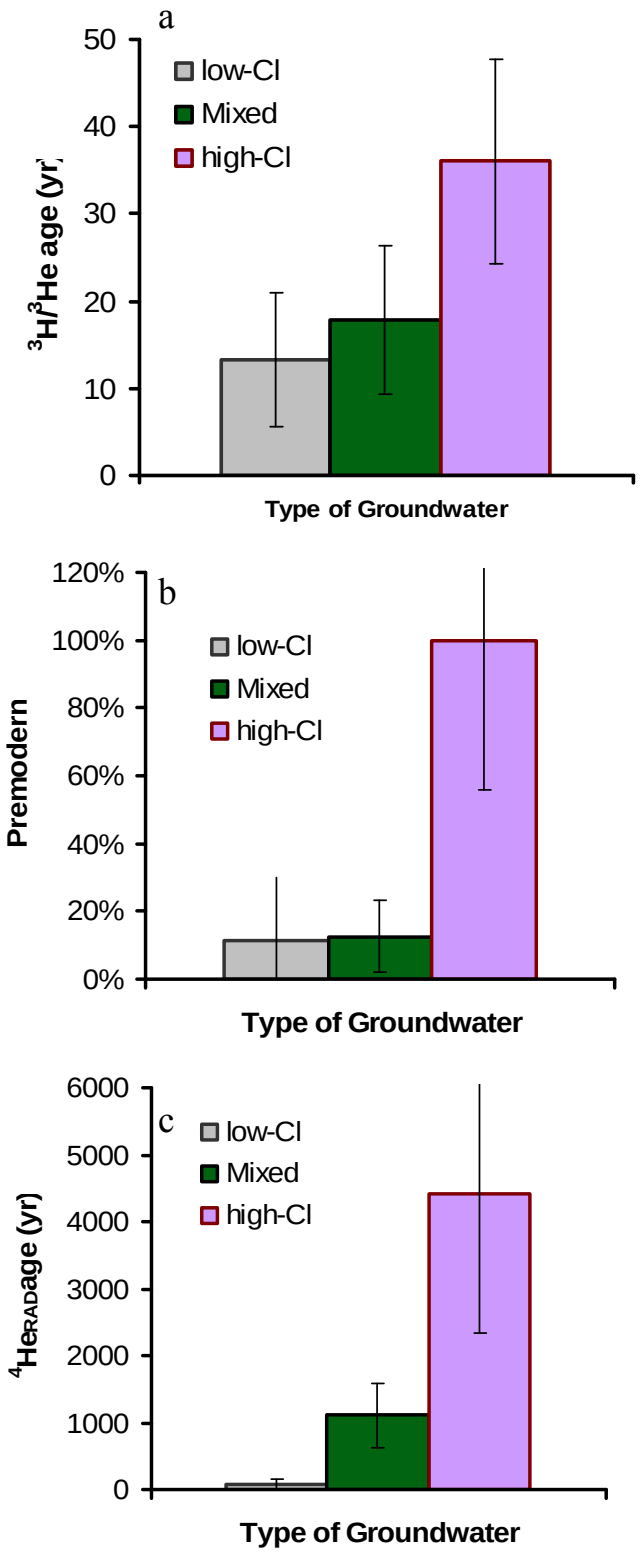

Figure B.6: Differences in low-Cl^- groundwater (14 samples), high-Cl^- groundwater (4 samples) and mixed samples (4 samples) are manifested in the a) $^3H/^3He$ ages, b) percent premodern water, and c) $^4He_{RAD}$ ages. The Error bars represent the standard deviation.

B.4 Seasonal Trends for Groundwater Fractions

The following figures (Figure B.7 to Figure B.10) illustrate the spatial distribution of groundwater fractions estimated from ^{222}Rn. These data were not included in Figure 4.6 for visual aide (i.e. too many data sets would result in difficulty in distinguishing spatial trends occurring throughout the catchment). The focus of Chapter 4 is on spatial, not temporal differences, in groundwater discharge to the Merced River so only the key datasets were included to indicate that similar spatial patterns occur throughout the year. Figures B.7 to Figure B.10 show similar patterns seen in Figure 4.6 (elevated fractions of groundwater occurring in Yosemite Valley, and much more variable groundwater fractions occurring downstream of Yosemite Valley).

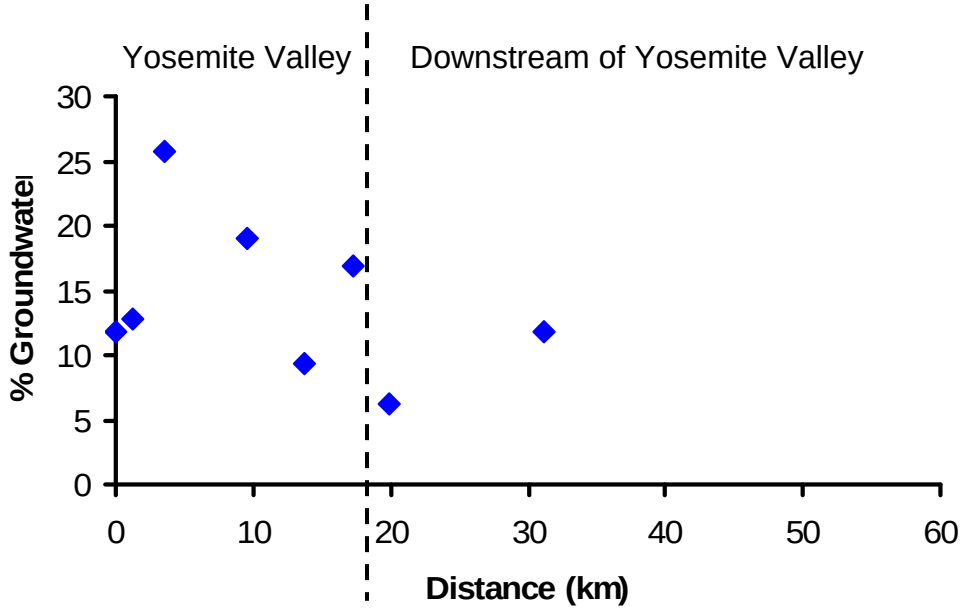

Figure B.7: Percent groundwater in the Merced River measured on January 31, 2007.

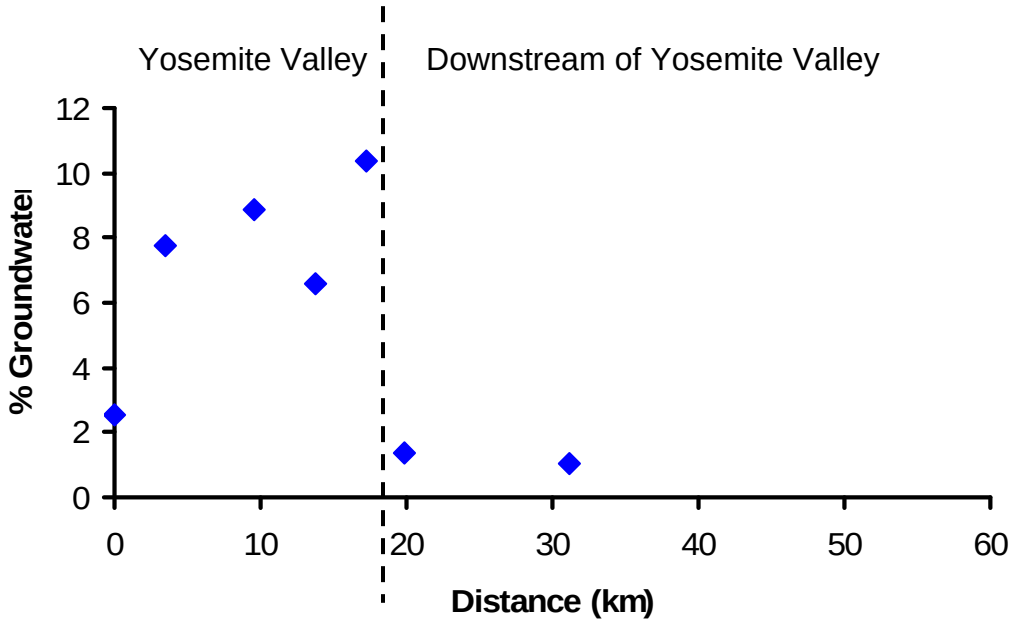

Figure B.8: Percent groundwater in the Merced River measured on May 24, 2007.

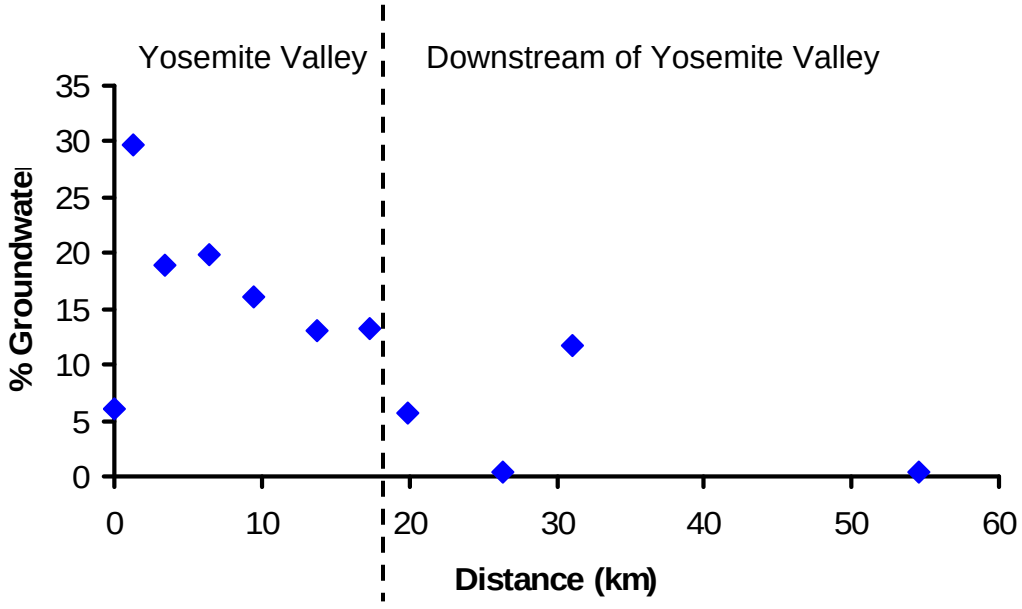

Figure B.9: Percent groundwater in the Merced River measured on July 12, 2007.

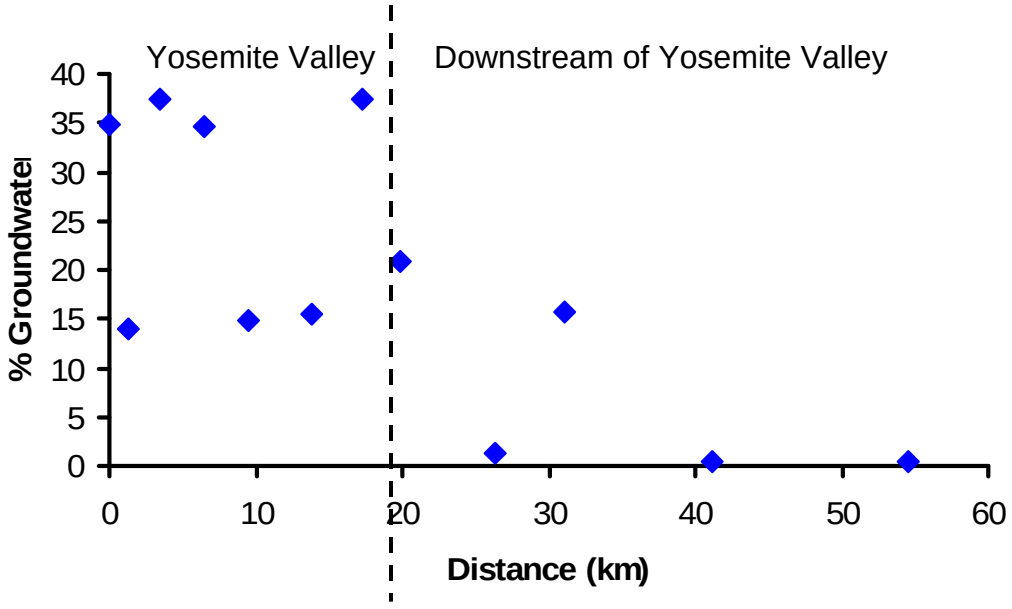

Figure B.10: Percent groundwater in the Merced River measured on October 10, 2007.

B.5 Analytical Methods for Determining Organochlorines

Öberg (2003), Öberg and Sanden (2005), and Svensson et al., (2007) measured Cl_{org} from soil by using the method for determining total leachable and total amounts of organohalogens (Asplund, et al., 1994). These authors assume that other organohalogens (i.e. bromine and iodine) are negligible compared to Cl_{org}. During the analytical procedure 20 mg of milled soil sample is combined with an acidic nitrate solution (20 ml, 0.2 M KNO_3, 0.02 M HNO_3) and shaken on a rotary shaker at 200 RPM for > 1 hr. The suspension was filtered through 0.45 μm polycarbonate filters. The suspension from the soil was then analysed according to the adsorbable organic halogen method described in (EU 1996) for Cl_{org} in water samples. This method includes diluting the filtered water to a 3:100 or 1:50 by volume ratio with deionized water, and placing the diluted sample in a 300 ml Erlenmeyer flask. Each sample had 50 mg of activated carbon, 5 ml of 0.2 M KNO_3, 0.02 M HNO_3 solution, and seven drops of concentrated HNO_3 added to it. The suspension sample was placed on a rotary shaker at 200 rpm for > 1 hr, and filtered using a 0.45 μm polycarbonate filter. The samples were rinsed with ~20 ml 0.01 M KNO_3, 0.001 M HNO_3 solution. The filter and filter cake was combusted under O_2 at 1000 °C in a Euroglas AOX analyzer. Formed hydrogen halides were determined by microcoulombmetric titration with silver ions. Samples were all analyzed with blanks, and the detection was ~5 μg Cl_{org} L^{-1}.

References

Asplund, G., A. Grimvall, and S. Jonsson, Determination of the total and leachable amounts of organohalogens in soil, *Chemosphere*, 28, 1467-1475, 1994.

EU, EU 1485 *Water Quality Norm*—Determination of adsorbable organically bound halogens (AOX), Approved April 1996.

Oberg, G., The biogeochemistry of chlorine in soil, *The Handbook of Environmental Chemistry*, 3, 43-62, 2003.

Öberg, G., and P. Sanden, Retention of chloride in soil and cycling of organic matter-bound chlorine, *Hydrological Processes*, 19 (11), 2123-2136, 2005.

Svensson, T., P. Sanden, D. Bastviken, G. Oberg, Chlorine transport in a small catchment in southeast Sweden during two years, *Biogeochemistry*, 82, 181-199, 2007.